Department of Civil and Environmental Engineering

Road network recovery from concurrent capacity-reducing incidents: model development and optimisation

By

ANTONIO PELLICER-POUS

A thesis submitted in fulfilment of the requirements for the degree of

DOCTOR OF PHILOSOPHY

October 2021

Declaration of Authenticity and Author's Rights

This thesis is the result of the author's original research. It has been composed by the author and has not been previously submitted for examination which has led to the award of a degree.

Signed: Antonio Pellicer-Pous

Date: 20/10/2021

ABSTRACT

Local and regional economies are highly dependent on the road network. The concurrent closure of multiple sections of the network following a hazardous event is likely to have significant negative consequences for those using the network. In situations such as these, infrastructure managers must decide how best to restore the network to protect users, maximise connectivity and minimise overall disruption. Furthermore, many hazardous events are forecast to become more frequent and extreme in the future as a result of climate change.

Extensive research has been undertaken to understand how to improve the resilience of degraded transport networks. Whilst network robustness (that is, the ability of a network to withstand stress) has been considered in numerous studies, the recovery of the network has captured less attention among researchers. Methodologies developed to date are overly simplistic, especially when simulating the dynamics of traffic demand and drivers' decision-making in multi-day situations where there is considerable interplay between actual and perceived network states and behaviour.

This thesis presents a decision-support tool that optimises the recovery of road transport networks after major day-to-day disruptions, maximising network connectivity and minimising total travel costs. This work expands upon previous efforts by introducing a new approach that models the damage-capacity-time relationship and improves the existing reinforcement-learning traffic-assignment models to be applicable to disrupted scenarios. An efficient metaheuristic approach (NSGA-II) is proposed to find optimal solutions for the recovery problem. The model is also applied to a real-world scenario based on the Scottish road network. Results from this case study clearly highlight the potential applicability of this model to evaluate different recovery strategies and optimise the recovery of road networks after multi-day major disruptions.

Keywords: RECOVERY, REINFORCEMENT LEARNING, RESOURCE ALLOCATION, TRAVEL BEHAVIOUR, OPTIMISATION, RESILIENCE, MULTI-DAY DISRUPTION, HAZARDOUS EVENT.

DEDICATION

This PhD thesis is dedicated to my family, for all the love and the endless support they give me. I would not have been able to complete this journey without their encouragement, patience, understanding and personal sacrifices.

ACKNOWLEDGEMENTS

First of all, I would like to thank my supervisor Dr Neil Ferguson for his support, guidance and encouragement throughout this research. Thanks also to my second supervisor Dr John Douglas for his valuable advice and comments on this work. Without their feedback and their guidance it would have not been possible to complete this thesis. This research has been made possible thanks to the funding and support of the University of Strathclyde.

Special thanks to IBI Group for their financial and technical support. In particular, to Graeme Scott (Director of IBI Group Glasgow) and David Salton (ITS consultant and project manager at IBI) who showed great interest in this project and provided very helpful insights.

An acknowledgement also goes to the Head of Network Maintenance at Transport Scotland, Scott Lees, who helped me to understand the roles and responsibilities of key organisations, such as Transport Scotland, involved in traffic incident management.

I would also like to thank my colleagues from the Department of Civil and Environmental Engineering, especially to Chago, Nui, Fiona, Eli, Cedric and Riccardo, for the moral support and the help they gave me throughout these years. Also thanks to all my friends from outside the department who knew how to cheer me up and support me in difficult moments and made my stay in Glasgow much more enjoyable.

Finally, I would like to thank to my parents, sister, family and friends in Spain for their continuous love, support and good wishes whenever I needed them. Thanks to all those who have helped me directly or indirectly in the successful completion of my thesis.

Antonio Pellicer-Pous

LIST OF AUTHOR'S CONTRIBUTIONS

1. Technical & published work (or in preparation).

The following manuscripts are being prepared for publication:

Manuscript1. Title: "A systematic review of road network recovery models and future directions".

Manuscript2. Title: "An improved reinforcement-learning departure time and route choice model: Application to multi-day road network disruptions".

Manuscript3. Title: "Optimising road network restoration from capacity-reducing damage in the north of Scotland".

2. List of conferences.

Pellicer-Pous, A., & Ferguson, N. S. (2020). Optimising road network restoration from capacity-reducing damage in North-East Scotland. 8th International Conference on Transport Network Reliability. 24th-26th June. Stockholm (Sweden). Accepted paper. The conference is postponed to June 2021 due to covid-19 crisis.

Presenter at the 1st Doctoral School Multidisciplinary Symposium, at the University of Strathclyde (Glasgow, UK) – June 2019. Title of the talk: "Optimising road network recovery from major multi-day disruptions". ISBN: 978-1-909522-53-4. University of Strathclyde Publishing.

Pellicer-Pous, A. and Ferguson, N. S. (2019) 'Optimising road network recovery from major multi-day disruptions. Application to the Scottish Road network', at the *Universities' Transport Study Group (UTSG) Conference*. Leeds, UK.

Pellicer-Pous, A. and Ferguson, N. S. (2019) 'Optimising road network recovery from major multi-day disruptions', in *Scottish Transport Applications Research (STAR)*. Glasgow, UK.

Presenter at the PhD Research Conference of the Department of Civil and Environmental Engineering (University of Strathclyde, Glasgow), 2017.

3. List of Awards

2017 – Second best speaker at the PhD Conference day (Department of Civil and Environmental Engineering, University of Strathclyde, Glasgow).

2019 - Shortlisted for the Images of Research Competition at the University of Strathclyde (Glasgow) with an image entitled 'Driving optimal decision-making'. (see Appendix 7).

2019 - Entry to Images of Research 2019 has been selected to appear in the year-long display along the River Clyde, outside the Glasgow Science Centre (Glasgow, UK).

4. External meetings

2017-2019. Regular Internal meetings with industry. IBI Group. The author has also presented and discussed the practical applications of this research with stakeholders at a series of internal meetings with the company IBI Group (sponsor of this project).

June 2017. Meeting with the Regional Manager of AIMSUN, Pete Sykes. In this meeting AIMSUN traffic modelling software was presented, highlighting the potential applications of the software. More specifically, the different types of traffic assignment models implemented in AIMSUN were presented and discussed.

February 2018. Meeting with the Head of Network Operations (Transport Scotland). The aim of this meeting was to understand the current state of practise of road network restoration and how operating companies cope with multiple incidents across the network. The meeting was also useful to understand their needs and opportunities for future improvements.

TABLE OF CONTENTS

LIST OF FIGURES

LIST OF TABLES

LIST OF NOTATIONS

Notation	Equation	Description
β_1, β_2, β_3, β_4	(6.4)	Coefficients of the terms included in the cost function.
β_z	(6.22) (6.23) (6.26) (7.7) (7.8) (7.9) (7.10) (7.11)	Binary variable (0-1) that indicates whether option z is favourable ($\beta_z = 1$) or not ($\beta_z = 0$) on day t, when the stimulus is positive.
β_{Fz}	(6.25) (7.12) (7.10)	Binary variable (0-1) that indicates if an option z is favourable ($\beta_{Fz} = 0$) or unfavourable ($\beta_{Fz} = 1$), when the stimulus is negative.
β_{Qz}	(7.8) (7.9) (7.11)	Binary variable (0-1) that takes a value of 1 ($\beta_{Qz} = 1$) if a packet of drivers h is aware of the disrupted route of option z. Driver knows of this disrupted
β_N	(6.25)	Binary variable (0-1) that takes the value of 1 if all options that are no chosen on day t are unfavourable and 0 if not all unselected options are unfavourable.
$\beta_{N'}$	(7.11) (7.13)	Binary variable (0-1) that takes the value of 1 ($\beta_{N'} = 1$) if all unselected options are unfavourable/disrupted, or 0 ($\beta_{N'} = 0$) otherwise.
$\rho_{h,CAR,t}$	(6.32)	Binary variable that indicates if the packet of drivers h travels by car on day t ($\rho_{h,CAR,t} = 1$) or decides not to travel by car ($\rho_{h,CAR,t} = 0$).
δ_{tij}	(3.17)	Binary variable that indicates if there is traffic demand from node i to node j at time t.
λ	(7.1)	User-defined threshold that is defined for each driver. It limits the maximum number of vehicles that can be on a road without triggering on-board decisions.
ε	(6.30)	Variable that weights the exploration and exploitation phases on the ε -greedy approach.
θ	(6.13)	Angle between the vertical axis and the decay of the bad-memory event function.
ϕ	(4.4)	Angle between the productivity-resource relationship and the x-axis.
γ_r	(3.13)	Binary variable that omits those trips whose post-disaster travel time is k times greater that the pre-disaster travel time.
γ_U	(6.28)	Variable that indicates the total number of options that are unfavourable.
$\nu_{h,LATE,t}$	(6.32)	Binary variable that indicates if the packet of drivers h arrives late to the destination on day t ($\nu_{h,LATE,t} = 1$) or on time ($\nu_{h,LATE,t} = 0$).
$\eta_{h,MODE,t}$	(6.32)	Binary variable that indicates if a packet of drivers h travels using another mode of transport that is not car-based ($\eta_{h,MODE,t} = 1$) or cancels the trip ($\eta_{h,MODE,t} = 0$).
ϑ_n	(4.2) (6.3)	A random value between 0 and 1.
ϑ_l	(4.1)	Random number (between 0 and 1) that is assigned to each road segment l. A road segment will be classified as damaged if the random number has a value below a pre-defined limit level.
ϑ_h	(5.2)	Random value between 0 and 1 that is generated for each packet h of vehicles.
φ_j	(6.9) (6.10)	Weighting factor that represents the memory level of travellers on day j.
Ω_h	(7.2)	Patience level of a packet h of vehicles.
ξ	(7.15)	User-defined value (between 0 and 1) that quantifies how the new pre-trip information is altering the mental probabilities of selecting travel options.
ς	(5.1)	Parameter of the Chang et al (1985) speed-density model.
a	(7.19)	BPR coefficient, often set at 0.15.
acc_a	(6.37) (6.38)	Accessibility variable that is given to an area a and it measures how close an alternative transit station is from the area where the user is located.
AA, BB, CC, DD	(6.32)	User-defined values that indicates the importance of each term in the calculation of the probability of selecting the option of 'not travelling by car'.
A_{ht}	(6.7)	Travel cost that packet of drivers h expects at time t.
AT_h^t	(5.8) (6.26) (6.27)	Previous arrival time of packet of vehicles h.
AT_h^{t+1}	(5.8)	New arrival time assigned to the queued packet of vehicles h.
AT_{hzt}	(6.5) (7.11)	Arrival time of packet of drivers h after choosing travel option z on day t.
b	(7.19)	BPR coefficient, often set to 4.
B_{hzt}	(6.11)	Bad-event memory variable that is used to further weight the travel cost of those bad experiences on day t identified by packet of drivers h.

Notation	Equation	Description
B_{max}	(6.11)	User-defined value that quantifies the maximum weighting value that the bad-memory variable (B_{hzt}) can take.
b_1 and b_2	(6.11)	User-defined limit values that characterises the bad-event memory function.
$comf$	(6.37)	Variable that defines the level of comfort that users experience by using this alternative transport mode.
ct	(7.14)	Number of consecutive days that an option is disrupted.
C_{hzj}	(6.7)	Travel cost of option z that packet of drivers h has experienced on day j.
$C_{h,FF}$	(6.17)	Free-flow travel cost of packet of drivers h.
$C_{r,pre}$	(3.14)	Cost in terms of travel time between the OD pair r during the pre-disaster stage.
$C_{r,post}$	(3.14)	Cost in terms of travel time between the OD pair r during the post-disaster stage.
CT	(7.4)	Current time that is being analysed (e.g. 8:04am).
CR_l	(7.16)	The remaining capacity of a disrupted link l.
$d_{r,post}$	(3.12) (3.13)	Post-disaster demand between the OD pair r that is satisfied.
$d_{r,pre}$	(3.12) (3.13)	Pre-disaster demand between the OD pair r that can be satisfied.
d_z	(7.14) (7.8) (7.10)	Variable that reduces the probability of selecting those options that contain at least a disrupted link.
D	Section 4.2.4	Value that indicates the amount of damage in units of resource*time.
D_l^0	(4.5)	Damage (in resource*time) that needs to be repaired on the damaged road segment l.
Dm_l	(4.1)	Binary variable that indicates if a road segment (or link) l is damaged ($D_l = 1$) or undamaged ($D_l = 0$).
DF_{hzt}	(6.18)	Difference between the expected travel cost (A_{ht}) on day t and the perceived travel cost (E_{hzt}) of each travel option, which is calculated to obtain the stimulus value.
$DF_{ht,max}$	(6.19)	Maximum difference between the expected travel cost (A_{ht}) on day t and the perceived travel cost (E_{hzt}) of all travel options available for packet of drivers h.
$DF_{ht,min}$	(6.20)	Minimum difference between the expected travel cost (A_{ht}) on day t and the perceived travel cost (E_{hzt}) of all travel options available for packet of drivers h.
DL_{ht}	(6.4)	Late arrival penalty assigned to packet of vehicles h on day t. It takes a value of 1 for late arrival or 0 otherwise.
DT_{zj}	(6.8) (6.26) (6.27)	Departure time of chosen option z on day j.
DT_{mt}	(6.8) (6.26) (6.27)	Departure time of chosen option m on day t.
DA_j	(8.1)	Total trip attraction at zone j.
E_{hzt}	(6.17)	Perceived travel cost of packet of drivers z on travel option z calculated on day t.
ET_h	(6.5) (6.26) (6.27)	Earliest limit of the preferred arrival time interval (PATI).
EAT_{hz}	(7.3)	Arrival time that packet h of drivers expects after choosing new travel option z.
EL	(7.3)	User-defined extra time that allows drivers to arrive later than the starting time of the activity.
$E[C_{hzt}]$	(7.20)	Estimated travel cost of option z that packet of drivers h receives from the GPS systems on day t.
EP_{DZ}	(8.4)	Employment at datazone level.
EP_{NTEM}	(8.4)	Aggregated employment at NTEM zone level.
$ETT_{route,h}$	(7.4)	Travel time of the new route that the packet h of drivers expects.
f	(8.3)	Factor that converts aggregated trips to disaggregated trips.
$freq_a$	(6.37) (6.39)	Frequency of the service that is provided by the alternative transport mode.
$f(c_{ij})$	(8.1)	Deterrence (travel cost) function between any pair of zones i and j.
F	(7.7) (7.8) (7.9) (7.10)	Binary variable (0-1) that indicates the presence or absence of the new feature that reduces the probability of selecting those disrupted options.
g	(4.4)	Gradient of the productivity-resource relationship. Note that $\tan(\beta) = g$.
gap	(5.7)	Average distance between two consecutive vehicles.
g_h	(7.20)	Binary variable that takes a value of 1 if packet of drivers h receives GPS information or 0 if packet h does not receive that information.
h	(5.8) (5.9) (5.10) (5.1) (5.5) (5.2) (6.7)	Packet of vehicles

Notation	Equation	Description
H_{hzj}	(6.17)	Binary variable that indicates if a travel option z has been used on day j ($H_{hzj}=1$) or it has not been used ($H_{hzj}=0$) by packet of drivers h.
HH, JJ, LL	(6.37)	User-defined variables that weight each terms of the formula that quantifies the service level satisfaction of drivers.
J_h	(7.2)	Number of disrupted links that driver h has experienced on the same day.
$\max J_h$	(7.2)	User-defined maximum number of disrupted links that limits the number of re-routes this driver can take.
κ	(3.13)	User-defined parameter that indicates that post-disaster travel time is "k" times greater than the pre-disaster travel times.
k_l	(5.1) (5.3) (5.5) (5.6) (7.1)	Traffic density only on the running part of link l.
k_o	(5.1) (5.4) (5.6)	Density associated with a maximum flow. In this model, it is assumed that this value is half of the jam density value (k_j).
$k_{Q,VMS}$	Section 7.6	Pre-defined limit value of the density of a link that is used by the VMS to give advice to drivers of busy roads.
k_j	(5.6) (7.1)	Jam density on link l. Equation (5.4) is used to calculate this value.
K_r	(3.8)	Weighting factor that indicates the importance of an OD pair r.
K_j	(3.17)	Weighting factor that indicates the importance of the destination node j.
KT_h	(6.36) (6.32)	The 'need to travel' variable that is included in the calculation of the probability of selecting the option of 'not travelling by car'.
l	(3.5) (7.1) (7.2)	Link (road segment) number.
ℓ_h	(6.16) (6.1)	Learning rate for each packet of vehicles h.
L_{ij}	(3.8) (3.15) (3.17)	Parameter that determines the level of connectivity between node i and node j at time t.
LA_l	(5.3) (5.4) (5.7)	Number of lanes on link l.
LE_l	(5.3) (5.4)	Length of link l.
LE_{queue}	(5.7)	Length of the queue.
LE_{veh}	(5.7)	Average length of a vehicle. It is assumed a value of 4.8m (Qu *et al.*, 2013).
LT_h	(6.5) (6.26) (6.27)	Latest limit of the preferred arrival time interval (PATI).
m	(6.3)	Selected travel option on day t
mt_1	(7.14)	Maximum number of consecutive days that a driver can face a disrupted route without reducing the probability of being selected.
mt_2	(7.14)	Minimum number of consecutive days that a driver can face a disrupted route without reducing completely to zero the probability of being selected.
M_{hzt}	(6.11)	Experienced travel cost after using travel option z by packet of drivers h on day t.
n	(3.8)	Total number of node pairs
nL	(3.5)	Total links of the network
N	(3.17)	Total number of nodes
OD_{ij}	(3.15) (8.1)	Traffic demand between node i and node j.
OP_i	(8.1)	Total trip production at zone i.
p_{zt}	(6.2) (6.3) (7.7) (7.8) (7.10)	Probability of selecting each travel option z on day t.
p_{mt}	(6.22) (6.23) (6.24) (6.25) (7.7) (7.8)(7.9) (7.10)	Probability of selecting travel option m on day t.
$p_{m(t+1)}$	(6.22) (6.24) (7.7) (7.9)	Probability of selecting the travel option m for the next day
$p_{z(t+1)}$	(6.23) (6.25) (7.8) (7.10)	Probability of selecting the travel option z for the next day.
p'_z	(6.30)	The new probability of selecting travel option z after the trade-off between exploration and exploitation.
$p_{z,Random}$	(6.30)	Random probability of selecting the travel option z on the ε-greedy approach.
$p_{z,mental\ mo}$	(6.30)	Probability of selecting travel option z that drivers store on their mental model.
$p_{zt,updated}$	(6.31)	Updated probability of selecting the travel option z on day t after incorporating the option of 'not travelling by car'.
$p_{z,new}$	(7.15)	New probability that is obtained as a combination of the $p_{z,mental}$ and the $p_{z,pretrip}$.
$p_{z,pretrip}$	(7.15)	Probability that is assigned to travel options based on the pre-trip information received.

Notation	Equation	Description
$p_{h,NC,t}$	(6.31)	Probability of selecting the option of 'not travelling by car' on day t by packets of drivers h.
$p_{h,NC(t+1)}$	(6.32) (6.33)	Probability of selecting the option of 'not travelling by car' on day $t+1$ by packets of drivers h.
$p_{h,MODE}$	(6.40)	Probability of choosing between cancelling the trip or using an alternative transport mode.
$P(\vartheta)$	(4.2) (4.3)	A uniform cumulative probability distribution.
P_{min}	(4.3)	Upper limit that defines the "minor" damage state on the probability distribution $P(\vartheta)$.
P_{mod}	(4.3)	Upper limit that defines the "moderate" damage state on the probability distribution $P(\vartheta)$.
P_{sev}	(4.3)	Upper limit that defines the "severe" damage state on the probability distribution $P(\vartheta)$.
PD_l^t	(4.4) (4.5)	Productivity (in units of resource-time/time) of repair teams allocated to damaged road segment l on day t.
PV	Figure 4.10	Priority value (PV) specified on each repair strategy. This value indicates the position of a damaged place in the list of priorities.
$PL_{\lim}$	(4.1)	Upper limit that is used to classify a road segment as damaged or undamaged.
P_a^{t+1}	(6.1)	Probability that the action a occurs at trial $t+1$, ranging from 0 to 1.
P_a^t	(6.1)	Probability that the action a occurs at trial t (expected probability), ranging from 0 to 1.
ΔP_a^{t+1}	(6.1)	Change in the strength of the action a for the next trial $t+1$. Note that the symbol Δ indicates a change in that variable
$PATI_h$	(6.5)	Preferred Arrival Time Interval of packet of drivers h.
$penalty$	(7.16)	User-defined value that penalises the undisrupted travel time of a link.
q_l	(5.5) (5.6) (7.19)	Flow of vehicles on link l.
q_{max}	(5.6) (7.19)	Maximum flow of vehicles on link l.
$q_{l,max,post}$	(3.11)	Post-disruption capacity of link l.
$q_{l,max,pre}$	(3.11)	Pre-disruption capacity of link l
Q_t	(3.3) (3.5)	Performance value in terms of total travel time.
Q_c	(3.17)	Performance value measured in terms of connectivity. It can take values between 0 and 1, being 0 null connectivity and 1 full connectivity.
r	(3.8)	Node pair
R	(3.11) (3.12)	Total number of origin-destination pairs.
RS_{DZ}	(8.4)	Residential population at datazone level.
RP_a^t	(6.1)	New probability of the action a after experiencing it on trial t (experienced probability), ranging from 0 to 1. In Bush-Mosteller model (1951).
RT	(4.4)	Number of repair teams that are assigned to a damaged place
RT_{min}	(4.4)	Minimum number of repair teams that needs to attend the damaged location in order to carry out repairs.
RT_{max}	(4.4)	Maximum number of repair teams that can attend the same incident location without reducing the total productivity
RU_z	(6.26) (6.27) (7.11)	Path/route of option z at day t.
RU_m	(6.26) (6.27) (7.11)	Path/route of chosen option m at day t.
RD_l^t	(4.5)	Percentage of damage that is repaired of damaged road segment l on day t
RD_l^{t-1}	(4.5)	Percentage of damage that is already repaired on day $t-1$
RC_h	(6.32) (6.34)	Late arrival coefficient that is used when the packet of drivers h does not reach its destination before the starting time of the activity a.
RS_h	(6.35) (6.32)	Rescaled value of the service level satisfaction (SL_h).
RE	(6.42)	Relative error.
s_{hzj}	(6.7)	Binary variable (0 or 1) that indicates if the travel option z, which was chosen on day j, has the same departure time as the option chosen on day t.
S_{hmt}	(6.16) (6.22) (6.23) (6.24) (6.25)	Stimulus value of packet of vehicles h after choosing travel option m on day t.
SL_h	(6.32) (6.40)	Service level satisfaction of using an alternative transport mode.
SDE_{hzt}	(6.4)	Amount of time that packet of vehicles h arrives early at the destination after choosing option z on day t.

Notation	Equation	Description
SDL_{hzt}	(6.4)	Amount of time that packet of vehicles h arrives late at the destination after choosing option z on day t.
SAT_{hmt}	(6.16)	"Satisfaction" value of packet of vehicles h after choosing travel option m on day t.
ST	(7.3)	Starting time of the activity.
t	(6.7)	Time (in days).
t_0	(3.3)	Time when the disruption occurs.
t_1	(3.3)	User-defined time horizon.
$t_{h,w}$	(5.8) (5.9)	Time that packet of vehicles h have to wait until the shockwave reaches its position.
$t_{h,queue}$	(5.8) (5.10)	Time to drive to the end of the link, assuming a free-flow travel speed.
t_{RC}	(6.34)	Time after the starting time of the activity that is needed to achieves a value of 1 on the RC_h variable.
tt_{lhj}	(7.6)	Travel time on link l that packet h of drivers have experienced on day j.
$tt_{withpenalt}$	(7.16)	Travel time of link l after being penalised due to the capacity reduction.
tt_O	(7.19) (8.1)	Free-flow travel time.
$T_{t,l}$	(3.5)	Average travel time on link l on day t. This is calculated using the BPR formula (Bureau of Public Roads, 1964).
$T_{t,V}$	(3.7)	Time that each vehicle V spends travelling on day t
TZ	(6.14)	Time when the bad-event memory variable takes a value of 1. It can be calculated using the value of the bad-event memory variable (B_{hzt}) of any day j.
TP_{NTEM}	(8.4)	Aggregated residential population at NTEM zone level.
TR_{DZi}	(8.3)	Number of trips that are assigned to the smaller zone i (datazone level).
TR_{NTEM}	(8.3)	Aggregated number of trips on the NTEM zone level.
TT_{hzt}	(6.4)	Time that packet of vehicles h spent on their journey after choosing option z on day t.
$\overline{TTC}_{ts}$	(6.42) (8.6)	Mean value of the total travel cost of s simulations on day t.
$\overline{TTC}_{t,30}$	(6.42) (8.6)	Mean value of the total travel cost of 30 simulations on day t
U	(6.36)	Number of days in a row in which drivers have not attended the activity.
U_f	(6.36)	Number of days in which activity is not essential and drivers may not attend the activity.
U_s	(6.36)	Initial value of the 'need to travel' variable
U_g	(6.36)	Number of days in which the 'need to travel' variable is increasing until it reaches the maximum value of 1.
v_h	(5.1) (5.5)	Speed of the packet h of vehicles.
$v_{h,min}$	(5.1)	Minimum speed of packet h of vehicles.
v_{max}	(5.2)	Maximum speed limit of the road.
$v_{h,FF}$	(5.1) (5.2)	Free flow speed of packet h of vehicles.
$v_{ff,l}$	(5.6)	Free-flow speed on link l.
va	(5.2)	Variable that limits the maximum variability of the speed of drivers.
$V_{t,l}$	(3.5)	Number of vehicles on link l on day t.
V_{net}	(3.7)	Total number of vehicles travelling on the network
$V_{l,run}$	(5.3)	Total number of vehicles travelling on the running part of link l at time t.
$V_{queue,l}$	(5.7)	Number of vehicles waiting on the queue of link l at time t.
$V_{l,max}$	(5.4)	Maximum number of vehicles that can use link l at time t.
V_{tij}	(3.17)	Total number of vehicles that completed their trip from node i to node j on day t.
$V_{ij,pre}$	(3.17)	Total number of vehicles that are expected to travel from node i to node j during the pre-disrupted stage.
W_r	(3.11)	Total number of paths between an OD pair r.
w_r	(3.11)	A path between an OD pair r.
$x(t)$	(8.7)	Results from the model simulation (e.g. traffic flow, speed).
$x'(t)$	(8.7)	Collected real traffic data (e.g. traffic flow, speed).
y_{RC}	(6.34)	Coefficient that indicates how important is to arrive on time to undertake the activity.
Y	(8.7)	Difference between model simulation and real traffic data.
z	(6.3) (6.7)	Travel option.
$\mathcal{Z}$	(6.2) (6.3) (6.7)	Total number of possible travel options that each driver knows.

LIST OF ABBREVIATIONS & ACRONYMS

Notation	Description
ATIS	Advanced Traveller Information System
BM	Bush-Mosteller model
DMRB	Design manual for Roads and Bridges
FIFO	First-in-first-out principle
FSM	Four-Step model
GA	Genetic Algorithms
HAZUS-MH	HAZard United States - Multiple Hazard (FEMA, 2013)
LA	Learning Automata
NSGA-II	Non-dominated Sorting Genetic Algorithm
OD	Origin-Destination
PAT	Preferred arrival time
PATI	Preferred arrival time interval
PUE	Partial User Equilibrium
REDARS	Risk from Earthquake DAmage to Roadway Systems (ImageCat, 2005).
RL	Reinforcement Learning
SLA	Stochastic Learning Automata
UE	User Equilibrium
VMS	Variable Message Signs

CHAPTER 1

Introduction

1.1. Context and problem definition

A road transport network is an essential infrastructure that contributes to the development of a country as it allows the movement of people and goods. Community and regional economies are highly dependent on the transport network as they need to use road infrastructure to provide their services to other communities. For example, the Trunk Road network in Scotland contributes around £1.38 billion to its economy each year through public transport, road freight and road construction and maintenance (Peeling *et al.*, 2016). It also provides access to education, jobs and services, which are essential for the society.

There is a growing concern for the vulnerability of these networks to disruption by natural or human-made hazards. Road networks are highly exposed to these hazardous events, which in some cases may produce damage to road sections, congestion and closures of some parts of the network. Direct impacts, which are related to the physical damage to the road infrastructure, and indirect impacts, which are associated with additional travel time and other extra costs borne by society, are important for the economy. Road closures produce longer journey times, additional delays, costs for businesses and impacts on the tourist market as fewer people are willing to travel with disruptions, among other consequences (Ekosgen, 2016). For example, a series of rainfall-induced debris flows in August 2004 affected the Scottish road network. Social and economic impacts were significant, closing some road segments for a few days and making access to and from some remote communities difficult (Winter *et al.*, 2013). An increasing incidence of extreme weather events is expected to happen in the future due to climate change, which may exacerbate the

effect of natural hazards on the transport network (IPCC, 2014). It is therefore important to plan for these events and ensure that transport networks are well prepared and if the impact is not avoided, guarantee a rapid recovery of the network with a minimal impact on society. Therefore, infrastructure owners and transport operators aim to provide resilient transportation systems that are capable of absorbing the impacts of disruptive events, adapting to new situations and recovering quickly if any infrastructure is damaged.

Recently, there has been a growing interest in the study of the impacts of hazards on transport networks and their resilience due to the increase in natural disasters and terrorist attacks (Mattsson and Jenelius, 2015; Chang, 2016; Postance, 2017; Carlos Lam *et al.*, 2020; Zhang *et al.*, 2020). The term *resilience* is used widely over many different fields of research from ecology (Standish *et al.*, 2014) to psychology (Schoon, 2006; Schwarz, 2018) as well as to infrastructure systems (Chen and Miller-Hooks, 2012). A review of previous definitions in the field of transportation systems is included in Wan *et al.* (2018). In all these definitions, three resilience capacities are clearly identified: adaptive capacity, absorptive capacity and recoverability. In the context of this thesis, *resilience* is defined as the ability of a system to withstand and respond to the impact of disruptions and to recover within an acceptable time after being affected, thereby achieving a desired state. Bruneau *et al.* (2003) conceptualise resilience as encompassing four principles (commonly known as 4R's): (1) *Robustness*, defined as the ability to withstand stress without losing functionality; (2) *Redundancy*, the ability to provide alternative routes/means of transport to continue operations even if some road segments are damaged; (3) *Resourcefulness,* the ability to identify problems, establish priorities and mobilise repair resources to achieve goals and shorten the time of recovery (Cimellaro, Reinhorn and Bruneau, 2010); and (4) *Rapidity*, which measures how quickly functionality is restored. The levels of robustness and redundancy determine the performance loss of transport systems, whilst resourcefulness and rapidity determine the ability to restore the functionality of the system.

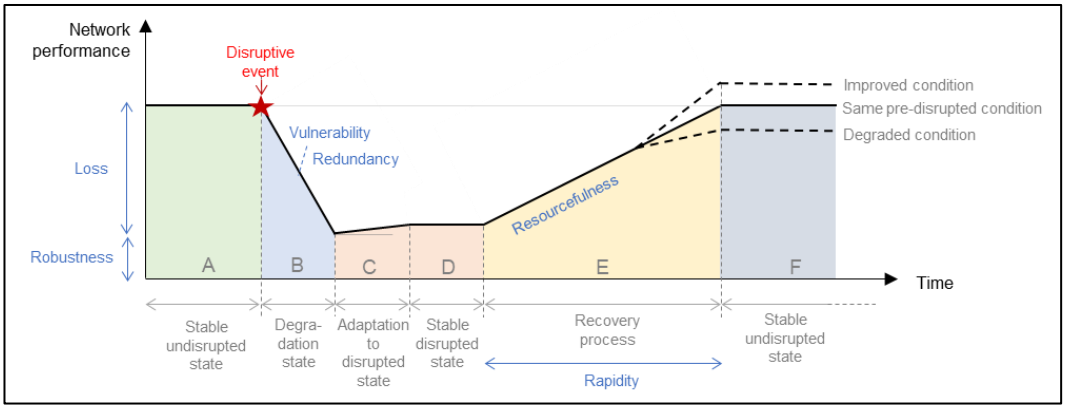

Figure 1.1. Typical disruption profile and posterior recovery
[Adapted from Henry and Ramirez-Marquez (2012)]

Graphically, these resilience principles are represented in Figure 1.1. Depending on how the network functionality is measured, different phases are identified. If it is measured using a flow-based approach (i.e. travel times), six phases are identified: (A) Undisrupted state, when the network has not yet been disrupted; (B) After the impact of a hazard, there is a degradation phase in which the performance of the system is decreasing; (C) Adaptation of drivers to the new disrupted situation (e.g. drivers might find alternative routes to get to their destination); (D) Stable disrupted state: the system remains disrupted for a period of time if no repair action is undertaken; (E) Recovery process when repairs are carried out; and (F) New undisrupted state after all repairs are completed. The new stable state can be the same as the pre-disrupted level or worse or better than this level. Note that the order of repairs and the allocation of repair resources to damaged places can determine the shape of the recovery profile (from C to F).

Vulnerability is defined in the context of this thesis as the susceptibility to events that can cause damage to road networks (Berdica, 2002). In this sense, susceptibility is defined as the likelihood of being harmed. Vulnerability of transport networks has attracted the attention of the research community (Mattsson and Jenelius, 2015; Reggiani, Nijkamp and Lanzi, 2015). Vulnerability assessments identify which components are the most important to the performance of the network and therefore more vulnerable when the hazard impact occurs. Although considerable research has been devoted to studying the vulnerability of transport networks, rather

less attention has been paid to studying the functionality restoration of transport networks after hazard impacts. These are referred to in the literature as *road restoration problems* (Tuzun Aksu and Ozdamar, 2014) or *road recovery problems* (Nakanishi, Matsuo and Black, 2013). The aim of these problems is to help find the 'best' distribution of resources to damaged locations so that models can assist decision makers in restoring the network in a prompt and efficient way under limited budgetary resources.

Several studies have addressed the problem of obtaining the optimal recovery strategy to certain damage scenarios. However, the lack of practicality, the low resolution and the assumptions made are unable to capture essential aspects of an actual road network restoration. In particular, the simulation of drivers' behaviour is a challenging area of research and strong simplifications and hypotheses make current transport models unrealistic in a fast and changing environment after hazard impacts. For instance, the assumption that drivers have 'perfect knowledge' of all network conditions before and after a hazard impact is not realistic. This assumption could be accepted in a long-term plan for infrastructure changes (Faturechi and Miller-Hooks, 2014b) but it cannot be accepted for a short-term period where network conditions are constantly changing. Understanding the dynamics of the individuals' behaviour is an important consideration to obtain more realistic results that current recovery models are missing.

Also, to date, most road recovery models are designed for catastrophic events, such as earthquakes and hurricanes. In these scenarios, short-term responses are fundamental to ensure safe evacuation, search-and-rescue and adequate relief distribution. In the long term, the repair of the infrastructure is the main concern. However, these approaches do not capture the impact of lower-risk weather-related hazards, such as landslides and floods, whose consequences are less often at a catastrophic level. In such cases, damage is repaired faster and network conditions are constantly changing due to repairs.

Information systems such as Intelligent Transportation Systems (ITS) and Advanced Traveller Information Systems (ATIS) are designed to provide external information on traffic conditions to drivers, which affects travel choices. These are expected to improve the system performance, helping recovery models to achieve the

desired outcomes faster. However, current road restoration models do not incorporate the effect of information technologies and therefore drivers' response to network changes is not affected by external travel information. ITS could also improve the efficiency of transport networks by distributing the flow of vehicles on the network to avoid congested areas.

A literature review conducted for this thesis (see Chapter 2) identified several challenging research areas that could improve the way that road transport recovery models and drivers' decision making processes are developed. These areas include:

(1) A better simulation of how drivers learn and make day-to-day and within-day travel decisions, avoiding the assumption of 'perfect knowledge' and providing different levels of external travel information after hazard impacts.

(2) The design of an optimisation model that finds the optimal repair strategies by taking into account the impact that repair resource allocation produces on drivers' behaviour and consequently on the overall system resilience.

(3) The practical applicability to real networks that are impacted not only by high impact and low probability events (e.g. disasters), but also by low impact and high probability events (e.g. winter storms, floods).

1.2. Research aim and objectives

The goal of this research is to develop a decision-support tool that assists network managers to devise the most effective and efficient way to restore a damaged road network. The tool recommends optimal repair strategies that allocate repair resources to damaged road segments, using an improved reinforcement-learning (RL) stochastic traffic model that simulates how drivers react to day-to-day and within-day network changes as well as learning from their mistakes. Such models find application in more challenging scenarios where, e.g., there are multiple damage locations across the network and resources to repair the network are limited.

In order to narrow the aspects of the recovery modelling field that are investigated, some questions that are addressed in this research are the ones described in Table 1.1. The research objectives pursued in order to answer the research questions are also included in the same table.

Table 1.1. Identification of research questions and objectives

Research questions	Research objectives	Chapter
RQ1. What is the current state-of-the-art in the field of recovery models of road transport networks after disruptive events?	**OB1.1**. Undertake a systematic literature review of current road recovery models and find potential gaps in the literature.	**2**
RQ2. How can the impact of different repair strategies on network resilience be measured? And, how can the 'best' repair strategy that produces the largest positive impact in terms of resilience be obtained?	**OB2.1.** Review previous metrics that measure the performance of systems and propose those metrics that will be used to measure the network functionality in this thesis. Review global indicators to measure the resilience of road transport networks. **OB2.2.** Review previous techniques to solve optimisation problems and select an algorithm that finds the 'optimal' repair strategies, thereby maximising the performance of the network.	**3**
RQ3. How can 'damage to infrastructure' be quantified and simulated using hazard susceptibility data?	**OB3.1.** Review how damage has been modelled in previous road recovery models. **OB3.2**. Select which road segments are damaged based on a probability distribution that is obtained from hazard susceptibility data. **OB3.3**. Assign a numerical estimate of damage to each damaged road segment.	**4**
RQ4. How can the infrastructure repair process be modelled, considering a resource-damage-time relationship and providing the evolution of road capacities over time?	**OB4.1.** Develop a resource allocation model that assigns repair resources to damaged roads, provides a repair scheduling plan and calculates the evolution of damage and repair over time.	**4**
RQ5. How can the movement of vehicles through the network be modelled, allowing a more flexible approach incorporating on-board decisions, such as re-routing or cancelling trips?	**OB5.1.** Review previous macroscopic, mesoscopic and microscopic traffic simulators. **OB5.2.** Outline the benefits/limitations of using existing traffic simulators. **OB5.3.** Propose my own framework that models the dynamics of vehicles when moving through the network, allowing the possibility of including on-board travel decisions.	**5**
RQ6. What is the current state-of-the-art in reinforcement-learning traffic models and their application to disrupted traffic networks?	**OB6.1.** Review current learning-based models in traffic assignment and their applicability to damaged road transport networks. Identify gaps in the literature.	**6**

Continuous in the next page

From the previous page

Research questions	Research objectives	Chapter
RQ7. How can the updating probability scheme of selecting travel options of previous RL traffic models be improved, taking into account departure time differences between travel options?	**OB7.1.** Understand the formulation presented in previous RL traffic models. **OB7.2.** Reformulate the RL updating probability scheme for selecting travel options incorporating departure time differences between travel options. Differentiate between favourable and unfavourable travel options.	**6**
RQ8. How can the RL traffic model incorporate the possibility of cancelling a trip or using alternative transport modes if disruptive events occur?	**OB8.1**. Incorporate an additional travel option within the set of alternative options that allows drivers to decide not to travel using their own car and use alternative transport modes or cancel the trip.	**6**
RQ9. To what extent can bad memories of previous trips affect drivers' travel decisions of future trips and how can it be implemented in the formulation of the RL traffic model?	**OB9.1**. Review previous research that outlines how bad experiences are remembered more than good ones. **OB9.2**. Introduce an additional factor in the travel cost formulation that considers how bad experiences are remembered more that good ones.	**6**
RQ10. What is the impact of the 'learning rate' parameter of the RL traffic model on the global network performance?	**OB10.1.** Undertake a sensitivity analysis of the learning rate parameter. Assign different values and observe how the system performance changes over time.	**6**
RQ11. How can the on-board drivers' decision-making process be modelled and implemented in the traffic simulator?	**OB11.1.** Introduce a triggering option that allows drivers to make on-board decisions (re-routing or abandoning trip) when they face disruptions on their route. **OB11.2.** Design a route choice algorithm that helps drivers find alternative routes when they face disrupted roads.	**7**
RQ12. How can the consequences of an on-board decision after a disruptive event impact future travel decisions and how can it be implemented in a RL traffic model? Or, in other words, how can the functions that update the option probabilities of the RL traffic model be reformulated in order to incorporate the consequences of on-board travel decisions?	**OB12.1.** Update the drivers' probability of selecting options for the next day, which are considered in the RL traffic model, incorporating the consequences of on-board decisions.	**7**

Continuous in the next page

From the previous page

Research questions	Research objectives	Chapter
RQ13. To what extent does providing information (pre-trip information, GPS navigation, Variable Message Signs, etc.) to drivers improve the recovery of transport networks?	**OB13.1**. Assign different types of external information to drivers and compare their impact on the network performance after disruptive events with and without providing external information.	**7**
RQ14. Is the proposed recovery model applicable to real case scenarios, obtaining a set of optimal repair strategies that can be selected to repair a disrupted road network?	**OB14.1**. Apply the recovery model to a real case scenario, which is the Scottish road network, and demonstrate that this model can obtain the (near-) optimal repair strategies that improve the recovery of disrupted road networks.	**8**

1.3. Scope

This research focuses on the restoration on road networks after disruptive events. However, certain areas are out of the scope of this research. The initial period of the post-event recovery process, which is called response recovery period or emergency phase (Miles, Burton and Kang, 2018), includes actions that vary from immediate emergency response actions that ensure human life is not in danger to shutting down some parts of the network in order to keep people safe. This research does not cover this initial response recovery period and it assumes that the situation is under control, damage is already assessed and only recovery actions are needed to ensure traffic gets back to normal conditions.

This model only accounts for physical damages that produce closures or capacity reductions of some parts of the network for at least a day. Those incidents that are cleared withing a few hours are not considered in this model. It is also assumed that damaged road segments are repaired overnight and therefore, no changes on the network occur during the simulation. Regarding the traffic modelling, this model assumes that all trips are repeated in a daily basis and only passenger cars are considered in the simulation.

1.4. Research significance: end-user benefits

Under limited resources, it is challenging to repair all damaged road segments simultaneously. Decision makers have to prioritise the interventions that provide the largest improvements to network performance. This research benefits both transport managers and transport authorities as this project provides a decision-support tool that assists them in making optimal and efficient recovery decisions.

From an operational point of view, immediately following a disruptive event, the recovery model can help network managers find optimal repair strategies that provide the maximum network performance during the restoration period. Transport operators may have some contingency plans in place for when these situations occur and this may help them to decide the priority order of repairs in a risk-based approach. However, the importance of this model is that it tries to predict the travel behaviour of drivers under these scenarios and select the optimal repair strategies based on the sum of individual performances. The model also estimates how long the service restoration is likely to take, so that managers can increase the number of restoration work crews or add redundancy to the network in order to reduce the recovery time. The model can also be used to test some traffic management strategies, so that transport operators may influence drivers' decisions when travelling after disruptions.

From a planning point of view, this model can also be used to identify critical road segments that, if disrupted, would cause the greatest disruption to the network. These are the areas that either transport authorities and/or transport operators may need to make more robust by allocating more resources during the recovery process or providing more information to drivers so that they can make more informed decisions, avoiding potential congestion in these areas if disrupted.

The model and its application example to the Scottish road network can guide the decision making of network managers in order to optimally restore the performance of transport networks after disruptive events.

1.5. Thesis structure

This PhD thesis is divided into nine chapters that describe the whole process that is carried out to develop this recovery model fully. Figure 1.2 shows a diagram that structures the whole thesis.

After this introductory chapter, a systematic literature review is presented in Chapter 2. It reviews previous recovery models that are applied to road transport networks. It also indicates potential research gaps in the area of road recovery modelling.

Chapter 3 presents the conceptual framework of the proposed recovery model and formulates the optimisation problem. Two network performance metrics are presented and different methods to solve the optimisation problems are also reviewed.

Chapter 4 introduces a damage scenario simulation using hazard susceptibility data and a repair process model to simulate how damage is repaired over time. The model is applied to the Sioux Falls Network (South Dakota, US).

The following chapters (5, 6 and 7) focus on the description of the dynamic modelling of drivers' behaviour and traffic simulation after the impact of hazardous events. Chapter 5 presents a mesoscopic traffic simulator that aims to model the dynamics of vehicles when moving through the network.

Chapter 6 presents an improved RL traffic model that aims to simulate the drivers' decision making process. The model is again applied to the Sioux Falls transport network (South Dakota, US) incorporating the RL traffic model.

Chapter 7 introduces some improvements (on-board decisions and external information) to the previous version of the RL traffic model included in Chapter 6. The updated model is also applied to the Sioux Falls transport network (South Dakota, US), illustrating the improvements introduced in this chapter.

Chapter 8 presents the application of the proposed recovery model to a real transport network in the north of Scotland. Finally the general conclusions of this PhD thesis are presented in Chapter 9 and future lines of research are also highlighted.

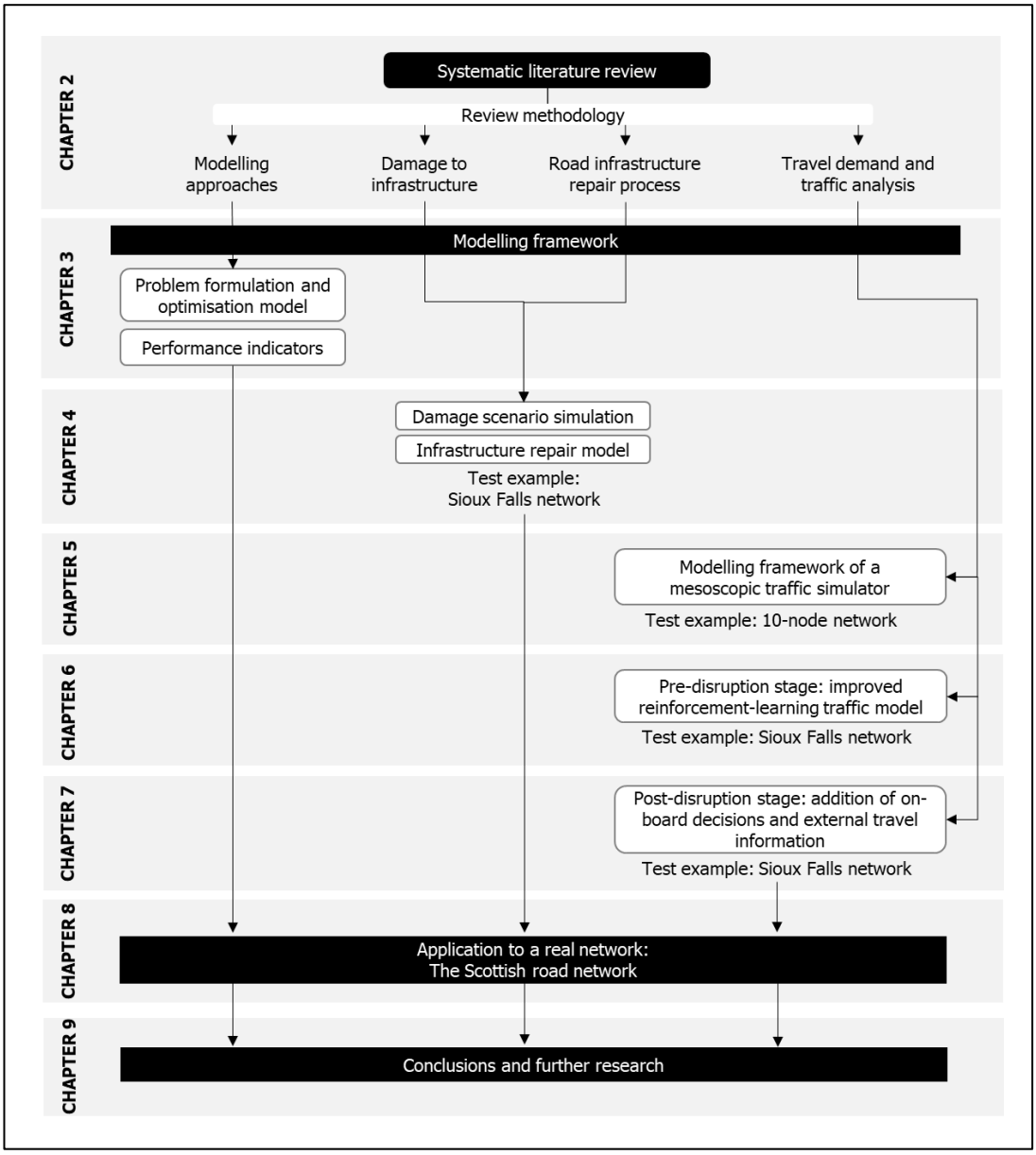

Figure 1.2. Representation of the thesis structure.

CHAPTER 2

A systematic review of road network recovery models and future directions

2.1. Introduction

Road networks enable the movement of people and goods, provide access to essential and desired activities and support social cohesion and economic development. However, these networks are susceptible to the impacts of natural or human-made hazard events that can reduce the performance of the network, producing negative consequences for individuals, organisations and communities relying on the network.

In recent years, there has been an increasing interest in the resilience of road networks by infrastructure managers and national governments. Their commitment to keep the transport network moving makes them show interest in identifying measures to protect and aid the recovery of the network from potential events that can cause disruption. If disrupted, it is in their interest to restore the network efficiently and expeditely so that society can return to normal and economic and social losses are minimised.

Although different definitions of the term *resilience* have been proposed in the literature, most of these agree that resilience includes the ability both to absorb and recover from the impact of a hazardous event[1]. Recent reviews of the definition and measurement of infrastructure system resilience include those by Faturechi and Miller-Hooks (2014a), Konstantinidou *et al*. (2014), Martinez-Pastor *et al.* (2015), Hosseini *et al*. (2016), Wang and Yodo (2016), Twumasi-Boakye and Sobanjo (2018), Sun *et al*. (2018), Wan *et al.* (2018), Rus *et al.* (2018) and Zhou *et al*. (2019). Most of them

[1] For example, the UNISDR (2009) defines resilience as "the ability of a system, community or society exposed to hazards to resist, absorb, accommodate, adapt to, transform and recover from the effects of a hazard in a timely and efficient manner, including through the preservation and restoration of its essential basic structures and functions through risk management."

highlight the lack of studies into the system recovery phase and acknowledge that this is an area where there is an opportunity to contribute to more sustainable and resilient systems.

The primary focus of this chapter relates to modelling the recovery of the road network from an event which causes damage to the road infrastructure and disrupts the operation of the network. As a cross-disciplinary concept, researchers have applied restoration models to different disciplines, such as psychology, ecology, engineering (water, energy, transport and structures), etc. The case of road transport systems adds an additional complexity as the performance of the system is directly affected by travel demand and individual drivers' routing decisions and the interaction between this demand and supply of infrastructure capacity. Çelik (2016) undertook a review of the recovery of general infrastructure systems in humanitarian operations, including relief distribution and inventory prepositioning. Although this review provided a general overview of restoration models, none of them captured the specific peculiarities of the road infrastructure system. There is a need to identify those models that specifically represent the recovery of road networks after disruptive events. The aim of this chapter is to provide a systematic review of relevant road restoration models which highlights the main components of these models, classifies the different approaches taken within each component, identifies gaps and limitations and considers options to improve restoration models.

The main contributions of this chapter are the following: (1) to the best of the author's knowledge, this is the first document that reviews in detail recovery models of road transport networks after hazardous events; (2) this chapter creates a framework to study and compare road recovery models; and (3) finally, it enables the identification of gaps in the literature and potential areas of further research.

2.1.1. Road network restoration models

A general framework for road restoration models is shown in Figure 2.1. The starting point is the occurrence of a hazardous event (e.g. earthquake, storm) which causes damage to road infrastructure and may also directly affect traffic demand or traffic flows before, during and after the event. Physical damage to road infrastructure may result in the partial or full closure of parts of the network or the reduction in maximum

speed on affected elements or both. Road users will respond to any changes in network capacity in one or more ways including re-routing, changing mode of transport, adjusting activity schedule (e.g. changing destination or departure time) or cancelling travel altogether. Road restoration represents all actions taken by the network manager including inter alia ensuring road user safety, informing users of existing or future network conditions, modifying the network and managing traffic during disruption, prioritising selected users such as emergency services and allocating resources to repair damaged network elements. In many cases, restoration will represent the restitution of the network to its former state, although on certain occasions full recovery may not be possible in which case the restored network would provide lower connectivity or capacity than before. Alternatively, the network manager may take the opportunity to enhance the network in some way.

The main purpose of a restoration model is to assist the network manager to devise the most effective and efficient way to restore a damaged road network. Such models find application in more challenging scenarios where e.g. there are multiple damage locations across the network and resources to repair the network are limited. Restoration is a complex, long-term process involving multiple steps and the opportunity to enhance the network is available.

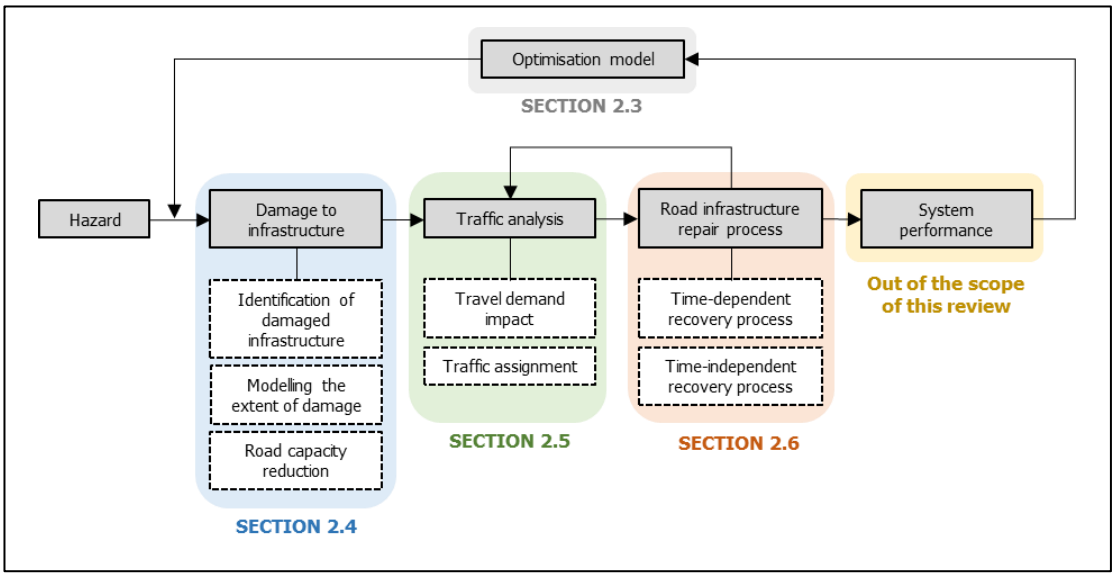

Figure 2.1. Key modules of a road recovery model. The sections of this chapter are divided according to this diagram.

2.1.2. Overview of terminology

Different definitions have been used to describe essential terms in the area of system resilience. As different authors have used these terms in a variety of ways and applied to different disciplines, the terminology presents in general inconsistency across the literature. This brief section aims to lay the foundations for essential resilience terms that might be used in some other sections of this chapter.

In the context of this thesis, *vulnerability* is defined as the susceptibility to events that can cause capacity reduction in a road network (Berdica, 2002). In this sense, a more vulnerable network would be one where a hazardous event of a given magnitude would result in more damage (performance reduction) than a less vulnerable network. As opposed to vulnerability, the term *robustness* is defined as the ability of the system to withstand stress without losing functionality. *Redundancy* is the ability to provide alternative routes/means of transport to continue operations even if some road segments are damaged. *Resourcefulness* is the ability of roads' authorities to identify problems, establish priorities and mobilise repair resources to achieve goals (Cimellaro, Reinhorn and Bruneau, 2010). Closely related to resourcefulness is the concept of *rapidity*, which is a measure of how quickly functionality is restored.

A *hazard* is defined as a phenomenon that may cause health impacts, property damage and social, economic or environmental disruption (UNISDR, 2009). A *hazardous event* is therefore the manifestation of a hazard in a particular place during a particular period of time. Hazards can be classified into three groups (Gill and Malamud, 2016): (1) Natural hazards, a natural process that may have negative impacts on society; (2) Anthropogenic hazards, human activity that may impact negatively; (3) Technological hazards, unintentional failure of technology. *Single hazards* are those independent hazards that are caused by different triggers. The effect of one hazard on the others is known as *hazard interactions*, and the term *multihazard* refers to all possible hazards and their interactions in a region. The terminology that defines the interactions between hazards is unclear in the literature. Hazard interactions are also known as *chains*, *cascades*, *domino effects*, *compound hazards* or *coupled events* (Dalezios, 2017). Five possible hazard interactions are highlighted (Gill and Malamud, 2016): (1) Natural hazards trigger other natural hazards; (2) Human activities trigger other natural hazards; (3) Human activities

exacerbating natural hazard triggering; (4) Cascades of hazards or networks of hazard interactions; (5) The concurrence of two (or more) hazard events. The probability that any hazard causes harm to society is known as *risk*. In other words, it is the composite of the probability for a hazard to occur and the resulting consequences of that impact.

The terms *restoration* and *recovery* are used interchangeably in the literature. Some authors name *restoration models* while others *recovery models*. The difference between both concepts is minimal. In the area of computer science, restoration is defined as the process of bringing something back to its original state. Whereas recovery is the process of regaining something lost. In the area of transportation, restoration is used as a more generic term that is related to the performance of the network (e.g. restore road functionality). However, recovery is more related to the process of planning and assigning resources to restore the functionality of the network (e.g. recovery strategies). In any case, both terms are used interchangeably in this thesis.

These terms are illustrated in the following Figure 2.2, which is a simplified version of Figure *1.1*. It shows a disruption and posterior recovery profile. As shown, the network performance is stable, achieving an equilibrium state before the disruptive event occurs. After the impact, the performance is disrupted and only when repairs are complete, the performance gets back to normal.

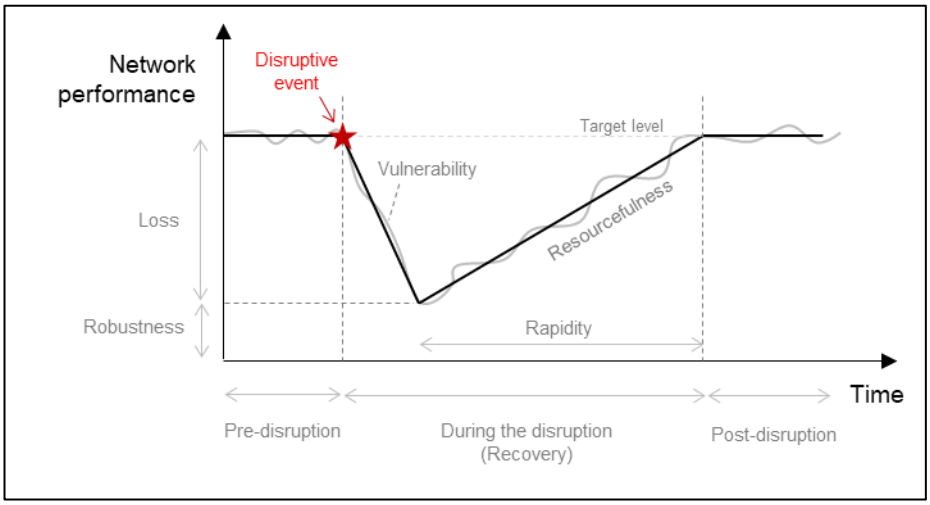

Figure 2.2. Simplification of the disruption and recovery profile considered in Figure 1.1.

2.2. Literature review methodology

A systematic methodology was used to identify relevant publications. The key stages of this process, including identification, screening and eligibility are explained below. A detailed PRISMA flow diagram (Moher *et al.*, 2009) with the corresponding number of publications (n) at each stage is provided in Figure 2.3. The scope of the review was restricted to publications in English, including journal papers, conference proceedings, doctoral dissertations, books and reports from 1995 to 2019.

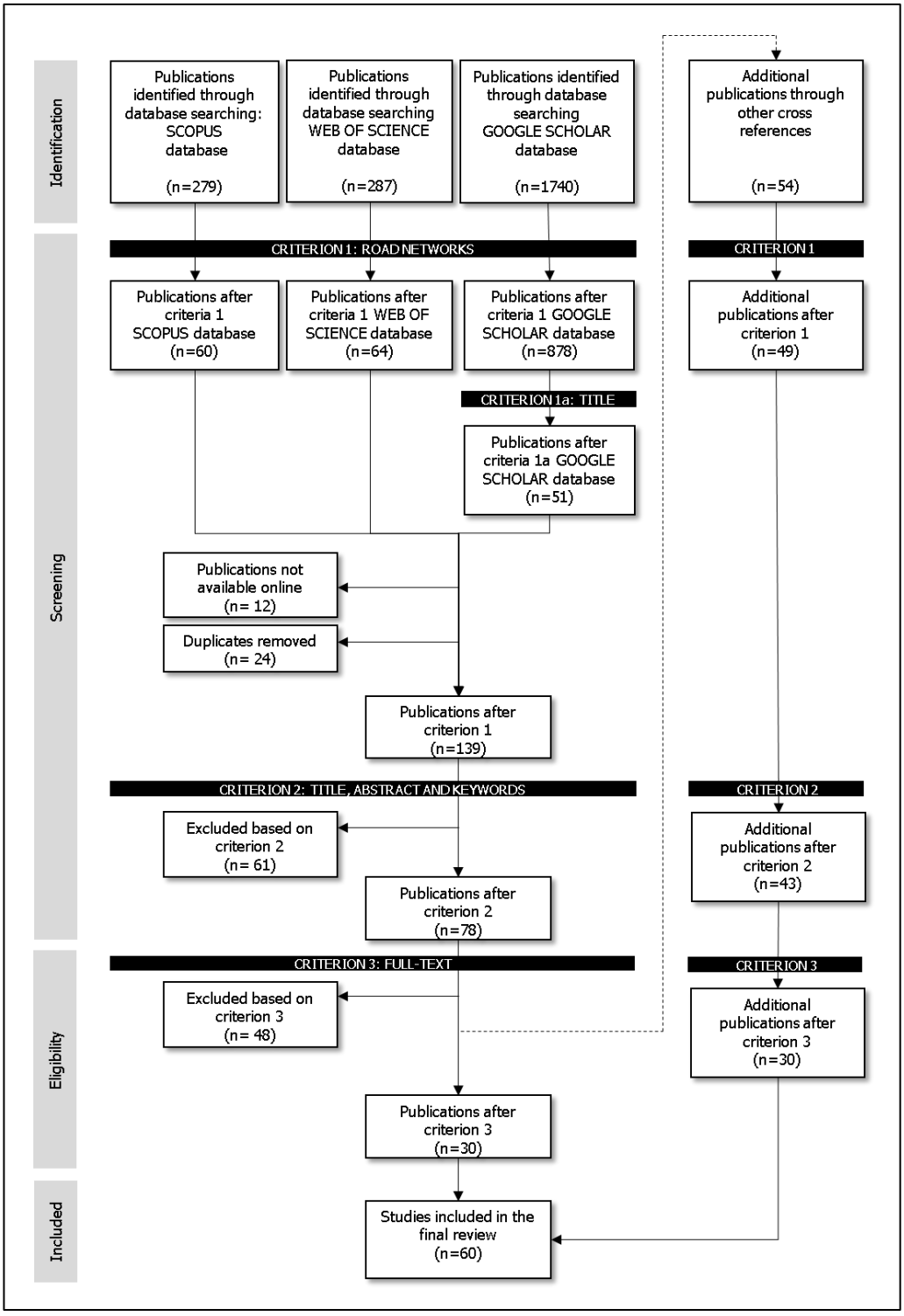

Figure 2.3. PRISMA flow diagram showing the selection process of the reviewed publications ("n" indicates the number of publications).

2.2.1. Identification of relevant publications

Three different databases were used to find published work within the field of engineering that addresses the topic of transport resilience: *Web of Knowledge*, *Scopus* and *Google Scholar*. Four groups of individual concepts were used to identify relevant publications within the first two databases as shown in Table 2.1. Any published work that contained one or more terms from each group, in either the title, abstract or keywords was added to the working sample. A single group of terms was used to search the *Google Scholar* database. If one of these terms appeared in the title or text of a publication it was added to the working sample.

Table 2.1. Groups of keywords for identifying publications

IDENTIFICATION						SCREENING
Web of Knowledge and *Scopus*				*Google Scholar*		Criterion 1
Group 1	Group 2	Group 3	Group 4	Group 1		
Resilien*	Recovery	Hazard*	Optim*	Resilience	Flood	Road*
	Restoration	Impact*	Simulat*	Repair	Earthquake	Transport
	Reconstruction	Disrupt*	Priorit*	Recovery	Landslide	network*
	Rehabilitation	Earthquake*	Allocat*	Restoration	Optimisation	Bridge*
		Flood*		Hazard	Simulation	Road
		Landslide*		Disruption	Allocation	infrastructure*
		Disaster*		Impact	Prioritisation	Link*
		Emergen*		model	Network	
					Infrastructure	

The truncation symbol * indicates that all words starting with this particular combination of letters will be looked for.

2.2.2. Screening

Two criteria were defined to screen the working sample and select relevant publications for review:

(1) CRITERION 1 was used to select only those publications that were related specifically to road networks. Any work that did not contain one of the terms in the final column of Table 2.1 either in the title, abstract or keywords was excluded from the review. For publications identified from the *Google Scholar* database, publications were selected only if the "road", "bridge", "link" or "transport" were used in the title or text, and the publications was found to be related to the topic following a manual inspection. Exceptionally, if a non-road-based restoration model could clearly be applied to road networks, this publication passed this criterion although further reading was required to

check its eligibility. Any publications that was not accessible in full text from a research library or publisher was also excluded.

(2) CRITERION 2 ensured that those publications that passed criteria 1 were in line with the general topic: "recovery of road networks after disruptive events". The title, abstract and keywords of each paper were read and if a publication addressed the topic, it was accepted for the next stage. Several publications relating to retrofitting of bridges prior to disruptions were found. Although these publications focussed principally on prevention rather than restoration, they also modelled the impact of hazards, the selection of retrofitting activities (similar to restoration activities) and the improvement of the network performance after these activities (similar to recovery). Due to their similarities with recovery models, these papers were also accepted after close reading.

2.2.3. Eligibility

Once all potential publications were identified, an exhaustive reading of the full-text was required to decide whether each piece of research would be included in the final review. Any work that modelled a detailed road restoration after the impact of disruptive events was accepted. Publications that analysed the performance of an individual asset (e.g. isolated bridges) rather than a network were excluded.

Relevant papers cited in selected publications which had not previously been identified were considered as potential publications for inclusion in the review. Any such publications which satisfied all criteria above were included.

2.2.4. Publications selected for review

A total of 60 publications met the selection criteria which included 47 journal papers, 5 doctoral dissertations, 5 conference papers, 2 book sections and 1 report. The distribution per 4-year interval is represented in Figure 2.4. It shows an increasing trend in recent years. A word cloud that displays the 50 most frequent words of all selected publications is also included in the same figure. The most frequent word is network followed by time, recovery, resilience, restoration, road and model. The main components of these recovery models are summarised in Figure 2.1. All of them simulated damage to infrastructure, modelled a repair process and used a

performance metric to measure the effectiveness of repairs. However, not all models undertook a traffic analysis as it was only needed if a flow-based metric was used. The following sections identify the similarities and differences between models on each key component. The 'performance metric' module is not considered in this review as there are already other reviews in the literature, such as the one carried out by Faturechi and Miller-Hooks (2014a) or another by Konstantinidou *et al.* (2014), that provide a comprehensive literature review on the measurement of transport system performance following disasters.

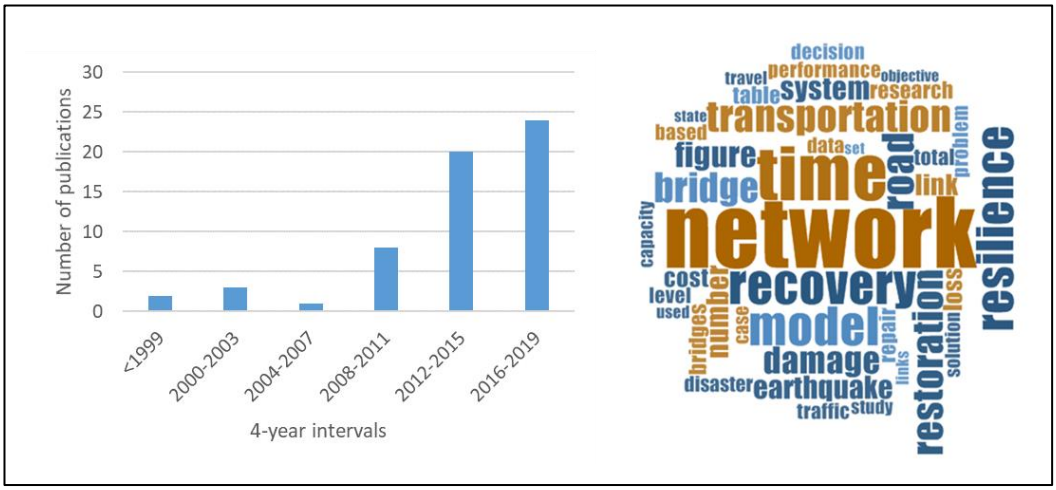

Figure 2.4. On the left, number of studies for each 4-year interval. On the right, word cloud that displays the 50 most frequent words of all selected publications. Produced using NVIVO software.

2.3. Road restoration modelling approaches

The aim of this section is to give a general overview of recovery models, understanding the different model purposes (problem types or potential outputs) and examine how models are mathematically formulated.

2.3.1. Classification based on model purpose and model uncertainty

Six types of problem were identified based on model purpose. Four of these problems aimed to find optimal solutions to the recovery problem: (1) Optimal repair scheduling problems, if the purpose of the model was to find the optimal start or end time for repairing each damaged asset; (2) Optimal repair sequence problems, if the model

focussed on finding the optimal priority list of repairs; (3) Optimal resource allocation problems, if the model sought to assign limited available resources to damaged locations in an optimal way; (4) Optimal routes to repair, if the model found optimal routes composed of different damaged assets that needed to be repaired by different repair teams. Some publications might be included in more than one category. The final types of identified problems did not necessarily involve trying to find an optimal solution: these were (5) those models that evaluated the performance and/or resilience of road networks and (6) those models that assessed the effectiveness of multiple repair strategies by using some network performance metrics.

Recovery models were also classified as *deterministic,* if non-random variables were included, or *stochastic,* if variable uncertainty was included. Variables such as recovery time, infrastructure damage, hazard intensity or link capacity may be unknown *a priori.* These uncertain variables were treated using Monte Carlo simulations, which generate random variables following a specified probability distribution. Table 2.2 differentiates between these two types of models and Table 2.3 identifies those random variables considered in stochastic models.

Table 2.2. Classification of publications based on problem type and approach.

	Problem type / Model purpose	Description	Deterministic approach	Stochastic approach
Optimisation-based	Optimal repair time scheduling	Find the starting or ending time for each repair	(Bocchini and Frangopol, 2012a, 2012b; Tuzun Aksu and Ozdamar, 2014; Unal, 2015; Li *et al.*, 2019)	(Zhang, Wang and Nicholson, 2017; W. Zhang *et al.*, 2018; Li *et al.*, 2019)
	Optimal repair sequence	Find the optimal list of repairs, so that repairs are made following the order of the list	(Sato and Ichii, 1995; Feng and Wang, 2003; Orabi *et al.*, 2009, 2010; Al-Rubaee, 2012; Lertworawanich, 2012; Bocchini, 2013; Vugrin, Turnquist and Brown, 2014; Karamlou and Bocchini, 2014, 2016; Ye and Ukkusuri, 2015; Nifuku, 2015; Lu *et al.*, 2016; Basavaraj *et al.*, 2017; Yamasaki and Miwa, 2017; Zamanifar and Seyedhoseyni, 2017; Vodák, Bíl and Křivánková, 2018; Li *et al.*, 2019)	(Furuta *et al.*, 2008; Barker, Ramirez-Marquez and Rocco, 2013; Baroud *et al.*, 2014; Li *et al.*, 2019)
	Optimal resource allocation	Assign available resources to damaged locations optimistically	(Sato and Ichii, 1995; Chen and Tzeng, 1999; Karlaftis, Kepaptsoglou and Lambropoulos, 2007; Orabi *et al.*, 2009, 2010; Ferreira, 2010; Duque and Sörensen, 2011; Bocchini and Frangopol, 2012b, 2012a; Tuzun Aksu and Ozdamar, 2014; Unal, 2015; Karamlou, Bocchini and Christou, 2016; Hackl, Adey and Lethanh, 2018; Kaviani *et al.*, 2018; Liao, Hu and Ko, 2018; Wu and Chen, 2019)	(Furuta *et al.*, 2008; Chang *et al.*, 2012; Chen and Miller-Hooks, 2012; Ozbay *et al.*, 2013; Faturechi and Miller-Hooks, 2014b; Zhang and Miller-Hooks, 2014; Zhang and Wang, 2016)
	Optimal routes to be chosen for repair	Identify and select routes of damaged assets to repair in an optimal way	(Mehlhorn, 2009; Vodák, Bíl and Křivánková, 2018)	(X. Zhang *et al.*, 2018)
Non-optimisation-based	Evaluate the performance and/or resilience of road networks	Assess the resilience of a transport network using performance metrics	(Stevanovic and Nadimpalli, 2010; Henry and Ramirez-Marquez, 2012; Nogal *et al.*, 2016; Twumasi-Boakye and J. O. Sobanjo, 2018; Kilanitis and Sextos, 2019; Twumasi-Boakye and Sobanjo, 2019; Vishnu, Kameshwar and Padgett, 2019)	-
	Evaluate different recovery scenarios	Evaluate a pre-set repair strategy based on some network performance metrics	(Chang, 2003; Zhang, Alipour and Coronel, 2018)	(Shinozuka *et al.*, 2003; Zhou, Banerjee and Shinozuka, 2010; Decò, Frangopol and Bocchini, 2013; Nifuku, 2015; Aydin *et al.*, 2018)

Table 2.3. Stochastic variables considered in stochastic models.

References \ Stochastic variables	Average daily traffic	Travel time	Recovery cost	Recovery time	Recovery speed	Restoration magnitude	Link capacity	Hazard intensity	Infrastructure damage	Component reliability	Component vulnerability	Target functionality	Idle time interval	Resource demand
(Shinozuka *et al.*, 2003)				✓										
(Furuta *et al.*, 2008)									✓				✓	
(Zhou, Banerjee and Shinozuka, 2010)				✓										
(Chang *et al.*, 2012)							✓	✓	✓					
(Chen and Miller-Hooks, 2012)							✓							
(Barker, Ramirez-Marquez and Rocco, 2013)				✓							✓			
(Decò, Frangopol and Bocchini, 2013)				✓			✓					✓	✓	
(Ozbay *et al.*, 2013)														✓
(Baroud *et al.*, 2014)				✓							✓			
(Faturechi and Miller-Hooks, 2014b)		✓					✓							
(Zhang and Miller-Hooks, 2014)		✓					✓							
(Nifuku, 2015)				✓					✓					
(Zhang and Wang, 2016)	✓		✓							✓				
(Zhang, Wang and Nicholson, 2017)	✓			✓										
(W. Zhang *et al.*, 2018)	✓			✓					✓	✓				
(X. Zhang *et al.*, 2018)					✓	✓	✓							
(Aydin *et al.*, 2018)				✓										
(Li *et al.*, 2019)				✓										

2.3.2. Classification based on mathematical modelling techniques

The methods used to solve the reviewed recovery models are identified in Table 2.4. Among these, exact methods (20% of all reviewed publications) and metaheuristic optimisation techniques (39% of all reviewed publications) were the most frequently used techniques. Analytical (or exact) methods are those techniques that are guaranteed to find an optimal solution at a high computational time. The algorithms have to solve strict mathematical formulations. As opposed to exact methods, numerical algorithms can find near optimal solutions at an acceptable computational cost. The main aim of these techniques is to find an optimal solution without searching the whole solution space (Sangaiah *et al.*, 2020). Numerical methods are further categorised into two types: heuristic algorithms and meta-heuristic algorithms. Among all reviewed publications that use metaheuristic algorithms, more than 75% use some sort of genetic algorithms. This is a metaheuristic search algorithm that, based on the evolutionary ideas of natural selection and genetics, selects the fittest individuals (solutions) for reproduction and produces their offspring for the next generation (Holland, 1975).

Exact, heuristic and metaheuristic optimisation problems are formulated using one or more mathematical functions (objectives) that need to be maximised or minimised. Table 2.5 compiles all objective functions identified in the reviewed work. If one publication used more than one objective function (multi-objective approach), it is included in more than one cell of Table 2.5. Some publications use generic terms such as *resilience* or *performance loss* as objective functions. In these cases, the variables that were used to measure these generic terms are included individually in the table, considering its maximisation or minimisation as appropriate. Note that some models include an optimisation to assign traffic to the road segments. This optimisation problem is not included in this section (see Section 2.5).

Simulation models are more problem-specific and are developed to evaluate the impact of a set of discrete decisions before implementing them in real life. This is usually justified by comparing the system performance before and after a disruptive event and during the recovery phase. Based on the results extracted from the simulation, transport authorities can make the most appropriate decision for each situation, not necessarily being the optimal one. About 20% of the reviewed

publications used this approach.

Table 2.4. Classification of publications based on solving method and technique

Solution method	Subtype	Solving technique/algorithm	Publication and year
Exact solution	(Mixed) integer programming	Branch and cut algorithm	(Tuzun Aksu and Ozdamar, 2014)
		Lagrangian relaxation	(Chang *et al.*, 2012)
		Branch and Bound method	(Kaviani *et al.*, 2018)
		Sequential quadratic programming	(Wu and Chen, 2019)
		Benders decomposition, column generation, and Monte Carlo simulation.	(Chen and Miller-Hooks, 2012)
		Progressive Hedging Algorithm	(Faturechi and Miller-Hooks, 2014b)
		Branch-and-cut decomposition and hybrid genetic algorithm	(Zhang and Miller-Hooks, 2014)
		P-Level Efficient Points (pLEP) algorithm	(Ozbay *et al.*, 2013)
		(I) (Implemented in General Algebraic Modelling System)	(Mehlhorn, 2009)
		(I) (solved by LINGO software)	(Feng and Wang, 2003)
		(I)	(Liao, Hu and Ko, 2018)
Heuristic optimisation	(I)	Greedy algorithm	(Lu *et al.*, 2016)
		Based on greedy algorithm(II)	(Basavaraj *et al.*, 2017)
	NP-Hard	(II)	(Yamasaki and Miwa, 2017)
Metaheuristic optimisation	(I)	Modified NSGA-II (MATLAB)	(Bocchini and Frangopol, 2012a) (Bocchini and Frangopol, 2012b)
		NSGA-II	(Orabi *et al.*, 2009, 2010; Unal, 2015)
		Genetic Algorithm	(Sato and Ichii, 1995; Furuta *et al.*, 2008; Bocchini, 2013; Karamlou and Bocchini, 2014; Li *et al.*, 2019)
		Simulated Annealing	(Vugrin, Turnquist and Brown, 2014)
		Algorithm with Multiple-Input Genetic Operators (AMIGO)	(Karamlou and Bocchini, 2016)
	NP-Hard	NSGA-II	(Zhang and Wang, 2016)
		Genetic Algorithm	(Karlaftis, Kepaptsoglou and Lambropoulos, 2007; W. Zhang *et al.*, 2018)
		Ant colony algorithm	(Vodák, Bíl and Křivánková, 2018)
		Weighted Sum Method + Genetic Algorithm	(Zhang, Wang and Nicholson, 2017)
		Fuzzy multi-objective Genetic Algorithm	(Chen and Tzeng, 1999)
	Dynamic programming	Particle swarm optimization	(Lertworawanich, 2012)
	Nonlinear integer programming	Tabu search	(Ye and Ukkusuri, 2015)
		GRASP and VND algorithm	(Duque and Sörensen, 2011)
Simulation models	(I)	(Chang, 2003; Shinozuka *et al.*, 2003; Zhou, Banerjee and Shinozuka, 2010; Stevanovic and Nadimpalli, 2010; Henry and Ramirez-Marquez, 2012; Decò, Frangopol and Bocchini, 2013; Nogal *et al.*, 2016; Zhang, Alipour and Coronel, 2018; Twumasi-Boakye and J. O. Sobanjo, 2018; Kilanitis and Sextos, 2019; Twumasi-Boakye and Sobanjo, 2019; Vishnu, Kameshwar and Padgett, 2019)	
Others	(I)	(I)	(Ferreira, 2010; Basavaraj *et al.*, 2017)
		Fuzzy VIKOR method (ranking method)	(Zamanifar and Seyedhoseyni, 2017)
		Copeland Score (CS)	(Barker, Ramirez-Marquez and Rocco, 2013; Baroud *et al.*, 2014)
		Analytic Hierarchy Process (AHP)	(Al-Rubaee, 2012; Nifuku, 2015)

(I) Not specified
(II) Authors implement their own algorithm

Table 2.5. Classification of studies based on the objectives used in the optimisation

	MAX / MIN	Objective	References
Connectivity	MAX	Number of independent pathways between locations	(Zhang and Wang, 2016)
	MIN	Time to connect critical locations	(Bocchini, 2013; Karamlou and Bocchini, 2014; Vodák, Bíl and Křivánková, 2018)
	MAX	Number of connected nodes	(Karamlou and Bocchini, 2016)
	MAX	Connectivity between nodes	(Yamasaki and Miwa, 2017; Liao, Hu and Ko, 2018)
	MIN	Indirect cost due to loss of connectivity	(Hackl, Adey and Lethanh, 2018)
Accessibility	MAX	Total length of accessible roads	(Feng and Wang, 2003)
	MAX	Total weighted earliness of all cleared paths	(Tuzun Aksu and Ozdamar, 2014)
	MIN	Weighted sum of the time to travel from each node to its closest regional centre	(Duque and Sörensen, 2011)
Travel time	MIN	Travel time expenditure	(Sato and Ichii, 1995; Chen and Tzeng, 1999; Bocchini and Frangopol, 2012a, 2012b; Bocchini, 2013; Ozbay *et al.*, 2013; Vugrin, Turnquist and Brown, 2014; Karamlou and Bocchini, 2014, 2016; Lu *et al.*, 2016; Basavaraj *et al.*, 2017)
	MIN	Additional travel time throughout the recovery duration	(Orabi *et al.*, 2009)
	MIN	Indirect cost due to temporal prolongation of travel	(Hackl, Adey and Lethanh, 2018)
	MAX	Travel time resilience	(Kaviani *et al.*, 2018)
	MAX	Ratio between travel time before and after the disrupted event	(Faturechi and Miller-Hooks, 2014b; Ye and Ukkusuri, 2015)
	MIN	Travel delay in areas of higher social vulnerability	(Unal, 2015)
	MIN	Indirect losses due to delays	(Unal, 2015)
Travel distance	MIN	Total travel distance	(Bocchini and Frangopol, 2012a, 2012b; Bocchini, 2013; Karamlou and Bocchini, 2014, 2016)
	MIN	Indirect losses due to increased travel distance	(Unal, 2015)
Flow/Capacity	MIN	Travel demand loss	(Chen and Miller-Hooks, 2012; Lertworawanich, 2012; Vugrin, Turnquist and Brown, 2014; Li *et al.*, 2019)
	MAX	Total flow to destination nodes	(Chang *et al.*, 2012; Zhang and Miller-Hooks, 2014)
	MAX	Demand satisfaction resilience	(Kaviani *et al.*, 2018)
	MAX	Number of lanes open to traffic	(Karamlou, Bocchini and Christou, 2016)
Repair costs	MIN	Reconstruction costs	(Karlaftis, Kepaptsoglou and Lambropoulos, 2007; Orabi *et al.*, 2009, 2010; Bocchini and Frangopol, 2012a, 2012b; Unal, 2015; Hackl, Adey and Lethanh, 2018; X. Zhang *et al.*, 2018)
	MIN	Reconstruction time	(Chen and Tzeng, 1999; Vodák, Bíl and Křivánková, 2018)
	MIN	Retrofit costs	(Chang *et al.*, 2012; Karamlou, Bocchini and Christou, 2016; Zhang and Wang, 2016)
	MIN	Total response cost	(Ferreira, 2010)
	MIN	Number of crews working in unit time	(Unal, 2015)
Repairs	MAX	Ratio of restored links to damaged links	(Furuta *et al.*, 2008)
	MIN	Idle time between repair teams	(Chen and Tzeng, 1999)
Benefits after repairs	MAX	Economic benefits of restoring a path	(Mehlhorn, 2009)
	MAX	Total condition improvements after repairs	(Karlaftis, Kepaptsoglou and Lambropoulos, 2007)
Human risk	MAX	Total number of life savings	(Feng and Wang, 2003)
	MIN	Risk of rescuers	(Feng and Wang, 2003)
	MIN	Total rescue time	(Wu and Chen, 2019)
Completion time	MIN	Time to reach a target functionality level	(Bocchini and Frangopol, 2012b; Unal, 2015)
	MIN	Time to full network service resilience	(Orabi *et al.*, 2010; Barker, Ramirez-Marquez and Rocco, 2013; Baroud *et al.*, 2014)
	MIN	Total recovery time	(Zhang, Wang and Nicholson, 2017; W. Zhang *et al.*, 2018)
	MIN	Skew of recovery trajectory (time units)	(Zhang, Wang and Nicholson, 2017; W. Zhang *et al.*, 2018)
No objective function			(Chang, 2003; Shinozuka *et al.*, 2003; Zhou, Banerjee and Shinozuka, 2010; Stevanovic and Nadimpalli, 2010; Al-Rubaee, 2012; Henry and Ramirez-Marquez, 2012; Decò, Frangopol and Bocchini, 2013; Nifuku, 2015; Nogal *et al.*, 2016; Zamanifar and Seyedhoseyni, 2017; Aydin *et al.*, 2018; Twumasi-Boakye and J. O. Sobanjo, 2018; Zhang, Alipour and Coronel, 2018; Twumasi-Boakye and Sobanjo, 2019; Vishnu, Kameshwar and Padgett, 2019; Kilanitis and Sextos, 2019)

2.4. Modelling vulnerability

This section reviews the approach taken by reviewed recovery models to simulate the location and extent of damage. It also describes how road damage is transformed numerically into a reduction of road capacity in these models.

2.4.1. Single vs. multi-hazard

Most of the reviewed recovery models only analyse the impact of single hazards on road infrastructure and these are treated as isolated and independent phenomena. The majority of these models treat these hazards as punctual reductions of road capacities on the day of the impact. In these cases repairs can start immediately after the incident. Other models consider hazards as a continuous impact for a certain amount of time. In such situations, the reduction of road capacity is maintained for a period of time until the perturbation is ended. As an example, Nogal *et al.* (2016) reduced the capacity of some road segments to 50% as a result of a road maintenance that lasted 15 days.

Regarding the type of hazard, more than half of the publications study the impact of earthquakes, whereas only 10% of the models consider the impact of floods and 6% of the models the impact of terrorist attacks. The rest of the publications try to develop generic models which do not focus on a specific type of hazard. Table 2.6 classifies each publication based on the type of hazard.

Only two publications have tried to incorporate the impact of multiple hazards on road infrastructure. Basavaraj *et al.* (2017) considered the susceptibility of nodes to different hazards simultaneously (concurrent multi-hazard events). However, their model was implemented as a single-hazard model and the only implication was that repair resource requirements for each node were different depending on the type of hazard considered. Yamasaki and Miwa (2017) initially tried to consider the effect of cascading hazards on the network. They considered that some links failed during the main shock of an earthquake event, while others failed in the aftershock. The model took into consideration these potential cascading link failures in their formulation. None of the other publications incorporate the effect of multi-hazard events within road restoration models. A single hazard approach is considered to be a good starting point to understand how individual or independent hazards affect road networks, but not enough to capture all interactions that multiple hazards may have. As Gill and

Malamud (2016) mentioned, single hazard approaches could potentially underestimate risk, distort management priorities or increase vulnerability to other ignored hazards. Therefore, further research needs to be done in this area in order to consider multi-hazard approaches in road recovery models.

2.4.2. The hazard-infrastructure damage relationship

The focus of this section is to understand how current recovery models have simulated the damage to infrastructure and the extent of that damage. Three major types of road infrastructure (links) are studied: general, bridges and road sections. Five categorical ways of classifying the extent of damage were identified: (1) bi-level damage classification in which road infrastructure is classified as damaged or undamaged states. See for example: (Henry and Ramirez-Marquez, 2012; Lertworawanich, 2012; Baroud *et al.*, 2014; Tuzun Aksu and Ozdamar, 2014; Vugrin, Turnquist and Brown, 2014; Nogal *et al.*, 2016; Basavaraj *et al.*, 2017; Yamasaki and Miwa, 2017); (2) tri-level damage classification, considering undamaged, damaged and collapse states (Lu *et al.*, 2016); (3) four-level damage classification, using undamaged, small damage, moderate damage and large damage (Furuta *et al.*, 2008); (4) HAZUS (FEMA, 2013) damage categories, which identify five damage states: undamaged, slight, moderate, extreme and complete damage (Mehlhorn, 2009; Orabi *et al.*, 2009, 2010; Al-Rubaee, 2012; Bocchini, 2013; Karamlou and Bocchini, 2014; Zhang, Wang and Nicholson, 2017); and for the particular case of bridges: (5) BRIME (Godart and Vassie, 2001) damage categories, which identify five classes of bridge deterioration (from class I to class V) (Karlaftis, Kepaptsoglou and Lambropoulos, 2007).

Four major approaches were identified to assign damage to road infrastructure: damage can be assigned (1) based on historical data or surveys; (2) based on hypothetical events; (3) based on fragility curves; and (4) based on a known probability distribution. A classification of the reviewed publications based on these four methods is provided in Table 2.6.

Table 2.6. Classification of publications based on hazard and damage modelling approach

Hazard types			Damage modelling approaches: Deterministic approach – Based on historical data / surveys, tests, etc.	Damage modelling approaches: Deterministic approach – Hypothetical damage	Damage modelling approaches: Stochastic approach – Based on fragility curves	Damage modelling approaches: Stochastic approach – Based on a known probability distribution of damages
Natural hazards		Earthquake	(Sato and Ichii, 1995; Feng and Wang, 2003; Bocchini and Frangopol, 2012b)	(Chen and Tzeng, 1999; Karlaftis, Kepaptsoglou and Lambropoulos, 2007; Furuta *et al.*, 2008; Mehlhorn, 2009; Orabi *et al.*, 2009, 2010; Karamlou and Bocchini, 2014; Yamasaki and Miwa, 2017; Li *et al.*, 2019)	(Shinozuka *et al.*, 2003; Zhou, Banerjee and Shinozuka, 2010; Stevanovic and Nadimpalli, 2010; Chang *et al.*, 2012; Decò, Frangopol and Bocchini, 2013; Nifuku, 2015; Unal, 2015; Karamlou and Bocchini, 2016; Karamlou, Bocchini and Christou, 2016; Zhang, Alipour and Coronel, 2018; Wu and Chen, 2019; Kilanitis and Sextos, 2019; Vishnu, Kameshwar and Padgett, 2019)	(Chen and Miller-Hooks, 2012; Bocchini, 2013; Faturechi and Miller-Hooks, 2014b; Zhang and Miller-Hooks, 2014; Zhang and Wang, 2016; Zhang, Wang and Nicholson, 2017; W. Zhang *et al.*, 2018)
		Flood	-	(Lertworawanich, 2012; Liao, Hu and Ko, 2018)	(Hackl, Adey and Lethanh, 2018)	(Chen and Miller-Hooks, 2012; Faturechi and Miller-Hooks, 2014b; Zhang and Miller-Hooks, 2014)
		Landslide	(Aydin *et al.*, 2018)	-	-	-
		Hurricanes	(Twumasi-Boakye and J. O. Sobanjo, 2018)	-	-	-
		No specified	(Bocchini and Frangopol, 2012a)	(Kaviani *et al.*, 2018)	-	(Basavaraj *et al.*, 2017)
	Human-made hazards	Terrorist attack	-	(Liao, Hu and Ko, 2018)	-	(Chen and Miller-Hooks, 2012; Faturechi and Miller-Hooks, 2014b; Zhang and Miller-Hooks, 2014)
No specified hazard			(Ferreira, 2010; Duque and Sörensen, 2011; Al-Rubaee, 2012; Ozbay *et al.*, 2013; Twumasi-Boakye and Sobanjo, 2019)	(Henry and Ramirez-Marquez, 2012; Baroud *et al.*, 2014; Tuzun Aksu and Ozdamar, 2014; Vugrin, Turnquist and Brown, 2014; Ye and Ukkusuri, 2015; Lu *et al.*, 2016; Nogal *et al.*, 2016; Vodák, Bíl and Křivánková, 2018)	-	(Barker, Ramirez-Marquez and Rocco, 2013; X. Zhang *et al.*, 2018)

The first and second approach consists of assigning damage to infrastructure deterministically. The first method identifies what infrastructure is damaged based on real data (e.g. historical data from previous events, surveys, inspections, field tests, etc.). For instance, Sato and Ichii (1995) optimised the restoration process of a road network in Japan damaged by the 1978 Off Izu-Oshima earthquake. The second method assigns damage to infrastructure according to the modellers' criteria and based on hypothetical hazardous events.

In contrast, the third and fourth approaches relate damage to hazard probabilistically, including those uncertainties involved in the damage process. For instance, two equal roads affected by the same hazard with the same intensity suffer differently due to other ignored factors, such as the construction or maintenance history.

In particular, the third method uses fragility functions (or fragility curves when expressed graphically) to determine whether infrastructure components are damaged or not and to what extent. Fragility curves express the probability of exceeding or attaining a certain level of damage, for a given value of hazard intensity. A graphical example of a generic fragility curve for each damage state is shown in Figure 2.5. Given a certain value of hazard intensity, the probability of having a certain level of damage is shown. The sum of all probabilities of all damage states for a given hazard intensity is equal to 1. This creates a spectrum of damages in which each damage state has a specific range of values. The shorter this range of values is, the lower the probability of being in that damage state will be. This probabilistic information can be used to identify which roads have more chance of being in a damaged state. Two different methods have been identified to assign damage using this probabilistic data: (a) range-based method and (b) risk-based method. Firstly, the most commonly used method for assigning damage to infrastructure is the range-based method (Chang, 2003; Shinozuka *et al.*, 2003; Zhou, Banerjee and Shinozuka, 2010; Chang *et al.*, 2012; Karamlou, Bocchini and Christou, 2016) and it consists on generating, using Monte Carlo simulation, a uniform-distribution random value (RV) between 0 and 1 for each damaged asset. This value falls to one of the ranges of damage states mentioned before and shown in Figure 2.5. The damage level of this asset corresponds to the damage state of that range. Secondly, Bocchini and Frangopol (2011) proposed a risk-based method to determine the damage state of each asset

without the need to generate random values. This method calculated the level of damage as a continuous value based on the concept of risk which is defined as a composite of the probability of being in a damage state and the consequences of that damage level. The authors quantified the consequences of each damage state as an integer value that varies from 0 (no damage) to 4 (collapse), using a five-level damage classification. As shown in Equation (2.1), given a certain hazard intensity, the damage level was obtained as a product of probabilities and consequences of each damage state. Then this numerical value was categorised into one of the five damage states by identifying in which range of damage levels the continuous value was included.

$$Damage\ level = 0 \cdot P(no\ damage) + 1 \cdot P(minor\ damage) + 2 \cdot P(moderate\ damage) + 3 \cdot P(extreme\ damage) + 4 \cdot P(collapse) \quad (2.1)$$

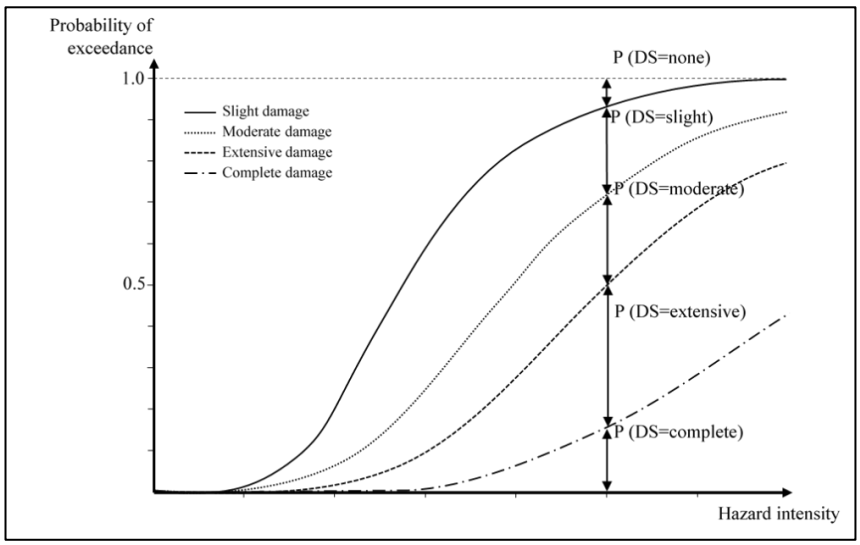

Figure 2.5. Fragility curves for five levels of damage. It shows probability (P) of being in a damage state (DS) given a value of hazard intensity.

Although this third major approach can be considered as a very straightforward way of assigning damage to infrastructure, the main difficulty falls on the development of fragility curves for each type of hazard-infrastructure relationship. Fragility curves can be obtained based on expert opinions, empirically if enough data

from past events are available (Shinozuka *et al.*, 2003; Zhou, Banerjee and Shinozuka, 2010; Nifuku, 2015) or analytically (Chang *et al.*, 2012). Other authors (Stevanovic and Nadimpalli, 2010; Unal, 2015; Karamlou and Bocchini, 2016) obtained data from a combination of analytical and expert-opinion models that were available in software packages developed in the United States, such as HAZUS-MH (FEMA, 2013) and REDARS (ImageCat, 2005). HAZUS-MH (HAZard United States - Multiple Hazard) is a software that estimates damage and losses to essential facilities after natural disasters (FEMA, 2013). REDARS software (Risk from Earthquake DAmage to Roadway Systems) also estimates damage but just to transportation components after earthquakes. This third approach is mostly limited to those publications that model the recovery of road networks under seismic conditions.

The fourth method uses Monte Carlo simulation to assign damage to infrastructure in a probabilistic approach. The main difference compared to the previous one is the non-use of fragility functions. Although this method might be considered a special case of the second approach as the authors are assuming 'hypothetically' that link failures follow a certain probabilistic distribution, it is preferred to separate both approaches due to the probabilistic nature of this last method. It consists on generating random variables with a given probability distribution to simulate random behaviours. Every time random values are generated, a possible network state or scenario is created. Basavaraj *et al.* (2017) assumed that the number of unavailable links in a network followed a binomial distribution whose parameters were the total number of links and the probability of link failure. Every time a random value which followed the binomial distribution was generated, a certain number of links were classified as unavailable. After a large number of samplings, the generated values of unavailable links covered all spectrum of possibilities. Similarly, Zhang and Miller-Hooks (2014) assumed that the number of damaged links followed a binomial distribution with a certain probability across the network.

2.4.3. Infrastructure damage and functionality relationship

This section describes how road damage is transformed numerically into a reduction of network functionality. This is measured as a capacity reduction of those damaged road segments. Two approaches to assign new values of capacity based on their

damage level are identified in the literature: (1) a deterministic-based approach, in which the reduction of road capacity is determined by a fixed value that depends on the damage level; and (2) a stochastic-based approach, in which a variability in the remaining road capacity exists.

Deterministic values of road capacity from different reviewed publications based on each damage state of links is synthesised in Table 2.7. According to Chang *et al.* (2010), there are three ways of developing damage-functionality relationships: empirical, analytical and expert opinion-based. As the reader can notice from the Table 2.7, expert opinion-based methods are the most widely used. Some models considered the functionality of links as a binary variable (opened or closed). Others also included the possibility of being partially opened. Some authors may appear more than once in Table 2.7 as they have also tried to perform a sensitivity analysis of link capacities by exploring different damage-capacity loss relationships. However, as Shinozuka *et al.* (2003) mentioned, most of these values are hypothetical and further research is needed to validate them. On the other hand, some other publications did not consider reductions in road capacity because they did not measure changes in traffic conditions.

Regarding the stochastic-based approach, some authors argued that road capacity should be considered as a stochastic variable due to the uncertainty associated with the hazard impact and the subsequent road damage. In this sense, link capacities could be treated as random variables with a known probability distribution. By generating random values of this distribution using Monte Carlo simulation, new remaining capacities were created for each damaged link. For instance, Chen and Miller-Hooks (Chen and Miller-Hooks, 2012), Zhang and Miller-Hooks (2014) and Zhang *et al.* (2018) assumed that the capacity reduction of each damaged link followed a uniform distribution on the interval from 0 to the link's original capacity.

Table 2.7. Classification of publications based on hazard and damage modelling approach

References	Based on:**		Affected infrastructure	Damage state (based on HAZUS damage classification (FEMA, 2013))				
				No damage	Minor damage	Moderate damage	Extensive damage	Complete damage
(Shinozuka *et al.*, 2003)		-	Bridges	100%	100%	75%	50%	50%*
(Zhou, Banerjee and Shinozuka, 2010; Nifuku, 2015)	EO	(Shinozuka *et al.*, 2003)	Bridges	100%	100%	75%	50%	0%
(Stevanovic and Nadimpalli, 2010)	EO	(Shinozuka *et al.*, 2003)	Bridges	100%	100%	50%	25%	25%*
(Zhou, Banerjee and Shinozuka, 2010; Nifuku, 2015)	EO	(Shinozuka *et al.*, 2005)	Bridges	100%	100%	50%	0%	
(Karamlou and Bocchini, 2016)	EM	(Applied Technology Council, 1985)	Bridges	100%	100%	25%	10%	10%*
(Zhou, Banerjee and Shinozuka, 2010; Nifuku, 2015)	EO	(Shinozuka *et al.*, 2005)	Bridges	100%	100%	25%	0%	0%
(Zhang, Alipour and Coronel, 2018)		-	Bridges	100%		50%		0%
(Nogal *et al.*, 2016; Li *et al.*, 2019)		-	Links	100%	50%		0%	
(Bocchini and Frangopol, 2012a, 2012b; Bocchini, 2013; Karamlou and Bocchini, 2014; Unal, 2015)	EO	(Bocchini and Frangopol, 2012a)	Bridges	100%		50%		
(Chang *et al.*, 2012; Karamlou, Bocchini and Christou, 2016; Hackl, Adey and Lethanh, 2018; Twumasi-Boakye and J. O. Sobanjo, 2018; Twumasi-Boakye and Sobanjo, 2019; Vishnu, Kameshwar and Padgett, 2019)	EO	(Padgett and DesRoches, 2007)						
(Lu *et al.*, 2016)	AN	(Sullivan *et al.*, 2010)	Links	100%		15-20%		0%
(Chen and Tzeng, 1999; Feng and Wang, 2003; Henry and Ramirez-Marquez, 2012; Baroud *et al.*, 2014; Tuzun Aksu and Ozdamar, 2014; Vugrin, Turnquist and Brown, 2014; Ye and Ukkusuri, 2015; Basavaraj *et al.*, 2017; Yamasaki and Miwa, 2017)		-	Links	100%		0%		
(Lertworawanich, 2012)		-	Roadways	100%		0%		
(Chang, 2003; Kilanitis and Sextos, 2019; Wu and Chen, 2019)		-	Bridges	100%		0%		
(Kaviani *et al.*, 2018; Liao, Hu and Ko, 2018)		-	***					
(Sato and Ichii, 1995; Karlaftis, Kepaptsoglou and Lambropoulos, 2007; Furuta *et al.*, 2008; Mehlhorn, 2009; Orabi *et al.*, 2009, 2010; Ferreira, 2010; Duque and Sörensen, 2011; Al-Rubaee, 2012; Ozbay *et al.*, 2013; Decò, Frangopol and Bocchini, 2013; Zamanifar and Seyedhoseyni, 2017; Aydin *et al.*, 2018; Vodák, Bíl and Křivánková, 2018)		-	Not mentioned / Not specified					

* Secondary local detour routes are considered. Then, a residual flow capacity is provided
** EO: Expert Opinion; EM: Empirical; AN: Analytical
*** Several link capacity reductions are applied

2.5. Travel demand and traffic analysis

Hazardous events not only impact physical road infrastructure but also drivers' behaviour. Traffic modelling becomes essential to understand behavioural changes after the impact of disruptive events. However, only those models that uses flow-based metrics (such as delay, traffic flow, travel time expenditure, etc.) are the ones that need to model the response of network users (i.e. system operation). This section aims to understand how traffic behaviour is modelled in reviewed publications.

Three different areas of traffic modelling may be affected by hazard impacts: (1) travel demand, which means that some drivers might decide to suppress or re-schedule their trips, redistribute them to other locations or change transport mode; (2) traffic assignment, which deals with route choices after changes in the physical road network; and (3) traffic operation, which means that drivers adapt their driving behaviour to changes on the road network (e.g. speed reduction). Impacts on traffic operation has received less attention among researchers. Shinozuka *et al.* (2003) proposed some hypothetical reductions of free-flow speed on partially-damaged links. However, most publications just assumed that free-flow speed does not change. The following sections describe in more detail the first and second areas of traffic modelling.

2.5.1. Impact on travel demand

After a hazard impact, some activities may not be available at the destination forcing drivers to supress or reallocate the trip to other places, re-schedule activities or switch to other transport modes. The majority of reviewed publications do not consider changes in travel demand. The lack of empirical travel demand data after hazard events makes the modelling of travel demand more difficult (Chang, 2003; Karamlou, Bocchini and Christou, 2016). After major disruptive events, some travellers might prefer much closer destinations, covering shorter distances and to spend less time travelling, which may appear an improvement in the system performance (Bocchini and Frangopol, 2012b). Therefore, in order to compute an unbiased metric of network performance and due to lack of empirical travel demand data, reviewed traffic models assume that travel demand remains constant before and after hazard impacts.

Nevertheless, only the work done by Zhou, Banerjee and Shinozuka (2010) captured changes in travel demand. They proposed a decreasing linear relationship,

originally developed by Shinozuka *et al.* (2005), between trip reduction rate and the length of time after a disruptive event. Immediately after the seismic impact, a maximum change in travel demand was produced, and travel demand gradually recovered as restoration continued over time.

2.5.2. Modelling traffic routing

Traditionally, traffic assignment problems are classified as: (1) *Dynamic*, if traffic demand varies with time, or *static* if there is no variation in time; (2) *User equilibrium* based or *system optimal* based models. The former defines a model whose travellers choose the routes that minimise their individual cost. In this sense, traffic flows are in equilibrium when no driver can improve his/her travel cost by shifting to other routes (Wardrop, 1952). The latter defines a model in which travellers choose the routes that minimise the total travel cost of the entire system, instead of their own travel cost.

Table 2.8 classifies the reviewed recovery models based on whether they use static or dynamic assignment and user equilibrium or system optimal. Most of the publications model traffic assignment under the assumption of static user equilibrium. These models assume that drivers are initially in an equilibrium state and, after the impact of a disruptive event, the system reaches a new equilibrium state with higher total travel cost due to the full/partial closure of some road segments. However, the reality is that equilibrium conditions cannot be reached immediately after the impact as drivers need time to get/receive information and adapt their travel behaviour to the disrupted network before reaching a new equilibrium state. In this case, shortly after the disruptive event, drivers do not have perfect knowledge of traffic conditions, which means that they cannot select the route with their minimal travel cost on a congested network. They cannot anticipate how other drivers will behave and therefore equilibrium conditions may not be reached immediately after the impact. Unless external travel information is provided via social media or navigation systems, drivers only know the travel costs on routes from previous travel experiences. What is more, under a dynamic assignment, not all drivers start their journey at the same time which means that there is variation in demand over the studied period and therefore drivers cannot know all traffic conditions on all routes under these circumstances. Faturechi and Miller-Hooks (2014b) admitted that this assumption

could be accepted only if there was enough time between network changes (e.g. road repairs) so that drivers were completely aware of new network conditions. However, it was not clearly defined how much time was considered as *enough*. To the best of the author's knowledge, this equilibrium-based assumption cannot be ensured after a hazard impact.

The concept of Partial (or Restricted) User Equilibrium (PUE) was introduced in the literature in order to avoid making the assumption that equilibrium conditions are reached in the aftermath of the impact. Faturechi and Miller-Hooks (2014b) used the concept of PUE developed by Sumalee and Watling (2008) which assumed that only drivers on affected paths might consider rerouting and the others remained in the same routes. Nogal *et al.* (2016) used the concept of Restricted User Equilibrium (RUE) in which a system impedance was introduced in the model to reflect the lack of knowledge of the new situation that drivers have and the lack of information of the behaviour of other drivers. In other words, this impedance is due to the capacity of adaptation of drivers to network changes. The global behaviour of users was analysed in a day-to-day basis. This impedance limited the variation of route flows between two consecutive time intervals (days). This meant that the quantity of flow that could be transferred from one link to another was limited between days. Thus, the model did not reach equilibrium conditions immediately after the perturbation and some time was needed to reach again equilibrium conditions. It was based on a macroscopic traffic model that simulated the dynamic response of the network after a disruption. Note that the model is included in Table 2.8 in the area of static assignment as the OD demand was assumed to be constant and departure time choice was not considered.

The level of information available to drivers in the aftermath of an incident plays an important role assisting drivers in making travel decisions. However, the reality is that not all drivers have the same level of information available to them and this makes modelling the aftermath of an incident more difficult. Intelligent Transport Systems (ITS) bring information technology and telecommunications together, in order to monitor traffic, identify incidents and inform drivers as quickly as possible of any disruption on the network. In this sense, providing some (or all) drivers with information about network conditions (closed links, travel times, congestion, etc.)

could help them making more informed travel decisions, which could (or not) reduce overall network expenditure (total veh-mins). In any case, it is difficult to anticipate exactly how drivers will respond to information of traffic conditions and therefore user equilibrium is not likely to be achieved. To the best of the author's knowledge, the provision of external travel information and its impact on drivers' decisions after disruptive events has not been considered on current recovery models. The assumption of 'perfect knowledge' can no longer be accepted and the network might not reach equilibrium conditions immediately after the disruption due to the existence of different levels of travel information.

Table 2.8. Classification of reviewed publications in terms of traffic assignment

	User equilibrium	Restricted/partial user equilibrium	System optimal
Static traffic assignment	(Chen and Tzeng, 1999; Shinozuka *et al.*, 2003; Chang, 2003; Orabi *et al.*, 2009; Zhou, Banerjee and Shinozuka, 2010; Bocchini and Frangopol, 2012b, 2012a; Lertworawanich, 2012; Bocchini, 2013; Vugrin, Turnquist and Brown, 2014; Karamlou and Bocchini, 2014, 2016; Nifuku, 2015; Unal, 2015; Ye and Ukkusuri, 2015; Lu *et al.*, 2016; Twumasi-Boakye and J. O. Sobanjo, 2018; Hackl, Adey and Lethanh, 2018; Kaviani *et al.*, 2018; Li *et al.*, 2019; Twumasi-Boakye and Sobanjo, 2019; Vishnu, Kameshwar and Padgett, 2019)	(Faturechi and Miller-Hooks, 2014b; Nogal *et al.*, 2016)	-
Dynamic traffic assignment	(Stevanovic and Nadimpalli, 2010; Zhang, Alipour and Coronel, 2018; Kilanitis and Sextos, 2019)	-	-
No traffic assignment	(Sato and Ichii, 1995; Feng and Wang, 2003; Karlaftis, Kepaptsoglou and Lambropoulos, 2007; Furuta *et al.*, 2008; Mehlhorn, 2009; Ferreira, 2010; Orabi *et al.*, 2010; Duque and Sörensen, 2011; Al-Rubaee, 2012; Henry and Ramirez-Marquez, 2012; Chang *et al.*, 2012; Chen and Miller-Hooks, 2012; Barker, Ramirez-Marquez and Rocco, 2013; Decò, Frangopol and Bocchini, 2013; Tuzun Aksu and Ozdamar, 2014; Zhang and Miller-Hooks, 2014; Baroud *et al.*, 2014; Karamlou, Bocchini and Christou, 2016; Zhang and Wang, 2016; Yamasaki and Miwa, 2017; Zamanifar and Seyedhoseyni, 2017; Zhang, Wang and Nicholson, 2017; Basavaraj *et al.*, 2017; Aydin *et al.*, 2018; Liao, Hu and Ko, 2018; Vodák, Bíl and Křivánková, 2018; W. Zhang *et al.*, 2018; X. Zhang *et al.*, 2018; Wu and Chen, 2019)		

NOTE: (Ozbay *et al.*, 2013) do not mention type of assignment, but they use a traffic simulation software whose name is not mentioned.

2.6. Infrastructure repair modelling

This section reviews the modelling process of how damaged infrastructure is physically repaired. Two types of recovery models are identified based on the repair

modelling process: (1) Those models that simulate how physical resources are allocated to damaged locations and consume time to undertake repair tasks (Resource-Task-Time relationship); (2) Those models that do not model the entire repair process and only select and prioritise repairs considering the benefits or impacts of getting damaged infrastructure back to normal.

The first group of models simulates the repair process by allocating resources to damaged locations. Traditionally, these resource are classified as personnel, plant and equipment. Recovery models group these resources in teams. For instance, Feng and Wang (2003) grouped resources in work-troops which included, in the context of that paper, machines, vehicles and manpower and then the whole work-troop attended a damaged location. These locations could be repaired by a single repair team or more than one. Henry and Ramirez-Marquez (2012) assumed that only one repair teams could attend an incident, while other models such as the one presented by Sato and Ichii (1995) considered that more than one team could attend the same incident and therefore speed up the repair process. There may also be some limitations in terms of availability of resources. Zhang, Wang and Nicholson (2017) limited the number of available teams that could work at the same time. This leads to the concept of *sequential* or *simultaneous* repairs. If there is just one available team to attend all incidents, damaged infrastructure needs to be repaired in a sequential way (e.g. Lertworawanich (2012) and Henry and Ramirez-Marquez (2012), among others). If there is more than one available team, these can attend more than one incident at the same time and therefore, repair damaged infrastructure in a sequential and simultaneous way (e.g. Orabi *et al.* (Orabi *et al.*, 2009), Karamlou and Bocchini (2014), Vugrin, Turnquist and Brown (2014), among others).

Resources need to undertake tasks to repair damaged assets. It can be a single task that represents the entire repair process or a series of connected tasks (Vugrin, Turnquist and Brown, 2014). The complexity of the problem is increased if different types of resources are required for each task. In turn, these tasks consume time that depends on the number of resources that undertake each task. The following Section 2.6.1 reviews how current models obtain the time required to repair damaged assets.

The second group of models do not obtain the time required to repair each damaged infrastructure. Instead, these models considered the benefits or impacts of getting damaged infrastructure back to normal (e.g. if bridge A, instead of bridge B, was repaired to its pre-disrupted condition, a higher network performance would be achieved). Karlaftis *et al.* (2007) allocated limited repair funding to some damaged bridges affected by a seismic event, maximising the total condition improvements after repairs and minimising reconstruction costs. If a bridge was selected to be partially or totally repaired, repairs were represented as an improvement in its damage condition and as an associated repair cost. Other bridges might also be selected and they would have other improvements and other costs. The final repair strategy was the one that maximised the condition and minimised costs. Therefore, there was not a time-dependent variable (e.g. repair time) involved in the process. Lertworawanich (2012) calculated the sequential list of repairs that minimised travel demand loss and network travel time. In this case, links were restored according to their relative importance. If a link carried the highest OD demand loss and its failure produced a considerable increase in travel time, it was clear that this link would be the first in the repair sequence. As observed, repairs do not use any time-dependent variable and thus, these are only based on the impact or consequences of repairs on the network performance. Similarly, Al-Rubaee (2012) proposed a road recovery priority model based on a similar Analytic Hierarchy Process (AHP) (Saaty, 1980) approach. It obtained a priority list of links that should be repaired based on several criteria, such as traffic, damage and financial factors, among others. Repairs, therefore, were only obtained based on the evaluation of these factors for each damaged link. Additionally, as repair time is not considered, these models do not give a total traffic delay cost, which is considered as an important variable to measure the performance of the system after a disruptive event. Also, in general, these models assume that repairs do not take place in parallel, which reflects how inaccurate this type of models could be.

2.6.1. Approaches to repair time modelling

This sub-section reviews different approaches of obtaining repair time in the literature. Three similar approaches are identified: (1) Repair time as a direct measure for damaged infrastructure; (2) Productivity of repair resources; or (3) The number

of repair steps.

The first approach consists on assuming that each damaged asset needs certain amount of time to be completely repaired. Repair time that is assigned to each location depends on the damage level. It can be obtained deterministically as follows: (1) Based on hypothetical repair times for each asset; (2) Using databases from the REDARS/HAZUS software (ImageCat, 2005) package that contains repair times of damaged transportation components under earthquake scenarios; or (3) Using expert opinion or previous real data from similar repairs. A classification of the reviewed models based on these three approaches is summarised in Table 2.9. Some authors also considered the uncertainty associated with the repair process (e.g. not finishing on time due to weather conditions, lack of personnel or plants, etc.) and suggested that repair time should be considered as a stochastic variable with a known probability distribution.

The second approach introduces the concept of resource, which has a fixed work pace that can be measured as "quantity of repair work per hour". If a damaged asset is measured in units of "quantity of work" or "amount of damage" and the work pace of each repair resource is known, then the time required to repair this infrastructure can be calculated by doing simple arithmetical calculations. Although this second approach can be reduced to the first approach by calculating the repair time, it is considered as a separate method in this review as it uses the concept of resource productivity and damage quantity to obtain repair time.

The third approach uses the concept of steps to determine the repair process. Damaged infrastructure needs a certain amount of steps to be carried out to achieve its pre-disrupted condition. The higher the damage level the asset has, the more steps are required to fully repair it. This number of steps can also vary depending on the availability of resources. As it can be seen, this approach can also be considered quite similar to the first one in the sense that if we know how long each step takes, we can estimate the amount of time taken to repair a road.

Table 2.9. Classification of publications according to the ways of modelling repair time

Recovery approach			References
Repair time	DA*	Hypothetical repair time	(Duque and Sörensen, 2011; Chen and Miller-Hooks, 2012; Henry and Ramirez-Marquez, 2012; Bocchini, 2013; Vugrin, Turnquist and Brown, 2014; Zhang and Miller-Hooks, 2014; Faturechi and Miller-Hooks, 2014b; Karamlou and Bocchini, 2014; Tuzun Aksu and Ozdamar, 2014; Ye and Ukkusuri, 2015; Nogal *et al.*, 2016; Vodák, Bíl and Křivánková, 2018; Hackl, Adey and Lethanh, 2018; Kilanitis and Sextos, 2019)
		Based on REDARS	(Mehlhorn, 2009; Stevanovic and Nadimpalli, 2010; Zhang, Alipour and Coronel, 2018)
		Based on HAZUS	(Vishnu, Kameshwar and Padgett, 2019)
		Based on expert opinion/real data	(Chang *et al.*, 2012; Karamlou and Bocchini, 2016; Karamlou, Bocchini and Christou, 2016; Twumasi-Boakye and J. O. Sobanjo, 2018; Twumasi-Boakye and Sobanjo, 2019)
	SA**	Stochastic repair time	(Shinozuka *et al.*, 2003; Zhou, Banerjee and Shinozuka, 2010; Barker, Ramirez-Marquez and Rocco, 2013; Decò, Frangopol and Bocchini, 2013; Baroud *et al.*, 2014; Nifuku, 2015; Zhang, Wang and Nicholson, 2017; Aydin *et al.*, 2018; W. Zhang *et al.*, 2018; Li *et al.*, 2019)
Resource productivity approach			(Feng and Wang, 2003; Furuta *et al.*, 2008; Orabi *et al.*, 2009, 2010; Ferreira, 2010; Bocchini and Frangopol, 2012a, 2012b; Unal, 2015)
Repair steps			(Sato and Ichii, 1995; Chen and Tzeng, 1999; Lu *et al.*, 2016; Basavaraj *et al.*, 2017; Yamasaki and Miwa, 2017; Kaviani *et al.*, 2018)

* DA: Deterministic approach
** SA: Stochastic approach

2.7. Conclusions and future directions

This chapter has presented a systematic literature review of current road recovery models after disruptive events. The methodology used to identify the final 60 publications included key stages such as identification, screening and eligibility. Road restoration models were analysed in terms of how road infrastructure was damaged and quantified, the impact on travel demand and drivers' decisions, how repairs were modelled and what mathematical modelling approach was used to undertake the analysis. By describing recovery models in such a way, the content of this chapter aims to serve as a guideline for researchers and practitioners in the field of transportation to identify what it is being done and detect potential research gaps in the area of road recovery.

Some general conclusions about the reviewed publications are the following. Despite the importance of multi-hazard impacts, only single-hazard events are simulated. The majority of the publications considered the impact of earthquakes on bridges which result in a reduction in network capacity. These damages are repaired by allocating physical resources and considering a single repair task that has a specific repair time. Sequential and/or simultaneous repairs are also considered depending on the number of available resources at a time. Once the network is damaged, most models load traffic onto the road network under the user equilibrium assumption which assumes that all drivers have full knowledge at any time of all travel costs in any route. Regarding the mathematical modelling approach, more than half of the reviewed publications solve the optimisation problem using exact methods or metaheuristic algorithms with genetic algorithms as the most common solution-search method. The most common purpose for which these models are used is the optimal allocation of resources to damaged locations and the optimal repair sequence. Most of them use deterministic approaches, although increasingly the uncertainty involved in the restoration process has been considered.

Existing challenges and future research directions, which are developed through the analysis of the selected publications, are discussed as follows. Regarding hazard impact analysis, recovery models should take into account that single hazards can trigger other hazards and it may affect the way that road networks are recovered under these situations. If a community is susceptible to more than one hazard and models are only considering isolated and independent hazards, it may result in taking wrong management decisions and this may increase the vulnerability of people to other ignored hazards. A more dynamic multi-hazard approach should be considered in current road restoration models. Also the vast majority of models are especially designed for extreme events, such as disasters, or emergency conditions. Less research in the area of road network recovery is done when dealing with incidents whose consequences are not high but have a medium likelihood of occurrence, such as winter storms, floods, etc. However, extensive research has been undertaken to study the vulnerability of road networks to the impact of these lower-risk weather-related hazards (i.e. floods) (Singh *et al.*, 2018; Arrighi *et al.*, 2019; Kasmalkar *et al.*, 2020; Wang *et al.*, 2020). The hazard-damage-functionality relationship should be

studied further as most of the current relations are based on expert opinions which would benefit from validation.

With regard to traffic modelling, the assumption of user equilibrium is not representative of how drivers react after these disruptive events. Although some authors justify the usage of this assumption for long-term recovery, it is still not clear where the boundary of long-term is defined. Further research should be done to simulate traffic behaviour under non-equilibrium conditions. In addition, it is also important to add that the world of Intelligent Transport System (ITS) is increasingly impacting the way that drivers get real-time information. User response changes depending on the level of information that is provided. Traffic modelling should be flexible enough to be able to adapt to future technological changes. Variations in travel demand on recovery models before and after disruptive events are also an important topic for future research.

Regarding infrastructure repair modelling, most publications consider that only one restoration team repairs one single asset. However, actual restoration works are undertaken by multiple teams. Models should also include repairs performed by multiple groups. External aid and temporary road solutions should also be taken into account in future road restoration models.

CHAPTER 3

Road recovery modelling framework and optimisation problem formulation

3.1. Introduction

The previous chapter presented a review of road recovery models that exist in the literature. Differences and similarities between models were highlighted and areas of improvement identified. Some of the major limitations of these models focused on how drivers' behaviour was simulated. Models assumed that drivers had full knowledge of all traffic conditions in any route at any time and the dissemination of external pre- or on-board travel information, via mobile phones or radio, was not simulated. This chapter introduces a new recovery model that tries to overcome these limitations found in previous models. The main aim of this chapter is to provide an overview of the entire model as an introduction to the rest of the parts of this thesis, describing the modelling framework and introducing the key models that form the global recovery model. The mathematical formulation of the optimisation problem is also presented and different numerical techniques are described in order to select the most suitable one that solves the optimisation problem. Additionally, this chapter also defines the objective functions considered in the optimisation process. Performance metrics that measure travel time and network connectivity used in previous models are reviewed and two metrics are proposed to use in this model.

3.2. Network modelling

The road network considered in this model is defined according to graph theory (Gibbons, 1985). A network (graph) consists of links and nodes. Every physical intersection or points representing changes in link attributes in a network is considered a *node* and two successive nodes are connected with a *link* that represents road segments. Both links and nodes have associated attributes (length, speed, capacity, turn penalties, etc.). The study area is divided into different zones (formerly

a travel analysis zone, TAZ) and each trip departs/arrives from/to the centroid of each zone, which represents the 'centre of activity'. Those centroids that act as origins and destinations for a trip are called *dummy nodes* as they do not represent a physical object/feature. These nodes are added to the network to allow vehicles to enter or leave the graph. Dummy nodes are connected to the network via *dummy links* (connectors), which are abstract links connecting TAZ centroids to realistic nodes on the physical network (Ortuzar and Willumsen, 2011). Dummy links are assumed to have infinite capacity. The number of trips originated from each origin node to their destination node forms the origin-destination (OD) matrix. In order to speed up the modelling process, vehicles can be grouped into packets that act as one entity. More information about how vehicles were grouped into these packets is provided in Chapter 5.

3.3. Modelling framework and problem formulation

This section introduces the general framework of the road recovery model proposed in this thesis and set out the optimisation problem. The areas that are excluded from this research are also mentioned in the following sections.

3.3.1. Conceptual framework

A general overview of the model is included in Figure 3.1. The occurrence of a natural hazard (e.g. landslides, floods, etc.) can significantly impact the road network causing concurrent failures across the network and producing damage to some parts of the infrastructure. A damage simulation model (described in Chapter 4) is implemented in order to simulate the damage created by the hazard. This model identifies those road segments that are physically damaged and need to be repaired. Although there are different ways of measuring damage (as mentioned in previous Chapter 2), this model gives a numerical value for each damaged link in units of "*required resources X time*" i.e. resource-minutes. The extent of damage is also linked to a reduction in link capacity. If a link is significantly damaged, then it may be totally closed or partially open to traffic.

Once the damage on all road segments is assessed, transport authorities and managers need to decide how to repair these incidents by giving priority to certain

damaged locations and allocating their required repair resources. A repair strategy, which will be described more in detail in Section 3.3.2, is a combined decision that provides a priority order of repairs and the number of repair teams that are allocated to each damaged incident. In order to know the effectiveness of the repair strategy, the model needs to simulate how repairs are undertaken considering the allocation of repair teams to damaged locations (which are repaired at a certain productivity rate) and how drivers using the network react to changes in link capacities from the time that damage occurs to when the network is fully recovered. A resource allocation and repair process model (Chapter 4) simulates how repairs are carried out on a day-to-day basis. The main aim of this module is to generate a resource allocation plan and a recovery schedule that includes a road restoration plan. With this information, the model knows exactly when each damaged road segment is partially or totally repaired and therefore the day when the link capacity returns to normal and is open to traffic again.

One of the other important parts of this model is the understanding of how drivers react to this network changes over time. The recovery model also includes a departure time and route choice model that applies the idea of artificial intelligence (AI), using the reinforcement learning (RL) technique (more information in Chapter 6 and 7), to simulate how drivers learn from their own experience and make day-to-day and within-day travel decisions. Additionally, the model also includes a novel feature, which has not been used in previous RL-based road recovery models, that provides external travel information to drivers. The movement of vehicles on the network is simulated using a mesoscopic traffic simulator which is implemented in order to send drivers from their origins to their destinations and calculate the travel cost spent on these journeys.

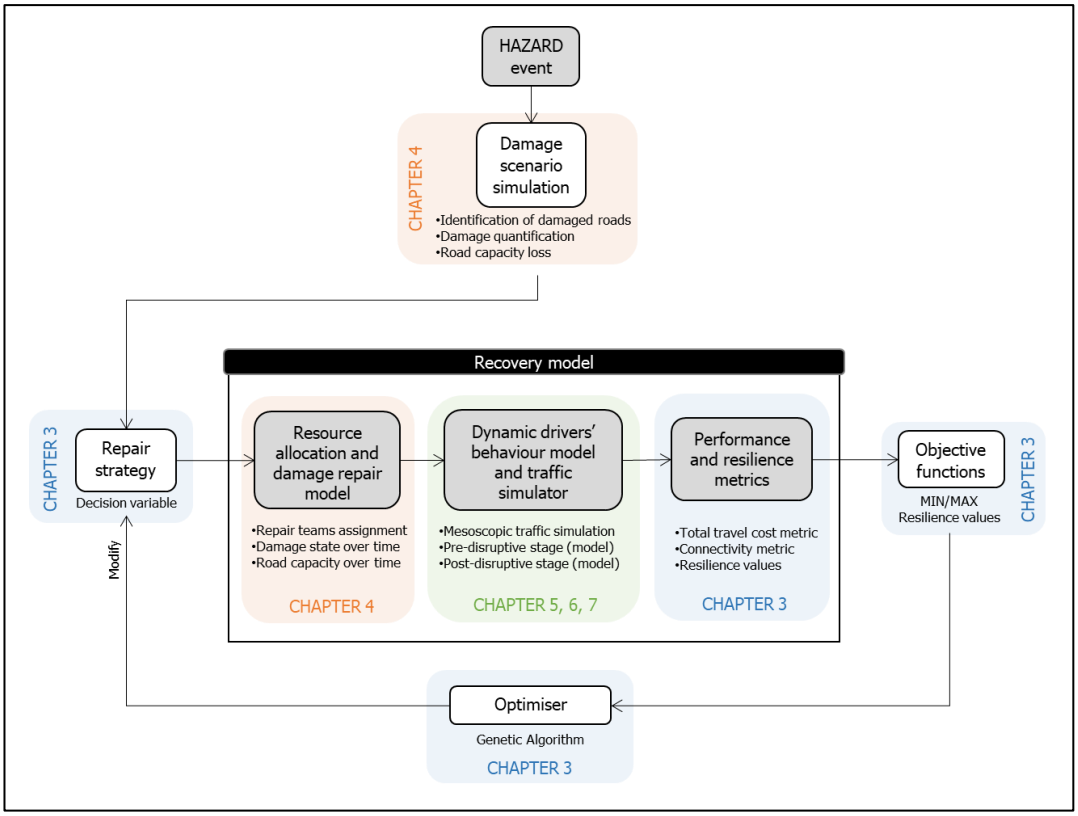

Figure 3.1. Conceptual framework of the optimisation problem

The effectiveness of the repair strategy that has been analysed can be measured using performance metrics. In this model, two metrics have been proposed: a traffic-related metric, which measures the total travel cost of all drivers and a connectivity metric that, to the best of the author's knowledge, combines for the first time a topological and demand characteristics of the network in a single metric. Performance metrics are updated on a daily basis to reflect the effect of implementation of repair strategies and driver response to the network state. Network resilience is defined as the aggregation of each metric over the duration of the repair strategy. Therefore, each repair strategy produces a single value of resilience for each metric.

As the aim of this project is to obtain the optimal repair strategy, an optimisation process is also included. The procedure consists of finding the repair strategy (decision variables) that maximises the objective function values while satisfying the constraints of the model. The objective functions considered in this model correspond to the resilience values measured on the 'total travel cost' curve

(objective 1) and 'connectivity' curve (objective 2). The optimisation aims to minimise travel cost and the possible delays that drivers may experience due to the disruptive events and maximise the connectivity of the network. The optimisation algorithm used in this model is called Genetic Algorithm (Holland, 1975), more specifically NSGA-II (Deb *et al.*, 2000), that is based on the Darwin's theory of natural selection (Darwin, 1859): the fittest solutions (repair strategies) survive and have more chance of being selected to breed and generate the next population of repair strategies. At the end of the last generation, a front of optimal (or close to the optimal) repair strategies is obtained and the selection of the final repair strategy is in modellers' judgement as they need to make a trade-off between total network cost and connectivity.

3.3.2. Problem formulation and decision matrix

The proposed optimisation model consists of three main elements: decision variables, objective functions and constraints. The mathematical expression is included in the following Equation (3.1).

$$\begin{gathered} min\ f(X)\ and\ max\ m(X) \\ subject\ to\colon\ resource\ limitation \end{gathered} \tag{3.1}$$

The problem considers two objective functions. The first objective function $f(X)$ quantifies the total travel cost experienced by all drivers that arrive to their destination. The second objective function $m(X)$ quantifies the network connectivity after the disruptive event. Both objective functions will be defined and explained more in detail in the following Section 3.4. It is important to consider mobility (obj1) and connectivity (obj2) aspects in the formulation because, after disruptive events, the capacity degradation of some road segments may lead to an increased travel time for some drivers compared to normal days and a reduction of partial travel demand that cannot be accommodated. In the particular case of a place that has been isolated after a hazard impact and attracts low travel demand, connectivity values acquire higher importance. If just total travel costs were considered, this lack of connectivity would not be reflected in the problem.

The decision variable X in this optimisation problem represents a repair strategy. Unlike most of the models reviewed in Chapter 2, this one defines a repair strategy as a combination of two main decisions: the identification of a priority order

of repairs and the allocation of repair resources to damaged locations. The repair strategy is mathematically materialised by the decision matrix $X = X[X_1, X_2]^T$ (see Equation (3.2)). Both, X_1 and X_2 are Inc-dimensional vector of integers, being Inc the total number of damaged locations on the network. The position in the vector represents the incident number. Note that a damaged location may include a single link failure or a two link failure if this is a two-way road. The integer vector X_1 represents the priority order of repairs. A value that varies from 1 (highest priority) to Inc is assigned to each position in the vector. Note that two damaged locations cannot have the same priority value, which means that the value on each position cannot be repeated. The integer vector X_2 represents the allocation of repair resources to each damaged location. Each value indicates the number of repair teams that are assigned to the corresponding damaged location. These values have an upper- and lower- limit as it is not possible to have ∞ repair teams and some incident locations also need a minimum of resources to start repairs. Note that this value can also indicate the maximum number of repair teams that can attend the incident location. The Example 1 has been included to clarify the values of the decision matrix.

$$X = \begin{bmatrix} X_1 \\ X_2 \end{bmatrix} = \begin{bmatrix} X_1^{Inc1} & X_1^{Inc2} & \dots & X_1^{Inc} \\ X_2^{Inc1} & X_2^{Inc2} & \dots & X_2^{Inc} \end{bmatrix} \tag{3.2}$$

***Example 1**. Some roads have been closed as a result of some landslides after the impact of a storm. Five locations have been identified as damaged. In this particular scenario, a possible repair strategy, and therefore the decision matrix, is defined as follows:*

$$X = \begin{bmatrix} X_1 \\ X_2 \end{bmatrix} = \begin{bmatrix} 5 & 3 & 1 & 4 & 2 \\ 3 & 7 & 5 & 3 & 4 \end{bmatrix}$$

In this case, as there are five incident locations, there are 5 columns in the matrix. First column represent the first incident location and so on. The highest priority of repairs (and therefore the first incident location that has to be repaired) is given to Incident number 3 (first row, third column). The rest of the order is Incident 5, 2, 4 and 1. Regarding the allocation of resources, 3 repair teams are assigned to incident 1 (second row, first column), 7 repair teams to incident 2 and successively.

3.3.3. Computer programming language/software

The model has been implemented using MATLAB software (The MathWorks Inc., 2018) and coded in MATLAB language. Due to the simplicity of MATLAB, it has been broadly used in the areas of science and engineering, especially in the field of Artificial Intelligence and Machine Learning to simulate and analyse behavioural dynamics of agents (Mohammadi Ziabari and Treur, 2019). One of the benefits of using MATLAB, as the abbreviation of MATLAB says ('*MATrix LABoratory*'), is that it works with matrices while other programming languages mostly work with numbers one at a time (The MathWorks Inc., 2018). Therefore, all data from this model is structured in matrices and arrays and MATLAB is able to carry out operations between these matrices/arrays according to the code that has been implemented, which is available under demand.

3.4. Resilience value and network performance metrics

This section presents the objective functions involved in the optimisation problem. Both objective functions are defined using metrics that measure the functionality of the network over time. This creates what is known as 'functionality curves' (Cimellaro, Reinhorn and Bruneau, 2010), which is a graph that measures on a vertical axis the network performance and on the horizontal axis the time. However, a single value needs to be obtained from these curves, which is ultimately the value that has to be maximised or minimised. This is also known as 'resilience value'. The challenging question of how to quantify resilience has been studied exhaustively in recent reviews (Francis and Bekera, 2014; Hosseini, Barker and Ramirez-Marquez, 2016; Rus, Kilar and Koren, 2018; Zhou, Wang and Yang, 2019). Despite the existence of more sophisticated resilience metrics, the model proposed in this thesis quantifies resilience (R) as the area under the functionality curve, starting from the day of the disruption until a user-defined day (in this case user refers to modeller), which is defined in this thesis as a certain amount of time after the last damaged road segment is completely repaired, so that there is enough time for network conditions to stabilise again. Originally formulated by Reed, Kapur and Christie (2009), it is expressed mathematically as shown in Equation (3.3).

$$Resilience = \int_{t_0}^{t_1} Q_t \, dt \tag{3.3}$$

Where,

Q_t, is the functionality curve.

t_0, time when the disruption occurs.

t_1, user-defined time horizon.

If the functionality curve (Q) is measured in the range of [0,1], the resilience value can also be normalised dividing the area under the functionality curve by the time interval as shown in Equation (3.4).

$$\overline{Resilience} = \frac{\int_{t_0}^{t_1} Q_t \, dt}{t_1 - t_0} \tag{3.4}$$

Where, $\overline{Resilience}$ is the normalised value of resilience in the range [0, 1].

Recent reviews provides an overview of the literature on transportation system performance metrics (Faturechi and Miller-Hooks, 2014a; Konstantinidou, Kepaptsoglou and Karlaftis, 2014; Rus, Kilar and Koren, 2018; Sun, Bocchini and Davison, 2018; Twumasi-Boakye and J. Sobanjo, 2018; Wan *et al.*, 2018; Zhou, Wang and Yang, 2019). Chapter 2 also provides a summary table (Table 2.5) with all performance metrics that have been used in those reviewed recovery models. The following sub-sections describe in detail the functionality metrics that are used in the model proposed in this thesis to measure the performance of the network. Two classes of functionality metrics are considered: traffic-related metrics (total travel cost) and a topological-related metrics (connectivity).

3.4.1. Total travel cost metric

3.4.1.1. A brief review of travel cost metrics

The impact of natural hazards on the network may produce the closure of some road segments and consequently, cause delays to some users on the network. Drivers may have to detour, making them take longer routes to get to their destination and/or produce more congestion in otherwise uncongested areas. The consequences of these

impacts have been traditionally measured by computing the travel time expenditure of drivers.

The majority of reviewed recovery models that measured travel time expenditure (Sato and Ichii, 1995; Chen and Tzeng, 1999; Bocchini and Frangopol, 2012a; Lu *et al.*, 2016) simulated traffic movements based on macroscopic models. These models represented traffic in an aggregate way as a continuous flow. This meant that individual movements of vehicles on the network could not be simulated and therefore, travel cost (time) was calculated based on aggregate volumes of traffic on each link at a given time. Equation (3.5) shows the link-based travel time formula which was used to calculate the network total travel time. In this case, performance metric (Q_t) in terms of total travel time was defined as a weighted sum of all link travel times, being the link weight the number of vehicles assigned to each link.

$$Q_t = \sum_{l=1}^{nL} V_{t,l} \cdot T_{t,l} \tag{3.5}$$

Where,

l, links

nL, all links of the network.

$V_{t,l}$, number of vehicles on link l on day t.

$T_{t,l}$, average travel time on link l on day t. This is calculated using the BPR formula (Bureau of Public Roads, 1964), which calculates the travel time on each link based on the number of vehicles using that link:

$$T_{t,l} = tt_O \cdot \left[1 + a \cdot \left(\frac{V_{t,l}}{q_{lmax}}\right)^{b}\right] \tag{3.6}$$

Where,

tt_O, free-flow travel time.

q_{lmax}, capacity of the link l.

a, BPR coefficient, often set at 0.15.

b, BPR coefficient, often set to 4.

3.4.1.2. Proposed total travel time metric

The model implemented in this thesis is able to simulate the trajectory of individual vehicles using a mesoscopic traffic model (see Chapter 5 for a detailed description).

This means that the travel time expenditure of each driver can be obtained and a value of total travel time can be extracted, which is more accurate than the aggregated link-based formula expressed in previous Section 3.4.1.1. Unlike the previous models that use this aggregated value of total travel time on each link, the performance metric shown in Equation (3.7) calculates the vehicle-based total travel time and is defined as the sum of the time spent to get to their destination by each vehicle.

$$Q_t = \sum_{V=1}^{V_{net}} T_{t,V} \tag{3.7}$$

Where,

V, vehicle on the network

V_{net}, all vehicles travelling on the network

$T_{t,V}$, time that each vehicle V spends travelling on day t

Note that this metric only computes those trips that have arrived to the destination. Those trips that have been cancelled or have not been completed are not included in the travel time calculation. These excluded trips will be considered in the complementary metric included in the following section.

3.4.2. Connectivity metric

3.4.2.1. A brief review of connectivity metrics

Besides travel cost related metrics, another key aspect to evaluate the performance of the transport infrastructure is the topological-related information. The concept of connectivity has been extensively used in the literature across various sectors (e.g. transportation, water, electricity) (Reggiani, Nijkamp and Lanzi, 2015; Soldi, Candelieri and Archetti, 2015; Billah Kushal and Illindala, 2020; Huck, Monstadt and Driessen, 2020; Rachunok and Nateghi, 2020). In essence, connectivity is defined as the ability to get from one place to another (Zhang, Alipour and Coronel, 2018). More precisely, in the context of graph theory, two nodes (also known as vertices) in a network are connected if there is at least a path between these nodes (Wilson, 1996). Over time, more definitions of connectivity have emerged among the literature and consequently several ways of measuring connectivity are identified.

The initial connectivity metrics come from the concepts of graph theory. Kansky (1963) developed several topological indices to measure the connectivity of transport networks by counting the number of links and nodes. Another way of measuring connectivity came from the concepts of k-edge connectivity and k-node connectivity. A graph was k-edge connected if there were k-1 links (or edges) that could be removed without disconnecting the network (Yamasaki and Miwa, 2017). Similar to k-edge connectivity, k-node connectivity described a graph that was disconnected if k nodes failed.

Kurauchi *et al.* (2009) also determined connectivity from a topological point of view. They defined connectivity as the number of disconnected paths between an Origin-Destination (OD) pair. Karamlou and Bocchini (2016) proposed a metric, which is shown in Equation (3.8), that included a weighting factor in order to show the importance of keeping certain OD pairs connected. This feature prioritised certain connections to hospitals, airports, schools, etc. If the weighting factor (K_r) was greater than zero for all OD pairs, then the loss/partial connection of a priority OD pair had a greater impact on Q_c than the loss/partial connection of a non-priority OD pair. However, in the hypothetical case that the weighting factor was zero for some OD pairs, then this metric implied that even if all OD pairs were not fully connected, network connectivity could still acquire its maximum value. Only when those important OD pairs were connected, the connectivity values would achieve the maximum value.

$$Q_c = \sum_{r=1}^{R} (L_r \cdot K_r) \tag{3.8}$$

Where,

r, a node pair.

R, total number of node pairs.

L_r, parameter that determines the level of connectivity between node pair r at time t. Note that a node pair is defined as fully (partially) connected if at least there is a path that is totally (partially) in service.

$$L_r = \begin{cases} 1 & if\ node\ pair\ r\ is\ fully\ connected \\ 0.5 & if\ node\ pair\ r\ is\ partially\ connected \\ 0 & if\ node\ pair\ r\ is\ not\ connected \end{cases} \tag{3.9}$$

K_r, weighting factor that indicates the importance of an OD pair r. This value is determined by engineering judgement and it has to satisfy the following constraint:

$$\sum_{r=1}^{R} K_r = 1 \tag{3.10}$$

The number of paths between an OD pair can be very large. That is the reason why Zhang and Wang (2016) proposed a new metric that quantified the number of independent paths between OD pairs. In this context, independent paths were defined as those routes that did not share any common road links. The advantage of considering just the number of independent paths was the limited number of paths that were identified. The authors also included a weighting factor in order to highlight the importance of certain OD pairs.

As the capacity of certain links might be reduced after the impact of disruptive events, it might result in connectivity failures. For that reason, Liao, Hu and Ko (2018) proposed a metric that quantifies network connectivity by considering the ratio between post- and pre-disruption link capacity.

$$Q_c = 1 - \prod_{w \in W_r} \left(1 - \prod_{l \in w} \frac{q_{l,max,post}}{q_{l,max,pre}}\right) \quad \forall r \in R \tag{3.11}$$

Where,

$q_{l,max,post}$, is the post-disruption capacity of link l.

$q_{l,max,pre}$, is the pre-disruption capacity of link l.

Q_c, performance value measured as connectivity value between the OD pair r.

W_r, set of paths between an OD pair r.

w_r, a path between an OD pair r.

R, set of OD pairs r.

Connectivity can also be defined in terms of incompleted trips. If drivers cannot get to their destination, cancel their trip or abandon in the middle of their journey, it can be considered as a lack of (demand-based) connectivity. In the field of freight

transport, Chen and Miller-Hooks (Chen and Miller-Hooks, 2012) proposed a metric (see Equation (3.12)) that quantified the expected fraction of demand that was satisfied before and after a disaster under certain recovery costs. It is assumed that no more than $d_{r,pre}$ trips can be satified.

$$Q_c = \frac{\sum_{r=1}^{R} d_{r,post}}{\sum_{r=1}^{R} d_{r,pre}} \tag{3.12}$$

Where:

R, total number of origin-destination pairs.

$d_{r,post}$, post-disaster demand between the OD pair r that is satisfied.

$d_{r,pre}$, pre-disaster demand between the OD pair r that can be satisfied.

Li *et al.* (Li *et al.*, 2019) modified the OD demand satisfaction ratio proposed by Chen and Miller-Hooks (Chen and Miller-Hooks, 2012). They added a binary variable (γ_r) that omitted those trips whose post-disaster travel time was k times greater that the pre-disaster travel time.

$$Q_c = \frac{\sum_{r=1}^{R} d_{r,post} \cdot \gamma_r}{\sum_{r=1}^{R} d_{r,pre}} \tag{3.13}$$

Where,

γ_r, binary variable that omits those trips whose post-disaster travel time is k times greater that the pre-disaster travel time. It takes the values considered in the Equation (3.14).

$$\gamma_r = \begin{cases} 1, & C_{r,post} \leq \hbar \cdot C_{r,pre} \\ 0, & C_{r,post} > \hbar \cdot C_{r,pre} \end{cases} \tag{3.14}$$

Being,

$C_{r,post}$, travel time between the OD pair r during the post-disaster stage.

$C_{r,pre}$, travel time between the OD pair r during the pre-disaster stage.

$\hbar$, user-defined parameter that sets the limit of those trips that are counted on the metric or those that do not.

Bocchini and Frangopol (2013) proposed a metric to quantify network connectivity based on the serviceability of routes between OD pairs. Connectivity was quantified as the total demand between those OD pairs that existed at least one route in service.

$$Q_c = \sum_{i}^{N} \sum_{j}^{N} L_{ij} \cdot OD_{ij} \tag{3.15}$$

Where:

L_{ij}, is the dummy variable that indicates if there exists at least a route in service (or not) between node i and node j at time t.

$$L_{ij} = \begin{cases} 1, & if\ there\ is\ at\ least\ a\ route\ in\ service\ from\ i\ to\ j \\ 0, & if\ there\ are\ no\ routes\ in\ service\ from\ i\ to\ j \end{cases} \tag{3.16}$$

OD_{ij}, demand between node i and node j at time t.

N, total number of nodes.

This metric considered the value of traffic demand (OD_{ij}) to indicate that some roads were more important than others because they carried higher traffic flows and therefore connects more important areas (Bocchini and Frangopol, 2013). Therefore, the more vehicles it carried, the more important that OD connection was.

3.4.2.1. Proposed connectivity metric

The previous section provided an overview of the main connectivity metrics proposed in the literature. Two classes of connectivity metrics could be highlighted: network-based connectivity metrics and demand-based connectivity metrics. The former focussed on measuring how many nodes were physically connected. The latter measured the fraction of travel demand that was satisfied. The problem observed from these metrics is that, for the same road network, different values of connectivity can be obtained depending on the type of metric that is used. As an example, consider a road network that is physically fully connected. Assume that there is a place located on a node that has been isolated from the rest of the network due to unforeseen circumstances. Under normal conditions, this place has very low intermittent demand (some days drivers need to reach that place and some other days no one needs to be there). If a demand-based connectivity metric is used, on those days that no one needs to get to that place, the connectivity gets the maximum value of 100% because the rest of the demand can easily arrive to their destinations. However, if a network-based connectivity metric is used, as not all nodes are physically connected, the connectivity value is less than 100% even when no one needs to reach that place. It is important to reflect the isolation of that node on the connectivity metric because,

under extraordinary situations, the travel demand that goes to the some places might be not zero/low values.

The proposed connectivity metric combines the supply side and the demand side in one formulation. For the supply side, the formula presented by Karamlou and Bocchini (2016) is used as an inspiration and for the demand side, the formula presented by Chen and Miller-Hooks (Chen and Miller-Hooks, 2012). The proposed formulation is included in the following Equation (3.17). To the best of the author's knowledge, this is the first time that a formula combines supply and demand side to measure the connectivity of the network. It quantifies the connectivity of all origin nodes to the rest of destination nodes of the network. Only the connectivity to nodes that are considered important is quantified.

The benefit of including a demand-based connectivity metric is that it also accounts for those vehicles that do not get to their destinations because of unconnected nodes, abandoned trips or cancelled trips. As Vishnu, Kameshwar and Padgett (2019) affirmed in their work, a robust resilience assessment requires an analysis that combines travel time and missed trips. Total travel cost (time) is already considered in the first metric on Section 3.4.1 and missed trips are considered in the metric that is being explained. As missed trips are not considered in the 'total travel cost' metric, no double counting of trips is involved.

A brief description of the formulation is included as follows. Equation (3.17) is divided into two main terms: a demand-based term ($\frac{V_{tij}}{V_{ij,pre}}$), which calculates the percentage of demand that is satisfied; and a topological-based term (L_{tij}), which determines if the node pair is physically connected. These are excluding terms, meaning that for the same node pair both terms cannot be computed at the same time. That is the reason of adding a binary variable (δ_{tij}). The importance of each destination node is computed using the factor K_j. In order to measure connectivity values in the range [0,1], the previous terms are divided by the number of node pairs whose connectivity is computed in the formula.

$$Q_c = \frac{\sum_{i=1}^{N}\left[\sum_{j=1}^{N} K_j\left[\delta_{tij}\left(\frac{V_{tij}}{V_{ij,pre}}\right) + (1-\delta_{tij})L_{ij}\right]\right]}{\sum_{j=1}^{N} K_j} \quad (3.17)$$

Where:

Q_c, performance value measured in terms of connectivity. It can take values between 0 and 1, being 0 null connectivity and 1 full connectivity.

N, total number of nodes.

K_j, weighting factor that indicates the importance of the destination node j. This value is determined by engineering judgement and it has to satisfy the following constraint (Equation (3.18)): the sum of the weighting factor of all destination nodes has to be 1.

$$\sum_{j=1}^{N} K_j = 1 \quad (3.18)$$

δ_{tij}, binary variable that indicates if there is traffic demand from node i to node j at time t.

$$\delta_{tij} = \begin{cases} 1, & if\ V_{ij,pre} > 0 \\ 0, & otherwise \end{cases} \quad (3.19)$$

V_{tij}, total number of vehicles that completed their trip from node i to node j on day t.

$V_{ij,pre}$, total number of vehicles that are expected to travel from node i to node j during the pre-disrupted stage.

L_{ij}, parameter that determines the level of connectivity between node i and node j from a supply side (Karamlou and Bocchini, 2016) on day t. It can take a value of 1 if nodes i and j are fully connected, or 0 if nodes i and j are not connected.

3.5. Multi-objective optimisation model

The optimal repair strategy that maximises/minimises the objective functions described in previous Section 3.4 is obtained using an optimisation model. The procedure of an optimisation problem consists of finding the combinations of design variable values that obtain the best objective function values, satisfying all the constraints. This is also called a combinatorial optimisation problem as it requires

searching for the best combination of variables among a large number of discrete solutions (Hosny, 2010). More specifically, it aims to find the best priority order of repairs and the best allocation of repair teams to those physically damaged road segments as described in Section 3.3.2.

There are mainly two type of methods to solve an optimisation problem (see Figure *3.2*): analytical methods and numerical methods (Cui *et al.*, 2017). The analytical (or exact) methods are those techniques that are guaranteed to find an optimal solution at a high computational time. The algorithms have to solve strict mathematical formulations but the problem is that some realistic problems cannot be represented by a series of formulas. As opposed to exact methods, numerical algorithms can find near optimal solutions at an acceptable computational cost. The main aim of these techniques is to find an optimal solution without searching the whole solution space (Sangaiah *et al.*, 2020). Numerical methods are further categorised in two types: heuristic algorithms and meta-heuristic algorithms.

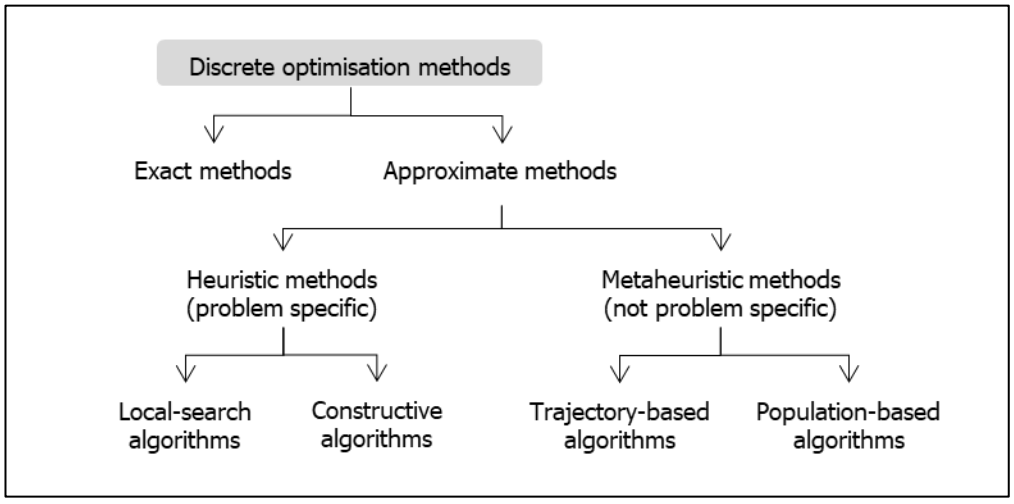

Figure 3.2. Classification of methods to solve optimisation problems

Heuristic methods are defined as techniques that seek good solutions at an acceptable computational cost but without the guarantee to achieve optimality (Reeves, 1996). It is also defined in the literature as a problem-dependent technique because these are solving methods for special and specific problems (Pillay and Qu, 2019). Examples of heuristic algorithms include local-search algorithms and constructive algorithms, among others. The former explores neighbouring solutions

in order to improve the solutions. The latter constructs the solution by making the best solution after a series of steps (Merz and Freisleben, 2002).

Metaheuristic algorithms are one level higher than the heuristic methods (Hussain *et al.*, 2018) as it combines heuristic methods in higher level frameworks with strategies that guide the search process (Alba, 2005). It is also known as problem-independent techniques because it is a more generic method that can be used for most optimisation problems (Hussain *et al.*, 2018). There exists multiple ways of classifying metaheuristic techniques in the literature but one that is commonly used is based on the number of solutions that is evaluated at a time. These are trajectory-based algorithms and population-based algorithms. The former evaluates one solution at a time and starts with a single initial solution. These algorithms create a trajectory in the search space. The latter initially explores a population of solutions. Then, after each iteration, a new population of solutions is created based on the results on the previous iteration and towards better search areas (Hussain *et al.*, 2018). Some commonly used trajectory-based algorithms are: simulated annealing, tabu search, basic local search, etc. On the contrary, some population-based algorithm are: genetic algorithms, scatter search, ant colony, particle swarm systems, etc. (Cotta, Talbi and Alba, 2005).

Metaheuristic techniques have become more popular over the exact methods in the last years due to the simplicity and robust results (Hussain *et al.*, 2018). However, the choice of the resolution technique needs to be based on the formulation of the problem (objective functions, variables constraints, etc.). The complexity of the problem presented in this thesis makes infeasible its resolution via exact methods. The model includes a number of constraints of the "if-then" form, the combinatorial nature of the model and other simulation modules that are implemented make the use of traditional mathematical resolution techniques difficult. Therefore, an approximate approach needs to be selected to solve the problem. Among all numerical techniques and due to the nature of the problem, the population-based approach is selected against the trajectory-based. The advantage of using a population-based is that the search space is explored more in depth as more solutions are run after each iteration. The procedure may also be faster as parallel computing can be used to run several solutions of the population in parallel. Also, as observed in the literature,

similar problems are solved using population-based techniques, obtaining fast and reliable results (Connor and Shah, 2014; Zhang, Zhang and Zheng, 2014; Míča, 2015; Gerami Matin, Vatani Nezafat and Golroo, 2017).

Depending on the number of objectives, optimisation problems can also be classified into single-objective problems and multi-objective optimisation problems. The problem proposed in this chapter optimises simultaneously two contradicting objectives (total travel cost and connectivity). This means that the optimisation does not provide a unique solution, but a set of optimal trade-offs between these potentially conflicting objectives. These set of solutions is called Pareto optimal set of solutions.

It is not possible to identify which population-based multi-objective optimisation algorithm is the best for a given problem (Lei and Shi, 2004). As the results obtained from an approximate approach are only an "approximation" of the optimal solutions, it is hard to know how close solutions are to the optimal value. That is the reason why it is difficult to compare between algorithms and in most cases the result may also be influenced by the parameter values of the algorithm taken on each problem (Míča, 2015). Therefore, the most appropriate algorithm to solve the problem presented in this thesis is selected based on the results obtained from similar problems already solved in the literature. Based on similar combinatorial optimisation problems, Genetic Algorithms have stood out over the rest of the population-based algorithms. Said *et al.* (2014) presented a comparative study between genetic algorithm, tabu search and simulated annealing for solving an assignment of facilities to different locations. The result showed that genetic algorithm had a better solution quality in comparison with the other metaheuristic algorithms. Connor and Shah (2014) evaluated the performance of three different metaheuristic techniques (Genetic algorithms, simulated annealing and tabu search) on a resource allocation and scheduling problem. The analysis suggested that the genetic algorithm performed better than the rest of algorithms. Matin *et al.* (Gerami Matin, Vatani Nezafat and Golroo, 2017) presented a problem that optimised road maintenance planning minimising the cost and maximising the pavement condition. It concluded that Genetic Algorithm performed better and provided the optimum solution. On the other hand, there are other studies that indicate that genetic algorithm performs not as good as

other metaheuristic algorithms (Zhang, Zhang and Zheng, 2014). However, as Abraham and Jain (2005) admit, optimisation techniques such as simulating annealing, tabu search, ant colony systems, etc. could generate the Pareto set of optimal solutions but the solutions very often tended to be stuck at a local optimum and there was no guarantee of finding the optimal set of trade-offs. On the contrary, evolutionary algorithms such as genetic algorithms was characterised by a population of solutions whose 'best' values were reproduced and combined to create new populations (natural selection).

Overall, genetic algorithm demonstrates an adequate and robust performance in similar combinatorial optimisation problems and therefore, this is the algorithm that is selected to solve the presented recovery problem.

3.5.1. Multi-objective Genetic Algorithm: NSGA-II

The Non-dominated Sorting Genetic Algorithm (NSGA-II) (Deb *et al.*, 2000) is a multiple objective optimisation algorithm, which is an extension of the classical Genetic Algorithm. The aim of the NSGA-II is to find the set of repair strategies that provides the (near-) optimal total travel cost and connectivity values. Apart from the reasons described in the Section 3.5, the NSGA-II is selected as the optimisation technique due to: (1) the effectiveness of generating optimal solutions for similar problems (Kandil and El-Rayes, 2006; Orabi *et al.*, 2009; Bocchini and Frangopol, 2012b; Gerami Matin, Vatani Nezafat and Golroo, 2017); (2) the nature of a multi-objective optimisation problem; (3) the advantage of fast running and good convergence of solution set (Deb *et al.*, 2000).

To clarify the terminology involved in a GA and to make it easier to the reader, some concepts are defined in this paragraph. Most of them are directly applied from the natural Darwinian theory (Darwin, 1859) and may be a bit confusing for those not specialised in the field. In this sense, an individual (in this model, a repair strategy) is characterised by a set of variables known as genes. These genes are the priority order of repairs and the allocation of repair teams to incidents. Each individual is a solution to the problem and the set of individuals is called a population.

The NSGA-II procedure is described as follows (Figure *3.3*). It starts with the generation of a random population of repair strategies. Then the recovery model

described briefly in Section 3.3.1 evaluates the performance of each repair strategy and a resilience value, which is used as a fitness value, is obtained for each objective. NSGA-II uses this fitness value to rank and sort these solutions. This is explained more in detail in the following Section 3.5.1.1. The genetic operators of selection, crossover, mutation and elitism are then applied to the best (highest ranking) solutions in order to generate a new population of solutions that are closer to the optimal (see Section 3.5.1.2 for more details). This procedure is repeated for a pre-defined number of generations or until the population has converged to the (near-) optimal, which means that the population does not produce offspring which are different from the previous generation. The Pareto front of solutions of this last generation forms the optimal set of repair strategies.

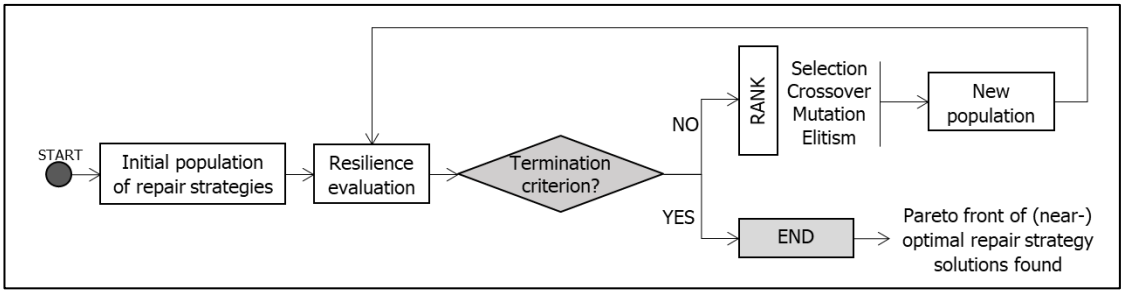

Figure 3.3. NSGA-II procedure

3.5.1.1. Ranking and sorting method

After the evaluation of each repair strategy, two fitness values (one for each objective) are assigned to each solution. However, the GA algorithm cannot optimise the value of two conflicting fitness values at the same time for each repair strategy. There are several methods in the literature that combine these two values and produce a single value that can be optimised by the algorithm. This value determines how "fit" an individual (repair strategy) is. The better the fitness value, the more probability this repair strategy has to be selected for reproduction. The Pareto rank-based technique used in this model to rank the solutions is the classical one formulated by Goldberg (1989). The advantage of this technique compared to other methods (e.g. weighted sum approach) is that the multi-objective vector is reduced to a scalar fitness value without combining the objectives in a weighted formula. The procedure of the Goldberg's method is the following: (1) Identify those non-

dominated repair strategies, which are those solutions whose objectives cannot be improved without degrading some of the other objective values. (2) Assign to these repair strategies a rank 1 and remove them from the population. (3) Identify again the non-dominated repair strategies of the reduced population. (4) Assign a rank 2 to these solutions and remove them from the population. (5) Repeat these steps assigning rank values until the whole population is totally ranked. A graphical example of this procedure is shown in Figure *3.4*.

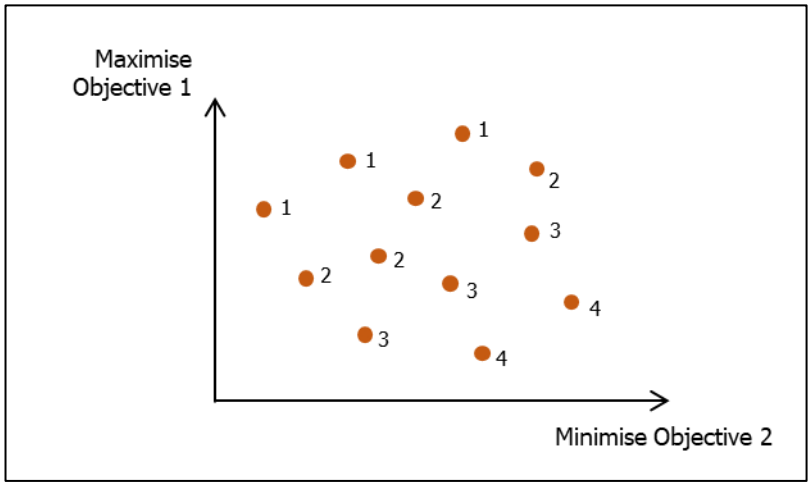

Figure 3.4. Graphical example of the Pareto ranking-based method used in this model. The numbers in the graph represent the ranking value associated with each repair strategy.

3.5.1.2. Genetic operators: selection, crossover, mutation and elitism.

The basic search mechanisms of the GA are the genetic operators. These are used to create new solutions based on the existing ones. In this model, two types of operators are considered: crossover and mutation. Crossover is one of the vital roles in a genetic algorithm. This operator selects some characteristics (genes) from selected repair strategies (parents) and creates new ones (kids). In terms of the process of natural selection, only the "fittest" strategies are the ones responsible for passing their genes to their next generation. The process of selecting those fittest solutions (or parents) is described as follows: (1) Select randomly two repair strategies from the same generation. (2) Find which of these two repair strategies is better in terms of the ranking value obtained in previous Section 3.5.1.1. That repair strategy whose ranking value is higher will be selected as a parent. If the ranking value of both repair strategies is the same, the modeller needs to define which conflicting objective

acquires higher importance and therefore, the parent will be selected based on the fitness value of the selected objective. (3) Store the selected repair strategy in a list of parents. (4) Repeat steps 1 to 3 to select the total amount of parents. In this model, the total number of parents are defined as the double of the number of offspring that are expected to produce. It is the double because two repair strategies (parents) can only create a single repair strategy (offspring).

Although a lot of crossover operators have been proposed in the literature (Kora and Yadlapalli, 2017), this model uses a uniform crossover operator due to its simplicity and randomness involved in the process. The idea behind this operator is that each gene of the repair strategy is randomly inherited from a parent. Initially, the operator creates a random binary (1 or 0) crossover mask of the same length of the repair strategy vector. Each "1" value means that a gene or variable from the parent 1 is transferred to the offspring. If there is a "0" value, then the gene is transferred from parent 2. A new crossover mask is generated randomly for each pair of parents considered in the model.

As described in Section 3.3.2, two damaged locations cannot have the same priority level. This means that a priority value assigned to each damaged location on a repair strategy cannot be repeated. For instance, if damaged road segment "A" is the second one on the list of priorities, damaged road segment "F" cannot be the second one on the list of priorities to be repaired. This restriction has to be imposed in the crossover operator as numbers need to be adjusted to avoid repetitions.

To introduce diversity in the new population of repair strategies, a mutation operator is also implemented in the algorithm. This operator introduces random changes in a variable ("gene" in nature selection theory) of a repair strategy. There are also different types of mutation operators, but in this model, a swap mutation is used due to the limitation of the non-repetitive integer values that the repair strategy can take. This type of mutation selects two positions at the repair strategy at random and interchanges their values.

In order to avoid losing good solutions from one generation to the next (Shumeet and Caruana, 1995), an elitist selection is also incorporated in the model. This operator selects the best repair strategies ('best' means the highest ranking

value) from the current generation and carry over to the next one, without altering the repair strategy. This method guarantees that the quality of the best solution does not decrease from one generation to the next (Shumeet and Caruana, 1995).

MATLAB (The MathWorks Inc., 2018) includes a global optimisation toolbox that incorporates a whole genetic algorithm module. However, due to the nature and singularity of the model presented in this thesis, the built-in MATLAB function of the Genetic Algorithm is not suitable for the purpose of this model. However, a similar algorithm has been implemented following the information provided in the online guides that MATLAB provides (The MathWorks Inc., 2018) and adapting the existing code to the structure and constraints of the presented model.

To run the optimisation algorithm, the user needs to define which percentage of the new population is created by using crossover operators, mutation operators or elitist selection.

3.6. Conclusions of the chapter

This chapter has provided an overview of the entire model which is used as an introduction to the remaining chapters of the thesis. It presented the conceptual framework of the recovery model which included a damage simulation model, a resource allocation and repair process model, a departure time and route choice model and an optimisation model. The chapter also described the formulation of the corresponding optimisation problem. Previous network performance metrics studied in the literature were reviewed and two functionality metrics were proposed to measure the effectiveness of each repair strategy: a traffic-related metric, which measured the total travel cost of all drivers and a connectivity metric that combined for the first time topological and demand characteristics of the network in a single metric. The model also quantified resilience as the area under the functionality curves. The higher the area under the 'total travel cost' curve is, the more travel time drivers experience to get to their destination. This means that the system is less resilient in terms of travel cost. Lower values of the area shows a better adaptation of drivers to the disrupted network. In the case of the connectivity values, the higher the value under the area of 'connectivity' curve, the more trips are completed. In this case the system is more resilient in terms of connectivity values.

Different types of methods to solve the optimisation problem were also reviewed. Genetic algorithms demonstrated an adequate and robust performance in similar combinatorial optimisation problems. The Non-dominated Sorting Genetic Algorithm (NSGA-II) was selected as a technique to solve the optimisation problem and find the Pareto set of repair strategies that provided the (near-) optimal total travel costs and connectivity values.

In conclusion, the key modules that form the proposed recovery model are successfully introduced in this chapter and a more detailed description of each module will be included in the following chapters. The performance metric considered in the proposed model provides a robust resilience assessment as it requires an analysis that combines the cost of each driver travelling through the network and the amount of trips that cannot be satisfied with the network conditions after hazard impacts.

CHAPTER 4

Damage scenario simulation and a three-stage road infrastructure repair model

4.1. Introduction

The impact of hazard events may produce physical damage to road infrastructure. The modelling of this impact is essential to support the strategic pre-disruption risk mitigation and post-disruption recovery planning. During the post-disruption planning phase, damage has already physically affected the infrastructure, and modellers just need to incorporate that real damage into the model and run it to find out the optimal repair strategy. However, for the pre-disruption planning phase, damage has not happened yet and modellers need to simulate possible scenarios of damage to infrastructure. Historical information on hazardous events can be used to recreate the impact of previous events on the road network. However, the limitation of historical data makes the development of new hazard-specific models more difficult. As an example, fragility models (which relates the intensity of a hazard to the probability that a particular damage state is exceeded, as described in Chapter 2) have been difficult to develop due to the limited post-event data for specific type of hazards (Tarbotton *et al.*, 2012). Most of the previous recovery models reviewed in Chapter 2 simply generate hypothetical damage scenarios and in most cases these are not even related to previous hazardous events. In order to overcome this lack of information, the first part of this chapter proposes a damage scenario simulation that uses existing hazard susceptibility data to identify those elements that are more vulnerable to damage from a hazard event. Based on a probabilistic approach, a damage state is

assigned to each damaged infrastructure and is quantified in units of repair resources-time. The second part of this chapter presents a repair model that simulates how damage is physically repaired over time. The resource allocation and repair process model is implemented in a three-stage model. It assigns resources to damaged places following a pre-defined priority order of repairs, updates the damage that is repaired on each day and converts this repaired damage into changes in road capacity. Therefore, the model combines a resource allocation module and a damage repair module to produce a road capacity recovery schedule.

Figure 4.1 shows how the output of the damage scenario simulation model is part of the input to the infrastructure repair model. The output of the repair model is the road capacity schedule for a specific repair strategy. Note that the model described in this chapter only involves the generation of a damage scenario and the physical repair of the damaged network. This means that the drivers' reaction to these network changes is still not simulated. This is incorporated in the model in chapters 5, 6 and 7 of this thesis.

The following sections of this chapter describe more in detail these two frameworks and apply the model to the Sioux Falls Network (South Dakota, US) in order to illustrate how it works.

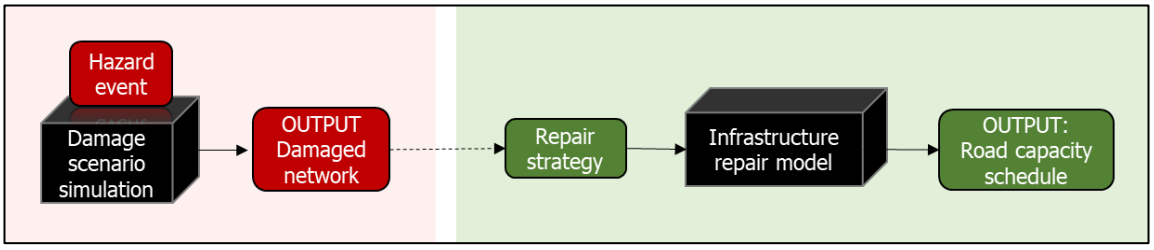

Figure 4.1. Simplified framework of the damage scenario simulation and infrastructure repair model

4.2. Damage scenario simulation: from hazard susceptibility to damage quantification

The determination of infrastructure damage is a very complex process that requires the help of engineers and professionals to assess the physical impact on road infrastructure. Damage is normally assessed by post-event inspections. A group of

engineers attends the incident location, assesses the severity of the damage and therefore, evaluates the amount of work that is required to repair this damage.

The review of previous road recovery models described in Chapter 2 identifies three major approaches that model damage to infrastructure: (1) an approach in which the modeller creates a hypothetical impact; (2) an approach in which the modeller use historic data to model damage of previous events; and (3) a stochastic approach, such as those based on fragility curves or based on a known probability distribution of damages. The creation of fragility curves for certain infrastructure under the impact of a specific type of hazard is a complex process that traditionally have been obtained based on seismic data (as observed in the review of Chapter 2) (Mai, Konakli and Sudret, 2017). One of the examples that uses fragility curves to analyse the vulnerability of transport networks and evaluate the system resilience is the work developed by Nogal *et al.* (2015).

However, the difficulty in obtaining these curves for some types of hazards would limit the application of the model presented in this thesis to certain hazards. In fact, if this approach were used in this thesis, the presented model would be limited only for seismic hazards. As the aim is to create a model that can be used for any type of hazard event, this approach has not been considered. In addition, the availability of data from previous hazard impacts is often scarce and modellers cannot use this data to predict future events because it is insufficient. As opposed to the most common recovery models that generate hypothetical impacts, the framework presented in this section describes an alternative methodology that uses the hazard susceptibility concept as a way to generate more realistic damage scenarios. Recently, hazard susceptibility modelling approaches have raised more interest among researchers and more advanced techniques have been developed (Pourghasemi *et al.*, 2020) which has made possible the application of the methodology to all types of hazards. A detailed description of the susceptibility concept is defined in the following Section 4.2.1.

The procedure that is followed to create damage scenarios is shown in Figure 4.2. Initially, a hazard susceptibility map is used to identify which road segments are damaged or undamaged. Then using a pre-defined probabilistic damage state function, a categorical severity of the damage is assigned to each damaged road

segment. Finally, a function that converts the categorical damage state to a numerical value is used to quantify the damage on each road segment. The following sections describe more in detail each aforementioned steps.

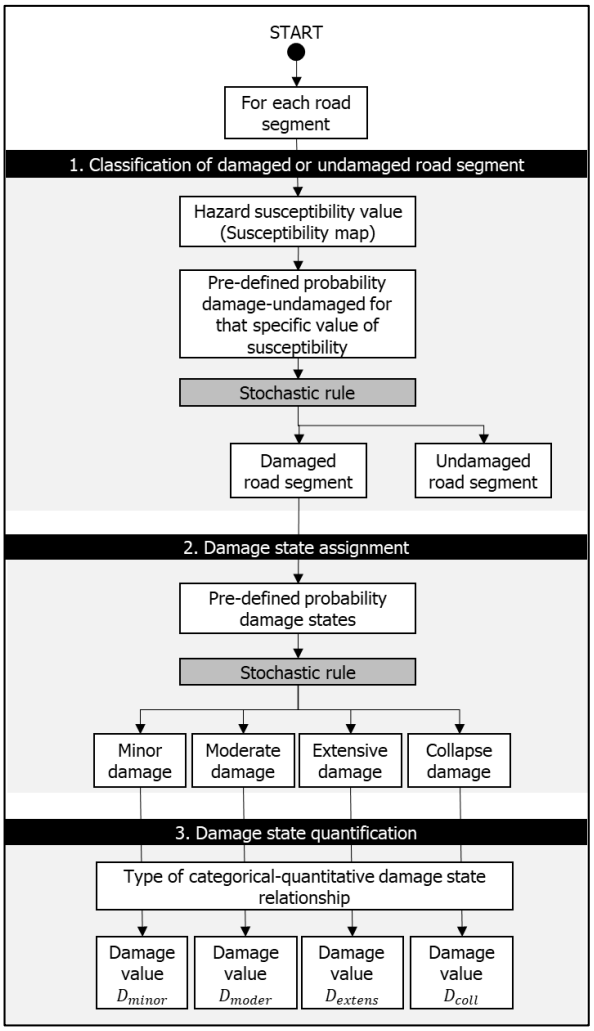

Figure 4.2. Process of assigning and quantifying a damage state to a road segment.

4.2.1. From hazard susceptibility to damage selection

The concept of hazard susceptibility is defined as the likelihood of a specific hazard occurring in an area (Brabb, 1984). In other words, it is the degree to which an area might be affected by the impact of any hazard event. Susceptibility answers the question of where the hazard is more likely to occur. It is important to mention that the concept of susceptibility does not consider the magnitude of the expected hazard impact nor the temporal occurrence of the hazard. It only accounts for the probability of spatial occurrence. This information can be useful as it allows the identification of

areas which are more prone to be impacted by certain hazards. However, the assessment of hazard susceptibility of an area is out of the scope of this project and therefore, already existing susceptibility data is used in this model.

In this project, hazard susceptibility is classified into four main groups: (1) high susceptibility; (2) moderate susceptibility; (3) low susceptibility and (4) not susceptible. If an area is highly susceptible to a certain hazard, road segments that are located in that area will be more likely to be affected by this hazard. Based on this idea, a stochastic rule is defined to identify which road segments are damaged: the higher the hazard susceptibility is, the more likely the road segment is identified as damaged. Figure 4.3 shows the relationship between damage probability and susceptibility classification. Each modeller needs to define the limit levels (a, b and c) that separate the damaged part and the undamaged part.

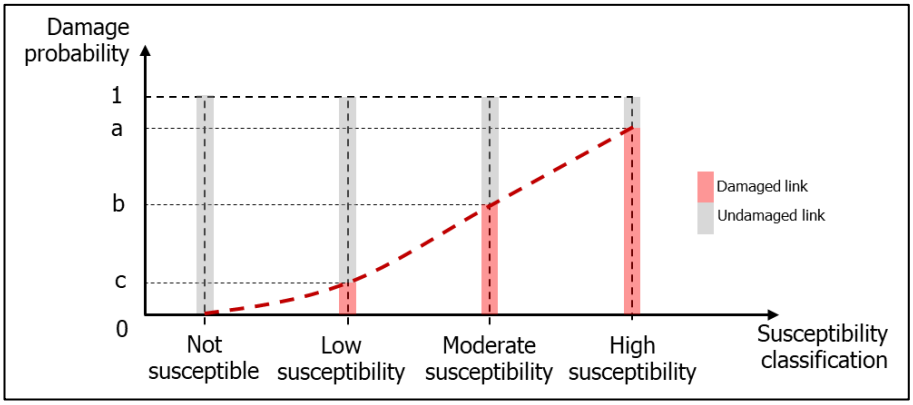

Figure 4.3. Hazard susceptibility vs. damage probability graph

A random number ϑ_l is generated for each road segment. A road segment will be classified as damaged if the random number has a value below the limit level. This is expressed in Equation (4.1) which defines the binary variable Dm_l as the value that indicates whether the road segment is damaged or not.

$$Dm_l = \begin{cases} 1 & if\ \vartheta_l \leq PL_{\lim} \\ 0 & otherwise \end{cases} \quad (4.1)$$

Where,

Dm_l, binary variable that indicates if the road segment l is damaged ($Dm_l = 1$) or undamaged ($Dm_l = 0$).

ϑ_l, random number for road segment l

$PL_{\lim}$, is the upper limit that is used to classify a road segment as damaged or undamaged. It takes different values depending on the level of susceptibility associated with each road segment: High susceptibility ($PL_{\lim} = a$), Moderate susceptibility ($PL_{\lim} = b$), Low susceptibility ($PL_{\lim} = c$) and Not susceptible ($PL_{\lim} = 0$).

4.2.2. Categorical damage states and damage assignment

Once road segments are identified as damaged/undamaged, the extent of the damage also needs to be simulated. HAZUS (FEMA, 2013) defined five qualitative damage limit states to evaluate the severity of damage on structural infrastructure after seismic impacts. These have been used extensively in previous studies as mentioned in the literature review (Chapter 2). These are: (1) No damage; (2) Slight/Minor damage; (3) Moderate damage; (4) Extensive damage; (5) Complete damage. It is not easy to define exactly the type of damage that each category includes because it depends on the hazard event and the type of infrastructure that is being affected. In this model, only the impact of a single type of hazard is considered. However, if multiple types of hazard concurrently impact the road network, it must be assumed that the damage state that is assigned to each damaged road segment requires the same recovery effort even if repair activities are different for each type of hazard. This means that, for instance, the amount of repair work involved in a 'minor damage' has to be similar when it is produced by a flooding event or by a landslide event, even if repair activities are different.

Once the amount of repair work is defined for each damage state, it needs to be assigned to each damaged road segment. As mentioned before, fragility curves are not always available to use for all type of hazards and all type of infrastructure. For that reason, the general model proposed in this chapter uses a stochastic rule and a uniform probability distribution function that assigns a damage state to each road segment. The procedure is the following: (1) Generate a new random number (ϑ_n) between 0 and 1; (2) For simplicity, a uniform cumulative distribution function is used in Equation (4.2) to obtain the probability value (also shown in Figure 4.4); (3) Identify the damage state using the Equation (4.3). Note that the probability distribution function can be changed by the modeller, if more information is provided.

$$P(\vartheta_n) = \vartheta_n \tag{4.2}$$

Where,

$P(\vartheta_n)$, is the uniform cumulative probability distribution.

ϑ_n, is a random value between 0 and 1.

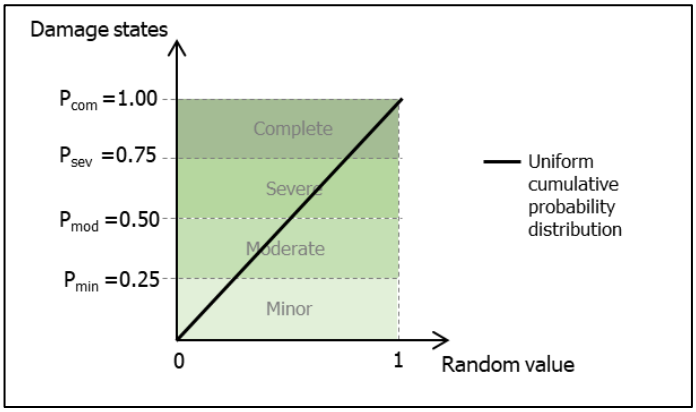

Figure 4.4. Example of a damage state assignment graph with values of $P_{min} = 0.25, P_{mod} = 0.5, P_{sev} = 0.75$.

$$Dam_{state} = \begin{cases} Minor, & if\ P(\vartheta_n) \leq P_{min} \\ Moderate, & if\ P_{min} < P(\vartheta_n) \leq P_{mod} \\ Severe, & if\ P_{mod} < P(\vartheta_n) \leq P_{sev} \\ Complete, & if\ P(\vartheta_n) > P_{sev} \end{cases} \tag{4.3}$$

Where,

$P_{min}, P_{mod}, P_{sev}$, is the limit that defines the minor, moderate and severe damage states, respectively.

$P(\vartheta_n)$, is the uniform cumulative probability distribution.

4.2.3. Units of damage

The question that arises here is: How is road damage measured? The quantification of damage requires the definition of a unit that is used to measure the amount of damage. The process of quantifying damage state on road infrastructure in a single variable is not straightforward.

As described in Section 2.5.1, previous recovery models use repair units to quantify damage. Some of them determine the number of steps to repair that

damage. Others assign directly repair time to each damaged infrastructure. And others consider the productivity of repair resources, so that repair time can be calculated. As described in previous Section 3.3, the model presented in this thesis is defined to allocate limited resources on multiple damaged road segments and this cannot be done if damage is quantified by simply using the number of steps or repair time. This model goes a step further and assigns repair teams (resources) to damaged places. In this case, the metric used to quantify damage on road infrastructure is measured in units of resource-time. It means that "R" amount of resources are required during "T" days (time) to repair the damage. This defines an "area" of damage that needs to be repaired. If fewer resources are assigned to this damaged infrastructure, more repair time is required to repair the same damage. Figure 4.5 shows the aforementioned relationship. The shaded area is the amount of damage that needs to be repaired. The brown area and the blue area contain exactly the same damage (because the area is the same). Depending on how many resources are assigned to each place, the damage can be repaired faster/slower because more/less resources are assigned to each place, respectively.

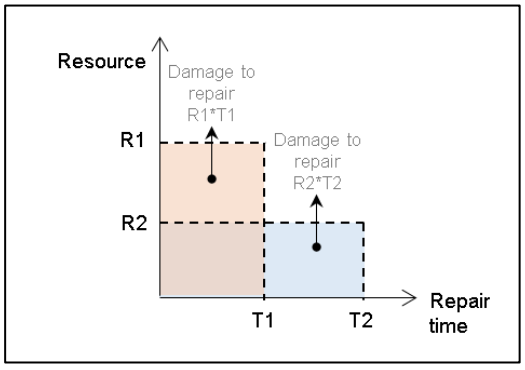

Figure 4.5. Damage quantification. Both shaded areas contain the same damage, but different number of resources and repair time.

4.2.4. From categorical damage state to quantitative damage

Based on the description of categorical damage states, each damaged infrastructure has been assigned to a specific damage state in Section 4.2.2. This state can be transformed into a numerical value in units of resource*time using a pre-defined step function. Figure 4.6 shows three types of categorical and quantitative damage state relationships. As observed, if there is no damage, then this value will be 0*D, being

D an initial damage value (Base Damage) defined by the user. If damage is complete, it is assumed to be 4*D in this case. Note that this categorical-quantitative relationship is not limited to the ones proposed in this section and other functions can be proposed. These relationships have been generated for the purpose of illustration assuming three different types of damage behaviour. Further research needs to be done in order to validate these values with real data.

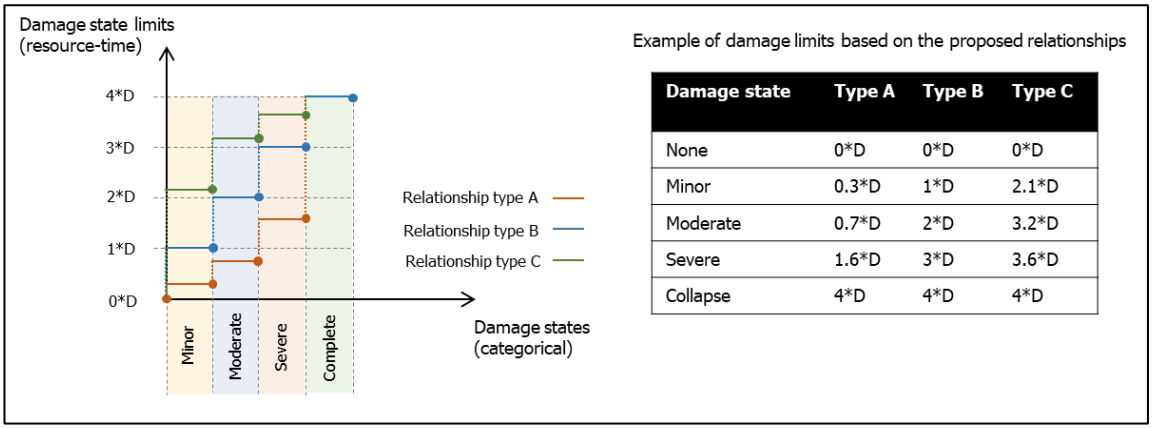

Example of damage limits based on the proposed relationships

Damage state	Type A	Type B	Type C
None	0*D	0*D	0*D
Minor	0.3*D	1*D	2.1*D
Moderate	0.7*D	2*D	3.2*D
Severe	1.6*D	3*D	3.6*D
Collapse	4*D	4*D	4*D

Figure 4.6. Categorical and quantitative damage state relationships. "D" is defined as the base damage applied to each type of relationship.

The fact that a 'Base damage' variable (D) is included in the relationship proposed in Figure 4.6 makes this method more flexible to be adapted to any type of hazard event. Depending on the type of hazard that is being analysed, the base damage can acquire a higher or a lower value. And then, based on the proposed relationships, the damage value on the rest of the other damage states can be easily obtained.

Note that if data from real damage of a past event is provided, then all this procedure is not needed and therefore the modeller can also introduce manually the damage values of each affected infrastructure.

4.3. Three-stage road infrastructure repair modelling: the framework

This section presents a resource allocation and repair process model that simulates how repairs are carried out in a day-to-day basis. The main aim of this model is to generate a resource allocation plan and a recovery schedule that includes a road

opening plan based on a pre-defined repair strategy (see Figure 4.7). These are explained more in detail in the following sections. The output of this model (network capacity plan) will be one of the inputs of the traffic simulator which will be used in Chapters 5, 6 and 7.

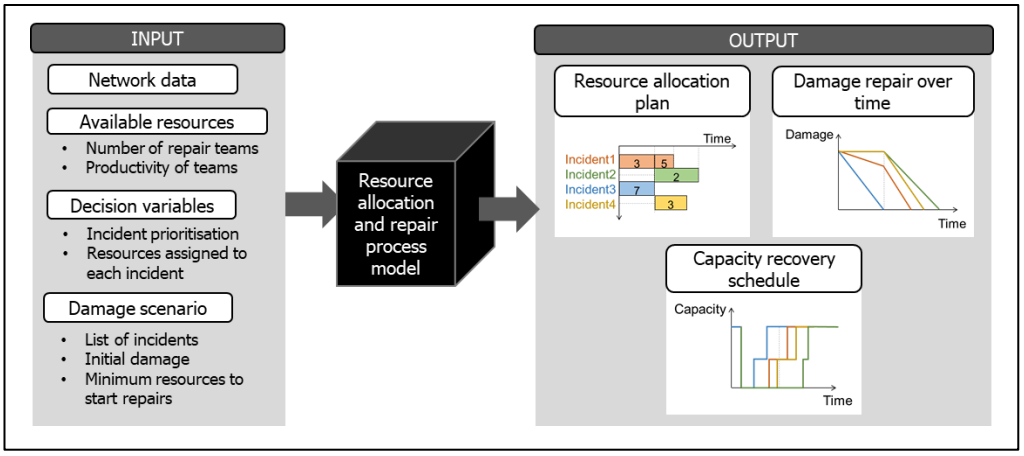

Figure 4.7. Inputs/Outputs of the resource allocation and repair process model

The model proposed is composed of three main stages as shown in Figure 4.8. The aim of the first stage of the model is to assign resources to each damaged road segment following the priority order of repairs that has been defined by the proposed repair strategy. This information will be used on the second stage of the model to measure the amount of damage that is repaired if these resources are allocated on this damaged road. This stage allows the monitoring of the damage and repairs at all times. The third stage of the model is therefore responsible for opening roads to traffic, once certain damage is repaired. All three stages are modelled sequentially during each day, so that information can be transferred between modules.

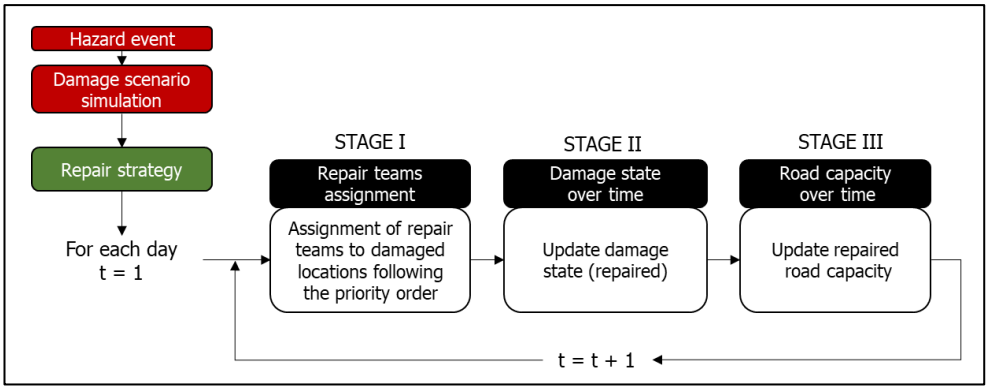

Figure 4.8. Three-stage resource allocation and repair process model

This model assumes that road capacity can only be increased between days and not within a day. The main reason is just to make the general problem easier. Changing the capacity of roads between days allows drivers to know at the beginning of their trip the state of the network. Although it may also be interesting the analysis of drivers' behaviour under dynamic changing network conditions within a day, this is out of the scope of this model. The rest of this section explains more in detail the three stages of this module.

4.3.1. STAGE I: Repair teams, resource productivity and resource allocation process

4.3.1.1. Repair team definition and productivity

The term *resource* defined in the damage quantification is a generic term that is used to represent those individuals or elements that carry out the repair process. Resources are grouped in repair teams, which are considered as the minimum indivisible unit of this repair model. Each repair team is formed by a group of personnel, plant and equipment, which are the main elements that are required to carry out the repair process. In this model, a repair team is a discrete variable. Depending on how many personnel, plant and equipment are within a repair team, the productivity of each repair team will be higher or lower. In this sense, productivity is defined as the amount of damage that can be repaired on a day by a repair team. Initially, the modeller has to decide how big the repair teams are in terms of personnel, plant and equipment

and according to this, assign a productivity per repair team. The current version of this model assumes that all repair teams have the same productivity. This implies that there is only one type of repair team, but further improvements could incorporate the possibility of adding different types of repair teams with different productivities.

In order to speed up the repair process, more than one repair team can attend the same incident location. As shown in Figure 4.9, this model assumes a linear relationship between repair teams and productivity. The more repair teams (RT) are assigned to the same place, the more damage they repair in a shorter amount of time (PD, more productivity). However, there is also a saturation point (RT_{max}) where the addition of more repair teams do not increase the productivity. It is also possible that certain damaged places need a minimum number of repair teams (RT_{min}) to start repairs. If there is only one available team and more than one repair team is required, then repairs cannot start as the difficulties of the tasks require more than one repair team.

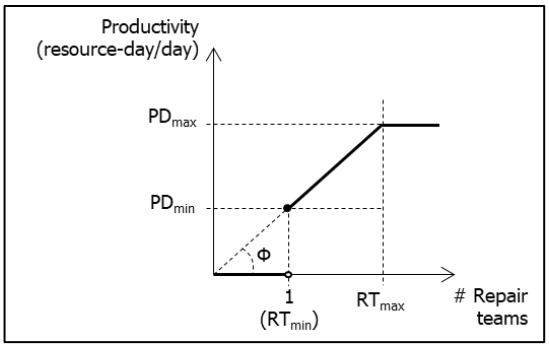

Figure 4.9. Productivity – number of repair teams relationship.

Equation (4.4) expresses mathematically the relationship between productivity and repair teams. The modeller needs to specify the maximum number of repair teams (RT_{max}) that can work at the same damaged location without reducing the productivity and the gradient or the slope (g) of the productivity-resource relationship. Knowing the number of repair teams assigned to each damaged location, the productivity can be obtained following the Equation (4.4).

$$PD = \begin{cases} \mathrm{g} \cdot RT_{max} & if\ RT \geq RT_{max} \\ \mathrm{g} \cdot RT & if\ RT_{min} \leq RT < RT_{max} \\ 0 & if\ RT < RT_{min} \end{cases} \quad (4.4)$$

Where,

RT_{max}, is the maximum number of repair teams that can attend the same incident location without reducing the total productivity.

RT_{min}, is the minimum number of repair teams that needs to attend the damaged location in order to carry out repairs. This is normally assumed to be 1.

g, is the gradient of the line. Note that $\tan(\phi) = g$.

RT, is the number of repair teams that are assigned to a damaged place.

PD, is the productivity associated with the RT number of repair teams (resource-day/day).

4.3.1.2. Resource assignment sub-model and assumptions

The principle of the simulation process of the stage I is the assignment of the required repair teams to each damaged location following the priority order specified in the repair strategy. If not enough resources are available, then repairs will have to wait until higher-priority roads have been repaired and their resources released to repair new damaged locations. Some assumptions are also considered in this model: (1) it is assumed that once the repair of a road segment begins, the repair team assigned to this damaged location must complete the restoration of this road before attending another incident location; (2) it is also assumed that no time or cost is spent when repair teams move from one damaged road to another. Consequently, the existence of depots is not considered in this model; (3) no more repair teams than the ones required by the repair strategy can be assigned to each road segment; (4) repairs can start on a road segment if there are equal or higher available teams than the minimum number of repair teams required to start repairs. The following Figure 4.10 shows the flowchart that has been implemented in MATLAB to develop this resource assignment submodel.

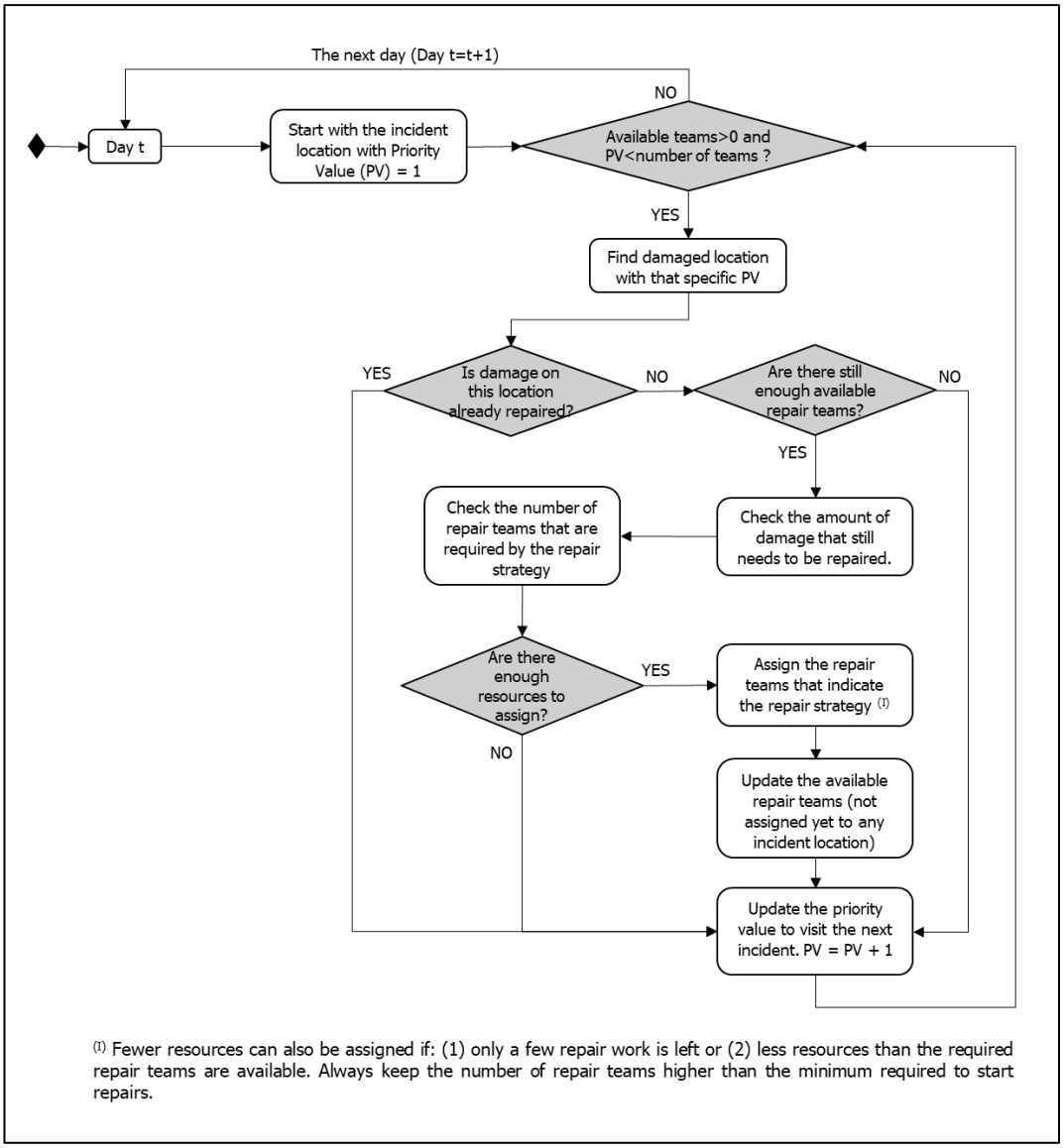

Figure 4.10. Flowchart of the resource assignment

4.3.2. STAGE II: Road damage repair over time

4.3.2.1. Damage-time relationship

Once all repair teams are assigned to each damaged road segment, damage repairs need to be simulated. The evolution of damage repair over time is directly connected to the previous stage I. Depending on the amount of resources assigned to each road segment on each day and based on their total productivity, a value of damage is repaired. Figure 4.11 illustrates the most general damage-time relationship that can be obtained from this sub-model. The line on this graph represents the evolution of damage repair over time. It is composed of five different parts: (PART A) Pre-

disrupted state. It is assumed that there is no damage before the disruption; (PART B) Waiting time, which is the time it takes for an already damaged road segment to receive repair resources. No damage is repaired in this section; (PART C) Fewer resources than the maximum number of required resources are assigned to this segment. In this sense, damage is repaired but in a slower pace as not all resources are completely assigned. Note that every time a new repair team attends the repairs of this road segment, there is a change in the slope of the damage-time relationship. This means that there can be more than just one PART C in Figure 4.11; (PART D) The maximum number of required resources are assigned to the road segment. This is the section of the graph that achieves the maximum vertical slope. Once resources are allocated, they are not reduced, except when the remaining damage requires less than the resources allocates for a single day, which is the case of the next part E; (PART E) Fewer resources than those required are assigned to the road segment because the amount of damage left does not require the maximum number of resources. This part usually takes a day of repairs.

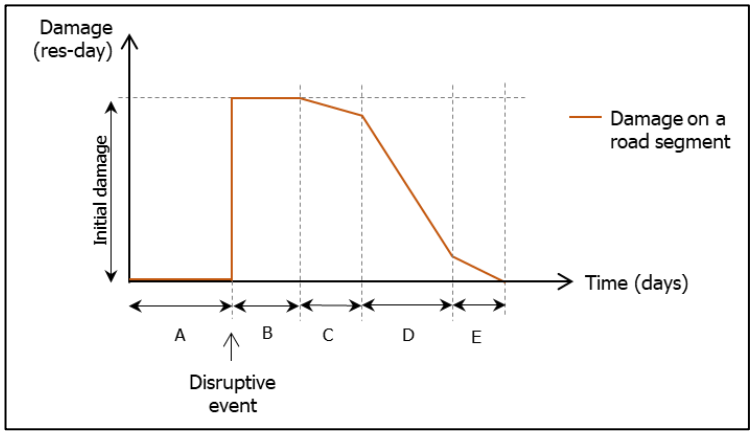

Figure 4.11. Evolution of damage over time during repairs

This damage-time relationship considered in this model adds an additional feature that is not contemplated in previous models. Normally damage-time relationship is only represented in previous models by parts A, B and D of Figure *4.11* (Bocchini and Frangopol, 2012b, 2012a; Karamlou and Bocchini, 2014; Unal, 2015). Orabi *et al.* (Orabi *et al.*, 2009) mentioned that repairs can start with fewer resources than their resource requirements, which indirectly implies the addition of part C as well. The model proposed in this section adds the possibility of having multiple parts C (different amount of resources are added on different days) and an additional part

E that releases some resources from current repaired place to other damaged places only when the damage left can be repaired by fewer resources rather than the maximum required resources. This is beneficial as it allows a more realistic representation of how repairs are carried out.

4.3.2.2. Update damage value after day-to-day repairs

The amount of damage that is repaired each day is calculated based on the number of repair teams that are working on site. Equation (4.5) describes this damage repair update. Figure 4.12 shows the flowchart that has been implemented in MATLAB to simulate this damage-time relationship.

$$RD_l^t = RD_l^{t-1} + 100 \cdot \left(\frac{PD_l^t \cdot \Delta t}{D_l^0} \right) \tag{4.5}$$

Where,

RD_l^t, is the percentage of damage that is repaired of damaged road segment l on day t.

RD_l^{t-1}, is the percentage of damage that is already repaired on day $t-1$.

D_l^0, is the total damage (in resource-day) that needs to be repaired on this damaged road segment l.

PD_l^t, is the productivity (in resource-day/day) of repair teams allocated to damaged road segment l on day t.

Δt, interval of time (in days) that the repair teams are working. In this model, this is always considered as one day ($\Delta t = 1$) which is the minimum indivisible unit of time.

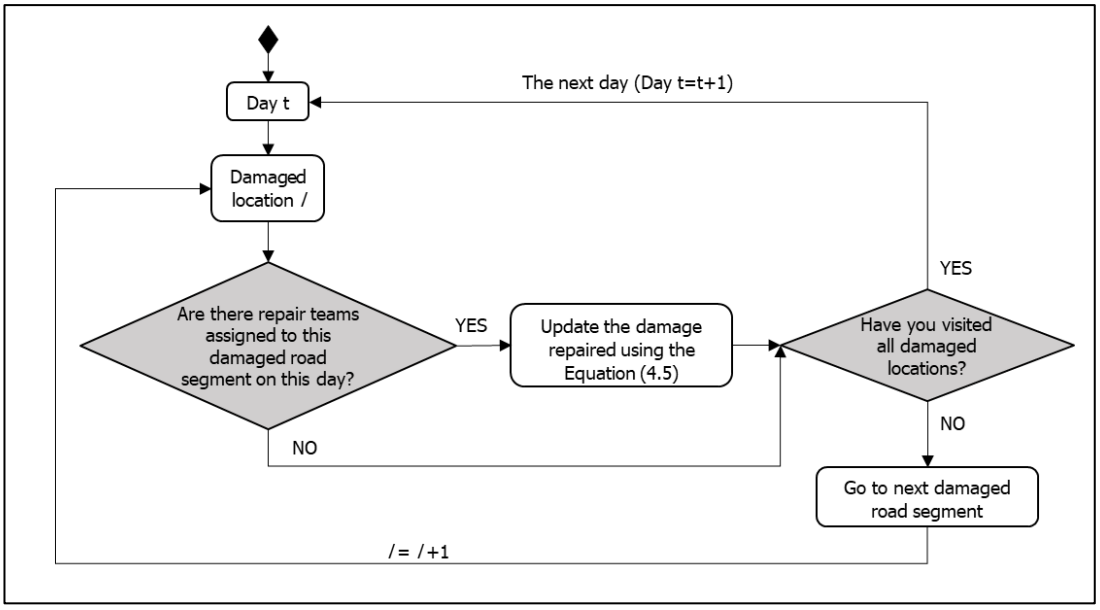

Figure 4.12. Flowchart of the damage repair progress model

4.3.3. STAGE III: Road capacity changes after repairs

4.3.3.1. Damage-Capacity relationship

As mentioned in previous sections, the extent of damage is linked to a reduction in road capacity. Once certain damage is repaired, road segments can be partially or totally open to traffic. To make it easier, if a road segment needs to be closed after a disruption (zero capacity), the damage-capacity relationship proposed in this model (as shown in Figure 4.13), which follows a deterministic approach, is defined as a three-step relationship in which road capacity can only take three values 0%, 50% or 100% of the initial road capacity (pre-disruption capacity) depending on the amount of damage that is repaired. This relationship could change depending on the decision of the corresponding transport manager/authority. Only when 50% of initial damage is repaired, is road capacity increased. And once all damage is repaired, then the road segment is totally open to traffic.

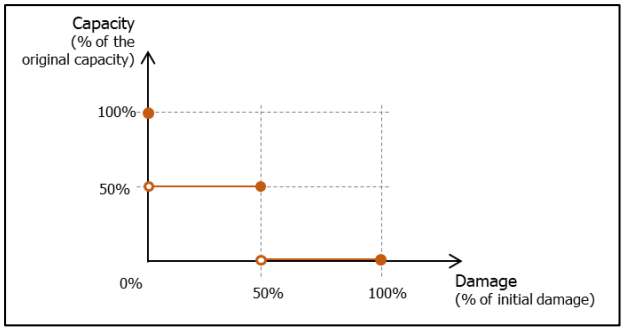

Figure 4.13. Damage-Capacity relationship used in this model when the capacity of the damaged road segment after the disruption is zero.

There can be cases in which road capacity after disruption is not zero (Figure 4.14). Capacity after disruption can be any value between 0% and 100% of the initial road capacity, being 0% when the road is totally closed to traffic and 100% when it is totally open. As shown in Figure 4.14, this model defines three cases: CASE A, when capacity after disruption is 0% of the initial road capacity (Figure 4.13); CASE B, when capacity after disruption is between 0% and 50% of the initial road capacity; or CASE C when capacity after disruption is between 50% and 100% of the initial road capacity. In Case A and B, road capacity takes the value of 50% of the initial capacity when 50% of the initial damage is repaired. On the contrary, in Case C, as the post-disruption capacity is higher than 50% of the initial road capacity, it only takes the value of 100% when repairs are complete. The flowchart that has been implemented in MATLAB is the one included in Figure 4.15.

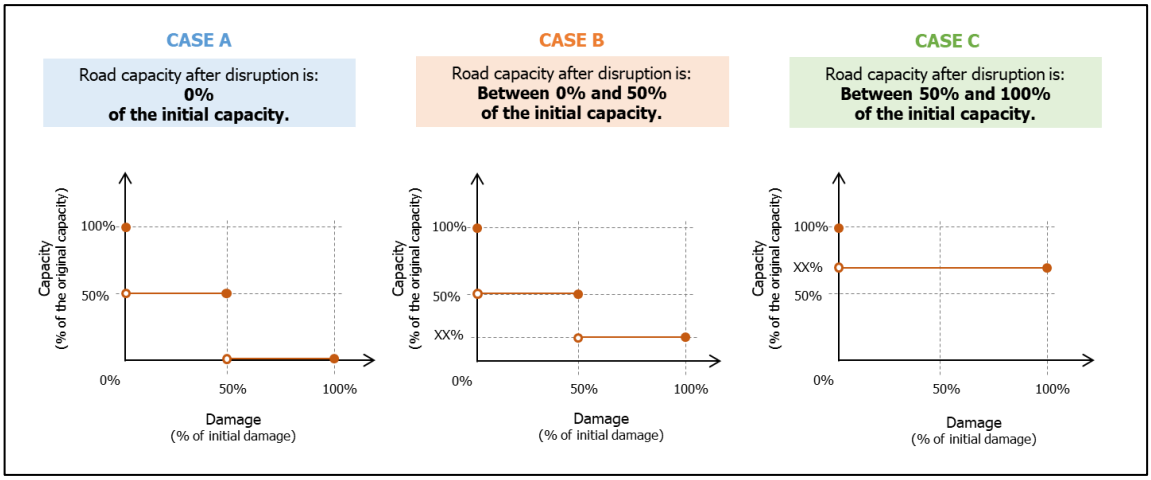

Figure 4.14. Damage-Capacity relationship when initial capacity is lower than 50% and higher than 0% (on the left) and lower than 100% and higher than 50% (on the right).

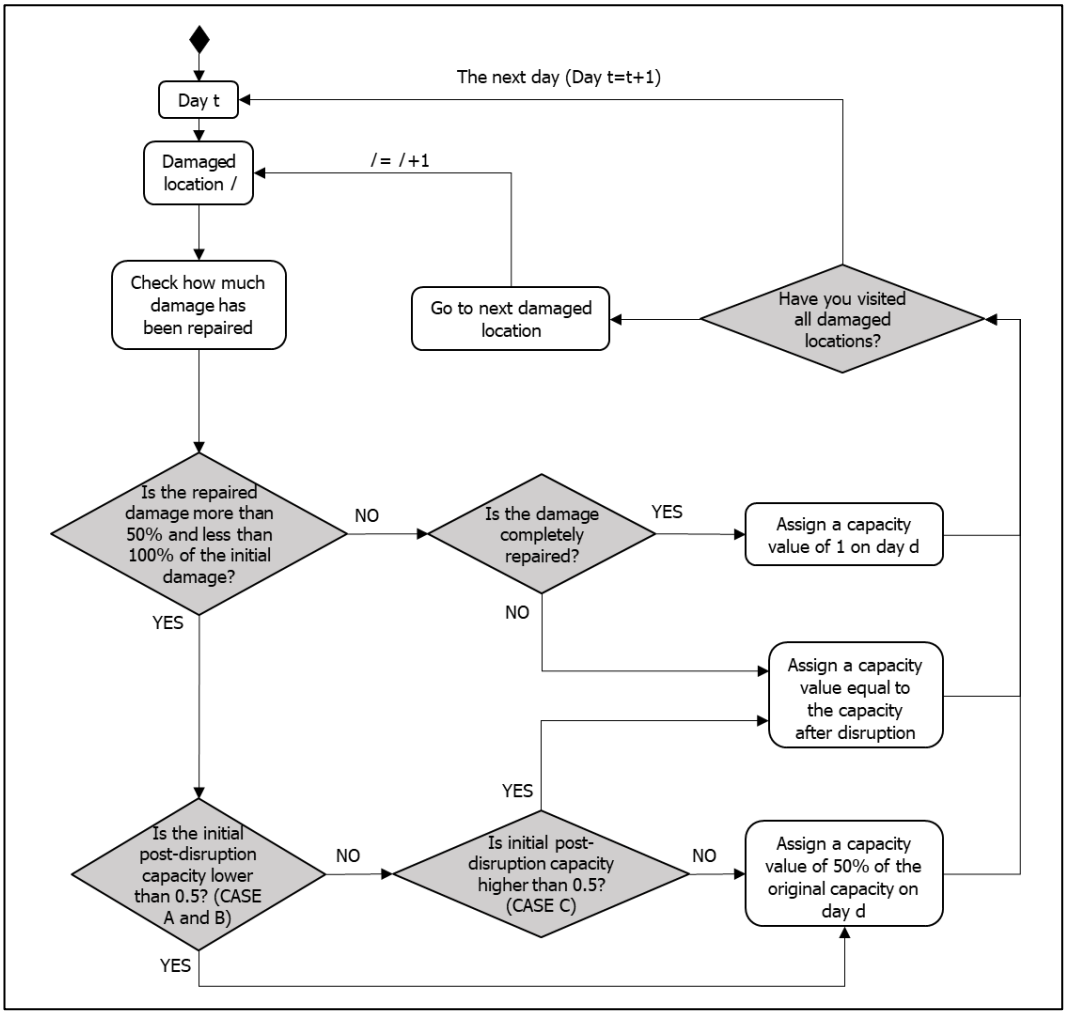

Figure 4.15. Flowchart of the damage-capacity sub-model.

4.3.3.2. Capacity-Time relationship

The final output of this submodel is the evolution of capacity over time on all damaged road segments. This is the information that will be used as an input on the traffic simulation module.

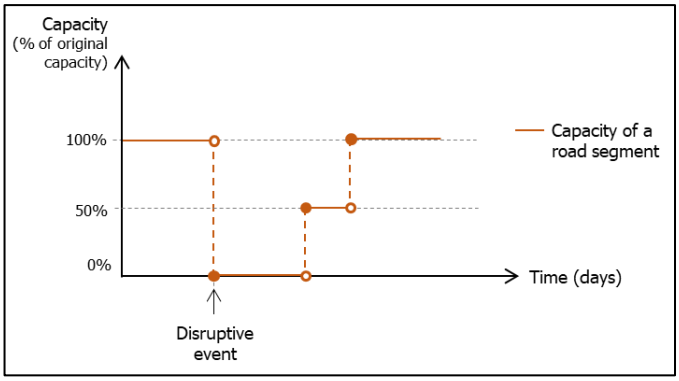

Figure 4.16. Example of the output of the resource allocation model: Evolution of road capacity over time

4.4. Illustrative example

To facilitate the understanding of the concepts described in this section, the resource allocation and damage repair model is applied to the well-known transportation network, Sioux Falls Network (South Dakota, US) which has been used in numerous researches (Chen and Tzeng, 1999; Orabi *et al.*, 2010; Ye and Ukkusuri, 2015; Lu *et al.*, 2016; Basavaraj *et al.*, 2017). The aim of this example is to illustrate the process that has been explained in the previous sections.

4.4.1. Road network data

The Sioux Falls network consists of 24 nodes and 76 links as shown in Figure 4.17 and whose characteristics are presented in Table A.1 and Table A.2 of the Appendix A. The original geometry proposed by Leblanc (1975) has been modified to adapt it to the real network. The vertex coordinates have been taken from Chakirov and Fourie (2014).

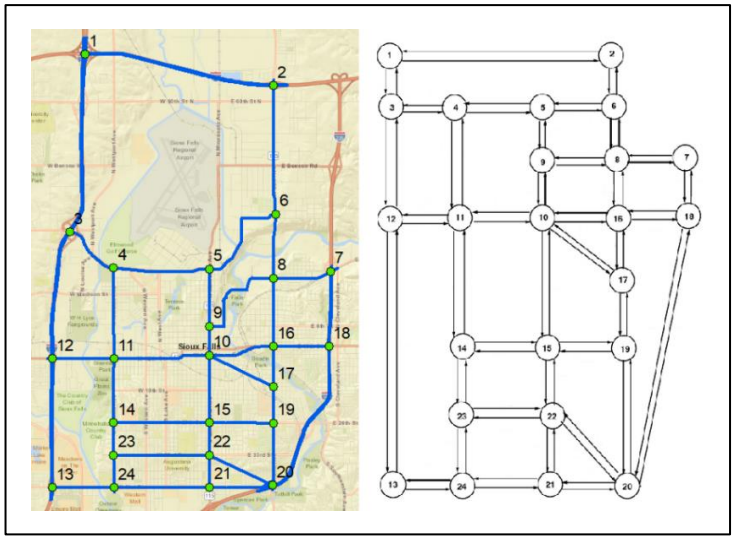

Figure 4.17. Sioux Falls network. On the left, adjusted geometry network (background from OpenStreetMap). On the right, the original Sioux Falls network used by Leblanc (1975).

4.4.2. Disruption scenario

This section aims to generate a damage scenario that simulates damage caused to multiple road segments as a result of a severe weather. A road segment susceptibility map (Figure 4.18) is used to show which road segments are more susceptible to be damaged by earthquakes. This map has been created by the author and does not correspond to any particular study done in the area. The susceptibility is represented by four categorical classes: not susceptible, low susceptibility, medium susceptibility and high susceptibility. As no more data was available, the damage probability associated with each level of susceptibility of each road segment is defined by the modeller. As described in Section 4.2, the level of susceptibility might indicate the likelihood that a road segment was affected by this hazard. This meant that if an area was highly susceptible to a certain hazard, road segments that were located in that area would be more likely to be affected by this hazard. Therefore, the probability of being damaged was higher. Based on this idea, Figure 4.19 shows the damage probability associated with each susceptibility level considered in this model. Initially, these values were assumed by the author, but if further data were available, these limits could change.

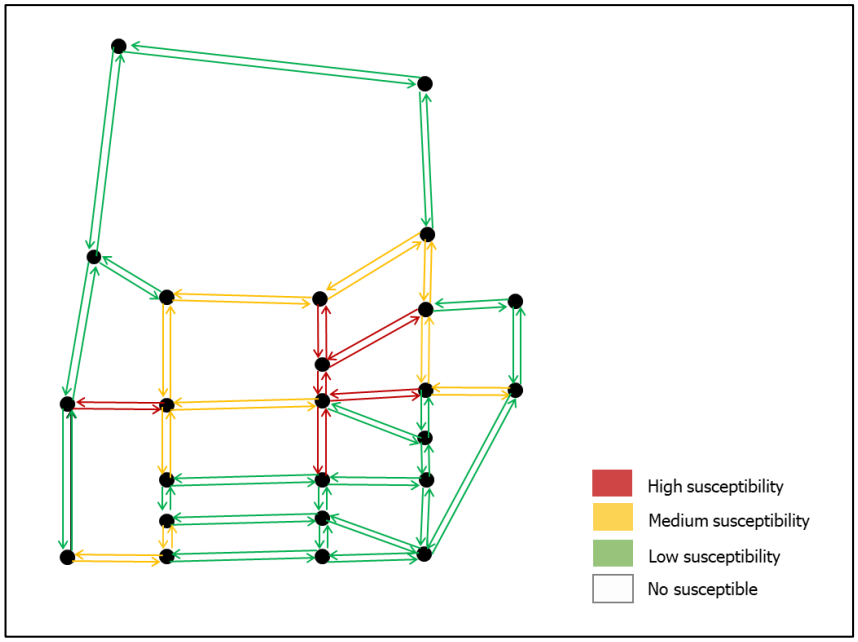

Figure 4.18. Hypothetic road susceptibility map of the Sioux Falls network.

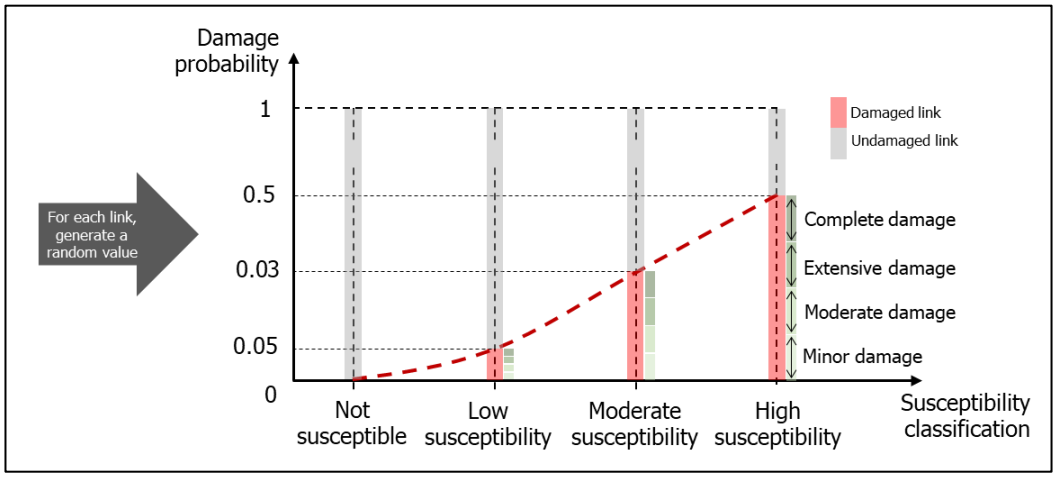

Figure 4.19. 'Hazard susceptibility vs. damage probability' graph. It shows the probability limits assumed for this example.

Based on the stochastic method presented in Equations (4.1), (4.2) and (4.3), several road segments are identified as damaged and a categorical damage state is assigned. The process of selecting which road segments are damaged is as follows: (1) Generate a random value for each road segment following a uniform probability distribution; (2) Depending on the susceptibility level of each road segment and considering a user-defined damage probability, it is classified as damaged road

segment (if the random value is above the probability associated) or undamaged road segment (if the random value is below the probability associated with that susceptibility level). This model assumes that if a road segment is damaged, the probability of having a minor, moderate, extreme or complete damage is selected according to a uniform distribution.

Ten bridges are identified to be susceptible to the impact seismic events on the Sioux Fall network. The location of the bridges is extracted from Chang *et al.* (2010). A hypothetical earthquake is assumed to impact the road network producing damage to certain bridges. A damage state has been assigned to each bridge as shown in Table 4.1 following a uniform probability distribution. The quantification of this damage state has been done using a linear relationship (see type B - Section 4.2.4). The value of the base damage is set to be D=10 res-day. As it is mentioned previously, damage is materialised as a reduction of road capacity. For this particular example, the damage-capacity relationship proposed by Padgett and DesRoches (2007) is adopted on this model.

Table 4.1. Disruption scenario: damage state, quantification and road capacity

Bridges	Damage state	Damage value (res-day)	Post-disruption road capacity (% original capacity)[1]
B1, B2, B9	No damage	0*D	100%
B3, B5	Minor damage	1*D	50%
B10	Moderate damage	2*D	0%
B7	Severe damage	3*D	0%
B4, B8, B6	Collapse damage	4*D	0%

Being base damage D = 10 res-day for this particular example

[1] Reference: Padgett and DesRoches (2007)

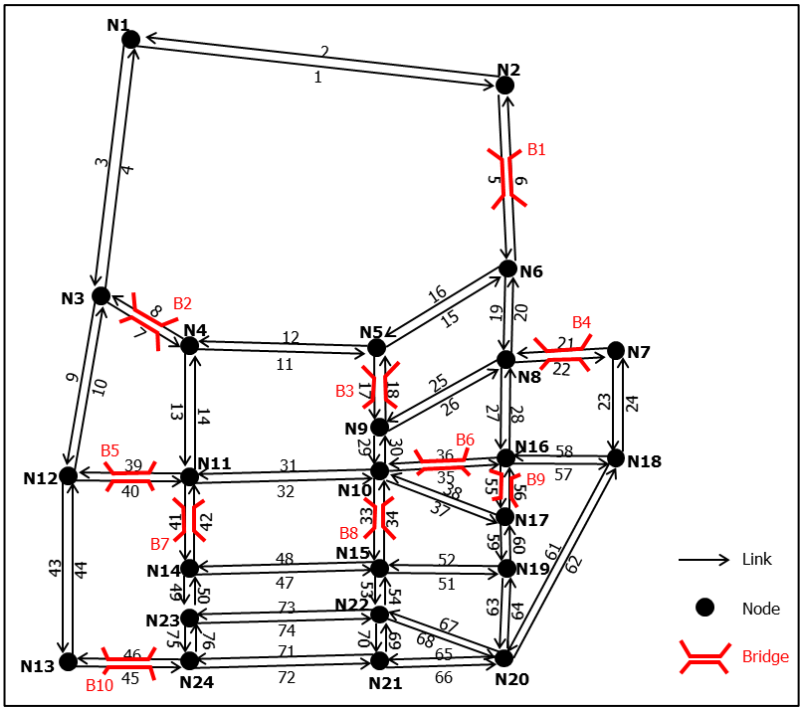

Figure 4.20. Simplification of the Sioux Falls network used in this model. The numbers correspond to the link and node number respectively. Bridges are shown in red.

4.4.3. Repair strategy and available resources

The initial proposed repair strategy is the one included in Table 4.2. It considers the priority order of repairs and the number of repair teams that are required to attend each incident location. This is the maximum number of resources that can be allocated to the same damaged place. The minimum number of repair teams must be defined by the modeller.

Table 4.2. Repair strategy proposed for this illustrative example

Repair strategy							
Damaged bridges	B3	B4	B5	B6	B7	B8	B10
Priority order of repairs (from higher to lower priority)	1	2	5	4	6	3	7
Number of required repair teams	5	5	5	5	5	5	5
Minimum number of repair teams	1	1	1	1	1	1	1

The number of resources that are available to repair all damaged places are 13 repair teams. It is assumed a linear relationship between the productivity and the

number of repair teams that work at the same damaged location, as shown in Figure 4.21. The saturation level of repair teams is set at 5.

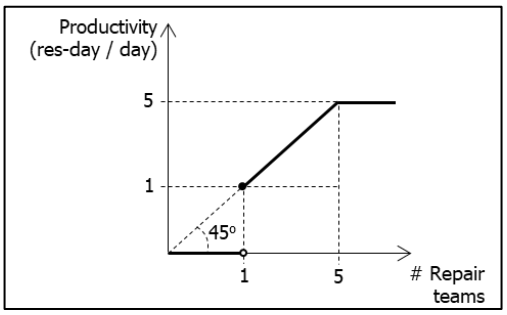

Figure 4.21. Productivity-repair team relationship for this example

4.4.4. Repair process and model outputs

The repair process follows the procedure described in Section 4.3. During the stage I, the number of required repair teams that are specified on the repair strategy are assigned to damaged locations following the priority order of repairs. The output of this Stage I is a road repair scheduling that is displayed using a Gantt chart. Figure 4.22 shows the output of this submodule. On day 1, all required repair teams are assigned to the bridge that has higher priority (in this case, B3). If there are spare resources, these are assigned to the bridge with the second-highest priority and so on.

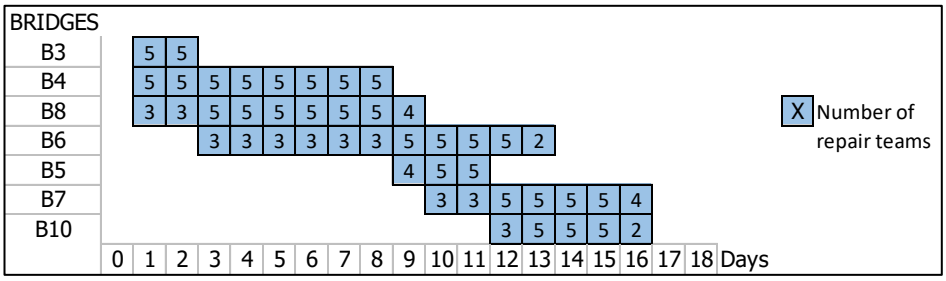

Figure 4.22. Road repair schedule using a Gantt chart

Once all repair teams are assigned to incident locations on day 1, repairs are carried out and damage values are reduced using the Equation (4.5). This process belongs to Stage II. Figure 4.23 displays the evolution of these damage values of each damaged bridge over time.

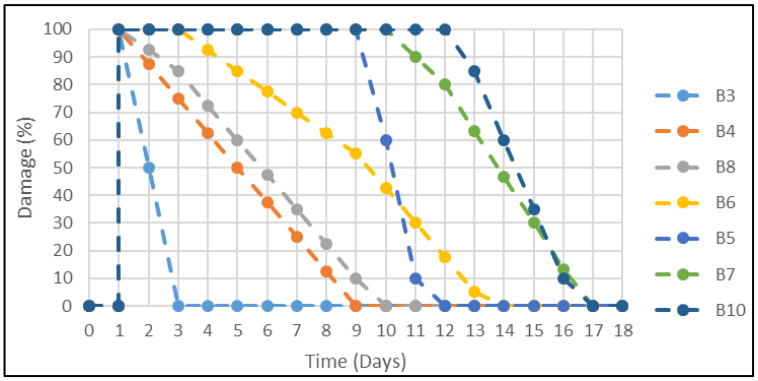

Figure 4.23. Evolution of the percentage of damage over time. Disruption happened on day 1.

From an operational point of view, after each damage is reduced, Stage III is responsible for checking if the road segment can be open to traffic or not. Using the pre-defined damage-capacity relationship shown in Figure 4.13 and Figure 4.14, an opening-closing schedule of damaged bridges can be obtained. Note that, in the relationship proposed in this model, road capacity only takes the value of 0, or the value of 50% of the initial capacity or the value of 100% of the initial capacity. However, other types of damage-capacity relationships can also be implemented. Figure 4.24 shows in red those bridges that are totally closed to traffic, in yellow those that are partially open and in green those that are totally open to traffic. As observed, this repair strategy requires 16 days of repairs to totally open the road network to traffic. On day 15, all network is open to traffic although only partially connected on bridges B7 and B10.

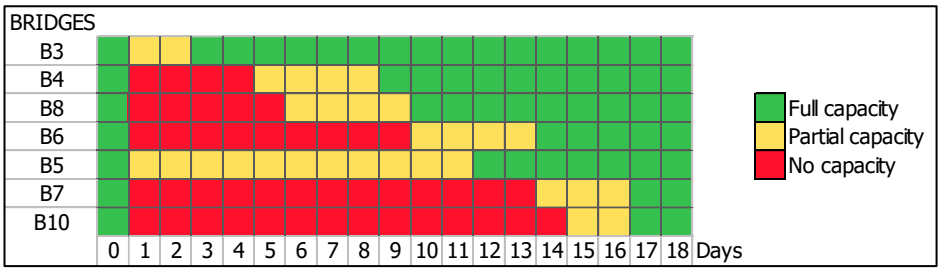

Figure 4.24. Closing-Opening dates of these damaged bridges. In green, totally open to traffic. In yellow, partially open. In red, totally closed to traffic.

A resilience index can also be used to compare different recovery strategies. In this case, using the output that this repair model is providing, the resilience index

can be defined as the earliest time that the network is fully recovered. In this example, the earliest time is 16 days, but there might be other recovery strategies whose earliest time was lower/higher. Instead of using the earliest time to fully recover the network as a resilience index, other ones can also be used: for instance, the earliest time to have all damaged road segments partially open to traffic, or the number of damaged road segments that are fully recovered on a certain day, among others.

4.4.5. Sensitivity analysis of parameters

This section analyses the sensitivity of the model to changes in: base damage value (D), available repair teams, productivity values and saturation level of repair teams. The 'one-at-time sensitivity' technique is used, whose aim is to create a variation of one parameter, keeping all the rest of parameters fixed, and observe the variation in the model outputs. Due to the limitation of space on this chapter, results from the tests are included in Appendix 2 and only general conclusions are provided in this section.

Results from the analysis evidence the importance of the variables. Some of them such as the base damage value and the available repair teams are variables that are considered as a given fixed value for all scenarios. This means that it is not possible to change their value, otherwise the problem would change in itself. However, the productivity values and saturation level of repair teams may have a significant impact on the repair process. The saturation level limits the number of teams that can work at the same time on the same damaged location. This has a significant impact as the higher the saturation level is, the faster the repair process is. Ideally the number of required teams selected by the pre-defined repair strategy (maximum repair teams) should be close to the number of saturation teams.

4.5. Contribution to the knowledge

The contribution that this chapter adds to the body of knowledge of road network recovery includes:

1. The development of a stochastic method to simulate damage scenarios. As opposed to previous models that just made up damage scenarios with no evidence of data, this method tries to provide a systematic framework that

allows the modeller the generation of new damage scenarios. In this model, hazard susceptibility data is used (if available) to identify which road segments are more vulnerable to the impact of hazard events. Then this information is used to assign a categorical damage state and quantify the damage that needs to be repaired. This method provides an alternative to the generation of new damage scenarios when data is limited (e.g. lack of historical damage data).

2. The definition of 'units of damage' (in units of resource-day) as a way to indicate the amount of work that needs to be repaired by those available repair resources.
3. The development of a novel three-stage model that simulates a road network repair process. It provides a framework that calculates the evolution of road capacities over time as a result of the allocation of repair teams to damaged road segments and the repair of damage over time.
4. The formulation of a dynamic sub-model that allows the assignment of resources to vary over time to damaged locations. It avoids the traditional way of assigning the same fixed number of resources until the damage is repaired. This allows the development of a five-step damage evolution graph (see Section 4.3.2.1). It also incorporates a productivity-resource relationship and saturation level of repair teams working at the same damaged place that most of the previous recovery modes do not include.

4.6. Simplifications and further improvements

The current version of the repair allocation and repair process model is still a simplification of how an actual restoration process is carried out. However, it provides the initial framework that sets the base for a potential more complex model. In this section, some simplifications that have been considered in the model are described and further improvements are proposed to overcome these limitations:

1. The current version of the model only requires a single task to completely repair the damage. Actual repair processes involve the completion of more than just one task that is done by teams of different types of resources. In fact, depending on the type of repairs that are required, some tasks may require more specialised equipment or personnel and this is not considered in

this version of this model. Although the current implementation seems to be a bit unrealistic by using just one task and one type of resource, it provides the first stage of what an actual road recovery process would look like. Further improvements should add more types of repair teams that include different numbers of personnel, plant and equipment and more variety of tasks. In this case, damage would be totally repaired when all tasks were completed. Different values of productivity should also be assigned to different repair teams. This can make the problem harder as there will be more decision variables on the overall optimisation problem, which in this case may slow the decision process.

2. In an actual restoration process, repair resources are located at strategic locations across the network and they are sent to damaged places from those locations. This is not considered in the current version of the model. Further improvements should include the addition of depots of resources at certain locations and also include the cost of sending them to repair damaged places. This may imply a first sub-optimisation model that allocates resources to damaged places minimising the cost of sending them to those places.
3. An improved definition of productivity of repair teams and their saturation level is required. The current model assumes that the productivity and the saturation level of workers is the same for all repair teams, no matter the damaged location. In reality, productivity values should change depending on the type of resources included on each repair team and the saturation level of teams working at the same damaged locations should change depending on the characteristics of each damaged location (available working space, difficulty of repairs, etc.).
4. As mentioned in the first point, damage may require more specialised resources. This may include resources from different sources (e.g. contractors) that are not available at all times. This implies that the repair process may be affected by the unavailability of these specific type of resources and it may require more time to bring these resources. This can produce that the damage-time graph explained in Section 4.3.2.1 acquires a different profile with more slopes representing the availability of resources at different times.

5. The current model can only repair the network with the available repair teams that are specified. However, if some damaged road segments need a specific type of resource that is not available with the existing resources, then there should be the possibility of bringing external resources (e.g. specific equipment, plant or personnel) from other places or other countries at a higher cost.

4.7. Conclusions of the chapter

This chapter aims to answer the following research questions: RQ3 "How can 'damage to infrastructure' be quantified and simulated using hazard susceptibility data?" and RQ4 "How can the infrastructure repair process be modelled, considering a resource-damage-time relationship and providing the evolution of road capacities over time?". This chapter presents a damage scenario simulation and a resource allocation and repair process model. The damage scenario simulation provides a framework to generate future damage scenarios. Using hazard susceptibility data, this method allows the identification of those elements more vulnerable to receive damage from a hazard event and, using a stochastic rule, the model classifies road segments as damaged or undamaged. It also identifies the damage state (minor, moderate, extensive or complete) that a damaged road segment suffers. Based on certain relationship between damage states and damage values, the model also transforms categorical damage values into numerical values, so that damage can be quantified.

The resource allocation and repair process model simulates how damage is repaired over time. This is implemented on a three-stage model. The first stage aims to assign resources to damaged places following the priority order of repairs. The second stage updates the damage that is repaired and the last stage converts this repaired damage into changes on road capacity.

This chapter also applies this model to a well-known transportation network, Sioux Falls Network (South Dakota, US). The aim of the example is to illustrate the process explained in the previous sections. The 'sensitivity' of some variables are also analysed. Results from this example show a resource allocation plan and a capacity recovery schedule that will be used as an input on the traffic simulator module, which

is described in chapters 5, 6 and 7 of this thesis. Future improvements are also proposed in order to achieve in future versions of this model a better representation of how an actual infrastructure repair process is carried out.

CHAPTER 5

Development of an event-based mesoscopic traffic simulation

5.1. Introduction

Traffic modelling aims to simulate and recreate how traffic moves in real life. Models are used for planning, implementation and traffic management. Depending on the level of detail, traffic simulation models are generally classified as microscopic, mesoscopic and macroscopic (Maerivoet and De Moor, 2005; Hoogendoorn and Knoop, 2013). Microscopic models capture the behaviour of individual vehicles in a very high level of detail. Macroscopic models represent traffic in an aggregate way as a continuous flow and it is measured in terms of speed, flow and density (Thonhofer *et al.*, 2018). And a combination of microscopic and macroscopic modelling is represented by the mesoscopic modelling. Mesoscopic models disaggregate the flow considered in macroscopic models and simulate the behaviour of individual or groups of vehicles as microscopic simulators do (Burghout, Koutsopoulos and Andreasson, 2006; Zhou and Taylor, 2014). The following section describes in detail each type of traffic model.

In this project, a mesoscopic simulator is selected to model the movements of vehicles through the network. During the first stages of this project, a macroscopic model was implemented in order to simulate in an aggregate level the characteristics of traffic. However, as the aim is to recreate how individual drivers make travel decisions and adapt their behaviour to changes in the network, it was necessary to increase the level of detail of the model and disaggregate traffic into individual vehicles. A microscopic modelling approach was discarded because the level of detail which these models provide at junctions was not required and it was expected to

simulate a large road network which was not ideal for a microscopic model due to their higher computational cost.

Therefore, the aim of this chapter is to present the mesoscopic traffic simulator that was developed and implemented for use in the restoration model. The content of the rest of the chapter is the following: the next section describes more in detail the different types of traffic models. Then, the next two sections explain the existence of different mesoscopic modelling approaches and the reasons why this traffic simulator was implemented in this chapter. Then, the structure of the mesoscopic model and the queue modelling approach are described. Finally, an illustrative example is used to demonstrate and evaluate the performance of the proposed model on a simple network.

5.2. Traffic modelling approaches

This section describes more in detail the three traffic modelling approaches (microscopic, macroscopic and mesoscopic models) that are classified in the literature according to the different levels of detail in the simulation.

5.2.1. Microscopic traffic model

Microscopic models describe traffic at a level of detail of individual vehicles and their interactions. The behaviour of a vehicle, which includes when the vehicle accelerates, decelerates, changes lanes, etc., is determined by the following models: car-following models, lane changing models and gap acceptance models (Ben-Akiva, Choudhury and Tomer Toledo, 2009; Bevrani and Chung, 2012). The car-following model describes the behaviour of a driver when following another vehicle. In this case, the motion of a vehicle depends on the distance to a leading vehicle and its speed. If the leading vehicle changes its speed, the following vehicles will also change its speed. It also describes the accelerating and breaking patterns that comes from the interactions of the driver and the leading vehicle (Burghout, 2004). The lane-changing model describes the decisions that drivers make to change lanes. Gap-acceptance models are used to model the execution of lane changes (Ben-Akiva, Choudhury and T.

Toledo, 2009). The available gaps are compared to the minimum accepted gap and if the available gap is greater than the minimum, the lane-change is executed.

The advantage of this high level of detail is that it allows the understanding of how vehicles interact and adapt their behaviour to small changes on certain parts of the network. However, it incurs a high computational cost as it has to model all interactions among vehicles and infrastructure and this cannot be afforded for large networks (Toledo *et al.*, 2005).

5.2.2. Macroscopic traffic model

On the other extreme, macroscopic models represent traffic in an aggregate way as a continuous flow and are based on the traffic flow theory describing the relationship between flow, speed and density (Thonhofer *et al.*, 2018). As opposed to microscopic approaches, these models analyse the average behaviour of a link instead of the behaviour of individual vehicles. Intersections are described in a low level of detail (Mohan and Ramadurai, 2013). These models usually have fewer parameter to calibrate.

The advantage of macroscopic models is that they can simulate large networks with low computational time. However, the level of detail provided by this model is very low to represent traffic behaviour at certain locations. The response of individual drivers to incidents is not possible to observe in these models.

5.2.2. Mesoscopic traffic model

A combination of microscopic and macroscopic modelling is represented by the mesoscopic modelling. Mesoscopic models disaggregate the flow considered in macroscopic models and simulate the behaviour of individual or groups of vehicles as microscopic simulators do (Burghout, Koutsopoulos and Andreasson, 2006; Zhou and Taylor, 2014). It describes the characteristics of traffic at a high level of detail, but the interactions and behaviour of drivers at a lower level of detail. However, a detailed model of the interaction between drivers is not needed. In this case, on each road (link), each vehicle or groups of vehicles are assigned an average speed which is

obtained from a speed-density relationship. Although the speed is calculated using aggregated values, vehicles are simulated individually or in groups of packets. The lane changes and acceleration/deceleration of vehicles are not modelled.

Nowadays, a wide variety of mesoscopic simulation models exists. A recent review, developed by Wang *et al.* (2018), highlighted the characteristics of the following mesoscopic models: CONTRAM (Leonard, Power and Taylor, 1989), DynaSMART (Jayakrishnan, Mahmassani and Hu, 1994), DynaMIT (Ben-Akiva *et al.*, 1998), MATSIM (Cetin, 2005), Mezzo (Burghout, Koutsopoulos and Andreasson, 2006), Dynus T (Chiu *et al.*, 2011), DTALite (Zhou and Taylor, 2014). Other mesoscopic models are: METROPOLIS (De Palma, Andre and Marchal, 1998), SILVESTER (Kristoffersson and Engleson, 2009), Dynameq (Mahut and Florian, 2011).

Two types of approaches are usually employed in mesoscopic models to simulate movements through the network: (1) Time-based (discrete-time) algorithms, which update the network state at every time period, even if there is no change on the network. Time, in this case, is an independent variable. (2) Event-based (discrete-event) algorithms, which simulate network changes as a discrete sequence of events in time. Each particular event marks a change of the network state. Time, in this case, is a dependent variable as it is only modelled when the event occurs. The main advantage of this second approach is the efficiency, in terms of computational costs, compared to a time-based approach as there is no need to update the network state at every single time interval.

Different approaches to model mesoscopic traffic simulators have been implemented in different software tools. The first form of mesoscopic model is the one considered in DynaMIT (Ben-Akiva *et al.*, 1998), which divides the road network into cells. A cell can include a single vehicle or a group of vehicles and vehicles can move between cells with or without overtaking other vehicles. A second approach models the movement of vehicles through the network based on a macroscopic model of traffic flow in which vehicles are assigned a speed using a specified speed-density relationship. Examples of this approach are the following models: CONTRAM (Leonard, Power and Taylor, 1989), DynaSMART (Jayakrishnan, Mahmassani and Hu, 1994), DTASQ (Mahut, 2001b), Mezzo (Burghout, Koutsopoulos and Andreasson, 2006). Finally, the last approach models individual vehicles through the network using

a simplified car following and lane changing models. Example of this approach is included in Mahut (2001a).

5.3. Why develop a new simulation model?

Despite the existence of other available mesoscopic models which are included in other already existing traffic simulation software packages, it was decided to implement a new mesoscopic model for the following reasons:

a) There is no free access to the code of some commercial mesoscopic models, such as CONTRAM or DynaSMART. This means that the existing codes cannot be altered and therefore new features cannot be added. In addition, a detailed description of how existing models are implemented is not always provided, which complicates the understanding of how models are developed.
b) Although some other traffic software packages are free and open source such as Mezzo, considerable time and effort are required to learn the programming language that was used to write the existing code and to understand the structure of how the code was implemented.

In addition, an advantage of writing a new code from scratch is that the modeller can easily understand how the model works, identify the assumptions made and areas for improvement.

5.4. Network structure modelling

The model proposed in this chapter follows the recent mesoscopic traffic approaches (e.g. Mezzo, DynaSMART) that model the movement of individual or groups of vehicles through the network at an aggregate level (based on the macroscopic fundamental diagrams). The model follows a discrete-event approach, which means that the model updates the traffic states only when there is an event. Events in this model are defined by vehicles entering the network, vehicles exiting or entering links or vehicles arriving at their destination. In order to speed up the modelling process, a minimum time unit is set by the modeller. This means that two consecutive events can only differ in time by a pre-defined value. By default, it was set to 0.01h (36 seconds).

Road network was represented using graph theory, which governs the relation between nodes and links. Nodes are points where traffic converges or diverges (e.g. road intersections), the origins and destinations of traffic (i.e. zone centroids) or locations where variations in geometric or functional characteristics of consecutive links are significant. Links are road segments that connect two nodes. The model was implemented using MATLAB programming language (The MathWorks Inc., 2018).

In order to speed up the modelling process, vehicles can be grouped into packets that act as a single entity. The more vehicles a packet contains, the lower the level of detail the model provides. If a packet is only formed by a single vehicle, then this model acts as an agent-based model in which each agent corresponds to one vehicle. If more than one vehicle are grouped in a packet, then the whole packet acts as a unique entity that travels through the network. It means that all drivers within the packet will make the same travel decisions. From now on, in this thesis when the term 'vehicles' is mentioned it also means 'packet of vehicles' and vice versa. Both terms are interchangeable.

The movement of packets is modelled on the link and node side. Interactions between vehicles within each packet and between packets when travelling on links are not modelled, although it has a macroscopic influence on the speed that is assigned to them as explained in Section 5.4.3.

5.4.1. Link model

A link is divided into two parts as shown in Figure 5.1: running part and queue part. The running part of the link contains those vehicles that are on the move to the downstream node and the queue part are those vehicles that are waiting to exit the link.

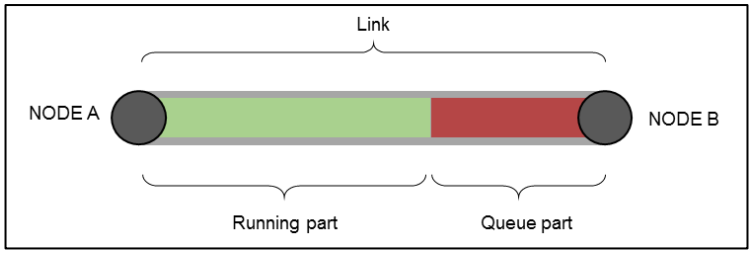

Figure 5.1. Link model representation.

When a vehicle enters a link, it is assigned to the running part with a speed that depends on the number of vehicles that are travelling on that running side. The more vehicles on that link (density), the lower the speed is as interactions between vehicles occur. The speed-density relationship used in this model is a modified version of the Greenshield's equation (Greenshields, 1933) included in Chang et al (1985). This relationship is explained more in detail in Section 5.4.3.

The speed that is assigned to each packet of vehicles is used to obtain the earliest time that a packet can reach the end node of that link. This arrival time is used to create a list of vehicles that want to exit the link. As this is not a microscopic traffic model, the acceleration of vehicles within the link is not modelled. For this reason, this model assumes that vehicles travel along the length of the road with a uniform speed (V_i). If drivers cannot exit the link on their earliest arrival time at the downstream node, they are sent to the queue part of the link. Only when there is enough capacity on the next link, are drivers allowed to leave the queue part. More information of this queue modelling approach is provided in the following Section 5.5.

5.4.2. Node model

Upstream links are connected to downstream links through nodes. In this model, these nodes are considered as intersections. It is assumed that each turning movement has an associated turning pocket as shown in Figure 5.2. All vehicles that want to use other links have to access first the turning pocket connected to the corresponding downstream link. Turning pockets are modelled as links that have a limited storage space, which is determined by the number of lanes and their length. Usually the length of these turning pockets, which is defined by the modeller, are negligible compared to the length of the links. By default it is set in 100m.

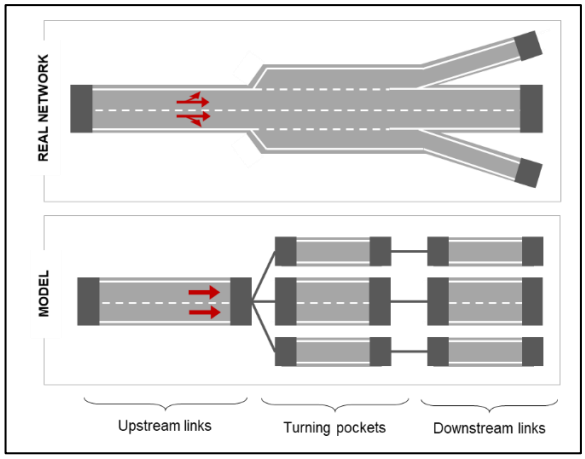

Figure 5.2. Representation of nodes using turning pockets

Once a vehicle arrives to the end of a link, it is immediately assigned to the turning pocket of that movement. If there is enough capacity on the upcoming link, then it is assigned to the next link. If not, this vehicle has to queue on the turning pocket until there is enough capacity to access the next link. If the length of vehicles queueing is longer than the physical length of the turning pocket, vehicles can block other turning movements even if there is still space for some vehicles to access other turning pockets. Figure 5.3 shows an example of a turning pocket that is blocking the immediate upstream link. Green vehicles occupy the full length of the turning pocket. As there is another vehicle that wants to access to the turning pocket, the rest of the vehicles queueing behind the green one cannot access the other turning pockets. Other types of intersections such as roundabouts, signalised intersections, etc. are not considered in this version of the model.

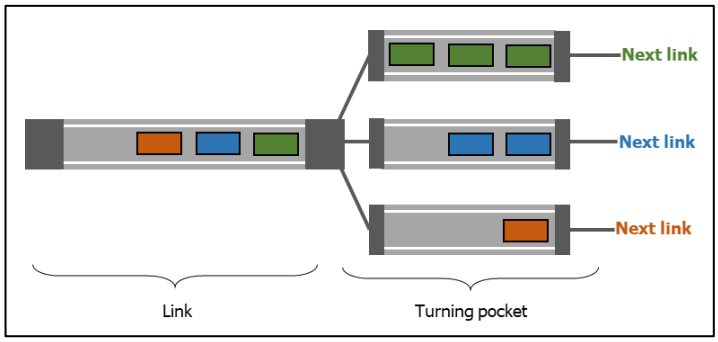

Figure 5.3. Turning pockets blocked and link blocked

5.4.3. Speed-density relationship

The speed-density relationship used in this model is a modified version of the Greenshield's equation (Greenshields, 1933) included in Chang *et al.* (1985). Figure 5.4 shows graphically the differences between these two models. The first one assumes a linear relationship between speed and density and the second one includes an additional parameter (ς) that modifies the curvature of the function. The second difference is that Chang *et al.* (1985) model adds a minimum speed. In our model, this characteristic is important as it allows the movement of vehicles on the queue dissipation, which will be explained more in detail in Section 5.5.2. The model needs to obtain the earliest exit time of those vehicles waiting on a queue. If speed were zero, the model would not be able to obtain an exit time. Therefore, the speed of vehicles at maximum density is limited by a minimum non-zero value. In the case of queue dissipation, this speed will be the queue dissipation speed.

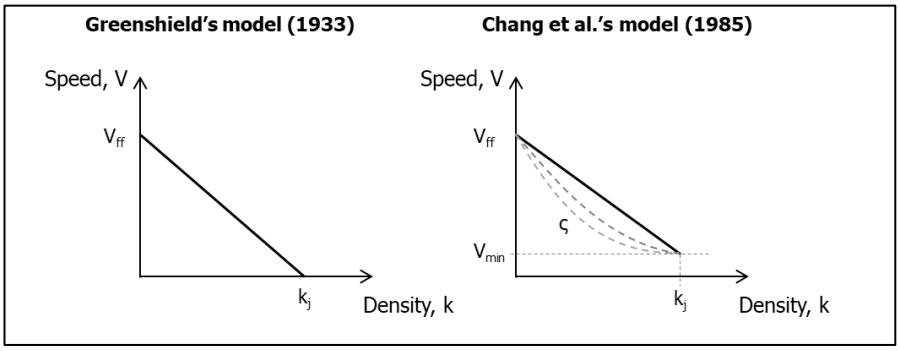

Figure 5.4. Comparison between the speed-flow relationship used in Greenshield's model (1933) and Chang *et al.* (1985) model.

Mathematically, Chang *et al.* (1985) model is expressed using Equation (5.1). When no vehicles are on the road, traffic density is zero which means that vehicles entering the link can travel under free-flow conditions (maximum speed). When traffic density is maximum (at a traffic jam), the model forces drivers to travel at a minimum speed to allow, at least, queue dissipation.

$$v_h = v_{h,min} + \left(v_{h,FF} - v_{h,min}\right) \cdot \left[1 - \left(\frac{k_l}{k_{max}}\right)\right]^{\varsigma} \tag{5.1}$$

Where,

v_h, speed of the packet h of vehicles.

k_l, traffic density only on the running part of link l.

k_{max}, maximum density of link l.

$v_{h,min}$, minimum speed of packet h of vehicles.

$v_{h,FF}$, free flow speed of packet h of vehicles.

ς, parameter of the Chang *et al.* (1985) model. This model assumes a value of 1 to be equivalent to the Greenshield's model. This value should be calibrated in future stages of the model.

Free-flow speed ($V_{h,FF}$) is limited to the maximum speed limit on the road. Therefore, depending on the type of road, the maximum speed may change. In order to account for variability of drivers, the maximum speed that an individual packet of vehicles can travel at is computed stochastically adding a random deviation (ϑ) from its pre-defined value as shown in Equation (5.2). The maximum difference between the maximum speed and the selected speed of drivers is set by the variable va. As an example, speed limits can vary 5% of the maximum if $va = 0.05$.

$$v_{h,FF} = v_{max} \cdot [1 - \vartheta_h \cdot (1 - va)] \quad (5.2)$$

Where,

$v_{h,FF}$, free-flow speed of packet h of vehicles.

v_{max}, the maximum speed limit of the road.

ϑ_h, random value between 0 and 1 that is generated for each packet h of vehicles.

va, variable that limits the maximum variability of the speed of drivers. It can take values between 0 (no variability) and 1 (highest differences between drivers).

The minimum speed of each packet of vehicles ($V_{h,min}$) is needed in order to allow the dissipation of the queues. Burghout *et al.* (2006) propose the value of $V_{h,min} = 6\ m/s$.

The density of each link (k_l) is calculated as the sum of all vehicles travelling on the running side of a link as shown in Equation (5.3). It is important to note that vehicles that are waiting at a queue are not included in the calculation. If the density of the link considered all vehicles (including running part and queue part), vehicles

could experience an additional delay while travelling (because those vehicles waiting at the queue were also considered) and then another extra delay due to the queue dissipation at the end of the link. In order to avoid this double counting of that delay, their speed is calculated based only on the vehicles that are travelling at that point on the running side (Burghout, Koutsopoulos and Andreasson, 2006). If there is a queue at the end of the link, vehicles will join the queue and they will have to wait until the queue is dissipated.

$$k_l = \frac{V_{l,run}}{LE_l \cdot LA_l} \tag{5.3}$$

Where,

k_l, density of each link l (vehicles per unit length)

$V_{l,run}$, the number of vehicles on the running part of the link l at time t.

LE_l, length of link l.

LA_l, number of lanes on link l.

The maximum density (k_{max}) is calculated as the maximum number of vehicles that can be physically storage on that link divided by the length of this link times the number of lanes available.

$$k_{max} = \frac{V_{l,max}}{LE_l \cdot LA_l} \tag{5.4}$$

Where,

k_{max}, maximum density (vehicles per unit length).

$V_{l,max}$, the maximum number of vehicles that can use link l at time t.

5.4.4. Entry flow restriction

Mathematically, under uninterrupted flow conditions, speed, density, and flow are all related by Equation (5.5) (May, 1990). In this sense, flow is determined by the speed-density relationship. The speed of new vehicles entering a link is obtained from the Equation (5.1) which depends on the density of vehicles at that time. However, in terms of computational modelling, the graph on the left of Figure 5.5 shows how the model simulates the entry of vehicles. Initially, there is a linear relationship between the number of vehicles entering the link per unit time and the density of vehicles on

the link (considering running and queue part). The capacity of the link limits the number of vehicles that can enter per unit time. However, when the density of vehicles is high ($k > k_o$), there are more interactions between vehicles and the number of vehicles entering a link should be affected by the number of vehicles on that link at that time. In fact, if the link density is high, the speed of vehicles is reduced and the entry flow should be reduced as well. However, as shown in the graph on the left of Figure 5.5, no matter the density of vehicles and speed on a link, if there is physical space, in the model, vehicles can still enter the link at their maximum rate (limited by the entry flow capacity of the link). The entry flow drops to zero when there is no physical space on the link so vehicles cannot enter. In contrast, what should happen in reality is what is shown in the graph on the right of Figure 5.5. The entry flow of vehicles should be influenced by the number of vehicles on the link. The higher the density of vehicles, the lower the number of vehicles that can enter per unit of time.

$$q = v \cdot k \tag{5.5}$$

Where,

q, flow (e.g. vehicles/hour)

v, speed (e.g. kilometres/hour)

k, density (e.g. vehicles/kilometre)

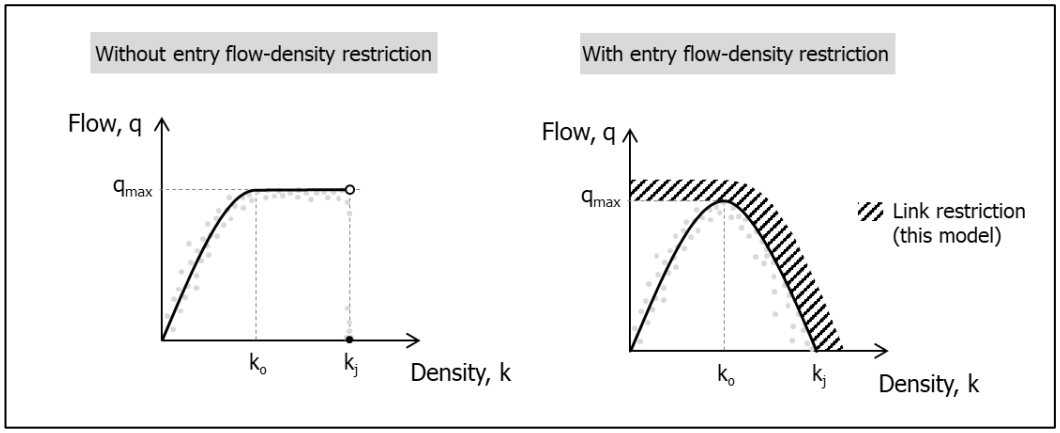

Figure 5.5. Flow-Density relationship with and without the restriction imposed to the entry flow.

In order to solve this issue, this model implements the relationship shown in the graph on the right of Figure 5.5, by incorporating an enter restriction on each link as shown in Figure 5.6. The capacity of the entrance of the link and the density (and speed) of vehicles on that link limit the maximum number of vehicles entering a link per unit time. This access restriction is expressed mathematically in Equation (5.6). If the density of the link is less than half of the density (k_o) at a traffic jam, the inflow cannot be higher than the capacity of that link. On the other hand, if the density is higher than the density k_o, inflow cannot exceed the limitation imposed on Figure 5.5. Adding this restriction, we allow a smooth transition between higher values of inflow and zero flow when the density is high (Figure 5.5). Therefore, this limits the maximum number of vehicles that can access the link per unit time during medium-high values of density.

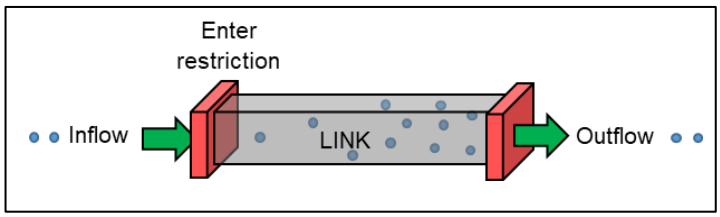

Figure 5.6. Enter restriction on a link

$$q_l = \begin{cases} q_{l,max} & if\ k_l \leq k_o \\ v_{\mathrm{ff,l}} \cdot k_l - \left(\frac{v_{\mathrm{ff,l}}}{k_j}\right) \cdot k_l^2 & if\ k_l > k_o \end{cases} \quad (5.6)$$

Where,

q_l, is the limit of vehicles per unit time that can enter a link l.

k_l, is the value of the density that is being analysed on link l.

k_j, jam density on link l. Equation (5.4) is used to calculate this value.

k_o, is the density associated with a maximum flow. In this model, it is assumed that this value (k_o) is half of the jam density value (k_j).

$v_{ff,l}$, is the free-flow speed on link l.

q_{max}, maximum flow.

5.5. Queue modelling

Modelling congestion acquires a significant importance in this model because it is expected to happen after the occurrence of disruptive events. One of the main reasons why congestion occurs is because travel demand exceeds the infrastructure capacity. As mentioned in Chapter 4, the impact of hazard events produces damage to infrastructure that is related to a reduction of road capacities. If road capacities are reduced as a result of the impact, congested conditions are expected to happen at certain locations of the network. In this cases, the capacity of certain roads may not be able to accommodate all traffic demand and it will result in growing queues. If these saturated traffic conditions persist for a long time, these queues may spill back to upstream road segments, blocking other roads and creating congestion in other roads of the network.

This section aims to describe how queue modelling is implemented in this traffic simulator. It explains how queues appear in the model and how this impacts the kinematic of vehicles travelling through the network. The procedure of how the formation and dissipation of queues are implemented are also included in this section.

5.5.1. Capacity constraints and virtual queue modelling

The formation of queues at intersections is also modelled in this traffic simulator. When the flow that tries to exit a link is higher than the outgoing capacity, a queue is formed from the downstream node towards the upstream node (see Figure 5.7). In this model, it is assumed that the outflow capacity of a link is the same as the inflow capacity of the next link. This assumption may underestimate delay experienced by vehicles. Note that in reality the capacity of the node may be more restrictive than the inflow capacity of the next link.

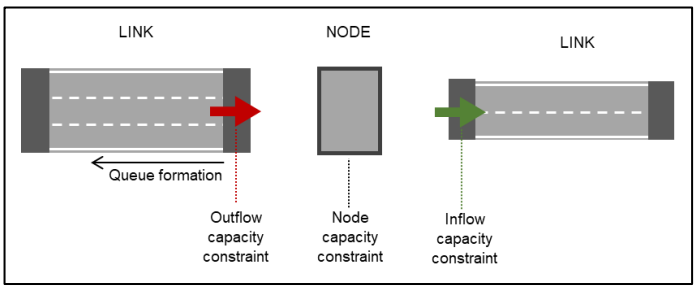

Figure 5.7. Capacity constraints on links and nodes

Packets of vehicles that cannot exit a link are sent to a virtual queue of vehicles. This virtual queue is created in order to have an order of vehicles that want to exit the link. The order is established based on the expected arrival time of each packet of vehicles. This means that this queue follows the FIFO principle (first-in-first-out): the first vehicle that enters the virtual queue is the first vehicle that leaves the queue. As the link model described in Section 5.4.1 is formed by a running part and a queue part, this virtual queue is transformed into a physical queue, so that it occupies space on the real link as shown in Figure 5.8. This has no implications *a priori* for new vehicles that enter this link. A new arrival time will be calculated and assigned to each of them considering just the vehicles that are travelling on the running part of the link. If there is a queue in front of them, these new vehicles will not be able to exit the link and they will join the queue. The only implication that the physical queue might have is related to the blockage of upstream links. If the length of the queue is longer than the length of the link, no more vehicles can enter the link and the queue starts to grow in the upstream links. Therefore, this model also takes into account the queue spillback implementation. The next section will explain how the queue is formed and dissipated and the process of implementing this in the model.

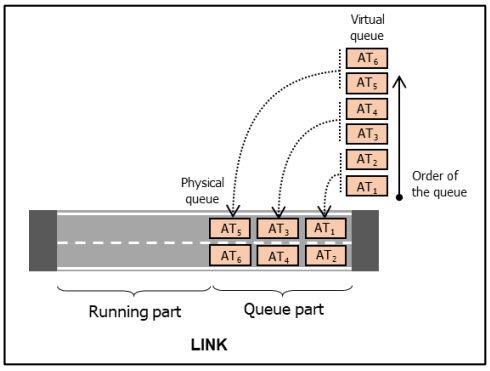

Figure 5.8. Virtual queue model implemented in this traffic simulation. Cars are represented by the rectangular shape and AT_X means the arrival time of each vehicle.

5.5.2. Queue formation and dissipation

The consequences of traffic congestion and queuing are the formation of shockwaves that are used to describe the propagation and dissipation of queues. Shockwaves are defined as boundaries that divide areas of different density (and thus flow and speed)

over time. These boundaries can be stationary or they can move over time. May (1990) classifies the type of shockwaves in six groups: frontal stationary, rear stationary, backward forming, forward forming, backward recovery and forward recovery. A graphical representation is included in Figure 5.9.

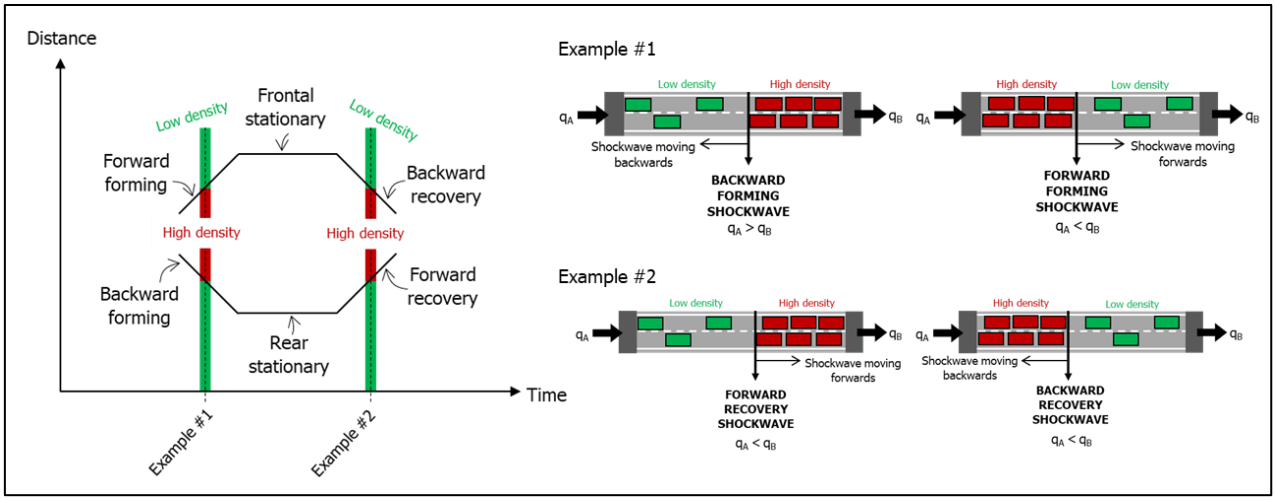

Figure 5.9. Classification of shockwaves. Graph on the left adapted from May (1990). Graph on the right, examples of shockwaves using sketches.

Most of these types of shockwaves are considered in the mesoscopic model that is proposed in this chapter.

a) Frontal stationary wave, which is a stationary boundary that divides an upstream area of higher density and a downstream area of lower density, is represented by the limited capacity of the turning pockets (intersection) or the capacity of the next link.

b) Backward forming and forward recovery waves are also represented on this model. When some vehicles cannot exit the link because there is a front stationary shockwave, vehicles are sent to the queue part of the link. These vehicles occupy physical space on the link. If more vehicles are joining the queue, there will be a wave that is moving backwards. This is the backward forming shockwave and it is quantified by updating the arrival time that will be explained more in detail in Section 5.5.2.1. When vehicles are leaving the link, then the queue is shrinking and the back of the queue moves forwards. This represents the forward recovery wave. This is also represented on the arrival time value.

c) Rear stationary wave is also represented as it is a particular case between a backward forming and a forward recovery wave and both are included in the model.
d) Forward forming wave, which is a downstream moving boundary that separates an upstream area of higher density and a downstream area of lower density of vehicles, is not considered in this model because the interaction between vehicles in links is not represented. For instance, this is the case of a lower-speed vehicle (e.g. truck) that causes the formation of a queue behind.
e) Backward recovery wave, which is when the demand flow rate becomes less than the capacity of the restricting section of the road, is also represented in this model using the queue dissipation method explained more in detail in Section 5.5.2.2. This method assumes a dissipation rate (wave) and depending on the length of each packet and the queue, it updates the departure time of each packet of vehicles, representing the backward recovery wave.

5.5.2.1. Queue formation: different arrival times

If packets of vehicles cannot leave a link because of the restricted capacity on the following node/link, a queue is starting to build up. As mentioned in Section 5.4.1, every time a packet enters a new link, an expected arrival time (to the end of the link) is calculated. If vehicles cannot leave the link at their corresponding time, they are sent to the queue part of the link and this is used to create a list of packets that shows the order of vehicles that want to exit the link. Therefore, the queue will be formed.

In this model, the queue occupies space. The length of the queue of vehicles waiting to exit the link is calculated following Equation (5.7). It depends on the average vehicle length, the gap between vehicles, the number of vehicles and the number of lanes.

$$LE_{queue} = \frac{V_{queue,l}}{LA_l} \cdot (LE_{veh} + gap) - gap \tag{5.7}$$

Where,

LE_{queue}, is the length of the queue.

$V_{queue,l}$, is the number of vehicles waiting on the queue.

LE_{veh}, average length of a vehicle. It is assumed a value of 4.8m (Qu *et al.*, 2013).

gap, average distance between two consecutive vehicles.

LA_l, number of lanes on link l.

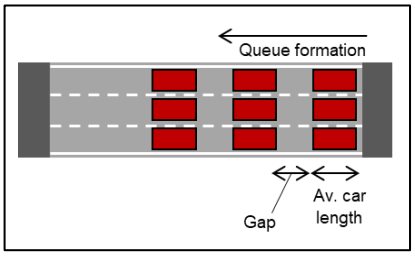

Figure 5.10. Sketch used to explain the calculation of queue length

5.5.2.2. Queue dissipation: updating arrival/departure times

When there is enough capacity on the following links and vehicles can exit the link, the queue of vehicles starts to move. In real-life, the leading vehicle starts accelerating instantaneously until they reach the expected speed. It provides a space headway so that the second vehicle can move. Then, this second vehicle starts to accelerate and the process is repeated to the third vehicle and so on.

This process, which follows Mezzo (Burghout, Koutsopoulos and Andreasson, 2006), is implemented in this model by changing the arrival time of each vehicle. Each queued packet of vehicles cannot move until the shockwave reaches them. So they have to wait a certain amount of time ($t_{h,w}$). Then these packets have also to travel to the end of the link, so there is another travel time associated ($t_{h,queue}$). The updated arrival time will be the sum of these two values as shown in Equation (5.8).

$$AT_h^{t+1} = AT_h^t + t_{h,w} + t_{h,queue} \tag{5.8}$$

Where,

AT_h^{t+1}, is the new arrival time assigned to the queued packet of vehicles h.

AT_h^t, is the previous arrival time of packet of vehicles h.

$t_{h,w}$, is the time that packet of vehicles i have to wait until the shockwave reaches its position.

$t_{h,queue}$, is the time to drive to the end of the link, assuming a free-flow travel speed.

The procedure that is followed in this model is the following. For each packet of vehicles that is on the queue:

(1) Obtain the speed (ω) of the backward recovery shockwave. Qu *et al.* (2013) conducted a qualitative and quantitative analysis based on video-collected data to study the motion characteristic of the queued vehicles at a signalised intersection. They concluded that the average shockwave speed is 4.42m/s and 4.94m/s, through the video survey and the mathematical calculation respectively. In this model, an approximate value of 5m/s (18km/h) will be used for the calculation.

(2) Calculate the length of vehicles (Len_{queue}) that are waiting just in front of this packet as explained in Section 5.5.2.1.

(3) Obtain the waiting time ($t_{h,w}$) until the shockwave reaches this packet of vehicles. It is obtained using Equation (5.9).

$$t_{h,w} = \frac{Len_{queue}}{\omega} \tag{5.9}$$

(4) Calculate the travel time ($t_{h,queue}$) of this packet of vehicles to drive to the end of the link. It is obtained using Equation (5.10), assuming a free-flow travel speed ($v_{ff,l}$). It is known that this will not be the speed that this packet will use at this moment because the vehicles are accelerating. However, it is assumed that vehicles instantaneously will reach this speed and therefore, the acceleration value would be negligible. It also makes the implementation of the formula much easier.

$$t_{h,queue} = \frac{Len_{queue}}{v_{ff,l}} \tag{5.10}$$

(5) Finally, the new arrival time will be calculated using the Equation (5.8). This value will be rounded to the nearest time unit (in this case multiples of 0.01h).

A graphical example is also included in Figure 5.11. Three packets of six vehicles are queuing waiting to exit the link. The expecting departure time is at 7am because the capacity of the next link is not restricted at that time. As the minimum time unit in this model is 0.01h (36sec), and due to the starting shockwave, this example will determine if all vehicles can leave at the same time (7am) or recalculate the departure time of the following vehicles. Based on the length of the queue and the speed of the shockwave, a waiting time is obtained from the graph on the right of the Figure 5.11. Then travel time is obtained based on the distance to the end of the link. The new arrival time will be the sum of both values.

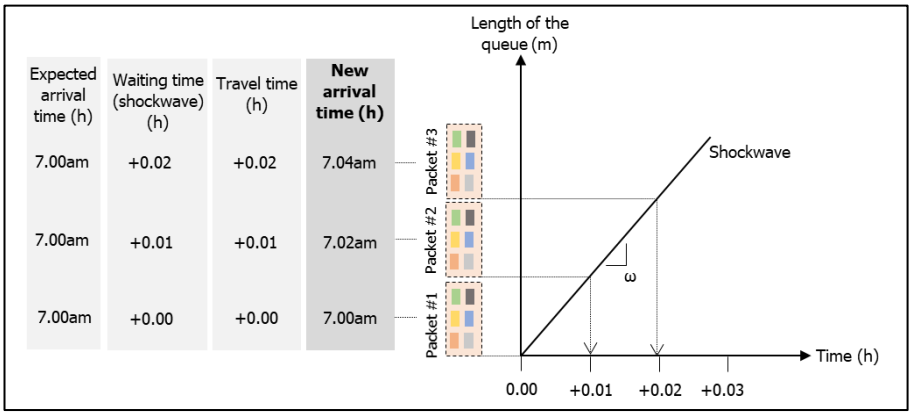

Figure 5.11. Example of the calculation of new departure times when multiple packets are waiting on a queue.

This procedure is also applied to new traffic demand that wants to enter the network for the first time. Even if they are not still on the network, not all vehicles can enter the network at the same time. The capacity of links determines the number of new packets of vehicles that can be added to the network. If some demand cannot be added because it exceeds the capacity of the link, they will form a virtual queue on the node (even if they are not still on the network), so that the departure time of each packet of vehicles is updated following the procedure that is explained in this section. This version of the model does not count towards network travel time the delay in entering the network. Future versions of the model could consider this additional delay.

Note that if the vehicles that are in at queue and cannot exit the link at the current simulation event time, the arrival time of those vehicles is updated by adding

a +0.01h (which is the minimum unit of time of the model) to the previous arrival time. In doing so, the model makes sure that the next running time, the model analyses these queued vehicles and checks if there is enough capacity. This is a modeller choice and could take other values.

5.6. Traffic simulator implementation

This section describes the procedure to simulate the movement of vehicles on the network. As mentioned in Section 5.4, this is an event-based traffic simulator which means that the model is only run when movements on the network are expected to happen. Therefore, the aim of the simulator is to find new events so that it keeps vehicles moving all the time. The modelling information that is described in this section is not freely provided by any of those existing mesoscopic traffic models mentioned in Section 5.2. For that reason, the content of this section can be considered as novel in a sense that it has never been shown before. It has been implemented from scratch, following the logical sense.

Figure 5.12 shows the general framework that has been implemented in this model. At the beginning of each new day, all packets of vehicles that want to enter the network for the first time are added to a list of traffic demand which includes the expected departure time of each packet, among other information such as the number of vehicles on the packet, the chosen route or the destination node. At this point, there is a module that finds the event with the earliest time. All vehicles that are expected to move at this time are sent to a 'list of movements'. These are the movements of the packets that are simulated. The three-step procedure shown in Figure 5.12, which will be explained more in detailed in the following sections, aims to simulate these movements sending vehicles to next links. Finally, the model checks if all vehicles have already arrived to their destination. If they have not arrived yet, then the model needs to find the next event so that more movements can be simulated. Once all vehicles have arrived to their destination, then no more movements are left and the simulation for the day in question is complete. The following sections explain the three steps that are responsible for simulating the movement of vehicles on the network.

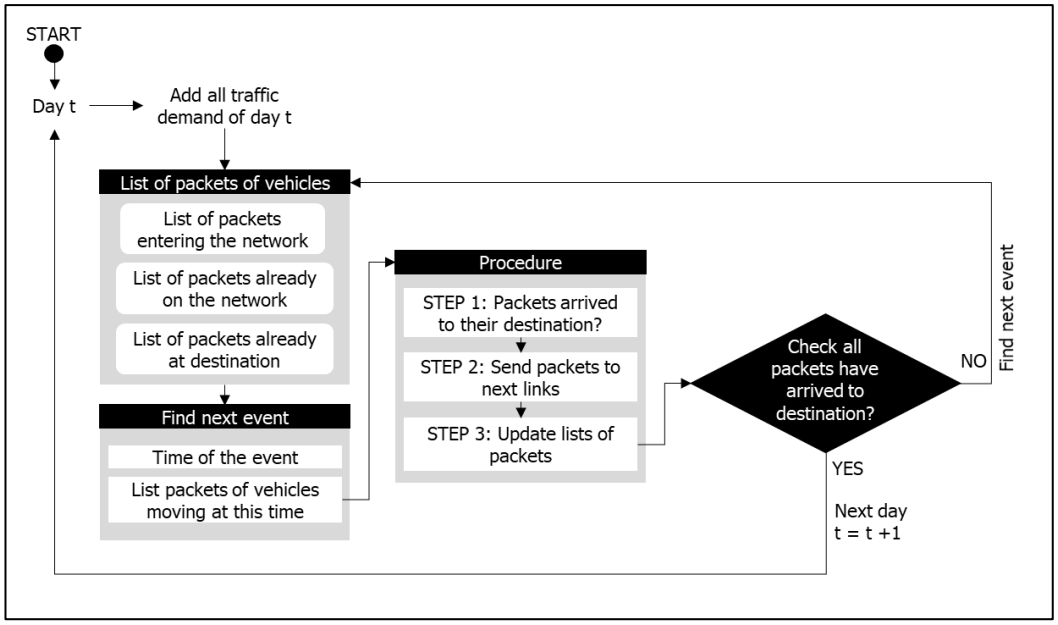

Figure 5.12. General traffic simulator framework considered in this model

5.6.1. STEP 1: Have vehicles reached destination?

The aim of this first step is to identify those vehicles that have already reached their destination. These vehicles are removed from the list of movements, removed from the network and added to the list of 'already arrived to destination'. This is done during the first step because in this way we avoid having vehicles on the network without being in motion. It also allows queues to get rid of vehicles that have already arrived to their destination. Another reason is also because the next step involves sending vehicles to next links and these vehicles have no next link as they have already reached their destination.

5.6.2. STEP 2: Add packets to next links

The aim of this second step is to send vehicles to next links when they have reached the end of a link. These vehicles have been travelling through the network and have reached a node that is not their destination. In this case, the model assigns vehicles to the next corresponding link if they satisfy some conditions that are explained further on in this section. To the best of the author's knowledge, the methodology proposed for this second step has not been explicitly included in previous mesoscopic models.

Two possible approaches were studied when implementing this second step: A) Analyse individually each packet of vehicles included in the list of movements in a random order and send it to the next link; or B) Analyse every single node of the network and send the vehicles that have reached this node to their next links. Although both approaches are totally acceptable, option B was preferred due to the following reason: analysing each node individually allows modelling the interaction between vehicles that arrive to the same node. The model can give priority to certain roads and reduce priority to other so that some vehicles need to wait until the movement of the other vehicles is completed. However, the disadvantage of this approach is that the algorithm has to visit all nodes on the network. If the network that is being analysed is large, it may take a long time to visit all possible nodes.

The procedure that is implemented in the model is summarised in Figure 5.13. The algorithm consists of two main loops: the 'node' loop and the 'packet' loop. Initially, the list of packets that are planning to move at this event is given. Remember that the 'event' has been found as described in previous sections, so the vehicles that are ready to move to the next link are known. At this stage, the algorithm enters into the node loop. Those nodes that have vehicles waiting to be sent to next links are analysed in this loop. This node can be the convergence point of more than one road, which means that a series of vehicles coming from different roads can reach the node at the same time. The algorithm can only simulate the movement of one packet of vehicles at a time. This means that an order of packets needs to be set in place. In this model, the order for simulating movements of packets is set depending on the hierarchy of roads. This means that if a road has a higher hierarchy than another road, the movement of those vehicles that are waiting on the first road will be simulated first. If all roads have the same hierarchy level, then the movement of vehicles will be simulated following the FIFO rule. This implies that those packets travelling through high-hierarchy roads may experience lower travel time compared to other packets that use lower-hierarchy roads.

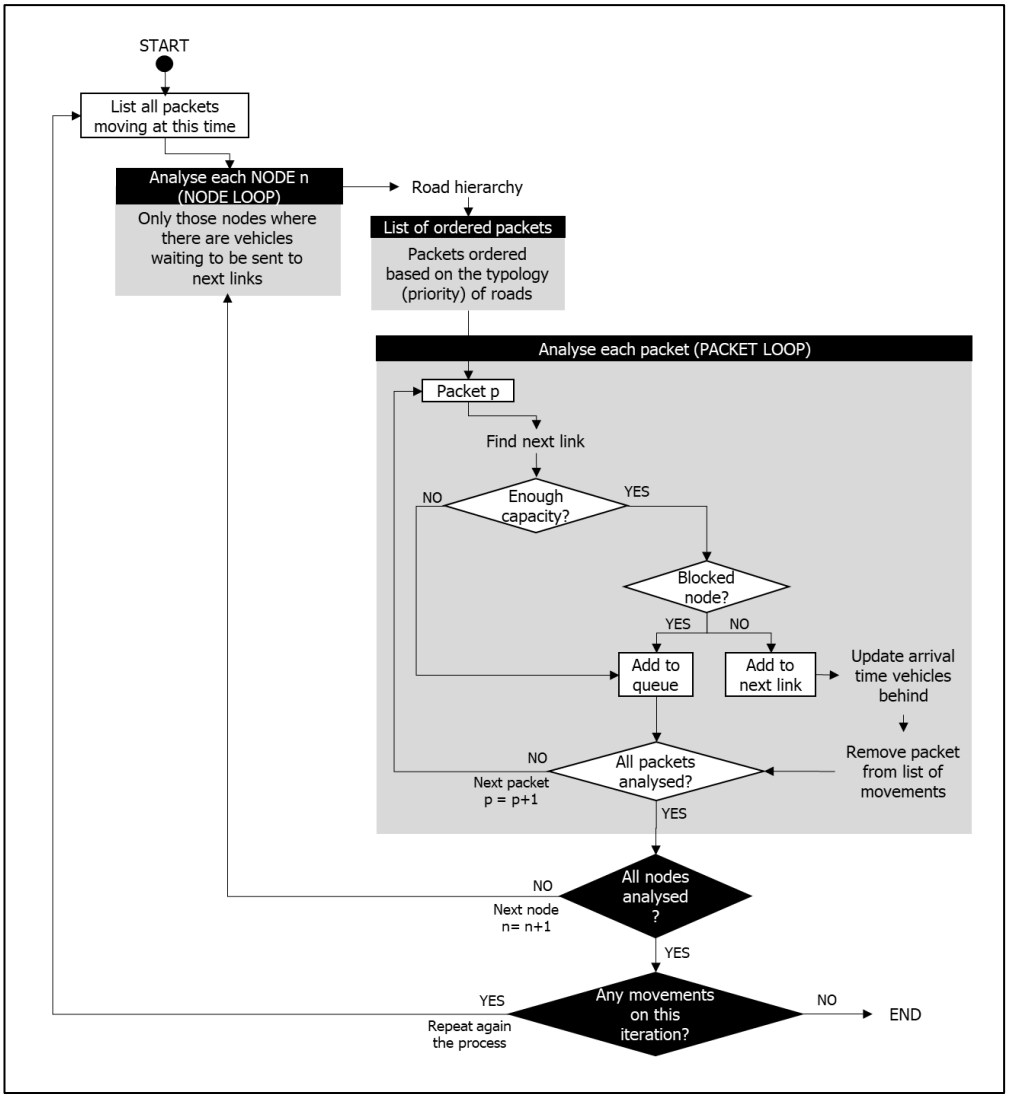

Figure 5.13. Flowchart of the step 2: Sending packets to next links

At this stage, a list of ordered packets of vehicles (based on the road hierarchy) is known. This means that the algorithm is ready to enter the 'packet loop'. In this loop, the movement of all packets of the list are simulated. The algorithm selects a packet of vehicles following the established order and find the next link.

Then the algorithm checks the capacity of this link for this time period of the selected event. As mentioned in Section 5.4, the minimum time period between events is 0.01h=36 secs. Therefore, there is a limit of the maximum number of vehicles that can physically access this link during these 36 secs. The number of vehicles that are entering the link during these 36 seconds is stored for the whole

simulation of the event. The capacity of each link is provided in vehicles per hour. This value can easily be transformed to vehicles per 36 seconds by simply multiplying the value by this factor (*36/3600). This is the maximum number of vehicles that can enter during this simulated event. If the number of vehicles per packet is higher than the maximum number of vehicles allowed to enter the link for that time period, vehicles can still enter the link (otherwise they will never enter that link), but the entering time of the following vehicles needs to be updated. Figure 5.14 shows an example of this particular case. In this case, the maximum number of vehicles is 4 per 36 seconds. The packet that wants to enter the link contains 10 vehicles. Not all of them can be sent to the next link during 36 seconds. This means that the entering time of the following vehicles needs to be updated, following the same methodology explained in Section 5.5.2.3.

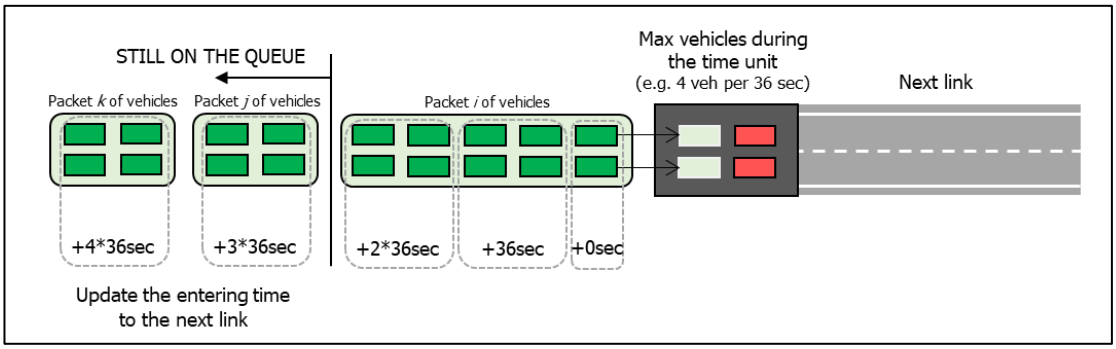

Figure 5.14. Graphical example of the method that updates the entering time of those vehicles that follow a packet of vehicles that contains more vehicles than the maximum number of vehicles allowed to enter the link per unit time.

Following the flowchart of Figure 5.13, if the number of vehicles exceeds the capacity of that link, then vehicles are sent to the queueing part of the original link. After that, the algorithm checks that the node is not blocked by other vehicles that are queuing in front of them (see Section 5.4.2). If the node is blocked, vehicles cannot use this node and they need to queue. However, if the node is not blocked, vehicles can be sent to their next link. Depending on the size of the packet, the arrival/departure time of vehicles that are behind them needs to be updated (as described in Section 5.5.2.2). Those packets of vehicles that are already sent to their

next links are removed from the list of movements, so that they are not analysed again.

Once all packets of the list of a specific node have been analysed, then a new node is visited and the process is repeated again. When all nodes have been successfully visited, the algorithm is coded in a way that repeats the exact same process only if there has been any movement during the current iteration. The reason is explained as follows. As this algorithm visits each node in a random order, it may visit some nodes whose vehicles cannot move because other nodes have not been analysed yet and next links are blocked. Figure 5.15 shows an example of this process. In this case, the algorithm visits the nodes in an ascending order (from N1 to N4). As link N2-N3 is physically completely full, vehicles that are located on link N1-N2 cannot move to the next link. When the algorithm visits node N3, a vehicle (the green one) can move to the next link N3-N4. This means that there is a new gap for one more vehicle in the link N2-N3 and the algorithm should send the first vehicle located in link N1-N2 (the blue one) to the next link. If the algorithm only considered one iteration, it would not be able to send that blue vehicle to the next link. That is the reason why the algorithm includes that iterative condition: 'if there has been any movement during an iteration, there should be one more iteration to run' just in case there are other vehicles that can fill some gaps.

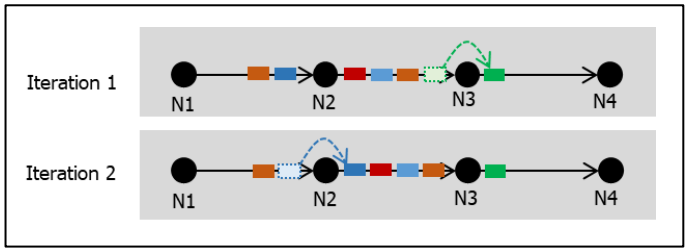

Figure 5.15. Example used to explain the iteration of the step 2.

5.6.3. STEP 3: Update arrival time

After sending packets of vehicles to next links, it is necessary to update their new arrival time to the next node. Therefore, the aim of this step is to calculate the new arrival time based on current traffic conditions. Every time a packet of vehicles enters a link, an arrival time is calculated using the Equation (5.11). The arrival time is

calculated as the current time when the packet has entered the link plus the time that each packet needs to travel through this link.

$$Arrival\ time = current\ time + additional\ time \tag{5.11}$$

The additional time is obtained considering that each packet travels at an average speed as shown in Equation (5.12). This speed is calculated based on the number of vehicles travelling only on the running part and its formulation has already been explained in Section 5.4.3, Equation (5.1). Note that the speed is assigned to each vehicle when it enters the link and it is assumed that this vehicle travels at this speed through the whole link.

$$additional\ time = \frac{distance}{speed} \tag{5.12}$$

Note also that if there are vehicles waiting on the queue part, the calculated arrival time of new packets cannot be earlier than the arrival time of these vehicles queueing.

5.7. 'Warm-up' and 'Cool-down' modelling periods

The road network implemented in the model is totally empty at the beginning of the simulation. The network requires some time to allow vehicles to enter the network and reach the real-world conditions. That is the reason why a 'warm-up' period is essential in this model. An additional 'cool-down' period is required to allow drivers already on the network to complete their trips. If a 'cool-down' period is not simulated, vehicles driving at the end of the peak period may experience faster travel times because no more vehicles are loading into the network and no interaction is produced.

The length of these additional periods may vary from project to project (*Traffic Engineering, Operations & Safety Manual*, 2005), but there are some rules of thumb that estimates the length of these periods. The manual done by the Federal Highway Administration (2004) and NSW Roads & Maritime Services (2013) says that the minimum warm-up period is twice the longest trip length of the network. But it states that after a few runs, the adequacy of the considered length should be verified and extended if required. The minimum cool-down period should be the time when the last vehicle of the peak period enters the network until the last vehicle of the peak period arrives to its destination. As this value is difficult to know *a priori,* in this model,

a certain number of preliminary runs will determine the length of this warm-up and cool-down period.

5.8. Illustrative example

In this section, the performance of the proposed model is evaluated over a sample network. This example tries to focus on the accomplishment of two main goals: (1) observe that the fundamental diagrams of traffic flow obtained from the model is in accordance to the theoretical diagrams proposed by Greenshield's model (1933) and the one modified by Chang *et al.* (1985) and (2) test that the queue formation and dissipation is working satisfactorily on congested networks.

The sample network, shown in Figure 5.16, consists of 10 nodes and 9 consecutive link segments of 1000 meters long each one. Each link segment have two lanes, a capacity of 2000 veh/h and a free-flow speed of 96 km/h.

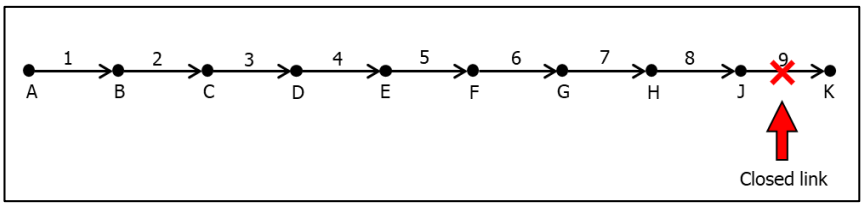

Figure 5.16. Network used to illustrate the mesoscopic traffic simulator of this chapter.

There is a traffic demand from Node A to Node K of 1700 veh/h. Individual vehicles are added following a uniform distribution from 8am to 9am. As the minimum time unit between events is 0.01h (~36seconds), vehicles are added into the network every 36 seconds.

An incident is introduced to alter the levels of flow, density and speed during a period of time. In this particular example, the last link (link 9) is closed to traffic at 8:24am (8.4h) and it is open again at 8:48am (8.8h). During this time, no vehicles can use link 9 and therefore, they need to wait until the road segment is open again. Note that the 'warm-up' and 'cool-down' periods are not modelled in this example.

5.8.1. Fundamental diagrams

The following section obtains the fundamental diagrams after running the model. Figure 5.17 shows the average data of flow, speed and density that is collected every minute on every single link of the model. In order to have a larger dataset, the same model has been run five times. Each colour indicates the data of each simulation. As the minimum time between events is 0.01h, data has been collected between events. In order to obtain data every minute, data has been averaged merging two consecutive events (0.01h+0.01h ~ 1 min). Flow is measured as the number of vehicles that enters each link at that period of time. The speed is obtained as an average of all speeds of all vehicles travelling through that link at that certain time. Note that the speed of those vehicles that are on a queue is assumed to be zero. In reality, vehicles should move at the speed of the queue dissipation. However, in this model, the speed of the queue dissipation is used to calculate a new arrival time to the end of the link (see Section 5.5.2.2). That is the reason why the Speed-Density diagram of Figure 5.17 shows the minimum speed in 0km/h.

Results from the model are compared to the theoretical fundamental diagrams. The resulting diagrams are in accordance to the theoretical ones (see Figure 5.4 and Figure 5.4 in Sections 5.4.3 and 5.4.4. respectively). Several aspects marked in red ellipses are explained more in detailed because these could be considered as anomalies of the model that are not shown in the classical fundamental diagrams.

Ellipse I highlights the assumption made in this section to obtain the average speed of vehicles on a queue. As observed in the diagram, the average speed on the link is zero but there are still vehicles on the link (density is not zero). This is possible because those vehicles that are still waiting on a queue to exit the link have zero speed.

Ellipse II shows the case of no inflow of new vehicles but high density of vehicles on the link. This is possible in this model because even if no more demand is entering the link, there are still vehicles waiting to exit that link and therefore the density is not zero at that time. As observed, the density is gradually decreasing until it gets a value of zero with zero inflow, as expected.

Ellipse III corresponds to a particular case of Ellipse II with vehicles still entering the link (moderate density and inflow). Generally, data of Ellipse III comes from the end of the simulation period when the number of new vehicles entering links is quite low. The trend is to have lower inflow (which at the end it will be part of Ellipse II) because no more demand is added into the network (demand stops at 9am). As opposed, the density of that link is still moderate/high because even if not a lot of vehicles are entering that link, there are still vehicles travelling or waiting on a queue to exit that link. The average speed of these vehicles at that time is quite low (~20km/h on average) because the speed of vehicles travelling through the network is averaged with the speed of vehicles waiting on the queue which is zero speed. This is the reason why the average speed of the link when there are vehicles waiting at the queue reduced the overall speed of the link.

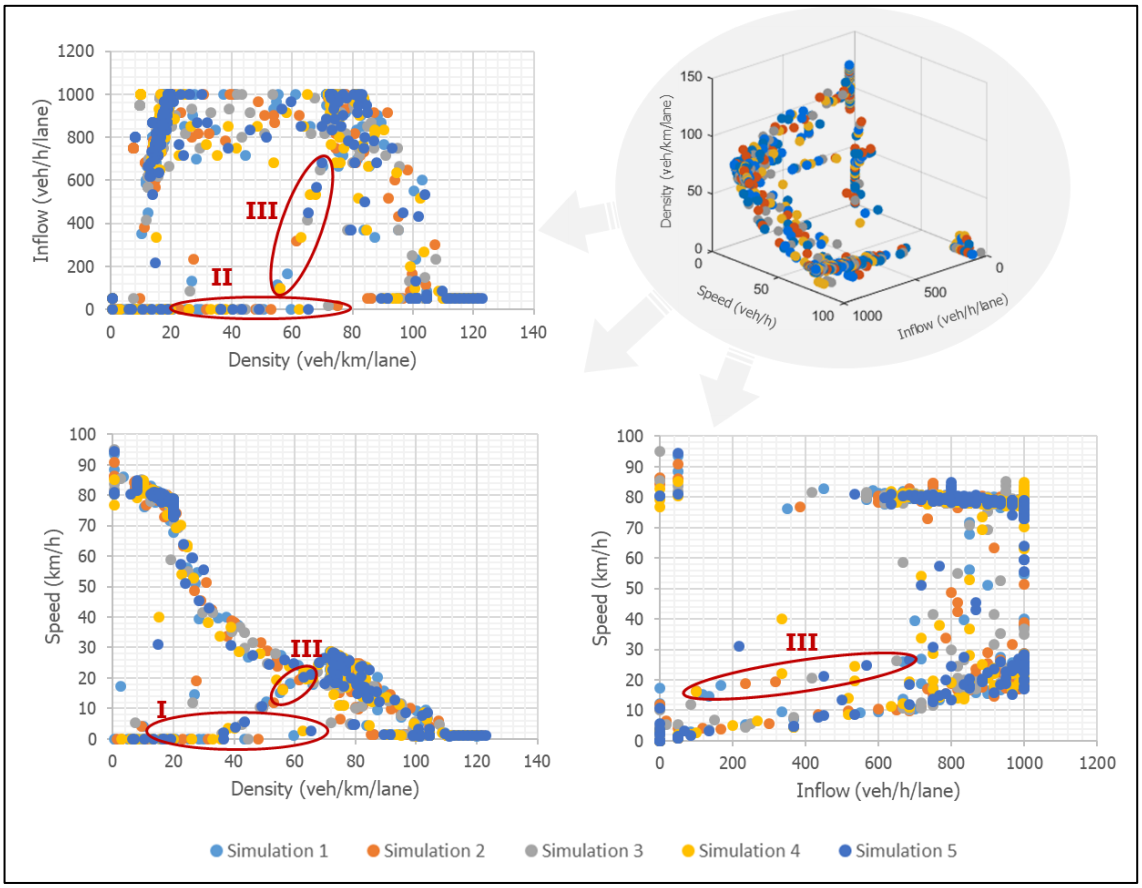

Figure 5.17. Fundamental diagrams of traffic flow obtained from the implemented mesoscopic model. Each dot represents an average data of flow, speed and density respectively that is collected every minute on every single link of the model. Five simulations have been run (see colours). Time period from 8am to 9am.

5.8.2. Queue propagation

This section illustrates the shockwave-propagation mechanism after the closure of one link located downstream. Figure 5.18 plots the cumulative number of vehicles entering each link over time. The slope of the lines represents the entering flow rate. As observed in the graph, vehicles are added into the network at 8am on link 1 and rapidly travel through the rest of the links. The first vehicle reaches the last link 9 after 10 minutes approximately. At 8:24am (8.4h in graph), Link 9 is closed and no more vehicles can use that link (slope of the line is zero – no flow rate). This means that the cumulative number of vehicles stays constant at that time. Vehicles that cannot access link 9 start to form a queue on link 8 from downstream to upstream waiting to exit the link. If the closure of link 9 extends for a long period, the formation of the queue on link 8 can reach the upstream node, producing the blockage of this link (queue spillback). Letter A in Figure 5.18 shows the time that it takes to block the link to new vehicles. In this case, after 7 minutes, link 8 is blocked and no more vehicles can use that link. The distance between lines represents the number of vehicles on each link (letter B in Figure 5.18). The queue formation is also blocking Links 7, 6, 5 and 4. This shows how the backward propagation of the queue is represented correctly (backward forming shockwave).

At 8.48am (8.8h in graph), the incident clears, vehicles can start using link 9 again and the queue start to dissipate and propagates via link 8, 7, etc. On link 3 the backward forming shockwave is caught up by the backward recovery shockwave which is moving faster. That is why links 1, 2 and 3 are unaffected by the incident.

For this particular example, as the capacity of all links is the same, the rate of vehicles leaving and entering a link is the same for all links. That is the reason why Figure 5.18 shows that the lines of entering flow and leaving flow rate (queue dissipation) are parallel. Lines come together when there is no new demand added into the network (at 9am).

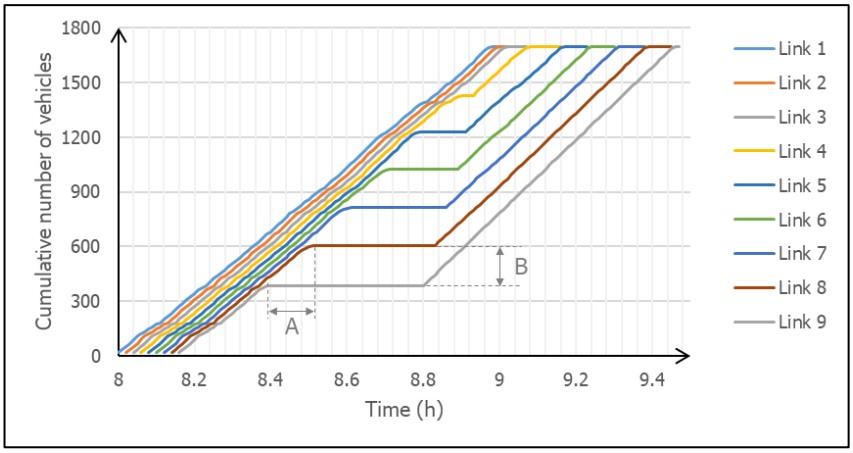

Figure 5.18. Cumulative number of vehicles that enters on each link. Incident starts on link 9 at time 8.4h and finishes at 8.8h.

Figure 5.19 shows another way of representing this queue propagation. It plots the number of vehicles waiting on a queue over time on each link. The vertical axis represents the simulation time and the horizontal axis the number of vehicles on a queue. Each colour represents a different link and the physical representation of the links is included at the bottom of the figure. As observed, at 8.4h the queue starts to build-up until it reaches link 3 at time 8.9h approx. Once link 9 is open again to traffic at 8.8h, a reduction of the number of queued vehicles on link 8 is observed because some vehicles are already sent to Link 9. The density of vehicles on link 8 starts to reduce and more vehicles that are waiting on a queue on link 7 can use link 8 and so on. As mentioned, when the queue dissipation line catches up the queue formation line, the queue is not propagated to more upstream links. In this example, even though the damaged link is open to traffic, the queue does not completely disappear until the end of the simulation. The main reason is that the entry flow rate and the exiting flow rate of each link is exactly the same for all links. In other words, the link capacity restrictions are the same for all links. In this sense, only limited number of queued vehicles of link 8 can enter link 9 due to capacity restrictions. The number of vehicles that enters link 9 is equivalent to the queue reduction of link 8. When no more vehicles can enter link 9 (due to the lack of capacity for the time interval 0.01h), queued vehicles that have not been able to enter link 9 will form a queue on link 8 until the next time interval (+0.01h) when link 9 will accept more vehicles. As some vehicles have left link 8, there is still space to access this link and therefore the same amount of vehicles that have entered link 9 will enter link 8 from

link 7. The process is repeated for all links. Therefore, as arrival and departure rates are the same, the queue is never completely dissipated unless flow rates changes. Only when the arrival rate becomes lower than the departure rate, the queue starts to clear from upstream to downstream links.

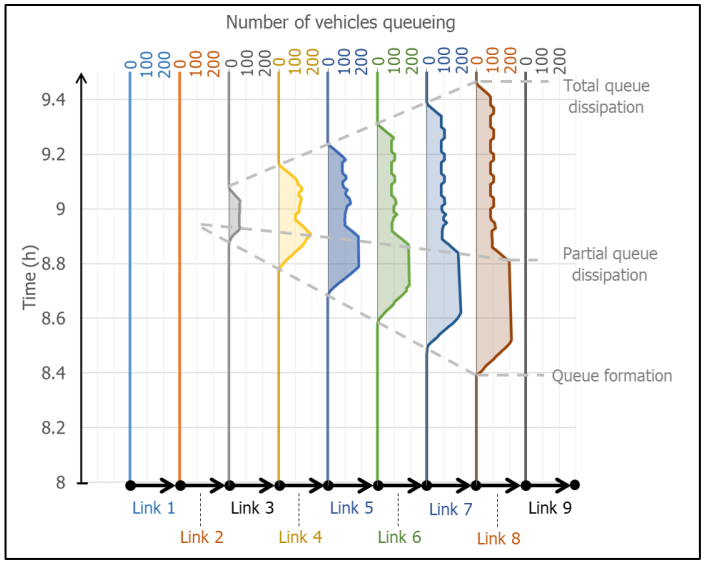

Figure 5.19. Number of vehicles queueing on each link vs. time

This Figure 5.19 also shows one aspect of the implemented relation between flow and density. As explained in the previous Section 5.8.1 and Section 5.4.4, the flow of vehicles that enters a link (entering rate) starts being affected once more than half of the jam density is reached, which means that the entering rate of vehicles is reduced. That is the reason why a queue can build up even without having the next link full. For instance, the queue on link 7 has started to build up without having the link 8 completely full. This means that the departure rate is lower than the arrival rate and a queue starts to build-up. On the other hand, the density of link 3 is less than half of the jam density, which means that inflow is not affected. Evidence of this is included in Figure 5.18 showing that the arrival rate of link 3 is not affected by the incident.

5.9. Contributions to the knowledge

This section provides an insight into those aspects that make this model slightly different from other existing mesoscopic models. However, it is worth mentioning that

the main aim of this chapter is not to present a novel traffic simulator. Already existing models work properly and although there are some areas of research that could be addressed to improve these models, that was not the intention of this chapter. However, due to the need to implement a bespoke mesoscopic model (see Section 5.3), several new aspects have been included, which contributes to the body of knowledge. This chapter provides a detailed explanation of a new three-stage process, which is explained in Section 5.6 and is used to simulate movements through the network. None of the models that have been consulted to develop this chapter (Mezzo, DynaSMART) provide an explanation of how they implement this modelling process of sending vehicles to next links. This model contributes to the body of knowledge by providing a detailed explanation of how this new procedure is implemented and it can be considered as a starting point for other researchers to develop new mesoscopic traffic simulators.

5.10. Drawbacks and areas of improvement

Some disadvantages regarding the implementation of the mesoscopic simulator and their possible areas of further improvement are included in the following section:

1. Code efficiency and computational cost. The method used in this model to simulate the process of moving vehicles across the network may not be the most efficient one. The 'node' loop and the 'packet' loop presented in Section 5.6.2 requires the simulation of all movements of all packets located on all nodes for several times. Every time there is a new movement on the network, the model needs to check that no more vehicles can move forward. If the network contains a large amount of nodes to visit and many packets of vehicles to simulate, the model may take a lot of time to run. However, there is still room for improvement in this area. Further work needs to focus on the improvement of the efficiency of the algorithm. The order of nodes that are visited during the 'node' loop should not be randomly selected and an order that maximises movements on the network should be implemented. This allows the algorithm to run fewer times and therefore, speed up the computational process.

2. Intersection modelling (nodes). This model considers that all intersections are simulated using turning pockets. For each next link, there is a turning pocket that drivers need to visit in order to be sent to the consecutive link. However, other typology of intersections should be implemented in future versions of this model. The addition of traffic signal control could also be an area of interest, which can provide different levels of priority to some roads after disruptions.

   Another aspect to consider in future versions of the model is that capacity of intersections may be more restrictive that the capacity of links. In this model, the capacity of the downstream link restricts the outflow of the upstream link, which means that junction delay is not considered. However, in reality, the capacity of the junction restricts the outflow of the upstream link.

3. Calibration and validation with real data. The model needs to be tested to larger networks, calibrated to specific traffic conditions to which they are applied and validated using real traffic data in order to be applicable to real life operations. Future work should focus all the efforts on the calibration and validation process.

4. Entry flow restriction. This model imposes that the flow of vehicles that enters in a link depends on the density of vehicles that are already on that link. The more vehicles that are circulating on the link, the lower the inflow of vehicles that can enter the link (see Section 5.4.4). However, this assumption implies that when the density of the link is already high (not necessarily a full link) and there is a high demand of vehicles that want to use that link, some drivers may not have access to the link and they start to build up a queue, even if the link is not completely full of vehicles. In reality, the queue spillback starts once all link is full of vehicles and no more vehicles can use that link. Further work needs to study this relationship more in depth.

5. Type of vehicles. This model only simulates the movement of cars. However, trucks are one type of heavy vehicles that also share the road with other cars. The interactions between vehicles are not modelled in this mesoscopic model

but it may have an impact as not all vehicles travel at the same speed. This model incorporates a variability in the free-flow speed that depends on the type of driver but it does not consider that these heavy vehicles can reduce the speed of other vehicles (interactions). The number of heavy vehicles that are travelling through the link may also influence the speed that is assigned to each vehicle that wants to enter the link. Further research needs to be done in this area.

5.11. Conclusions of the chapter

This chapter has presented a mesoscopic traffic simulator that models the dynamics of vehicles when moving through the network. Although there are already available existing mesoscopic models, this chapter has explained the reasons why another model has been implemented. The model represents the network using nodes and links, which are divided into running and queueing part. The fundamental diagrams based on aggregated macroscopic quantities dictate the movements of vehicles through the network. This model has also described how a queue is formed and dissipated when the network is congested. The contribution of this chapter to the body of knowledge is focussed on the provision of a detailed explanation of a new three-stage process that is used to simulate movements through the network and how it could be implemented in MATLAB. None of the consulted mesoscopic models (Mezzo, DynaSMART) have provided a detailed explanation of how they implemented this modelling process of sending vehicles to next links. It could be considered as a starting point for other researchers to develop new mesoscopic traffic simulators. An illustrative example has also been included and it demonstrates that the implemented model is able to replicate the fundamental diagrams of traffic flow and it forms and dissipates queues successfully. Further work needs to be done in order to calibrate the model to specific traffic conditions to which they are applied and validate it with real traffic data.

CHAPTER 6

A reinforcement-learning model of departure time and route choice

6.1. Introduction and background

Traffic assignment models, which are part of the traditional four-step model (Ortuzar and Willumsen, 2011), are widely used as a transport planning tool to predict traffic loads on the network. Results from these models, such as traffic flows, travel times and congestion levels, are used by transport planners to make important decisions regarding infrastructure investment and transport policies. Within restoration modelling, the current approach is to use static user equilibrium-based traffic assignment models (see literature review in Chapter 2). These models are based on the Wardrop's first principle (1952) which states that, under congested conditions, every traveller seeks to minimise his/her travel cost. User equilibrium (UE) is then reached when no traveller can reduce his/her travel cost by unilaterally switching to another route. However, in reality, drivers do not have 'perfect knowledge' of costs on all routes at all times and therefore, they may not select the route that has the minimum travel cost for them. Drivers only know information about traffic conditions on those routes that have been used in previous days or based on real-time information that is provided by traffic information services. After the impact of a hazard, parts of the network can be severely damaged, which may require the immediate closure of some road segments. Not all drivers may be aware of all network changes and therefore, it is unrealistic to think that after these incidents all drivers have perfect knowledge of traffic conditions (Hackl, Adey and Lethanh, 2018). Although static user-equilibrium assignment is still a preferred tool to assign traffic on

the network due to its simplicity and computational efficiency (Bliemer *et al.*, 2013; Kaviani *et al.*, 2018), the unrealistic assumptions made are likely to lead to output errors.

In recent years, there have been attempts to incorporate a non-equilibrium or transient drivers' behaviour in vehicle assignment (Faturechi and Miller-Hooks, 2014b; Nogal *et al.*, 2016). A system impedance was introduced in these models to reflect the drivers' lack of knowledge of the new situation.

Drivers need to make travel decisions that, in most cases, are repeated in a daily basis. As human beings, they have an inherited ability to learn from past experiences and therefore, they make current travel decisions based on the consequences of previous ones. Therefore, drivers can build their own travel memory and create their own travel expectations based on previous days. In this case, as drivers do not have perfect knowledge of network conditions, user equilibrium may not be reached. Learning-based algorithms for modelling travel behaviour result in more realistic traffic assignments (Wahba and Shalaby, 2006).

Therefore, the aim of this chapter is to develop a model that assigns traffic loads on the network, avoiding the user equilibrium condition and providing a more realistic drivers' decision-making modelling approach. The rest of this section describes the process of how human beings learn from their past experiences and use this information to make future travel decisions. Current learning-based traffic models are identified and their limitations are highlighted. Section 6.2 presents the modelling framework of the RL traffic model proposed in this chapter. Section 6.3 to 6.8 describe different parts of the model more in detail (expected travel cost calculation, stimulus functions, option probability updating functions). Section 6.9 applies all these concepts to the same transport network used in Chapter 4 (the Sioux Falls Network, US). Finally, Section 6.10 to 6.12 includes some limitations, further work and conclusions.

6.1.1. Psychological principles of learning behaviour

One of the first attempts that applies psychological principles to the area of learning comes from Thorndike's experiments (Thorndike, 1898, 1911). He studied the process

of how animals learn over time. In his experiments, he placed a cat inside a puzzle box and then a piece of meat outside the box. The only way to escape the box was through a door that was opened by pressing a lever. He observed that even though during the first time the cat opened the door probably by accident, the cat became more likely to repeat the action as it received a reward immediately after opening the door. Thorndike also noticed that cats became much faster at escaping the box. The reason was because opening the door led to a positive reward and thus, cats were more likely to repeat the same action in the future. This learning process is defined by Thorndike (1911) as the "Law of effect" and two key aspects are highlighted from this theory:

a) Any behaviour that leads to positive consequences is MORE likely to be repeated in the future.
b) Any behaviour that leads to negative consequences is LESS likely to occur again.

To the best of the author's knowledge, the term "reinforcement" appeared for the first time in the work done by Ivan Pavlov (1927) on his conditioned reflexes. The author, creator of *classical (or Pavlovian) conditioning*, demonstrated through his experiments why dogs started salivating even without having food in front of them. He suggested that any stimulus (e.g. the sound of a bell) could have the same effect of salivation if it was initially paired with the original stimulus (e.g. food). In this sense, this process of strengthening a behavioural pattern (e.g. salivating even without having food) is known as reinforcement.

6.1.2. Introduction to reinforcement learning and learning automata.

Reinforcement learning (RL) is a major branch of Machine Learning, which is an important research area of Artificial Intelligence (AI). RL allows agents to determine automatically the optimal behaviour based on the response of the environment, as shown in Figure 6.1. This feedback allows agents to learn from their behaviour. If the response is satisfactory, the agent receives a positive reward. And if it is not satisfactory, a negative reward (or punishment) is received.

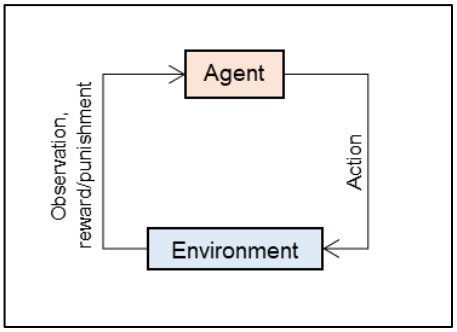

Figure 6.1. Diagram of the Reinforcement Learning system
[Adapted from (Sutton and Barto, 1998)]

There are some terms of the RL field that the reader must know at this point. Table 6.1 summarises some of these RL terms.

Table 6.1. Reinforcement learning terms.

Term	**Description**
Agent	Individual that makes a decision.
Action	A set of decisions that the agent can undertake.
Environment	Where the agent learns and makes decisions. The environment can be deterministic (if the same action leads to the same state) or stochastic (if the agent takes an action and the resulting state might not always be the same).
State	The observations that the agent receives from the environment.
Reward	The output after selecting an action by the agent.
Policy	A strategy that an agent uses in pursuit of goals.

Two types of RL models are classified in the literature (Gläscher *et al.*, 2010; Kurdi, Gershman and Banaji, 2019): model-based RL and model-free RL. Model-based RL algorithms are formulated as a Markov Decision Process (MDP), which represents how the environment reacts to the actions that an agent might take. It includes two functions (Haith and Krakauer, 2013): (1) a transition function (or transition model) that gives the probability of moving to any of the next states, given the current state of the environment and an action that an agent might take, and (2) a function that provides the reward to the agent. The "dynamics" of the environment are determined

by the transition function and the reward function. In this sense, the agent can potentially predict the dynamics of the environment. In summary, this system uses a predictive model of the world that answers questions such as "what will happen if the agent does X?" (Janner *et al.*, 2019).

However, in the absence of the transition and reward functions, MDP is unknown and the agent does not know *a priori* what the effects of the actions that the agent might take are. Therefore, the agent needs to interact with the environment and learn from their mistakes using a 'trial and error' approach. In this sense, and by taking actions, the agent starts to understand the unknown environment and the response to his/her actions. This is also known as 'model-free RL algorithm'. Therefore, this algorithm estimates the optimal policy directly from experience, without using any transition and reward function. Examples of this type of algorithms are: Learning automata (Narendra and Thathachar, 1974) and Q-learning (Watkins, 1989; Watkins and Dayan, 1992), among others.

The model that is proposed in this chapter belongs to the category of model-free algorithms because *a priori* agents (or drivers in this case) do not know the consequences of the actions they could take. They need to undertake the actions in order to gather information about the environment and with this information they can make future decisions.

The difference between the two model-free RL algorithms – Learning automata and Q-learning – is described as follows. Learning automata belong to the category of 'policy iteration methods', which search directly for the optimal policy in the space of policies (Wauters *et al.*, 2013). This algorithm defines a starting policy, estimates the state value of that policy and iterates towards the best policy by making changes to action choices (Buşoniu *et al.*, 2010). This is expressed using an action probability distribution that is updated using some reinforcement schemes (Wauters *et al.*, 2013). In contrast, Q-learning, which belongs to the 'value iteration methods', do not search for the optimal policy (also known as 'off-policy' algorithm (Violante, 2019)) and instead it evaluates the 'Quality' of a state-action pair through a value function (Wauters *et al.*, 2013). In this sense, 'quality' shows how useful an action is in obtaining the maximum reward (Violante, 2019). The optimal policy can be derived at the end from the obtained values (Habib, 2012).

Robert Bush and Frederick Mosteller (1951), using some considerations of Estes (1950), developed the first mathematical learning model in the area of psychology and biology to describe human behaviour. The idea behind the Bush-Mosteller (BM) model is that an agent is able to make a decision based on the consequences of their previous actions. In terms of probabilities, the Bush-Mosteller model (see Equation (6.1)) updates the probability P that an action a occurs on trial $t+1$ as a function of its value in the previous trial t and a correction term (ΔP_a^t) that is based on the agent's experience on trial t. This term increases or decreases the probability P_a^t. The term $r \cdot (1 - P_a^t)$ of Equation (6.1) corresponds to an increment in P_a^t which is proportional to the maximum possible increment, $(1 - P_a^t)$. The term $-p \cdot P_a^t$ corresponds to a decrement in P_a^t which is proportional to the maximum possible decrement, $-P_a^t$. The parameters r and p are also known as *reward* and *punishment*, respectively, and they take values between 0 and 1. Note that if an action is rewarded ($r > 0$), it cannot be punished ($p = 0$) and vice versa. These terms are multiplied by ℓ, which is also known as the *learning rate*. If the learning rate acquires the maximum value ($\ell = 1$) and the agent receives the maximum reward ($r = 1$, $p = 0$), then $P_a^{t+1} = 1$ which means that the probability that the action occurs on the next trial is immediately updated based on what the agent has experienced just the trial before. If the value of the learning rate is small (non-zero value), then the value of P_a^{t+1} is slowly increased or decreased, depending on the value of the reward/punishment.

$$P_a^{t+1} = P_a^t + \Delta P_a^t$$
$$\text{Being } \Delta P_a^t = \ell \cdot [r \cdot (1 - P_a^t) - p \cdot P_a^t] \tag{6.1}$$

Where,

P_a^{t+1}, is the probability that the action a occurs at trial $t+1$, ranging from 0 to 1.

P_a^t, is the probability that the action a occurs at trial t, ranging from 0 to 1.

ΔP_a^t, is the change in the strength of the action a, ranging from 0 to 1.

ℓ, is the learning rate, ranging from 0 to 1.

r, is the parameter that increases the probability P_a^{t+1}. It is also known as *reward*. It lies between 0 and 1.

$\wp$, is the parameter that decreases the probability P_a^{t+1}. It is also known as *punishment*. It lies between 0 and 1.

6.1.3. Reinforcement learning in the area of transport modelling

Reinforcement learning have been applied to other areas of engineering (Obaidat, Papadimitriou and Pomportsis, 2002), such as computer vision (Maravall, de Lope and Fuentes, 2013), transportation (Unsal, Kachroo and Bay, 1999; Barzegar *et al.*, 2011), automated system design (Oommen and Hashem, 2010). A review carried out by Abdulhai and Kattan (2003) about the reinforcement learning and their applications shows the potential of this technique in the transportation field. These authors and others (Bartin, 2019) admitted that the most researched part in the transport area was the use of RL in optimising traffic signal control operations (Roozemond and Veer, 1998; Abdullah, Pringle and Karakuls, 2003; Shoufeng, Ximin and Shiqiang, 2008; Bombol, Koltovska and Veljanovska, 2012; Zang *et al.*, 2020). However, they also mentioned that the application of the RL in the area of transportation field needed to be examined and explored further more.

In the area of route choice modelling, only a few models that apply the RL to the route choice problem have been identified in the literature. The following Table 6.2 summarises the characteristics of these models.

Table 6.2. Models found that use RL in route choice modelling

Reference	Description
(Ozbay, Datta and Kachroo, 2001)	A day-to-day route choice model using stochastic learning automata (SLA). The authors used a Linear Reward-Penalty Scheme to represent the day-to-day learning process. They used a macroscopic traffic model. The model was applied to simple 2-route network.
(Ozbay, Datta and Kachroo, 2002)	This model updated the previous one (Ozbay, Datta and Kachroo, 2001) by allowing drivers to choose a departure time (in addition to the route). Drivers were grouped into packets. They also used a macroscopic model. The model was also applied to a 2-route network.
(Wahba and Shalaby, 2005)	A day-to-day and within-day transit assignment model. The authors used a RL algorithm to simulate the adaptation process of passengers to the dynamics of the public transit network. Passengers made their travel choices (including departure time, origin-destination bus stops and route choice) based on the experience over time. It was modelled using a microscopic transport simulator.

Continuous in the next page

From the previous page

Reference	Description
(Yanmaz-Tuzel and Ozbay, 2009)	The authors improved the SLA originally proposed by Ozbay *et al.* (2001) to a Bayesian SLA model. The learning parameters were modelled as probability distributions rather than deterministic values and were estimated via a Bayesian Inference approach.
(Wei, Ma and Jia, 2014)	A day-to-day route choice model based on RL and multi-agent simulation. The authors applied the classical learning Bush-Mosteller model to simulate how individual drivers made daily route choices. The Reward-Penalty Scheme was represented as a stimulus function that represented the degree of satisfaction or dissatisfaction of each driver's choice. They used a macroscopic traffic model. The authors applied the model to a network of 13 nodes, 19 links and a demand of 2062 vehicles.
(de Oliveira Ramos and Grunitzki, 2015)	Route choice model that compared the Q-learning algorithm and the learning automata algorithm. The authors proposed a new mechanism that updated the drivers' set of routes, allowing faster routes to be learned. They applied the model to a network of 13 nodes and 24 links and modelling 1700 vehicles (4 OD). It also used a macroscopic traffic model.
(Bazzan and Grunitzki, 2016)	Traffic assignment model that allowed each driver to create his or her own route by deciding, at each node, how to continue their trips to their destination. The authors used the Q-learning algorithm to solve the problem. The difference between this model compared to the other models was that drivers decide to go to nodes instead of the classical method of selecting entire routes.
(Zhou *et al.*, 2020)	The authors combined a learning automata approach with a congestion game to address the route choice problem and reach the optimal route choice strategy. They pointed out that the BM model is an effective method to learn the optimal route choice strategy.

6.1.4. Limitations of current RL traffic models

Reinforcement learning algorithms have been used to model drivers' behaviour. However, current models do not capture essential aspects that characterise drivers' decisions. Some of the limitations of previous models are described as follows:

1. Reviewed RL traffic models have not dealt with the situation where one or more links have been closed. In such situations, drivers need to divert to other routes or even decide to abandon the trip and return home. These travel decisions may also influence future ones.

2. Especially after disruptive events, drivers may decide not to travel using their car and use other modes of transport or even cancel the trip. Current RL traffic models should incorporate a multi-modal approach and add the possibility of not travelling by car.
3. Emerging technologies and Intelligent Transport Systems (ITS) are helping drivers to make more informed decisions. Nowadays, drivers have access to pre-trip information and on-board information via GPS navigation, radio and social media. Travel decisions can be altered based on this new information. In this sense, current RL traffic models need to incorporate pre-trip and en-route travel information and understand how this new information alters the habitual travel behaviour and how it is integrated in the driver's cognitive model.
4. Current reward-penalty schemes of the RL traffic models reward the chosen option if it was a good decision or penalise the option if it was a bad decision. Consequently, the model rewards (penalises) the rest of the unselected options so that it stimulates drivers to use (or not use) them. If the model rewards the chosen option, then it penalises the rest and vice versa. However, models should not consider all the rest of options as a fixed block. Some of them may be favourable to use while others may not. A clear example is described as follows: according to current models, if a driver departs at 8am and arrives late at the destination, this option is penalised and all the rest of options are rewarded. However, this driver would never choose an option that departs later than 8am because there is a high chance of arriving late again. Modifications to current reward-penalty schemes should differentiate between travel options that drivers are also willing to use (favourable options) and those options that they prefer not to use (unfavourable options), instead of just differentiating between selected and unselected options.

These potential improvements are relevant to this study because it allows a more realistic approach in which drivers can make on-board travel decisions, learn from their past mistakes, influence future ones and make more informed decisions, among others. This acquires special importance after the impact of disruptive events.

Therefore, Chapters 6 and 7 aim to develop a model that overcomes the limitations observed in previous RL traffic models.

6.2. Modelling framework

6.2.1. Drivers' decision making process framework

The model proposed in this chapter is a departure time and route choice model that applies the idea of RL to simulate how drivers learn from their own experience and make day-to-day and within-day travel decisions. Learning techniques are ideal methods to model drivers' reactions to a changing environment without necessary converging to an equilibrium state (Brenner, 2004). This allows a more dynamic representation of drivers' adaptation to changing network conditions.

Based on the original idea of Bush and Mosteller (1951), this model allows drivers to learn from their own mistakes (as a 'trial and error' approach) and move towards minimising their day-to-day travel cost. Among the RL techniques, learning automata algorithm is the one selected to use in this model. The reasons why this approach have been selected are the following: (1) The LA algorithm is more intuitive compared to a Q-learning algorithm and reflects accurately drivers' decision-making as it describes the internal states of drivers as a probability distribution according to which actions are chosen. (2) LA searches directly for the optimal policy instead of evaluating the 'Quality' of a state-action pair through a value function (Wauters *et al.*, 2013). (3) A comparison between LA against QL algorithm which was done by de Oliveira Ramos and Grunitzki (2015) shows that LA converges faster to a preferred solution and needs to explore less of the network. (4) Easier to implement than other algorithms, such as the Q-Learning algorithm.

The inspiration of the model which is described in this chapter is based on the previous work done by Ozbay *et al.* (2002) and Wei *et al.* (2014). The former because they provide the idea of incorporating a departure time and a route choice as an inter-related decision on these types of models and the latter because they present an easy and understandable formulation for the reward-penalty scheme that can be directly applied to the transport area. Therefore, a combination of both models and several improvements are presented in this chapter.

Drivers' day-to-day behaviour can be represented as a dynamic process of repetitive travel decision making. They have to plan their trips in an uncertain environment and through making day-to-day decisions, drivers learn by 'trial and error' the dynamics of the system. Drivers acquire knowledge during the first days about the environment and store and update this information on their mental model. Over time, drivers may choose different travel options and learn which of these choices are the 'best' for them in achieving a certain goal. In the context of this model, a travel option is defined as a combined decision in which drivers choose a departure time and a route to get to their destination. Note that the model does not tell drivers the action that they should take. Instead, it allows them to discover which actions give them the maximum reward.

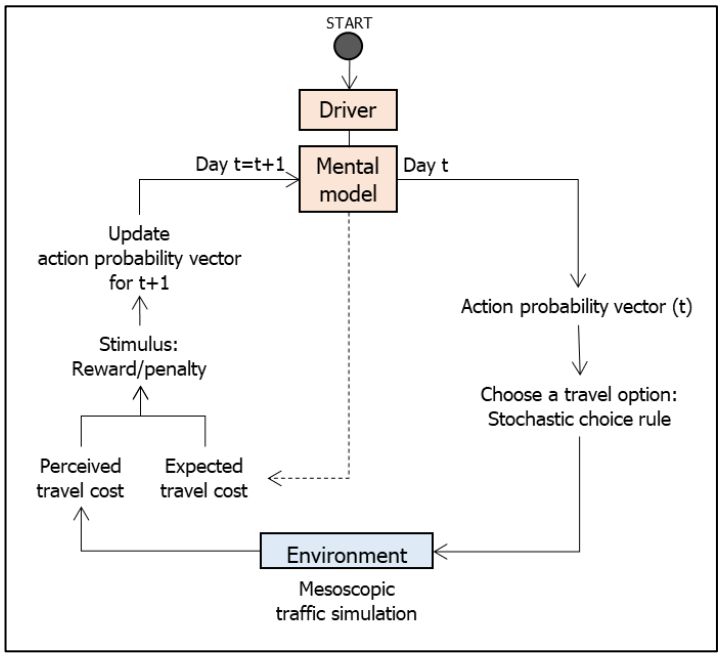

Figure 6.2. Drivers' decision-making process based on a reinforcement learning approach

The framework of the RL traffic model proposed in this chapter is shown in Figure 6.2. In this model, each driver has a 'brain' (mental model) that stores travel information from previous trips. These travel memories are represented by the LA algorithm as an internal state of each possible travel option. The consequences of selecting a travel option on each day updates the internal state of each option.

Mathematically, it is described as a probability distribution according to which travel options are chosen. The probability associated with each option indicates how likely the option is to be chosen by the driver. In this model, this is stored in an action probability vector (probability mass density) and it satisfies the condition shown in Equation (6.2): the sum of the probabilities of all possible travel options that a driver knows must be equal to 1. Initially drivers have zero knowledge about the environment and they learn while they select travel options on each day. This model assumes that all initial probabilities of selecting options are equal.

$$\sum_{z=1}^{\mathcal{Z}} p_{zt} = 1 \tag{6.2}$$

Where,

$\mathcal{Z}$, is the total number of possible travel options that each driver knows.

p_{zt}, is the probability of selecting each travel option z at time t.

Each driver selects stochastically the travel option for next day. This is done by using the stochastic choice rule presented in Equation (6.3). The bigger the probability of an option is, the more likely this option is selected by the driver. Each day, a uniform distributed random value (ϑ) is generated for each driver and it is compared to the cumulative probability distribution of all options. Each possible travel option is given randomly a unique number (z), which are then ordered from lowest to highest. The travel option ($z = m$) that satisfies Equation (6.3) is the one selected by the driver for that day.

$$\sum_{z=1}^{m-1} p_{zt} < \vartheta \leq \sum_{z=1}^{m} p_{zt} \tag{6.3}$$

$$\forall\, m \in \mathcal{Z}$$

Where:

p_{zt}, is the probability of selecting a travel option z on day t.

m, is the future selected travel option on day t.

z, is a travel option.

$\mathcal{Z}$, is the total number of possible travel options that each driver knows.

ϑ, is the random value (ranging from 0 to 1).

Once the driver has chosen a travel option for the day, a mesoscopic traffic model simulates the movement of vehicles through the network. This has already been explained in Chapter 5. At the end of the simulation, drivers receive a response from the environment in the form of the travel costs, which are stored in their mental models. Comparing this perceived travel cost and the travel cost that the driver expects from previous travel experiences, each driver receives a positive stimulus (reward) towards repeating the same travel option again or negative stimulus (punishment) that penalises the selection of this travel option. The action probability vector is adjusted for the day $t + 1$ according to the success or failure of the action taken on day t. Note that, as mentioned in previous Chapter 5, drivers can be grouped into packets in order to speed up the modelling process. Therefore, all drivers within the packet are treated as a homogenous group.

6.2.2. Preferred Arrival Time Interval (PATI) and types of drivers

The purpose of travelling is to undertake activities at the destination place. These activities may include work, recreational and social activities, among others. The importance of knowing the reason why drivers travel is because activities can be treated differently in this model. The starting time of all activity types may not be the same. Some activities have more restrictive starting times than others. For instance, the starting time of a work-based activity may not be as flexible as a leisure-based activity in general. This model considers this feature by assuming different starting times for different activities.

Drivers may have a period of time that they preferred to arrive before the activity starts. Some authors (Jenelius, Mattsson and Levinson, 2011; Thorhauge, Cherchi and Rich, 2014) use a Preferred Arrival Time (PAT) while others (Xiao, Liu and Huang, 2014) define a Preferred Arrival Time Interval (PATI) instead of a single point in time. If drivers do not arrive before the PAT or PATI, it may affect negatively producing stress, nerves, etc. If they arrive earlier, it may be too early and they would prefer to depart later. If they arrive later, that could be too late and they could arrive not in time to undertake the activity. In both cases, drivers are penalised for being late/early as it will be explained in the Section 6.3. The model proposed in this chapter

includes the possibility of adding both PAT and PATI. In fact, PATI can be transformed into PAT if the extreme values of the interval are equal.

Heterogeneity between drivers have also been considered in this model. As not all drivers prefer to arrive at the same interval time, different types of drivers have also been implemented in this model. Different types of drivers mean different PAT/PATI. Although this model opens the possibility to include these additional features, the lack of enough data may complicate the model and simplifications may be added, such as assuming a single starting time for all activities, or adding just one type of driver and therefore just one PAT or PATI.

6.2.3. Subset of initial routes

A large set of paths connects an origin and a destination in a real network. However, all these alternative routes cannot be generated in the model because it would be computationally expensive. Instead, a subset of routes is defined for each origin-destination pair. The modeller needs to define the number of routes (K) that the subset includes.

Routes are obtained using the Yen's K-Shortest Path algorithm (1971) based on free-flow travel times. This algorithm initially finds the shortest path between the origin node and the destination node using the Dijkstra's algorithm (1959) and then finds K-1 deviations of this previously-discovered shortest path without repeating nodes in the path. Yen (1971) identifies every node of the main shortest path and calculates another shortest path (spur) from each node to the last node, avoiding selecting already visited nodes and links from the root path (loopless). The process is repeated calculating a spur path from each node in each new shortest path (Brander and Sinclair, 1996; Chen *et al.*, 2020).

6.3. Travel cost function

Traditionally, the function that quantifies the travel cost depends on the time spent by a driver from an origin to a destination. However, more generalised cost functions than just travel time have been suggested by other researchers. As this model also considers the option of choosing a departure time, the cost function should consider

the effect of arriving earlier or later than the PAT/PATI. In fact, drivers may adjust their departure time for future trips depending on how early or late they arrive to the destination. This function usually consists of a trade-off between the travel time spent between an origin to a destination and some penalties for early or late arrivals.

There is a group of studies in which a simple linear cost function is considered, assuming that disutility is proportional to the delay. For instance, and based on previous work done by Gaver (1968), Vickrey (1969) and Cosslett (1977), Small (1982) proposed a utility function, which was extended by Noland and Small (1995), that considers the cost of early or late arrivals relative to some specific preferred arrival time. De Palma *et al.* (1983) changed this model and proposed a preferred arrival time interval, instead of a single preferred arrival time.

For the simplicity of the function, we use the one proposed by Small (1982), with the considerations of De Palma *et al.* (1983). Equation (6.4) shows the implemented generalised cost function.

$$C_{hzt} = \beta_1 \cdot TT_{hzt} + \beta_2 \cdot SDE_{hzt} + \beta_3 \cdot SDL_{hzt} + \beta_4 \cdot DL_{ht} \quad (6.4)$$

Where,

TT_{hzt}, time that packet of vehicles h spent on their journey after choosing option z on day t.

SDE_{hzt}, amount of time that packet of vehicles h arrives early at the destination after choosing option z on day t.

$$SDE_{hzt} = \begin{cases} ET_h - AT_{hzt}, & if\ AT_{hzt} < ET_h \\ 0, & otherwise \end{cases} \quad (6.5)$$

Being,

ET_h, earliest limit of the preferred arrival time interval (PATI).

$$PATI_h = [ET_h\ ,\ LT_h]$$

AT_{hzt}, arrival time of driver h choosing option z

SDL_{hzt}, amount of time that packet of vehicles h arrives late at the destination after choosing option z on day t.

$$SDL_{hzt} = \begin{cases} AT_{hzt} - LT_h, & if\ AT_{hzt} > LT_h \\ 0, & otherwise \end{cases} \quad (6.6)$$

Being,

LT_h, latest limit of the preferred arrival time interval (PATI).

$$PATI_h = [ET_h \ , \ LT_h]$$

AT_{hzt}, arrival time of packet of vehicles h choosing option z

DL_{ht}, late arrival penalty assigned to packet of vehicles h on day t. It takes a value of 1 for late arrival or 0 otherwise.

β_1, β_2, β_3, β_4, coefficients. These can take any value between 0 and 1. If it takes a value of 0, the corresponding term does not interfere in the cost function.

6.4. Expected travel cost

Every time drivers want to undertake a trip, they recall the travel cost spent on previous trips with similar characteristics. In this sense, the travel cost that drivers expect after choosing a route and a departure time is obtained from previous experienced trips that drivers have undertaken on previous days using the same route and departure time. This is called the expected travel cost, which is an aggregation of experienced travel costs. When a driver finishes a trip, the experienced travel cost of this journey is stored in his or her mental model. This creates a collection of memories that are used to estimate future travel costs.

The formulation of this expected travel cost is based on the formula proposed by Wei *et al.* (2014), which also use the Bush-Mosteller model. These authors proposed a formula to calculate the expected travel cost as a weighted average of all travel costs of all routes that a driver has used in the past. In this sense, they calculate an average travel cost specifically for that origin-destination (OD) pair. However, their model only accounts for route choice. Departure time choice is not considered. Due to the demand variation along a day, the travel cost of a route varies at different times. For instance, the travel cost of a route is not the same in the peak period as in a non-peak period. That is the reason why there is a need to update the previous formulation to account for departure time variations.

The formulation proposed in this model is designed to overcome the above limitation. The developed expression is shown in Equation (6.7). It calculates the expected travel cost (A_{ht}) between an OD pair as the average travel cost of all travel

options (z) that depart at a specific time based on previous travel experience. In other words, the travel cost that a driver expects once he or she knows the departure time for that day is calculated considering the travel cost of previous trips that have departed at the same time, no matter which route they take. That is represented by the third equation in the group of Equations (6.7).

If drivers have never used any route that has the same departure time, they cannot expect a travel cost at that time. In this model, it is assumed that if this happens, the expected travel cost will be calculated considering all routes and departure times, without including the previous limitation of having the same departure time. It is known that this is not a realistic assumption but at least the model still allows drivers to calculate an expected travel cost. This is represented by the second equation in the group of Equations (6.7).

Note that if drivers have no previous knowledge of travel options (that is the case on day $t = 1$), it is assumed that the expected travel cost is zero. Alternatively, the free-flow travel time could also be used to obtain the expected travel cost.

$$A_{ht} = \begin{cases} 0 & if\ t = 1 \\ \dfrac{\sum_{j=1}^{t-1} \sum_{z=1}^{Z} (C_{hzj})}{t-1} & if \sum_{j=1}^{t-1} \sum_{z=1}^{Z} s_{hzj} = 0 \\ \dfrac{\sum_{j=1}^{t-1} \sum_{z=1}^{Z} (s_{hzj} \cdot C_{hzj})}{\sum_{j=1}^{t-1} \sum_{z=1}^{Z} (s_{hzj})} & otherwise \end{cases} \quad (6.7)$$

Where:

z, is the travel option number.

h, is the packet of drivers.

t, is the time (in days).

A_{ht}, is the travel cost that packet of drivers h expects at time t.

C_{hzj}, travel cost of option z that packet of drivers h has experienced on day j. If a travel option has not been used on day j, then $C_{hzj} = 0$. This means that only one travel option can be selected on each day and therefore only one travel cost per day is computed in the formula.

s_{hzj}, binary variable that takes the value of 1 if the travel option z, which was chosen on day j, has the same departure time as the travel option m

chosen on day t. Otherwise, it takes a value of 0. Note that if a travel option z is not chosen on day j, then $s_{hzj} = 0$. This means that only one travel option can be selected per day and therefore the maximum value of s_{hzj} on each day j can only be 1.

$$s_{hzj} = \begin{cases} 1, & if\ DT_{zj} = DT_{mt} \\ 0, & otherwise \end{cases} \quad (6.8)$$

Being,

DT_{zj}, departure time of chosen option z on day j.

DT_{mt}, departure time of chosen option m on day t. Note that option m may not use the same route as option z.

6.4.1. Weighting factor φ_j: memory level of drivers

The mental model represents the driver's memory where previous travel experiences are stored. Every time a driver undertakes a trip, he or she is able to remember the cost associated with this travel option. However, as Anderson *et al.* (1994) say, all species that have memory forgets. This means that humans are able to remember experiences but at the same time these experiences can be lost over time.

Hermann Ebbinghaus (1880) was the first person who studied how memories decay over time. In his experiments, he proposed a mathematical equation that described the shape of forgetting, also worldwide known as Ebbinghaus' forgetting curve (see Figure 6.3). He found that this curve tends to be exponential in nature, so that memory loss is rapid within the first few days.

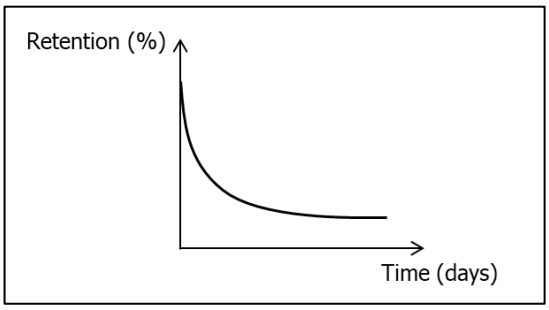

Figure 6.3. Simplified Ebbinghaus' forgetting curve

Previous models, such as the one developed by Wei *et al.* (2014), also incorporate the effect that memories decay over time when calculating the average travel cost. Drivers are able to remember more recent travel experiences than old ones. That is the reason why, in the drivers' mental model, recent travel experiences are stronger than old travel experiences.

The effect of memory decay is added to the group of Equations (6.7) and is updated in Equation (6.9). In these modified equations, the travel costs of all days are not counted as equal on the formulation. The effect of memory is represented by adding different importance (weights) to the values of different days, which are shown in green in Equation (6.9). As old travel experiences are remembered less than recent ones, their weighting values are lower. As opposed, recent travel experiences have the greatest impact with higher weighting values.

$$A_{ht} = \begin{cases} 0 & if\ t = 1 \\ \dfrac{\sum_{j=1}^{t-1} \left[\varphi_j \cdot \left(\sum_{z=1}^{Z} C_{hzj} \right) \right]}{\sum_{j=1}^{t-1} \varphi_j} & if \sum_{j=1}^{t-1} \sum_{z=1}^{Z} s_{hzj} = 0 \\ \dfrac{\sum_{j=1}^{t-1} \left[\varphi_j \cdot \left(\sum_{z=1}^{Z} s_{hzj} \cdot C_{hzj} \right) \right]}{\sum_{j=1}^{t-1} \left[\varphi_j \cdot \sum_{z=1}^{Z} s_{hzj} \right]} & otherwise \end{cases} \quad (6.9)$$

Where:

φ_j, weighting factor that represents the memory level of travellers.

The rest of variables are defined in Equation (6.7)

Different forgetting functions represent different ways of how drivers remember previous experiences. Although Ebbinghaus (1880) represents the memory decay as an exponential function, to simplify the complexity of the model, a linear function is proposed. However, the way that the model is coded allows the modeller to decide which forgetting curve prefers to use. Equation (6.10) expresses mathematically the calculation of the weighting factor (φ_j) that represents the memory decay of drivers. Note that if $\varphi_j = 1$, Equation (6.9) is equivalent to Equation (6.7).

$$\varphi_j = \begin{cases} 1 & constant\ function \\ j & linear\ function \\ e^j & exponential\ function \end{cases} \quad (6.10)$$

Where,

φ_j, is the weighting factor the represents the memory level of drivers on day j.

j, is the day that is being analysed.

6.4.2. Weighting factor B_{dkj}: bad memories

By nature, human beings tend to weight losses more than gains. For instance, Kahneman and Tversky (1979) found that people are more upset about losing £10 than happy finding £10, meaning that people are more afraid of losses. This idea that bad things are stronger than good ones have been present in the literature for quite long time. The literature proposes a 'loss aversion coefficient' to quantify the importance that people give to losses and gains (Kahneman and Tversky, 1979; Shalev, 2000; Abdellaoui, Bleichrodt and Paraschiv, 2007). As an example, in financial context, a loss aversion coefficient of 2 indicates that a loss should be valued up to 2 times more than a gain. Most of these loss aversion values have been empirically estimated using some financial experiments. Fishburn and Kochenberger (1979) proposed a median coefficient of 4.8 for the loss aversion value. Tversky and Kahneman (1992) suggested that people tend to value losses about 2.25 times higher than gains of the same value. Gottman (1995) proposed an index to evaluate the success or failure of a relationship, indicating that the number of positive interactions must outnumber the negative ones by five to one. Baumeister *et al.* (2001) and Rozin and Royzman (2001) reviewed a large number of studies that evidenced that bad things were stronger than good ones. They could not find any study that found the opposite. In fact, they found that bad events had stronger and more lasting consequences than good events. They also came to the conclusion that people's brain retained the memory of bad things and tended to learn faster from bad events (e.g. punishment) than from good ones (e.g. reward). Tugend (2012) also mentioned how bad experiences worn off more slowly than good ones.

This idea could be extrapolated in order to incorporate how bad experiences are remembered more that good ones in the drivers' decision making process. To the best of the author's knowledge, the model proposed in this chapter is the first one that takes into account and incorporates in the formulations how bad experiences are more retained than good ones in the memory of drivers when making travel decisions. The next section explains more in detail how this model has implemented this new feature.

6.4.2.1. Implementation: the importance of bad experiences

The question that arises here is: what is a bad experience for a driver? As an example, a 50-minute delay can be considered as a bad experience for a driver while a 10-minute delay can be considered a bad one for another driver. As bad experiences can differ from driver to driver and from journey to journey, it is necessary to quantify different levels of bad experience. In this model, a bad experience is defined as those journeys whose travel time goes beyond the expected one for that route. The more difference between the experienced and expected travel time, the worse the event will be for the driver and therefore, it will be remembered for a longer time.

A new variable that is called *bad-event memory* (B_{hzt}) has been created in order to further weight the travel time of those bad experiences. This variable is defined using a step-defined function shown in Figure 6.4. It can take the following range of values: a minimum value of 1 when the experience is not considered bad, which means that this term is not further weighted; and a maximum value of B_{max} when it is considered as a bad experience. Equation (6.11) includes the mathematical description of this function.

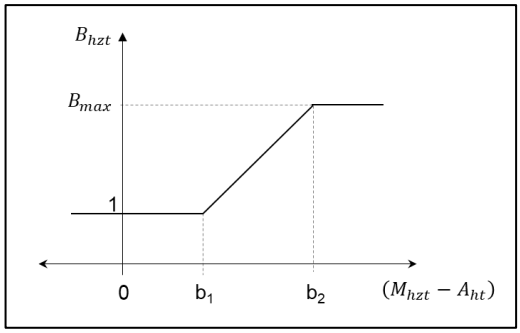

Figure 6.4. Graphical representation of the bad-event memory function

The advantage of the function presented in this section is that if the modeller does not want to consider this additional feature of further weighting bad memories, the value of B_{max} can be set to 1 and therefore, bad and good memories are equally weighted.

$$B_{hzt} = \begin{cases} 1 & if \quad (M_{hzt} - A_{ht}) \leq b_1 \\ \left(\frac{B_{max} - 1}{b_2 - b_1}\right) \cdot (M_{hzt} - A_{ht}) + \left(\frac{b_2 - b_1 \cdot B_{max}}{b_2 - b_1}\right) & if \quad b_1 < (M_{hzt} - A_{ht}) < b_2 \\ B_{max} & if \quad (M_{hzt} - A_{ht}) \geq b_2 \end{cases} \quad (6.11)$$

Where,

A_{ht}, is the expected travel cost of packet of drivers h on day t.

M_{hzt}, is the experienced travel cost after using travel option z by packet of drivers h on day t.

b_1 and b_2, are limit values defined by the modeller.

B_{max}, is a user-defined value that quantifies the maximum weighting value that the bad-memory variable can take.

B_{hzt}, is the bad-event memory variable on day t when a bad experience is identified.

This bad-event memory weighting factor is also added to the group of Equation (6.9) that calculates the expected travel cost and is updated in the following group of Equations (6.12) – Marked in green the weighting factor in the formulation. Note that if the bad-event memory weighting factor (B_{hzj}) is not considered in the formulation, Equation (6.12) turns into Equation (6.9).

$$A_{ht} = \begin{cases} 0 & if\ t = 1 \\ \dfrac{\sum_{j=1}^{t-1}\left[\varphi_j \cdot \left(\sum_{z=1}^{Z} B_{hzj} \cdot C_{hzj}\right)\right]}{\sum_{j=1}^{t-1}\left[\varphi_j \cdot \sum_{z=1}^{Z} B_{hzj}\right]} & if \sum_{j=1}^{t-1}\sum_{z=1}^{Z} s_{hzj} = 0 \\ \dfrac{\sum_{j=1}^{t-1}\left[\varphi_j \cdot \left(\sum_{z=1}^{Z} B_{hzj} \cdot s_{hzj} \cdot C_{hzj}\right)\right]}{\sum_{j=1}^{t-1}\left[\varphi_j \cdot \sum_{z=1}^{Z}\left(B_{hzj} \cdot s_{hzj}\right)\right]} & otherwise \end{cases} \quad (6.12)$$

Where,

B_{hzj}, is the bad-event memory variable of packet of drivers h after choosing option z on day j.

The rest of variables are defined in Equation (6.7) and Equation (6.9).

6.4.2.2. Bad experiences lose importance over time

An old well-known proverb says that *time heals all wounds.* Based on this expression, it was assumed that people tend to soften the importance of bad memories over time. After a certain amount of time, these bad experiences are considered equally important as good ones and therefore, there is no need to further weight these bad memories. That is the reason why a bad-memory decay function has been proposed in this section. It consists on a linear equation that decreases the value of the bad-event memory variable (B_{hzt}) over time until it reaches the value of 1, which is when memories are not further weighted. Figure 6.5 shows graphically how the additional weighting value decreases over time evidencing that drivers forget those bad experiences. Mathematically, this function is expressed in Equation (6.13) and it is used to update the value of the bad-event memory variable.

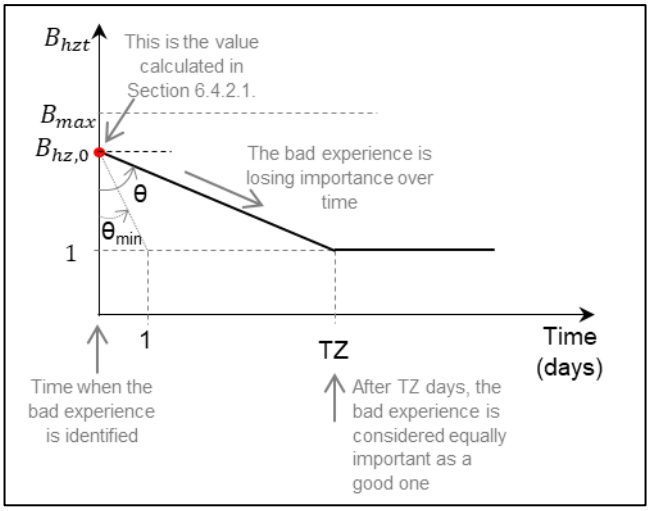

Figure 6.5. Graphical representation of the bad memory decay function

$$B_{hzt} = \begin{cases} B_{hz(t-1)} - \dfrac{1}{\tan\theta} & if\ t \leq TZ \\ 1 & otherwise \end{cases} \quad (6.13)$$

Where,

$B_{hz(t-1)}$, is the value of the bad-event memory variable on the previous day.

B_{hzt}, is the bad-event memory variable at time t.

t, is the time in days.

θ, is the angle between the vertical axis and the inclination of the decay function. This is a value defined by the modeller. It is measured in degrees and this can only take these values $\theta \in [\theta_{min}, 90)$. θ_{min} is described more in detail in Equation (6.15).

TZ, is the time when the bad-event memory variable takes a value of 1. It can be calculated using the value of the bad-event memory variable (B_{hzt}) of any day t.

$$TZ = (B_{hzt} - 1) \cdot \tan\theta + t \quad (6.14)$$

The angle (θ) between the vertical axis and the inclination of the decay function is a user-defined value that indicates how fast a driver forgets a bad experience. Low values of this angle indicates that drivers forget really fast the importance of previous bad events, while high values of the angle show that drivers retain in their mind these bad experiences for longer time.

It is important to limit the values that this angle can take. A minimum value θ_{min} (steepest slope) is defined in order to reach at least one-day gap (see Figure 6.5) between the day when the bad experience is identified and the next day. The formula used to calculate this value is shown in Equation (6.15). The maximum value has to be less than 90 degrees as the tangent of 90 cannot be mathematically calculated. Therefore, this angle can only take these values: $\theta \in [\theta_{min}, < 90)$

$$\theta_{min} = \tan^{-1}\left(\frac{1}{B_{hz,0}-1}\right) \quad (6.15)$$

Note that not all drivers are the same and therefore, we cannot assign a unique value of this angle to all drivers. For that reason, a different value of this angle will be assign to each driver. In the model, it is assigned randomly for each driver a different value between the minimum and 90 degrees (excluding this last one). If the angle is almost 90 degrees (e.g. 89.99), then it is considered that bad experiences do not lose importance over time. In this case, it is assumed that drivers will remember forever all these bad experiences and they will weight them more than good ones.

6.4.3. Calibration of memory parameters

The calibration process aims to find the parameters of the model that provide a good representation of the drivers' behaviour. This process can be achieved by confronting model results with actual measurements performed on the network. In particular, the calibration of the parameters that affect the memory of drivers is a complex process due to the entity of the information that is required. Data could be obtained through surveys in which drivers define what a bad experience is for them and how this bad experience is forgotten over time. Another possibility is to create a web-based travel simulator (Ozbay, Datta and Kachroo, 2001) that could be used to store drivers' decisions and therefore, acquire data that could be used in the model.

6.5. Stimulus function (reward-punishment function)

The consequences of the decisions that drivers make every day are accounted by a stimulus function. If drivers are satisfied with the travel decision on that day, they receive a positive stimulus towards repeating the same action the next day. If drivers

are not satisfied, they have less stimulus to repeat the same option the next day. The formulation that this section includes is based on the idea of the classical Bush-Mosteller model (1951) and modifies some models that have been applied to the transport area (Narendra and Thathachar, 1974; Ozbay, Datta and Kachroo, 2001; Wei, Ma and Jia, 2014).

The stimulus function that is proposed considers the difference between the expected and perceived travel cost of each driver on each day and it also includes some penalties for early or late arrivals. Based on this stimulus value, the probabilities of selecting travel options for the next days will be updated (see next Section 6.7).

The formulation of the stimulus function is described in Equation (6.16). The stimulus value (S_{hmt}) is formed by a satisfaction value (SAT_{hmt}) and a learning rate (ℓ_h). The satisfaction value indicates how happy (or satisfied) the driver is with the selected option on day t compared to the experience of previous days. The following Section 6.6.1 describes more in detail the calculation of this value.

$$S_{hmt} = \ell_h \cdot SAT_{hmt} \tag{6.16}$$

Where,

S_{hmt}, stimulus value of packet of vehicles h after choosing travel option m on day t. It can take values between -1 (negative stimulus towards repeating the same action the next day) and 1 (positive stimulus towards repeating the same action the next day).

ℓ_h, the learning rate for each packet of vehicles h. It can take values between 0 (excluded) and 1.

SAT_{hmt}, is the "satisfaction" value of packet of vehicles h after choosing travel option m on day t. This variable can only take values between -1 (totally dissatisfied) and 1 (totally satisfied).

The learning rate is commonly known in the field of machine learning as a 'hyper-parameter', which is a parameter value that is used to control the rate at which the algorithm learns (Smith, 2017; Blier, Wolinski and Ollivier, 2019; Gulde *et al.*, 2020). It determines how fast or slow the algorithm will move towards optimal

solutions (Rakhecha, 2019). To understand this better, a simple example is described as follows.

EXAMPLE. Imagine that 10 boxes are placed in a room. Four of them contain a prize of £50, £100, £500 and £1000 (each one) while the rest are empty. Each day, a person chooses one of the boxes and win the prize that is inside the box. The prizes are always placed in the same box on each day, which means that once the person opens a box, he/she knows the prize that is inside for the rest of the days. However, the person does not know how much money the maximum prize contains or how many prizes there are. The experiment is repeated for 10 days. In order to understand the concept of 'learning rate', the learning process of this person is analysed under two situations: when the learning rate is (CASE A) a high value or (CASE B) a low value.

The experiment starts. On day 1, the person opens the box and finds no prize. The next day, the person selects another box and finds no prize again. On day 3, the person selects another different box and finds a prize of £100. At this point, if the learning rate is too high, the person will instantly start to believe that this is the best prize he/she can get based on previous experience and therefore there is a very high probability of choosing the same box for the next days. On the other hand, with a low learning rate, the person is not completely sure that this is the maximum prize he/she can get and therefore the probability of choosing the same box for the next day is higher than choosing another box but he/she also gives the chance to try other boxes and find out if there is a higher prize.

To sum up, a higher learning rate could result in selecting rapidly a box that might not contain the maximum available prize and this person would never know if that is the maximum reward he/she can get. A lower learning rate means that the person might explore

the content of other boxes before sticking to the final one which means that more time is needed to converge but better prizes might be reached.

In this model, the learning rate represents the parameter that controls the learning process of drivers. If the learning rate is very high, drivers will rapidly stick to a travel option (not necessarily the optimal one) and if it is too small, drivers will take more time to learn and converge to the best values. A desirable learning rate is the one that is low enough so that it finds a (near) optimal solution but high enough so that it can be found in a reasonable amount of time. The consequences of choosing different values of the learning rate and the impact of these values on the model are analysed in an example proposed in Section 6.9 (more specifically in Section 6.9.3).

6.5.1. "Satisfaction" value (SAT_{hmt}).

The core of the stimulus value is the satisfaction (or dissatisfaction) of drivers after each travel decision. It compares the difference between the expected travel cost and the perceived travel cost. If the result of this difference is positive, it means that the perceived travel cost on that travel option is less than the expected one and therefore, drivers are satisfied with that decision. On the contrary, if the difference is negative, the perceived travel cost on that travel option is higher than the expected travel cost, meaning that drivers were expecting less travel cost on that option. Figure 6.6 summarises the procedure that is proposed to obtain the value of satisfaction or dissatisfaction, which is described as follows:

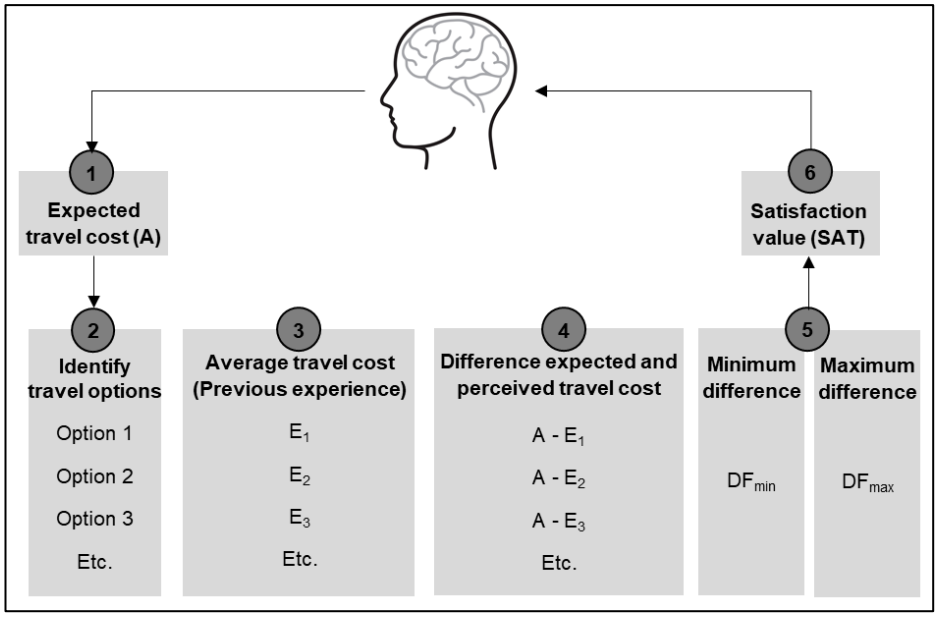

Figure 6.6. Process of satisfaction value calculation

1) Calculate the expected travel cost (A_{ht}) for each driver on each day using Equation (6.12), as described in Section 6.4, which is obtained before travelling on day t.
2) For each driver, identify all possible travel options that this driver could have chosen on day t. These options include those travel options that driver has used on previous days and those travel options that driver knows but he or she has never used. Other models (Ozbay, Datta and Kachroo, 2001; Wei, Ma and Jia, 2014) include all possible options instead of just considering the travel options that each driver knows. It is important to make this distinction because options that a driver does not know yet cannot be considered in the calculation. The reason is because this driver is not able to select this option due to the lack of knowledge.
3) Calculate the perceived travel cost (E_{hzt}) for each travel option identified in step 2. This is obtained as a weighted average of travel costs, calculated specifically for each travel option, as shown in Equation (6.17). There are two main differences between the perceived travel cost of option z and the expected travel cost [Equation (6.12)]: (1) the perceived travel cost of option z is calculated as the weighted average of travel costs considering only those days in which travel

option z is used. In contrast, the expected travel cost is obtained considering the weighted average of travel costs of all options; (2) The perceived travel cost also includes in the average the experienced travel cost on day t while the expected travel cost does not include this value. If other travel options different to z are used, these are not included in the weighted average value. If an option has never been used, it is assumed that the travel cost of that option is calculated using the free-flow travel cost. This is an assumption that needs validation in future stages of this model.

$$E_{hzt} = \begin{cases} \dfrac{\sum_{j=1}^{t} \left[\varphi_j \cdot \left(\sum_{z=1}^{\mathcal{Z}} B_{hzj} \cdot H_{hzj} \cdot C_{hzj} \right) \right]}{\sum_{j=1}^{t} \left[\varphi_j \cdot \sum_{z=1}^{\mathcal{Z}} \left(B_{hzj} \cdot H_{hzj} \right) \right]}, & if \sum_{j=1}^{t} \sum_{z=1}^{\mathcal{Z}} H_{hzj} > 0 \\ C_{h,FF}, & otherwise \end{cases} \quad (6.17)$$

Where,

E_{hzt}, perceived travel cost of packet of drivers h on travel option z calculated on day t.

C_{hzj}, travel cost of option z that packet of drivers h has experienced on day j.

φ_j, memory level of drivers ($0 < \varphi \leq 1$). This variable is explained more in detail in previous Section 6.4.1.

B_{hzj}, is the bad-event memory variable that is used to further weight the travel cost of those bad experiences on day t identified by packet of drivers h. This variable is explained more in detail in Section 6.4.2.

H_{hzj}, binary variable that indicates if a travel option z has been used on day j ($H_{hzj} = 1$) or it has not been used ($H_{hzj} = 0$) by packet of drivers h.

$C_{h,FF}$, free-flow travel cost of packet of drivers h.

4) Calculate the difference (DF_{hzt}) between the expected travel cost (A_{ht}) on day t and the perceived travel cost (E_{hzt}) of each travel option calculated in previous steps.

$$DF_{hzt} = A_{ht} - E_{hzt} \quad , \quad \forall z \in \mathcal{Z} \quad (6.18)$$

Where,

A_{ht}, is the travel cost that packet of drivers h expects at time t.

E_{hzt}, is the perceived travel cost of packet of drivers h on travel option z calculated on day t.

5) Find the maximum ($DF_{ht,max}$) and minimum difference ($DF_{ht,min}$) in travel cost obtained in the previous step. This indicates which travel option z would be the best and worst for each driver on that day by just comparing the expected and perceived travel cost.

$$DF_{ht,max} = max(D_{hzt}) \ , \qquad \forall z \in \mathcal{Z} \tag{6.19}$$

$$DF_{ht,min} = min(D_{hzt}) \ , \qquad \forall z \in \mathcal{Z} \tag{6.20}$$

6) Obtain the 'satisfaction' value of each packet of drivers h on day t after choosing option m by normalising the differences of travel costs to the $[-1, 1]$ range, being -1 the worst option that packet of drivers h could choose on day t and 1 the best option. With this scaling factor, the satisfaction value (SAT_{hmt}) is always greater or equal to -1 and lower or equal to 1. Equation (6.21) shows mathematically how to calculate the satisfaction value. The denominator indicates how good or bad a travel option z is, compared to the rest of options.

$$SAT_{hmt} = \begin{cases} \frac{DF_{hmt}}{DF_{ht,max}}, & if\ DF_{hmt} \geq 0 \\ \frac{DF_{hmt}}{|DF_{ht,min}|}, & if\ DF_{hmt} < 0 \end{cases} \tag{6.21}$$

6.6. Option probability updating functions

The heart and soul of the learning automata is the reinforcement scheme (Najim and Poznyak, 1994). Based on the selected travel option, the response of the environment and the stimulus value obtained from previous section, the model updates the probability vector of selecting travel options for the next day.

The formulation used by the classical Bush-Mosteller model (1951) adopts a very flexible approach and it leaves space for further improvements. The updating scheme of the classical model is based on the value of the stimulus (or drivers' satisfaction). After choosing an option m on day t, driver has a positive or negative

stimulus towards repeating the same option the next day. If the stimulus is positive, the probability of repeating the same option m the next day is increased and the probability of all the rest of options z is decreased. On the contrary, if the stimulus is negative, the driver is less likely to repeat the same option the next day. This means that the probability of choosing the selected option m is decreased and the probability of selecting the rest of options z is increased.

Recent models that are applied to transport modelling (Ozbay, Datta and Kachroo, 2001; Wei, Ma and Jia, 2014) keep the essence of the original model and do not introduce new improvements to the updating probability formulation. However, the formulation proposed in this section improves the previous updating scheme by considering a different approach, which is a direct consequence of the additional departure time choice module. As described in Section 6.2.2, each driver has an arrival time interval of preference (PATI). In this sense, there might be cases that some drivers are satisfied with the selected travel decision on day t but they arrive earlier or later than the PATI. There might be other travel options that use the same route but with different departure times, which means that drivers still have the chance to leave earlier if they have arrived late or leave later if they have arrived early. That is the reason why in this model the approach of increasing/decreasing the probability of selecting again the chosen travel option m and decreasing/increasing the probability of the rest of options z is not used and instead, a novel way of updating probabilities is presented in this chapter considering departure time differences between travel options. In this sense, travel options are classified as favourable options, which are more likely to repeat them the next day, and unfavourable options, which are less likely to repeat them the next day.

The following subsections present the new updating scheme of the proposed model. Two different formulations are presented according to the satisfaction of the driver (positive stimulus) or dissatisfaction (negative stimulus). For each particular case, the description of the favourable and unfavourable travel options are specified more in detail in each section.

6.6.1. Positive stimulus

A positive stimulus ($S_{hmt} \geq 0$) means that drivers are satisfied with the selected travel decision for that day, and therefore they are more likely to repeat the same option the next day.

Following the traditional BM model (Bush and Mosteller, 1951), the probability of choosing the selected option m on this day should be increased and the probability of choosing the rest of options z should be decreased. However, depending on the arrival time of each packet of drivers, some of them may not arrive within the PATI. If drivers arrive earlier/later than the preferred arrival time, other travel options that use the same route but later/earlier departure time may also be good travel decisions. Note that only those travel options with the same route are considered to be on the selection.

In this sense, a travel option z that is not selected by the driver on day t is considered a favourable option, which means that are more likely to be repeated the next day, in the following cases:

a) Driver that chooses option m on day t arrives earlier than the PATI and this alternative travel option z that is being analysed has the same route but later departure time than option m.
b) Driver that chooses option m on day t arrives later than the PATI and this alternative travel option z that is being analysed has the same route but earlier departure time than option m.

All the rest of travel options are considered unfavourable, which are less likely to be repeated the next day.

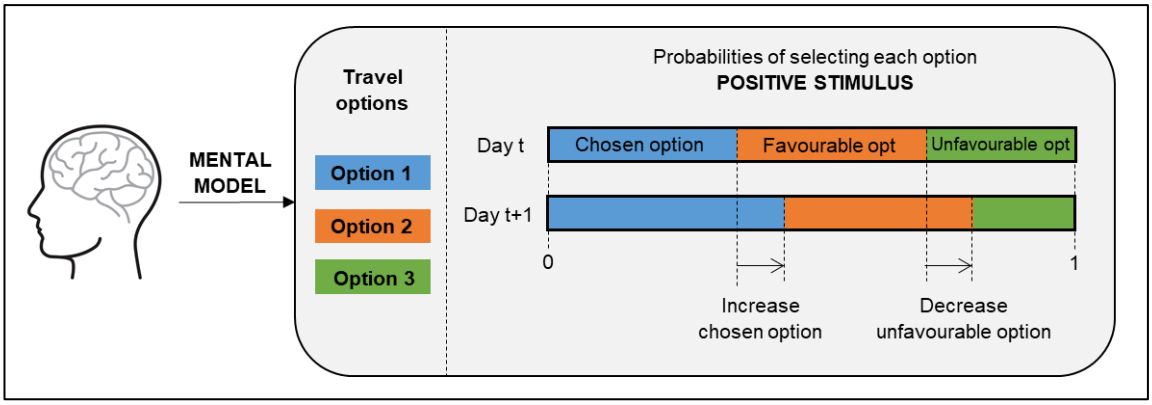

Figure 6.7. Graphical example of the option probability updating process when stimulus is positive.

The formulation, which is shown mathematically in Equations (6.22) and (6.23) of Table 6.3 and graphically in Figure 6.7, increases the probability of choosing again the selected travel option and decreases the probability of choosing unfavourable travel options. In this version of the model, the probability of choosing a favourable option is not increased or decreased. Although it is debatable, drivers who are satisfied with a travel decision are more likely to repeat the same option the next day but that does not mean that they are more/less likely to select a more favourable option instead. Future stages of the model should update the formulation in order to add the possibility of increasing the probability of selecting these favourable travel options. In any case, they certainly know which option they do not have to select and these are the ones whose probability is reduced.

Equation (6.22) updates the probability of choosing the option m for the next day ($p_{m(t+1)}$). Note that this option m is the one that has been chosen on day t. The new probability value is calculated by adding to the previous probability (p_{mt}) an additional value that comes from the reduction of the probabilities of selecting unfavourable options: the term $\left(1 - p_{mt} - \sum_{z=1}^{Z} p_{zt} \cdot \beta_z\right)$ calculates the remaining probability after removing the chosen option and favourable options and only the S_{hmt} part of the remaining probabilities constitutes the additional value that is added to the previous probability (p_{mt}).

For the rest of the options that have not been chosen on day t, Equation (6.23) updates the probability of selecting them for the next day. If the option is favourable, the probability remains the same as the previous day. If the option is

unfavourable, the value that has to be reduced from the probability of unfavourable options is the additional value that has been added to the selected option m on the previous Equation (6.22) $[(1 - p_{mt} - \sum_{z=1}^{Z} p_{zt} \cdot \beta_z) \cdot S_{hmt}]$. The quantity that is reduced to each unfavourable option is directly proportional to the value of the probability of each option $[\frac{p_{zt}}{\sum_{\substack{z=1 \\ z \neq m}}^{Z} [(1-\beta_z) \cdot p_{zt}]}]$. This means that if an unfavourable option has a high probability of being selected, the reduction will be higher. This is done in order to keep in zero (and not negative values) those options with zero probability of being selected.

A particular case is when the satisfaction value (SAT_{dct}, see Section 6.5.1) is 1, which is the maximum value it can take, and the packet of drivers arrives to the destination within the PATI. As this is the best outcome a driver can get on a single day and in order to accelerate computationally the convergence to the best option, drivers are forced to select the same travel option for the next day. Due to the stochastic nature of the model, if this condition is not imposed, some drivers choose on a day their best travel option and then the next day, instead of making the same decision, they might choose an alternative option. Common sense indicates that drivers will choose the decision that gave them the best possible outcome. Only in this case, the stochastic choice rule presented in Equation (6.3) (Section 6.2.1) is not considered and drivers will choose exactly the same option. However, probabilities are still updated according to the previous formulas. Ultimately, the modeller can decide if this imposed travel decision is considered or not in the model.

6.6.2. Negative stimulus

A negative stimulus ($S_{hmt} < 0$) means that drivers are not satisfied with the selected travel decision for that day and therefore, they are less likely to repeat the same option the next day.

According to the traditional model (Bush and Mosteller, 1951), the probability associated with the selected option on this day should be decreased and the probability of choosing the rest of options should be increased. However, as mentioned in Section 6.6, some travel options may be favourable and others

unfavourable. It means that the probability of selecting certain options cannot be increased and therefore the updating functions needs to be reformulated.

In this sense, a travel option z that is not selected by the packet of drivers h on day t is considered unfavourable in the following cases:

a) Driver that chooses option m on day t arrives earlier than the PATI and this alternative travel option z that is being analysed has the same route but earlier departure time than option m.
b) Driver that chooses option m arrives later than the PATI and this alternative travel option z has the same route but later departure time than option m.

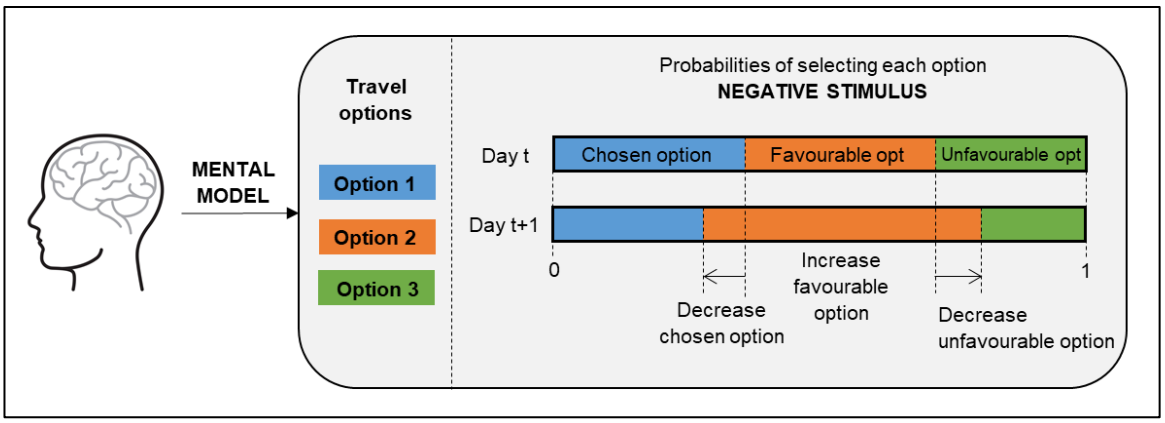

Figure 6.8. Graphical example of the option probability updating process when stimulus is negative.

The formulation proposed in Equations (6.24) and (6.25) of Table 6.3 and graphically in Figure 6.8 indicates that, when the stimulus is negative, the probability of the selected option m on day t is reduced. The probability of choosing those unfavourable options is reduced as well. And the probability of selecting favourable options is increased.

Equation (6.24) updates the probability of choosing the option m for the next day ($p_{m(t+1)}$). This option m is the one that has been chosen on day t. The new value is obtained by reducing from the previous probability (p_{mt}) a certain value that depends on the stimulus value of that driver.

Equation (6.25) updates the probability of choosing those options that have not been selected by the driver on day t. In order to make it easier for the reader, a breakdown of this equation is included in Figure 6.9. The equation is divided into three terms. The first one corresponds to the probability value of the previous day. The second and third ones are either-or terms because both cannot be computed at the same time. One of these terms is cancelled out while the other is calculated. It depends on the number of unfavourable options (β_N). If all unselected options are unfavourable $\beta_N = 1$, as the probability of the selected option m has to be decreased (because stimulus is negative), the probability of selecting the rest of options (even if they are unfavourable) has to be increased. This means that the second term is not calculated and only the third term is obtained. If not all options are unfavourable ($\beta_N = 0$), then the formulation differentiates between favourable and unfavourable options and increases the probability of selecting favourable options and decreases the probability of selecting unfavourable options.

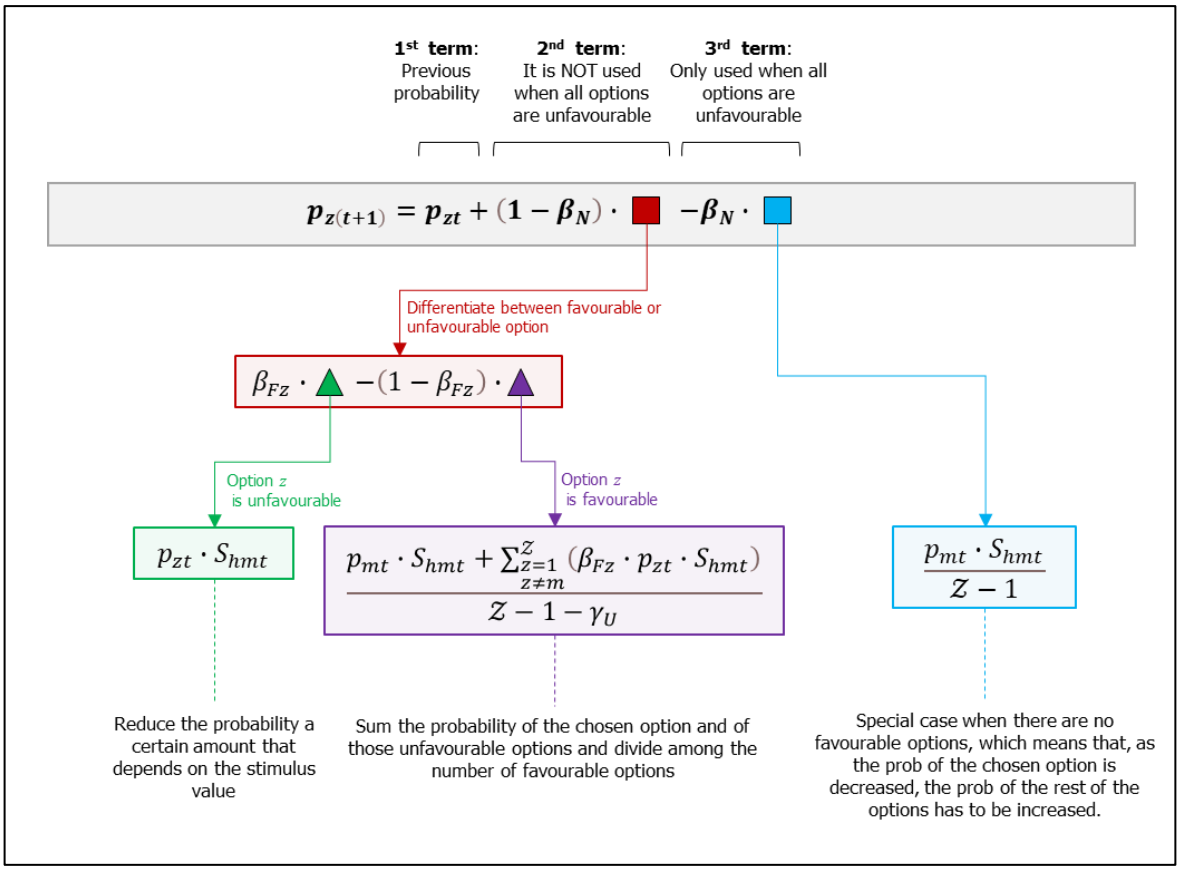

Figure 6.9. Breakdown of Equation (6.25) that updates the probability of selecting travel options that are not chosen on day t when the stimulus is negative.

Table 6.3. Option probability updating functions when stimulus is positive and negative.

		Formulation	Equation
Positive stimulus ($S_{hmt} \geq 0$)	Chosen option m on day t	$p_{m(t+1)} = p_{mt} + \left(1 - p_{mt} - \sum_{z=1}^{\mathcal{Z}} p_{zt} \cdot \beta_z\right) \cdot S_{hmt}$	(6.22)
	Rest of options z	$p_{z(t+1)} = p_{zt} - (1 - \beta_z) \cdot \left[\frac{p_{zt}}{\sum_{\substack{z=1 \\ z \neq m}}^{\mathcal{Z}} [(1 - \beta_z) \cdot p_{zt}]}\right] \cdot \left[\left(1 - p_{mt} - \sum_{z=1}^{\mathcal{Z}} [p_{zt} \cdot \beta_z]\right) \cdot S_{hmt}\right]$	(6.23)
Negative Stimulus ($S_{hmt} < 0$)	Chosen option m on day t	$p_{m(t+1)} = p_{mt} + p_{mt} \cdot S_{hmt}$	(6.24)
	Rest of options z	$p_{z(t+1)} = p_{zt} + (1 - \beta_N) \cdot \left[\beta_{Fz} \cdot p_{zt} \cdot S_{hmt} - (1 - \beta_{Fz}) \cdot \left[\frac{p_{mt} \cdot S_{hmt} + \sum_{\substack{z=1 \\ z \neq m}}^{\mathcal{Z}} (\beta_{Fz} \cdot p_{zt} \cdot S_{hmt})}{\mathcal{Z} - 1 - \gamma_U}\right]\right] - \beta_N \cdot \frac{p_{mt} \cdot S_{hmt}}{\mathcal{Z} - 1}$	(6.25)

$z \in \mathcal{Z}, \quad z \neq m$

Where:

z, travel option that is not chosen on day t.

m, option that is chosen on day t.

$\mathcal{Z}$, total number of options.

p_{mt}, is the probability of selecting option m on day t.

p_{zt}, is the probability of selecting another option z on day t.

$p_{m(t+1)}$, is the new probability of selecting the travel option m for the next day.

$p_{z(t+1)}$, is the new probability of selecting the travel option z for the next day.

S_{hmt}, stimulus value of packet of drivers h after choosing option m on day t.

β_z, binary variable (0-1) that indicates whether option z is favourable ($\beta_z = 1$) or not ($\beta_z = 0$) on day t, when the stimulus is positive.

$$\beta_z = \begin{cases} 1, & if\ AT_{hm} < ET_h \ \ and \ \ RU_z = RU_m \ \ and \ \ DT_z > DT_m \\ 1, & if\ AT_{hm} > LT_h \ \ and \ \ RU_z = RU_m \ \ and \ \ DT_z < DT_m \\ 0, & otherwise \end{cases} \tag{6.26}$$

$$z \in \mathcal{Z}, \quad z \neq m$$

RU_z, path/route of option z at day t

RU_m, path/route of chosen option m at day t

DT_z, departure time of option z at day t

DT_m, departure time of chosen option m at day t

ET_h, earliest limit of the preferred arrival time interval (PATI).

LT_h, latest limit of the preferred arrival time interval (PATI).

AT_{hm}, arrival time of packet of drivers h after choosing option m

β_{Fz}, binary variable (0-1) that indicates if an option z is favourable ($\beta_{Fz} = 0$) or unfavourable ($\beta_{Fz} = 1$), when the stimulus is negative.

$$\beta_{Fz} = \begin{cases} 1, & if\ AT_{hm} < ET_h \ \ and \ \ RU_z = RU_m \ \ and \ \ DT_z < DT_m \\ 1, & if\ AT_{hm} > LT_h \ \ and \ \ RU_z = RU_m \ \ and \ \ DT_z > DT_m \\ 0, & otherwise \end{cases} \tag{6.27}$$

γ_U, variable that indicates the total number of options that are unfavourable:

$$\gamma_U = \sum_{\substack{z=1 \\ z \neq m}}^{\mathcal{Z}} \beta_{Fz} \tag{6.28}$$

β_N, binary variable (0-1) that takes the value of 1 if all options that are no chosen on day t are unfavourable and 0 if not all unselected options are unfavourable. This is done in order to avoid having a denominator with a value less than 1 in equation (6.25). If $\beta_N = 1$, the second term of the equation (6.25) cannot be computed in the formulation and only the third term is be calculated.

$$\beta_N = \begin{cases} 1, & if \ \ (N - 1 - \gamma_U) < 1 \\ 0, & otherwise \end{cases} \tag{6.29}$$

6.7. Balancing Exploration and Exploitation

One of the problems identified in previous RL models that are applied to the transport field (Ozbay, Datta and Kachroo, 2001; Wahba and Shalaby, 2005; Wei, Ma and Jia, 2014; de Oliveira Ramos and Grunitzki, 2015) is that drivers quite rapidly stick to certain travel options without even trying all the rest of options that are available to them. If they do not give the chance to try other options, they will never know if these options are better than the chosen one. The models mentioned above use a learning rate value (see Section 6.5) that represents the speed at which drivers stick to good options. For instance, if a driver finds a good travel option, the probability of selecting this option again for the next day is increased higher if the learning rate is high or lower if the learning rate is low. However, even considering low learning rates, sometimes some drivers do not have the chance to try new options.

As drivers must try new ones since these may lead to even higher rewards, in addition to the learning rate, an additional mechanism is added to the current model in order to consider a trade-off between exploration (e.g. find new information about other options) and exploitation (e.g. use past information to select the travel option that maximises rewards). The method used in this model is called ε-greedy (Sutton and Barto, 1998). This classical algorithm consists in choosing a random travel option (exploration) with probability ε or choosing the best travel option (exploitation) for each driver with probability $(1 - \varepsilon)$. Equation (6.30) shows the new probability that is assigned to each travel option z after balancing exploration and exploitation. This new probability is the one that is used in the stochastic rule choice presented in Section 6.2.1 and that is used to choose stochastically a travel option for each day.

Independently of this new probability, drivers are still updating the probabilities on their mental model based on the consequences of their travel experiences as explained in the same section. Figure 6.10 incorporates the ε-greedy approach in the general framework of drivers' decision making of Figure 6.2. As observed, the whole process is the same but the stochastic rule choice is done using a new probability vector that is obtained from the greedy approach.

$$p'_z = \varepsilon \cdot p_{z,Random} + (1-\varepsilon) \cdot p_{z,mental\ model} \tag{6.30}$$

Where,

p'_z, is the new probability of selecting travel option z after the trade-off between exploration and exploitation.

$p_{z,Random}$, is the probability of selecting the option z. It is assumed that all options have the same probability.

$p_{z,mental\ model}$, is the probability of selecting travel option z that drivers store on their mental model.

ε, variable that weights the exploration and exploitation phases.

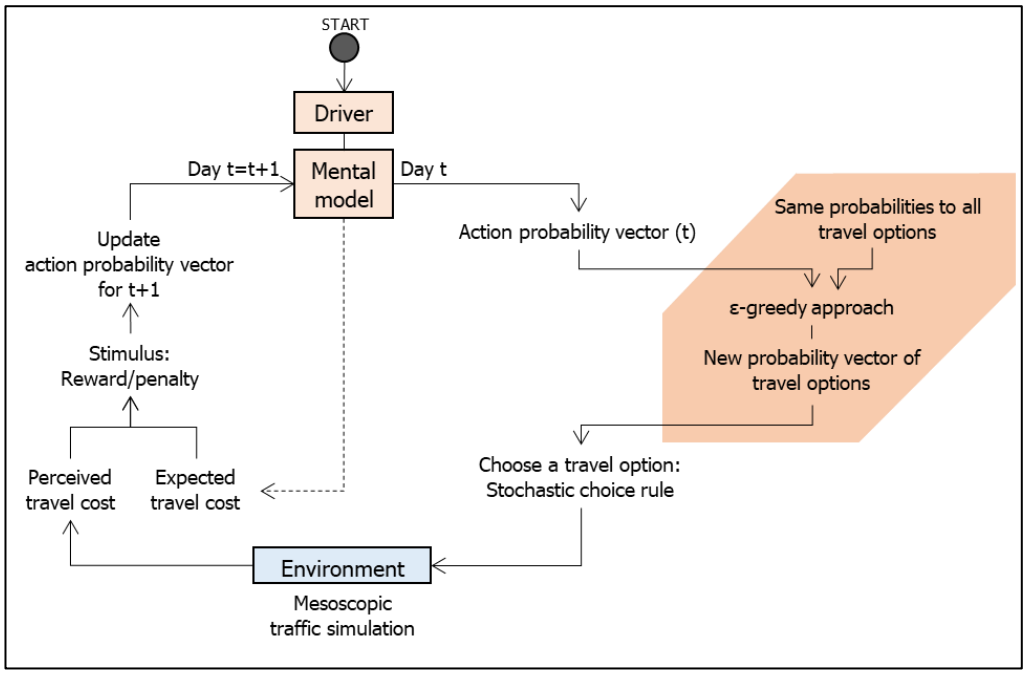

Figure 6.10. Updated drivers' decision-making process incorporating the ε-greedy approach (shaded part).

Different ε functions are proposed in this model in order to consider different ways of balancing exploitation and exploration. At the beginning of the exploration phase (usually at day t=1), ε starts with a high value which means that more random travel options are chosen by each driver in order to explore the possibilities the network is offering. Depending on the type of function that the modeller has decided to use, different ε values are considered on each day. If a constant function is chosen with a constant value of 1, drivers will choose their travel options randomly during the exploration phase. On the contrary, if the constant function takes the value of 0, we allow drivers to select their options based on their knowledge. Initially, all the options will have the same probability to be selected. Other possible ε-functions include linear, quadratic and exponential functions that start with a high value of ε and decreases with time, leading to high exploitation in the end. All these functions are acceptable, however, due to the simplicity of its formulation and the lower value of additional variables, a linear function has been chosen to be used in this model. The modeller has to define the end date of the exploration phase.

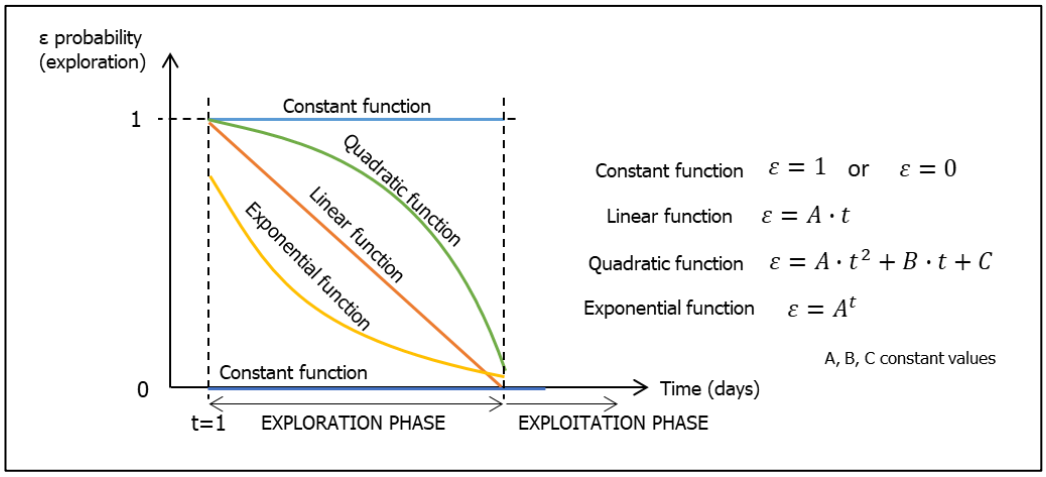

Figure 6.11. Different ε-functions proposed in this model

6.8. Extra option of 'not travelling by car'

After disruptions, some parts of the network may be closed to traffic and drivers may expect longer detours, communities may be isolated and some trips may be cancelled (Dalziell, 1998). The model adds the novel option of allowing drivers to decide if they want to travel using their car or, instead, they prefer to cancel the trip or use an alternative mode of transport to get to their destination. All reviewed transport

recovery models do not include this additional option and just assume that drivers have to travel every day. It is important to note that the aim of this model is not the implementation of a multimodal approach. The model adds this new feature in order to account for those trips that in real life would be cancelled because of the isolation of some disrupted destinations, the possibility of facing long detours or the existence of alternative transport modes. Also, in the light of Covid-19, the modelling of trip cancellation/suppression becomes more important as more people is able to work from home for short periods of time.

The new decision of 'not travelling by car' that drivers can choose is added as another option z, which has a probability of being selected by each driver on each day. Based on the consequences of driver's decisions on day t, the probability of 'not travelling by car' is updated independently, ranging from 0 to 1 following the process that is explained later on in this section. Initially the model described in previous sections only considered those travel options with a route and a departure time and the sum of probabilities of selecting these travel options was already 1. However, the incorporation of a new option that drivers can choose implies the recalculation of the probabilities associated with each travel option. Equation (6.31) calculates the updated probability of selecting each travel option after incorporating the additional option of 'not travelling by car'. Graphically it is also explained in Figure 6.12. Note that on day $t = 1$ (the first day of the simulation), it is assumed that the probability of selecting the option of 'not travelling by car' is zero.

$$p_{zt,updated} = p_{zt} \cdot \left(1 - p_{h,NC,t}\right) \quad \forall\ z\ \in\ \mathcal{Z} \tag{6.31}$$

Where,

$p_{zt,updated}$, is the updated probability of selecting the travel option z on day t after incorporating the option of 'not travelling by car'.

$p_{h,NC,t}$, is the probability of selecting the option of 'not travelling by car' on day t by packets of drivers h. The calculation of this value is explained later on in this section.

p_{zt}, is the probability of selecting the travel option z on day t.

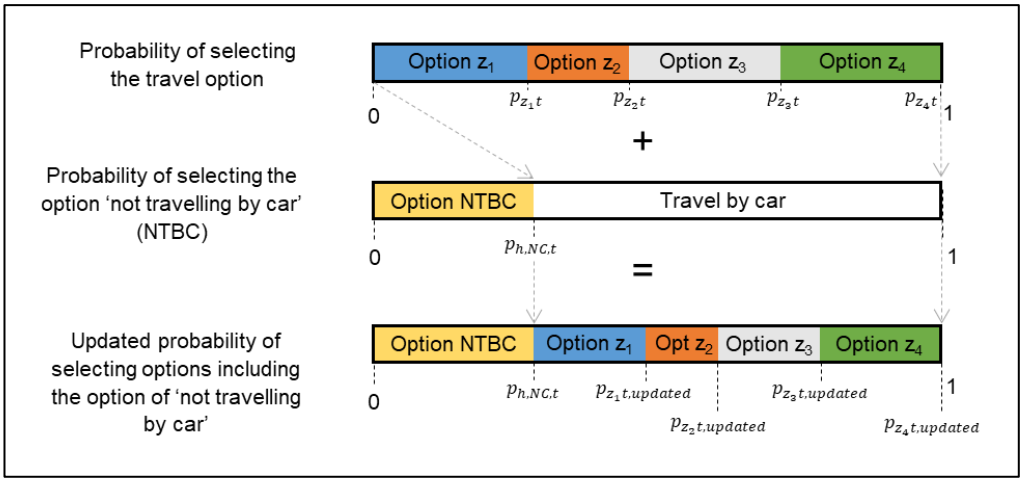

Figure 6.12. Graphical description of how to update probabilities of selecting travel options after incorporating the option of 'not travelling by car'.

The algorithm that is behind the increase or decrease of the probability of not travelling by car is shown in Figure 6.13. As observed in this figure, if drivers have travelled on day t using their car, they could have arrived late or not to undertake the activity. If they have not arrived late, then they are more likely to keep travelling by car on day $t+1$. On the contrary, if they have arrived late to the destination, they need to evaluate if they have alternative travel options or other transport modes to get to that place. If there are no other modes of transport or the service is deficient but they have more travel options (e.g. leaving earlier), they are more likely to keep travelling by car. However, if there are other alternatives, they may prefer to use them which means that drivers are more likely to travel using these other transport modes. On the other hand, if drivers have cancelled the trip on day t, they are more likely to try and travel the next day. The model captures an increasing need to undertake a trip from day to day. The rate at which this "need" increases is a topic worthy of research on its own. On the contrary, if drivers that have decided to travel by an alternative mode of transport are satisfied with the service, then they are more likely to continue using this service. If they are not satisfied, they are more likely to keep travelling using their car.

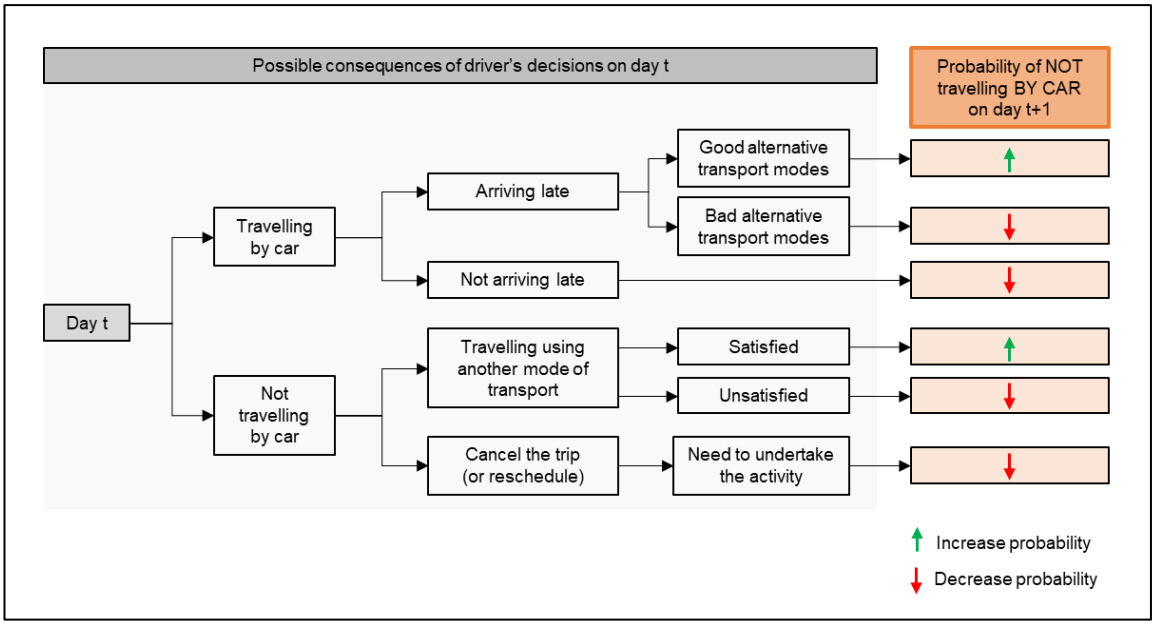

Figure 6.13. Increasing or decreasing the probability of NOT travelling by car based on the travel decisions on day t

Mathematically, this is expressed in Equation (6.32) and to make it easier for the reader a breakdown of the equation is included in Figure 6.14. Three main terms are identified. The first term represents the probability of not travelling by car on day t. The second and third term increase or decrease the probability of the first term based on the algorithm stated in Figure 6.13. Note that the second and third terms cannot be considered at the same time. For example, if a driver travels by car on day t, the second term is considered and the third term is excluded from the formulation and vice versa.

The second term of the Equation (6.32) modifies the probability of not travelling by car when the driver travels on day t. If the driver arrives late, the probability of using again the car can be increased or decreased depending on the service level of the alternative transport modes. On the contrary, if driver arrives on time, the probability of using the car again is increased.

The third term of the Equation (6.32) also modifies the probability of travelling by car but only when drivers decide not to use the car on day t. If drivers use another mode of transport, then the probability of using a car the next day can be increased or decreased depending on the service level of the alternative transport modes.

However, if drivers have decided to cancel the trip on day t, the probability of travelling the next day $t+1$ is increased depending on the type of activity.

$$p_{h,NC(t+1)} = p_{h,NC,t} + \rho_{h,CAR,t} \cdot \left[\nu_{h,LATE,t} \cdot (AA \cdot RC_h \cdot SL_h) - \left(1 - \nu_{h,LATE,t}\right) \cdot BB\right] + \left(1 - \rho_{h,CAR,t}\right) \cdot \left[\eta_{h,MODE,t} \cdot (CC \cdot SL_h) - \left(1 - \eta_{h,MODE,t}\right) \cdot \left(DD \cdot KT_h \cdot (1 - RS_h)\right)\right] \quad (6.32)$$

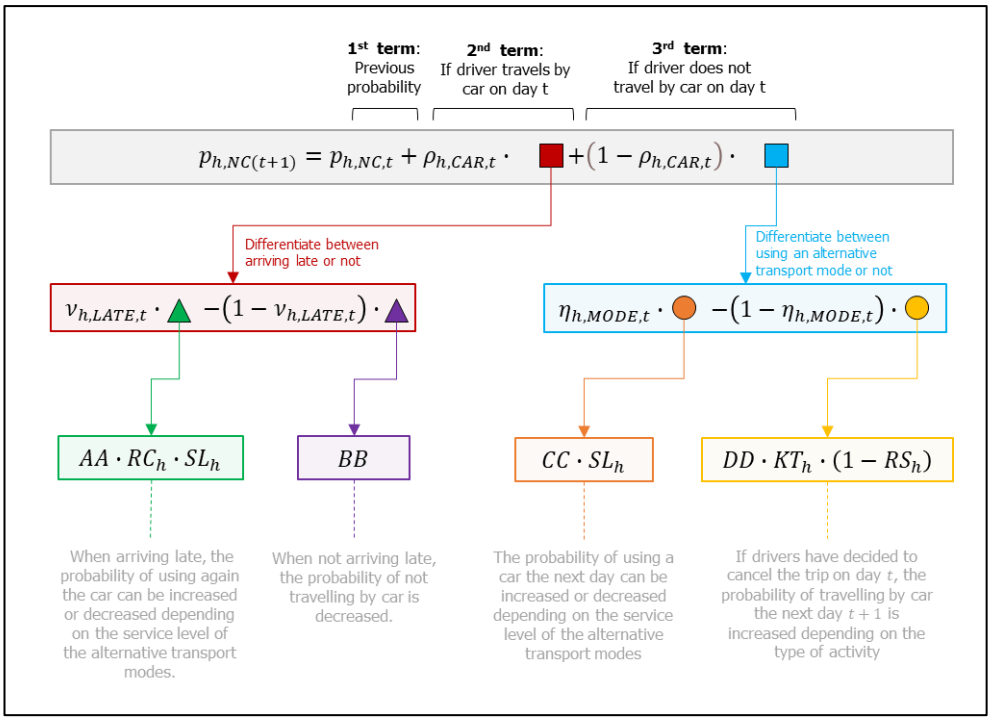

Figure 6.14. Breakdown of Equation (6.32) that updates the probability of selecting the option of 'not travelling by car' on day t+1.

Where:

$p_{h,NC(t+1)}$, is the probability of selecting the option of 'not travelling by car' on day $t+1$ by packets of drivers h. It is necessary to limit the range of values of $p_{d,NC(t+1)}$ to a number between 0 and 1, which is done using the following Equation (6.33).

$$p_{h,NC(t+1)} = \begin{cases} \max\left(\ 0\ ;\ p_{h,NC(t+1)}\ \right), & if\ p_{h,NC(t+1)} \leq 0 \\ p_{h,NC(t+1)}, & if\ p_{h,NC(t+1)} \in (0,1) \\ \min\left(\ 1\ ;\ p_{h,NC(t+1)}\ \right), & if p_{h,NC(t+1)} \geq 1 \end{cases} \quad (6.33)$$

$p_{h,NC,t}$, is the probability of selecting the option of 'not travelling by car' by packet of drivers h on day t.

$\rho_{h,CAR,t}$, is a binary variable that indicates if the packet of drivers h travels by car on day t ($\rho_{h,CAR,t} = 1$) or decides not to travel by car ($\rho_{h,CAR,t} = 0$).

$\nu_{h,LATE,t}$, is a binary variable that indicates if the packet of drivers h arrives late to the destination on day t ($\nu_{h,LATE,t} = 1$) or on time ($\nu_{h,LATE,t} = 0$).

$\eta_{h,MODE,t}$, is a binary variable that indicates if a packet of drivers h travels using another mode of transport that is not car-based ($\eta_{h,MODE,t} = 1$) or cancels the trip ($\eta_{h,MODE,t} = 0$). The procedure to obtain the value of this variable is described in Section 6.8.2.

AA, BB, CC, DD, are user-defined values that indicates the importance of each term in the calculation of the probability of selecting the option of 'not travelling by car'. These can take any value between 0 and 1. If it is 0, the corresponding term of the Equation (6.32) is not considered.

RC_h, late arrival coefficient that is used when the packet of drivers h does not reach its destination before the starting time of the activity a. It depends on the type of activity that is undertaken and the consequences of not arriving on time. This variable can take any value between 0 (not important if drivers arrive late) and 1 (important to arrive on time) – see Equation (6.34).

$$RC_h = \begin{cases} \left(\frac{1 - y_{RC}}{t_{RC}}\right) \cdot t + y_{RC} & if\ t < t_{RC} \\ 1 & if\ t \geq t_{RC} \end{cases} \quad (6.34)$$

Where,

y_{RC}, coefficient that indicates how important is to arrive on time to undertake the activity. It can take any value between 0 and 1.

t_{RC}, time after the starting time of the activity that is needed to achieves a value of 1 on the RC_h variable.

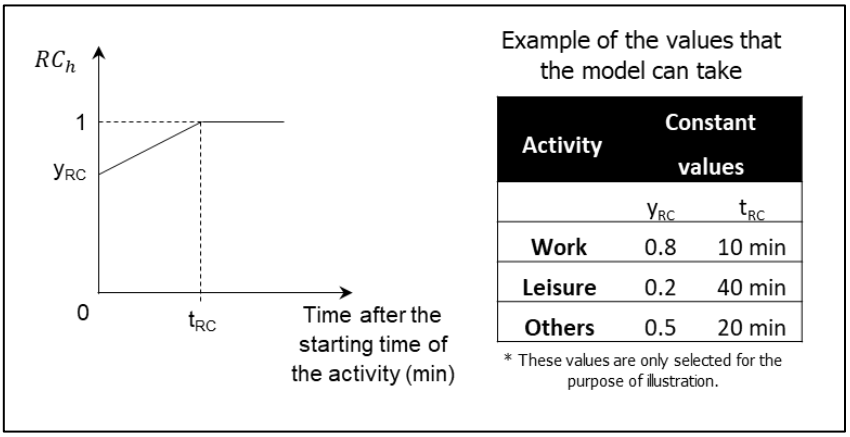

Figure 6.15. Late arrival coefficient (RC_h) and example of some parameters. The example values of the table are selected for the purpose of illustration.

SL_h, service level satisfaction of using an alternative transport mode. Depending on the origin and the destination of each packet of vehicles, there might be some areas that are very good connected to others. This variable reflects how the level of the service is. It can take values between 1 (e.g. good frequencies, journey times, stop distances, etc.) to -1 (bad frequencies, no comfort, always late, etc.). If it takes a value of zero, the probability is not increased nor decreased. A more detailed description of the values that this variable can take is included in Section 6.8.1.

RS_h, is the rescaled value of the service level satisfaction (SL_h). The original value of the SL_h is measured between -1 and 1. However, this value has been rescaled within the range of 0 to 1 because the rest of the values of the term of Equation (6.32) is measured in the range of 0-1.

$$RS_h = \begin{cases} 0 + (SL_h + 1) \cdot 0.5 & if\ SL_h \in [-1, 0] \\ 0.5 + (SL_h) \cdot 0.5 & if\ SL_h \in (0, 1] \end{cases} \quad (6.35)$$

KT_h, is the 'need to travel' variable. Depending on the type of activity and the number of days in a row without undertaking the activity, this variable can take any value between 0 and 1, being 0 the case that the activity is not essential and there is no need to travel, and 1 the case that drivers

need to travel. Figure 6.16 shows two cases that summarises the values that this variable can take [see Equation (6.36)]. Case 1 represents a typical leisure-based activity in which the variable takes a value of 0 during the first days, which means that the activity is not essential. On the other hand, Case 2 represents a work-based activity in which the variable already takes values close to 1 during the first days, which means that there is a need to travel. The more days without undertaking the activity, the higher the coefficient is (up to 1).

$$KT_h = \begin{cases} \left(\frac{1-U_S}{U_g}\right) \cdot U + U_S & if\ U_f = 0 \\ 0 & if\ U_f > 0\ \ and\ U < U_f \\ \frac{U-U_f}{U_g} & if\ U_f > 0\ and\ U \geq U_f \end{cases} \quad (6.36)$$

Where,

U, number of days in a row in which drivers have not attended the activity.

U_f, number of days in which activity is not essential and drivers may not attend the activity.

U_s, initial value of the 'need to travel' variable.

U_g, number of days in which the 'need to travel' variable is increasing until it reaches the maximum value of 1.

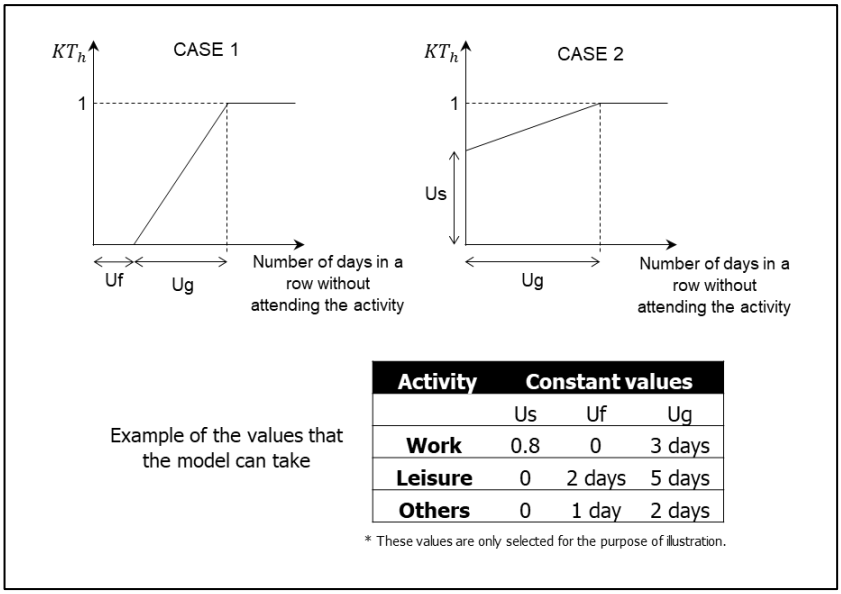

Example of the values that the model can take

Activity	Constant values		
	Us	Uf	Ug
Work	0.8	0	3 days
Leisure	0	2 days	5 days
Others	0	1 day	2 days

* These values are only selected for the purpose of illustration.

Figure 6.16. 'Need to travel' variable. Values on the table are selected for the purpose of illustration for different activities.

6.8.1. Service level satisfaction (SL_h) of alternative transport modes

One of the advantages of this model is that it allows drivers to decide not to travel using their car and instead they can use another transport mode or cancel a trip. This decision depends on the level of satisfaction of drivers towards using other transport modes. Different factors may influence these decisions, such as the frequency of the service, comfort, price, journey time, accessibility, reliability of time schedule, safety, aesthetics, etc. Although the aim of this model is not to develop a multi-modal approach, it was necessary to introduce some variables that evaluate the level of service of alternative transport modes. In this model, the service level satisfaction has been quantified using three variables: accessibility, frequency of the service and comfort. Mathematically, the calculation of the level of service is shown in Equation (6.37). This satisfaction level can vary between -1 (dissatisfied with the provided service) and 1 (really satisfied with the service). The difficulty of this approach is based on the need to incorporate real data from surveys to obtain the satisfaction of drivers towards the use of alternative transport modes of the study area. Unfortunately, the data collection is out of the scope of this thesis and information obtained from other surveys or the one provided by alternative transport modes

should be initially used. If more information is obtained, more variable can be incorporated into the equation (6.37).

$$SL_h = \frac{HH \cdot acc_a + JJ \cdot freq_a + LL \cdot comf}{3} \tag{6.37}$$

Where,

acc_a, is the accessibility variable that is given to an area a and it measures how close an alternative transit station is from the area where the user is located. As no data is available at this stage, the use of a piecewise-defined function expressed in Equation (6.38) is proposed. The function varies between -1 (difficulty in accessing other transport modes) and 1 (easy access to other transport modes). The variable $Dist_{walk}$ quantifies in an approximate way the distance between the user origin and the nearest transit station of the alternative transport mode. A graphical representation of this function is also shown in Figure 6.17.

$$acc_a = \begin{cases} 1 & if\ Dist_{walk} \leq 100m \\ 0.5 & if\ 100m < Dist_{walk} \leq 500m \\ 0 & if\ 500m < Dist_{walk} \leq 1km \\ -0.5 & if\ 1km < Dist_{walk} \leq 1.5km \\ -1 & if\ Dist_{walk} > 1.5km \end{cases} \tag{6.38}$$

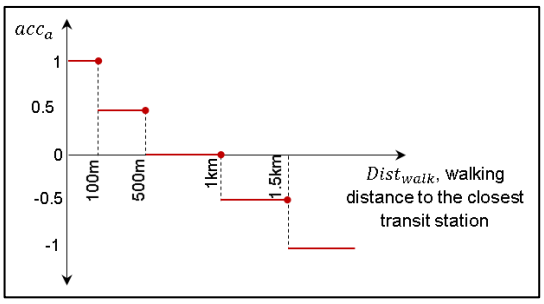

Figure 6.17. Graphical representation of the accessibility variable of alternative transport modes

$freq_a$, is the frequency of the service that is provided by the alternative transport mode. Due to the lack of data, it is proposed a linear function which increases or decreases based on the amount of time that a user has to wait to start his/her journey at the transit station. This value varies between -1 (really bad service frequency) and 1 (good service

frequency). The mathematical expression is included in Equation (6.39) and a graphical representation of this formula is considered in Figure 6.18. Users will be satisfied if the service is running every less than t_{min} minutes. However, if they have to wait more time to get the vehicle, the level of service satisfaction will decrease until it reaches a maximum limit (-1).

$$freq_a = \begin{cases} 1 & if\ t_{wait} \leq t_{min} \\ \left(\frac{-2}{t_{max} - t_{min}}\right) \cdot t_{wait} + \left(1 + \frac{2 \cdot t_{min}}{t_{max} - t_{min}}\right) & if\ t_{min} < t_{wait} \leq t_{max} \\ -1 & if\ t_{wait} > t_{max} \end{cases} \quad (6.39)$$

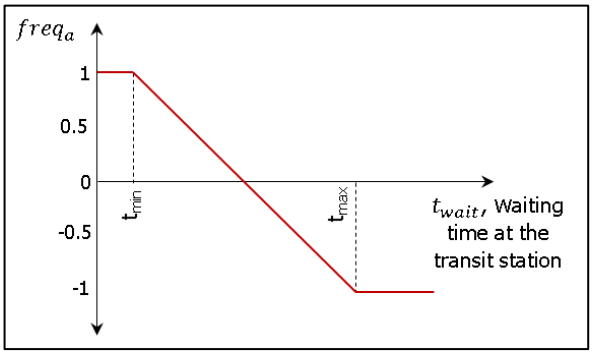

Figure 6.18. Graphical representation of the function that quantifies the value of the frequency of alternative transport modes

$comf$, is the variable that defines the level of comfort that users experience by using this alternative transport mode. This value varies between -1 (not comfortable at all) and 1 (comfortable).

HH, JJ, LL, are user-defined variables that weight each terms of the formula. Note that the sum of these variables has to be one ($HH + JJ + LL = 1$).

6.8.2. Decision of changing to other transport mode or cancel the trip

When drivers decides not to travel by car, they can still reach the destination if there are other available modes of transport. However, drivers will only use this alternative transport modes if the level of service satisfies their requirements. Therefore the probability of using another transport mode is influenced by the service level

satisfaction (SL_h) of each driver. If the service level is good for a driver (closer to 1), then this driver will be more likely to use it in a close future. On the contrary, if the service is bad (close to -1), then there is small chance that this driver chooses this transport mode to travel. If a driver decides not to use this alternative transport mode, although there can be other options (e.g. rescheduling the trip, etc.), it is assumed in this model that the driver opts for cancelling the trip.

The function that determines if a driver chooses another mode of transport or prefers to cancel the trip is expressed mathematically in Equation (6.40) and graphically in Figure 6.19. This is a piecewise-defined function in which its value depends on driver's satisfaction towards the use of the alternative transport modes. If the satisfaction is less than zero, driver has 100% probability of cancelling the trip. On the contrary, if the satisfaction is greater than 0, it is assumed that the probability of using another mode of transport will increase linearly with the satisfaction of the service.

$$p_{h,MODE} = \begin{cases} 0 & if\ SL_h < 0 \\ SL_h & if\ SL_h \geq 0 \end{cases} \quad (6.40)$$

Where,

SL_h, is the service level satisfaction of packet of drivers h towards using another mode of transport. This is calculated as explained in Section 6.8.1.

$p_{h,MODE}$, is the probability of choosing between cancelling the trip or using an alternative transport mode.

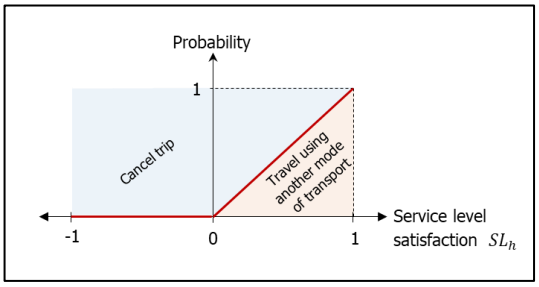

Figure 6.19. Graphical representation of the proposed probability distribution for cancelling trips or using another mode of transport

The modeller can simplify the model by omitting the existence of alternative transport modes. This means that those drivers who do not travel on a day cannot

find alternative transport modes and therefore, they have to cancel the trip. This can be done assigning a service satisfaction value lower than zero for all drivers. In this sense, according to Equation (6.40), the probability of using alternative modes of transport would be zero and drivers would have to cancel the trip.

The process of deciding if a driver chooses an alternative transport mode or cancel the trip consists on the following steps: (1) Generate for each driver a random value (ϑ) between 0 and 1 with a uniform-distribution probability. (2) Given a specific value of the service level satisfaction (SL_h), obtain the corresponding value of the probability distribution using Equation (6.40). (3) Compare the random value (ϑ) with the probability distribution ($p_{h,MODE}$) following the Equation (6.41) in order to identify if this driver decides to use other non-car-based transport modes ($\eta_{h,MODE,t} = 1$) or driver decides to cancel the trip ($\eta_{h,MODE,t} = 0$).

$$\eta_{h,MODE,t} = \begin{cases} 0 & if\ \vartheta > p_{h,MODE} \\ 1 & otherwise \end{cases} \quad (6.41)$$

6.9. Illustrative example

To facilitate the understanding of the concepts introduced in this section, the departure time and route choice model is applied to the same transport network used in Chapter 4, the Sioux Falls Network (South Dakota, US). The aim of this example is to illustrate how the proposed model works. It shows how the reinforcement-learning algorithm is used to simulate day-to-day drivers' travel decisions. Only the pre-disruption stage is analysed, which means that there is no network disruption involved. The following Section 6.9.2.1 analyses the process of how an individual packet of vehicles make travel decisions. However, in section 6.9.2.2, the behaviour of all drivers is analysed together in order to observe the overall state of the network on any given day. As this is a stochastic model, it needs to be run several times in order to obtain representative results. At the end of the section, the results that are obtained using multiple simulations are compared to the results of a single simulation.

6.9.1. Road network and traffic demand data

The Sioux Falls network consists of 24 nodes and 76 links as shown in Figure 6.20 and whose characteristics are presented in Table A.*1* and Table A.*2* of the Appendix 1. The vertex coordinates have been taken from Chakirov and Fourie (2014).

The traffic demand used in this example is extracted from the work done by Martinez-Pastor (2017). A total number of 4840 trips per hour are simulated in that work, which are grouped into 18 OD pairs as shown in Table A.*3* of Appendix 1. It is assumed a maximum set of 2 initial routes for each OD pair and it is expected that drivers choose between 3 possible departure times (8am, 8:15am or 8:30am). Therefore, the total number of possible options for each OD pair is 7 (2 routes and 3 departure times/route and the additional option of 'not travelling by car'). For this reason, the peak period modelled in this example is adapted to these 3 departure times (every 15min) and therefore the period of demand that is analysed is between 8am and 8:45am. This means that the total number of trips is (proportionally) 3636 for that time period. A warm-up and cool-down 30-min period are also simulated with a proportional number of trips for that amount of time. The number of vehicles per packet considered in the model is 10.

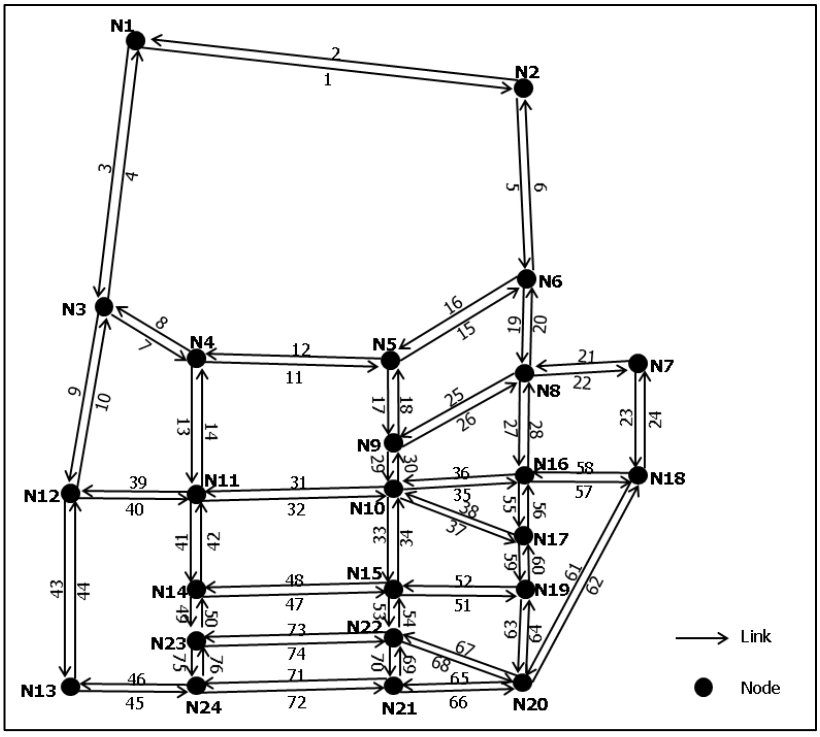

Figure 6.20. Sioux Falls network, defined by links and nodes.

It is assumed that all drivers are going to work (activity purpose) and the activity starts at 9am for all users. In order to consider the heterogeneity of drivers, two preferred arrival time intervals (PATI) have been included in this model. It is assumed that 50% of drivers prefer to arrive between 20 min and 10 min before the activity starts. For the rest 50% of drivers, PATI is defined between 10 min and 5 min.

A linear memory function is considered when calculating the expected and perceived travel cost over time. It is assumed a learning rate of 0.2. The additional feature of considering that bad memories are remembered more than good ones is also included in this example. The only information that drivers know is the one they have collected on previous travel experiences. No external travel information is provided to them. The value of the rest of parameters used in this example is included in Table 6.4.

Table 6.4. Values of the variables considered in this example.

Variable	Value	Variable	Value
Travel cost function (Section 6.3)		**General**	
$\boldsymbol{\beta_1 = \beta_2 = \beta_3 = \beta_4}$	1	Vehicles/packet	10
Memory function (Section 6.4.1)		Simulation time	25 days
Linear function		Linear exploration function	
$\boldsymbol{B_{max}}$	3	Exploration time	10 days
$\boldsymbol{b_1}$	10min	Exploitation time	15 days
$\boldsymbol{b_2}$	30min		
$\boldsymbol{\theta}$	Uniform distribution [0,90]	Learning rate	0.2
Option of not travelling (Section 6.8)			
$\boldsymbol{y_{RC}}$	0.8	acc_a	Probability distribution of Figure 6.21.
$\boldsymbol{t_{RC}}$	10 min	$freq_a$	Uniform distribution [-1,1]
$\boldsymbol{U_s}$	0.8	$comf$	Uniform distribution [-1,1]
$\boldsymbol{U_f}$	0 days	g	3 days
$\boldsymbol{t_{min}(freq_a)}$	10 min	$AA = BB = CC = DD$	1
$\boldsymbol{t_{max}\ (freq_a)}$	1 h		

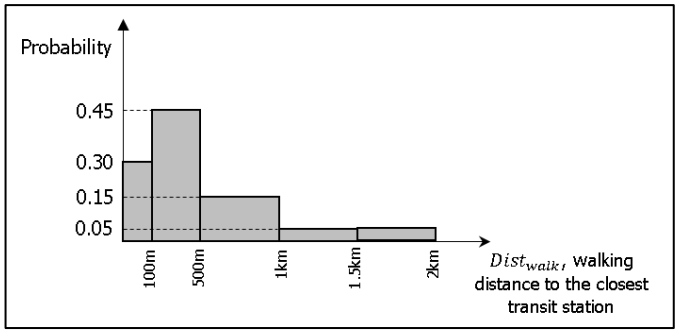

Figure 6.21. Probability distribution of walking distance to the closest transit station for each node.

The model is performed on a computer with 8GB memory and a quad-core 3.3 GHz Intel i5-3550 processor. Based on this, the computational time to run 10 simulations is approximately 20 minutes.

6.9.2. Results and discussion

6.9.2.1. Disaggregated results: understanding individual driver's travel decisions

Driver's decision making process is studied in this section by selecting randomly a packet of vehicles and analysing its travel decisions over time. In this example, a packet that travels from node 1 to node 20 has been selected. Table 6.5 includes a summary of the travel options that this packet can choose from.

Table 6.5. Travel options between origin node 1 to destination node 20

Option	Route	Departure time
Option 1	N1-N3-N4-N11-N14-N23-N22-N20	8:00am
Option 2		8:15am
Option 3		8:30am
Option 4	N1-N3-N4-N11-N14-N15-N22-N20	8:00am
Option 5		8:15am
Option 6		8:30am
Option not travel		

Results from the model are included in Figure 6.22. The first graph (A) represents the evolution of the probability of selecting travel options. Each option (route and departure time) is drawn as a line and the cross symbol in the figure

indicates the travel option that this packet of drivers has chosen on each day. Note that the number of the option is shown on the second axis. Initially, all options except the option of 'not travelling by car' have the same probability of being chosen by the driver. Following the stochastic rule choice (Section 6.2.1), this packet of drivers selects travel options. As an example, this packet chooses option #2 for day 1.

The second graph (B) in Figure 6.22 shows the departure and arrival time of this packet of vehicles. This graph also includes the starting time of the activity and the preferred arrival time interval for this packet. If the arrival time is beyond the red line (activity starting time), the packet of drivers will have arrived late to undertake the activity.

The third graph (C) represents the travel cost on each day and the weighted average of travel costs of previous days (expected and perceived travel costs). On day 1, the expected travel cost is not considered because drivers do not have previous travel experiences. As observed, the sudden high travel costs evidences the penalties that are applied to the travel cost functions due to late or early arrivals.

The last graph (D) displays the stimulus values (positive in green and negative in red). On day 1, as the perceived travel cost is greater than the expected travel cost, the stimulus is negative. This means that this packet of vehicles is less likely to repeat option #2 for the next day. At this point, this packet updates its option probability vector according to the stimulus value obtained from the previous day. Note that one of the improvements of this model compared to the previous ones (Ozbay, Datta and Kachroo, 2001; Wei, Ma and Jia, 2014) is shown on this updating scheme. After selecting option #2, this packet has departed at 8:15am on day 1 and it has arrived earlier than PATI. In these previous models, the probability of selecting option #2 for day 2 would be reduced and the probability of selecting the rest of options would be increased. However, in reality, it is very unlikely to increase the probability of option #1 because it has even an earlier departure time than the selected option on day 1. Drivers know that if they select option #1, the probabilities of arriving even earlier than option #2 are high. Therefore, this option #1 is considered in this case as an unfavourable travel option (see Section 6.6) and drivers will be less likely to choose it for the next day. For that reason, the probabilities of

selecting option #1 and #2 are reduced and the probabilities of selecting the rest of the options are increased.

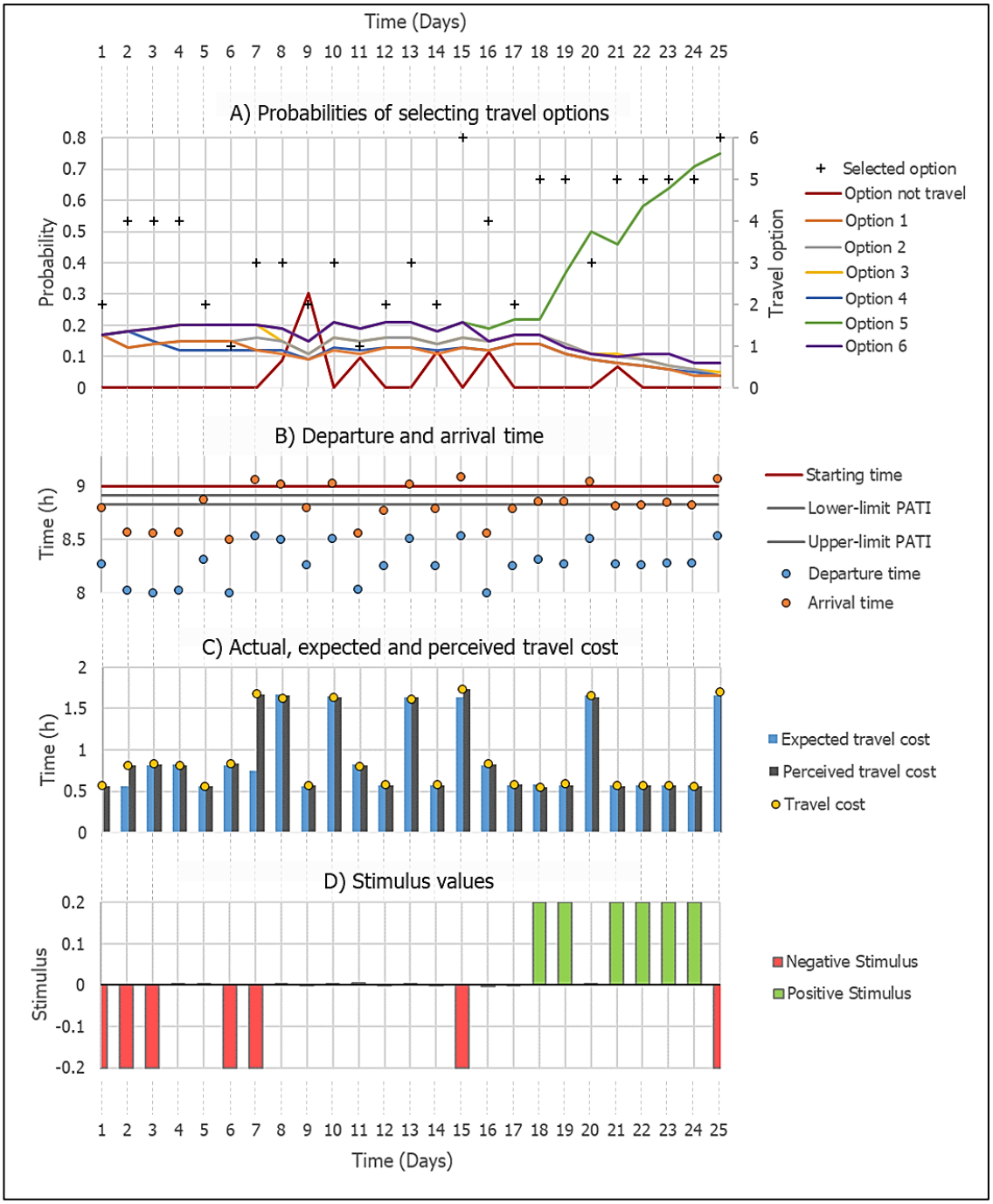

Figure 6.22. Mental model of packet of drivers #4 that travels from node 1 to node 20. Learning rate=0.2.

The process is repeated again for the next days. Based on the option probability vector and using the stochastic rule choice, a travel option is selected. The travel costs are obtained after travelling and a new stimulus value is calculated that is used to update the probabilities of selecting travel options for the next day.

Every time the packet of drivers arrives later than the starting time of the activity there is an increase on the probability of selecting the option of 'not travelling by car'. In this case, drivers can use any alternative transport mode or even cancel the trip. More specifically, on day 7 this packet arrives late and the next day the probability of not travelling increases. If drivers continue arriving late, the probability of not travelling will continue increasing. Due to the stochastic nature of the model, drivers may select the option of 'not travelling by car'. After a few days, the probability of not travelling is reduced because drivers have a 'need' to travel by car as mentioned in Section 6.8.

The core of this reinforcement model is the stimulus values and the updating scheme. Only when there are big changes in stimulus values, the probabilities of selecting options experience huge changes. In some cases of Figure 6.22, the stimulus values are close to zero. This means that the driver see no difference between the expected travel cost and the perceived travel cost compared to alternative options. If stimulus is close to zero, it implies that the probabilities of choosing travel options remain almost the same as the previous day.

The stimulus achieves the maximum positive value on day 18. It seems that both expected and perceived travel cost are similar in the graph, but numerically there is a slight difference. The expected travel cost on day 18 is 0.58h and the perceived travel cost is 0.55h., this being the maximum difference among all possible alternative options. That is the reason why stimulus get the maximum value. This implies that the probability of selecting the same option (#5) for the next day is increased the maximum possible value. At the end of this simulation period, option #5 stands out as the preferred travel option for this packet of drivers.

ε-greedy approach

This example has also used the ε-greedy approach explained in Section 6.7. Figure 6.23 shows the difference between the evolution of probabilities with and without

considering the ε-greedy linear approach. As observed, the ε value decreases linearly until it gets a value of zero after 10 days (exploration phase). This means that at the beginning all options have the same probability of being selected and then, as the ε value goes down, the probabilities acquire their 'undisturbed' value (without the ε-greedy consideration). As the probabilities of all options on day 1 are the same and the exploration phase is limited to 10 days, the ε-greedy linear effect is limited. An alternative would consider an extension of the exploration phase (more than just 10 days) or an alternative ε-greedy approach.

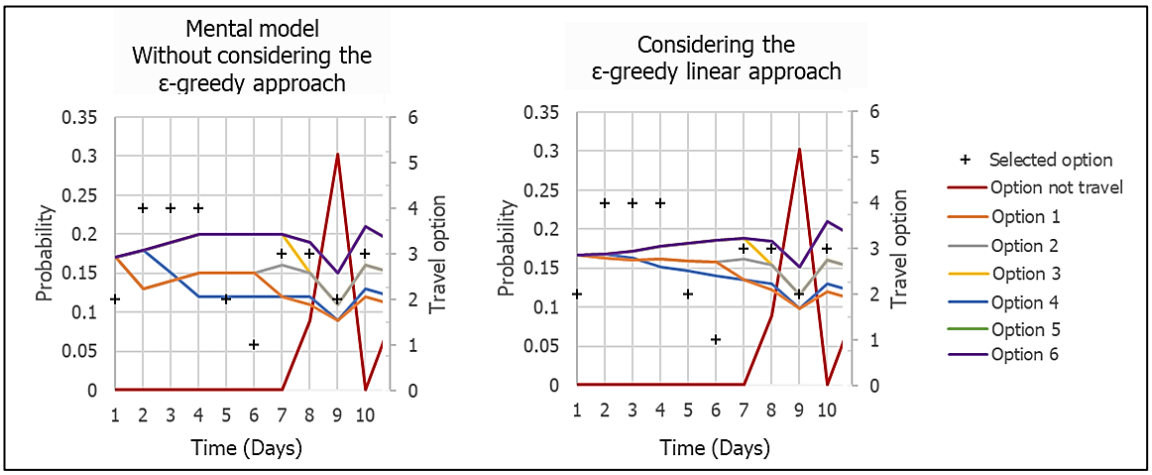

Figure 6.23. Evolution of probabilities of selecting travel options without and with the e-greedy linear approach. Packet of drivers #4.

Memory variables

Memory variables also have a high impact on the expected and perceived travel cost calculation. Figure 6.24 shows the memory coefficients that are used by packet of vehicles #57 to calculate travel costs on each day. These are obtained by multiplying the linear memory value (φ) and bad memory value (B_{hzt}) on each day. Each column of the graph represents the coefficients that are used on the weighted average of travel cost calculations on Equations (6.7) and (6.17). The black boxes highlighted on Figure 6.24 show the additional bad memory consideration and the corresponding decay over time. Note that for this example, a bad memory is considered as a journey whose travel time exceeds 10 min the expected travel time. The decay feature in which drivers forget the importance of bad memories over time is also shown in the graph. It is observed that the coefficient of bad memories is reduced over time until

it reaches its memory value alone (φ). In order to fully understand how to use this graph, an example is also included Figure 6.24. The idea of this example is to calculate the perceived travel cost on day 12 (highlighted column in the graph). This 12th column shows the memory values for the decisions that this packet made on each day (rows). As observed, the travel cost on day 12 (12th row) is weighted a value of 12. Travel cost on day 11 (11th row) is weighted a value of 11 and so on. However, the weighting coefficient on day 9 is 14 because this packet has considered the journey on day 9 as a bad experience and therefore, it is remembered more than some good ones.

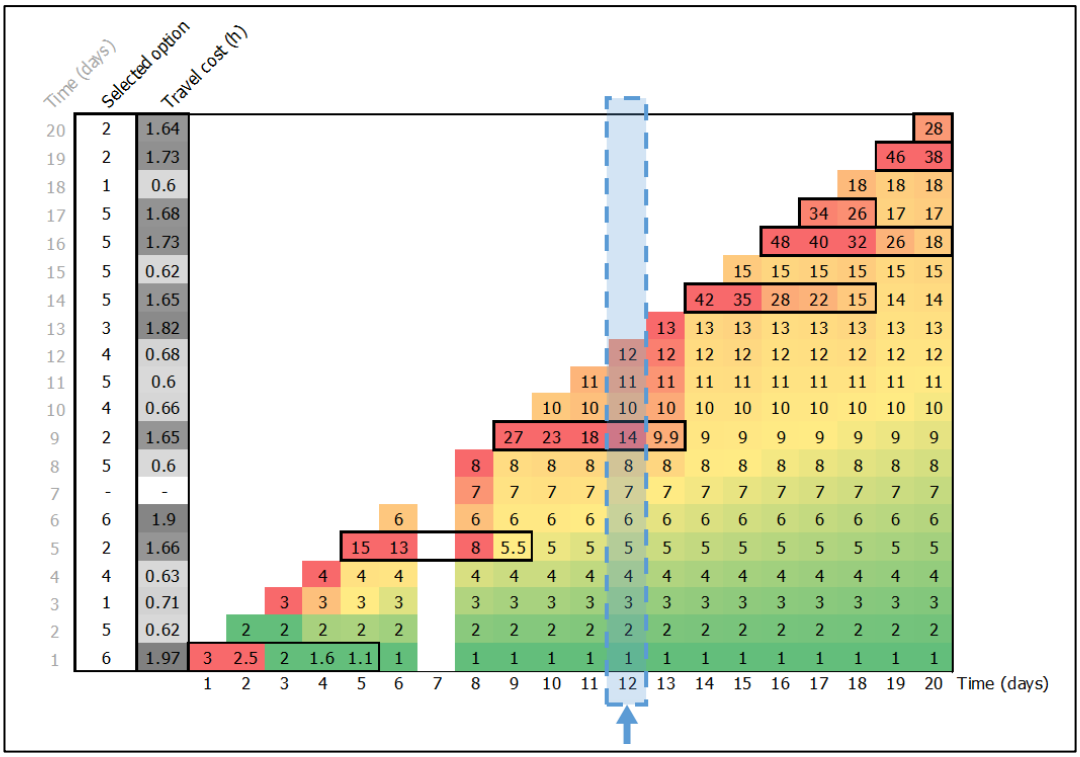

Figure 6.24. Memory coefficients (φ times B) over time used by the packet #57 of vehicles from node 1 to node 20. Memory decay (θ) of 64 degrees. Linear memory function. Highest bad memory value (B_{max}) is 3.

As mentioned, the additional bad memory variable loses importance over time. It depends on the decay value that is assigned to each packet of drivers. Figure 6.25 shows the decay of bad memory values depending on different decay angles (θ). The higher the angle, the longer the packet of driver remembers the bad event. If the modeller decides not to consider the bad memory feature, then the values located in

black boxes in Figure 6.24 would be their corresponding values of the memory levels (φ) and values on Figure 6.25 would be all 1 ($\theta = 0$). For instance, if a packet of drivers is characterised by a decay angle of 70 degrees, the bad memory weights more than a good one during 6 days. On the 7th day, this bad memory is considered equally important as a good one.

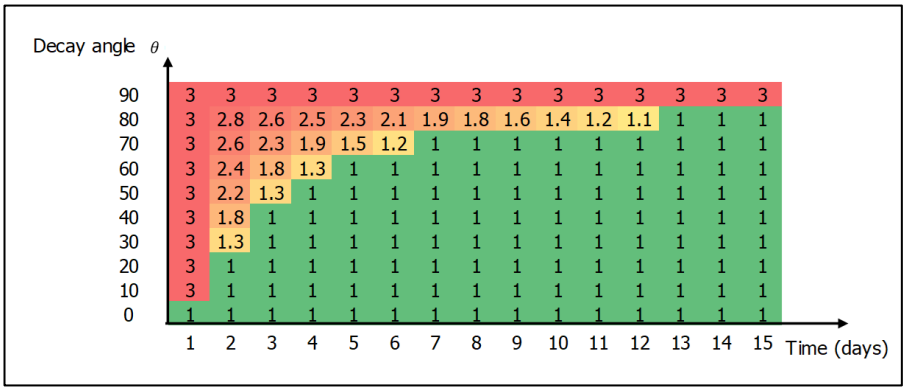

Figure 6.25. Bad memory variable decay depending on different values of the decay angle (θ). Highest bad memory value (B_{max}) is 3.

The impact that the bad memory formulation has on the calculation of the travel cost is shown in Figure 6.26. This graph provides two values of the expected travel cost on each day. One of them is when the maximum value of the extra weighting factor of bad experiences (B_{max}) is 3, meaning that a bad experience is remembered 3 times more than a good one. And the second one is calculated when the value of B_{max} is 1, which means that bad experiences are not stronger that good ones. Expected cost is not calculated on day 1 (because it is not computed during the first day of the simulation) and day 7 (because this packet of drivers decide not to travel on this day). Those expected travel costs that consider the additional weighting factor due to bad experiences have a higher cost compared to the others. This simulates the fact that drivers tend to remember slightly more those bad experiences.

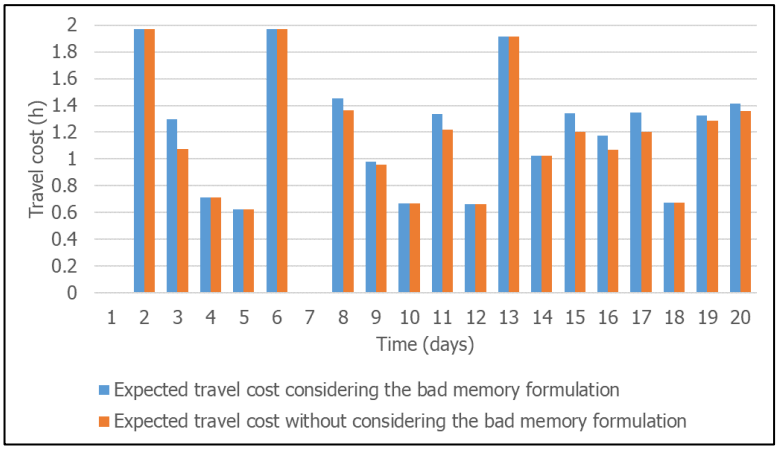

Figure 6.26. Impact of the additional weighting of bad experiences on the calculation of the expected travel cost. Packet #57 of vehicles from node 1 to node 20. Learning rate=0.2; Linear memory function.

6.9.2.2. Aggregated results: network level analysis

An aggregated analysis provides an overview of the state of the network on each day. Figure 6.27 shows the results of all travel cost spent on the whole network on each day during the simulation period. Due to the stochastic nature of the model, the algorithm is run 10 times and results are displayed on the same figure using a Box and Whisker plot. Total travel cost is obtained as the sum of all travel costs of all drivers travelling through the network on each day. Results evidence that travel cost stabilises and drivers tend to find the travel option that minimises their travel cost over time. Initially, drivers are on the exploration phase, which means that they are trying new travel options and choosing their best one. After 10-15 days, the gradient of the total travel cost trend is reduced, having a period of almost no changes in total travel cost from days 20 to 25. It is also observed that the difference between the 1st quartile and 3rd quartile is also reduced over time.

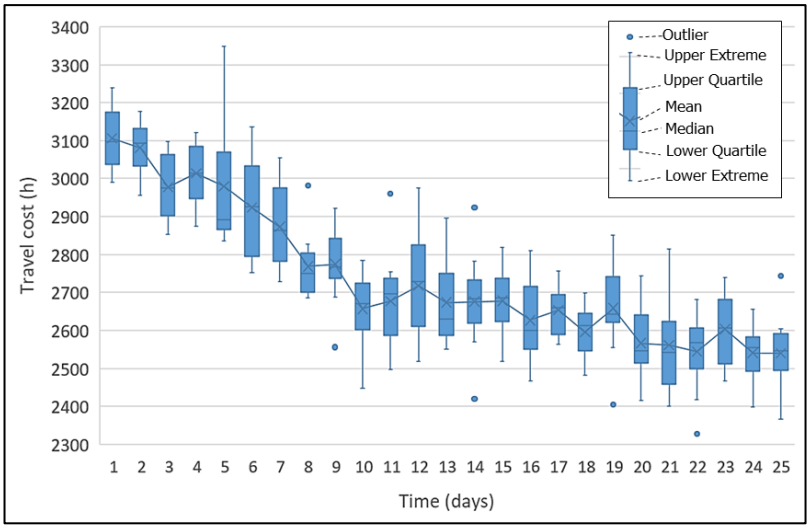

Figure 6.27. Box-Whisker plot: sum of travel costs for all drivers on each day. The graph includes 10 simulations. Learning rate=0.2.

It is important to analyse if 10 simulations are enough to rely on these results. For this reason, the model has been run 20 and 30 times and a comparison of the results are included in Figure 6.28. Graph A shows a comparison of the evolution of travel costs. The line that crosses all boxes represents the mean values on each day. Assuming that travel costs on the 30-sim results are reliable, the relative error (RE) is calculated in order to quantify how far each solution is from the 30-sim one. The error is calculated using Equation (6.42). A comparative of the relative errors is shown in Graph B of Figure 6.28. As expected, 10-sim results differ more than 20-sim results. However, the maximum error is less than 3% which means that there is not a huge difference between considering the 10-sim results or the 30-sim results. In addition, as the total travel cost metric used to measure the resilience of the network (Section 3.4.1) is calculated as the area under the travel cost curve, these slightly differences are not significant.

$$RE(\%) = \frac{\overline{TTC}_{ts} - \overline{TTC}_{t,30}}{\overline{TTC}_{t,30}} \cdot 100 \tag{6.42}$$

Where,

$\overline{TTC}_{ts}$, is the mean value of the total travel cost of s simulations on day t.

$\overline{TTC}_{t,30}$, is the mean value of the total travel cost of 30 simulations on day t.

RE, relative error in %.

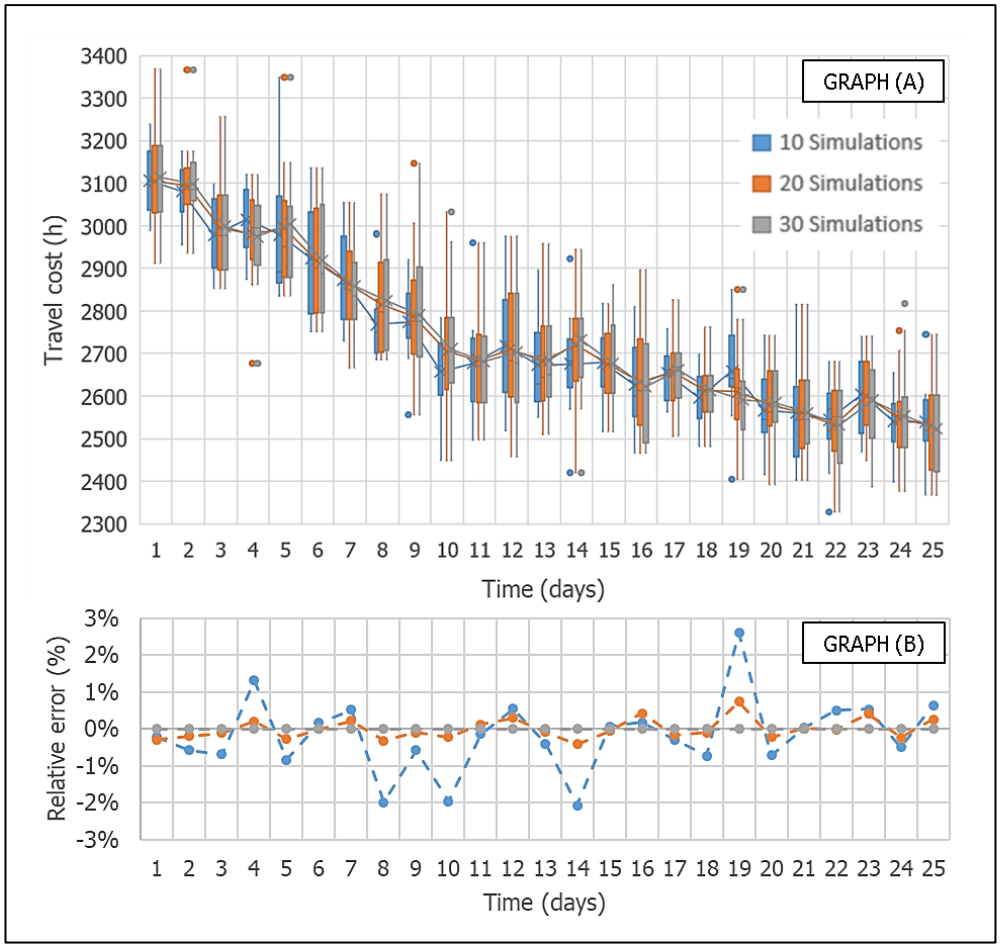

Figure 6.28. Graph A represents the evolution of travel cost over time of 10, 20 and 30 simulations using a multiple box plot representation. Graph B represents the relative error of the 10-sim and 20-sim considering the 30-sim as the right value.

Some drivers may not have the chance to use all available options before deciding the best travel option for them. Figure 6.29 shows the average number of travel options that drivers have already used on each day. It is obvious that the first day every driver has only used an option. As days go by, drivers are using other travel options and that is reflected on the increasing line on the graph. However, if drivers find an option that provides good results for them, they stick to it and no more options are used, even if these options may be better in terms of travel cost. This is reflected on the (almost) horizontal asymptote of the final days of the graph. It seems that, in this example after 25 days, almost all drivers have already tried all the 6 available travel options.

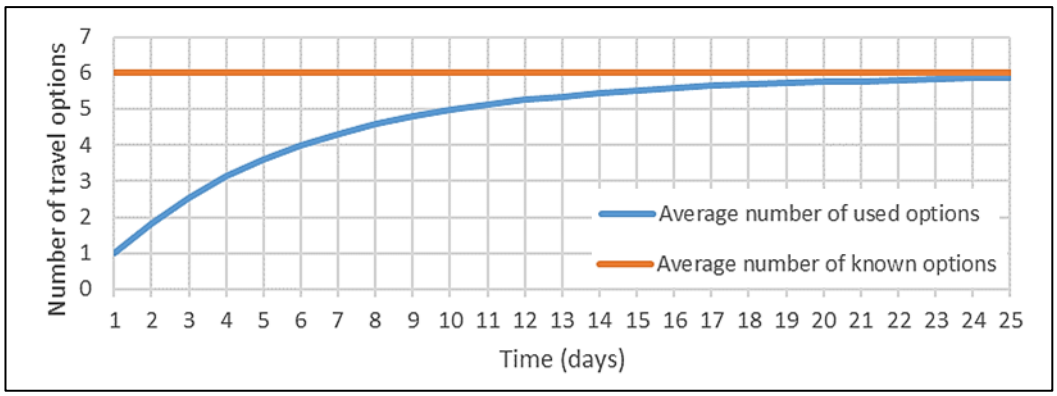

Figure 6.29. Average number of used/known travel options – route and departure time – on each day (10 simulations). The option of 'not travelling by car' is not considered in the graph.

6.9.3. Sensitivity analysis: learning rate

This section analyses the sensitivity of the model to changes in the learning rate (ℓ_h, see Section 6.5). The 'one-at-time sensitivity' technique is used and whose aim is to create a variation of one parameter (learning rate, in this case), keeping all the rest of parameters fixed, and observe the variation in the model outputs.

The learning rate is the parameter that indicates how fast drivers learn from the environment. The stimulus value, which is already described in Section 6.5, is a function of this learning rate. The higher the learning rate is, the higher the value of the stimulus is. This directly affects the updating scheme as a higher value of the stimulus implies a higher increase/decrease in the probabilities of selecting travel options.

Figure 6.30 shows the average total travel costs on each day for 10 simulations using different values of the learning rate. Low values of the learning rate show that drivers take more time to find their best travel option. The maximum value of the stimulus is limited to the learning rate, which means that if the learning rate is low, the stimulus is low as well. In these cases, after each day, the amount of probability that is increased/decreased is also reduced, meaning that the rate at which a travel option stands out among the rest is reduced as well. On the other hand, the higher the value of the learning rate is, the faster drivers learn and find their 'best' travel option. In these situations, when drivers find a very good option, the stimulus value

that is assigned to that option is high because the learning rate is high as well. This means that the probability of selecting that travel option is increased/decreased a quantity that is proportional to the stimulus value. As observed in the graph, when the learning rate is 1, drivers are able to find rapidly their best travel options so that the total travel cost is reduced almost at its minimum value on day 10. However, if the learning rate is 0.1, even after 30 days drivers are still trying to find their best option and they are not still close to reduce the total travel cost to its minimum value.

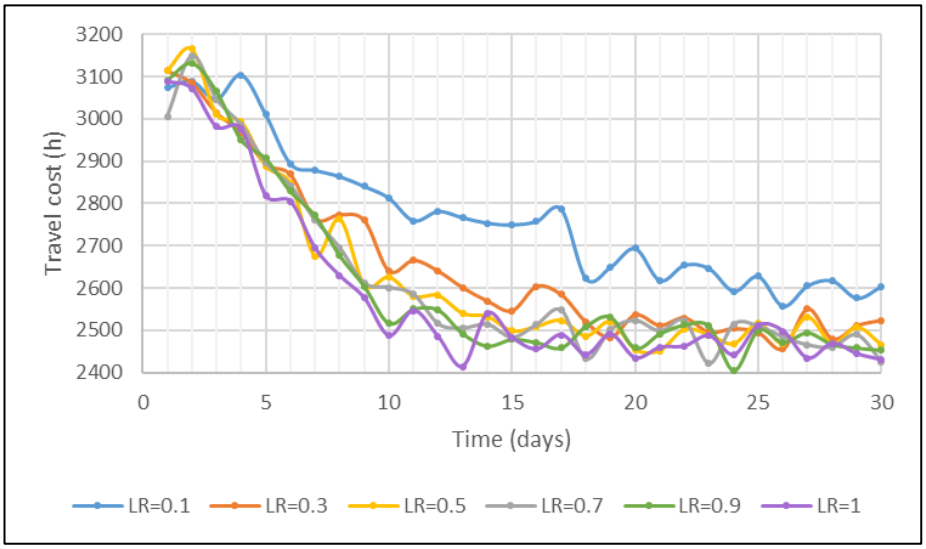

Figure 6.30. Average total travel cost (10-sim result) using different values of the learning rate.

However, taking high values of the learning rate can have side effects. Figure 6.31 represents the cumulative number of travel options that are used on average by drivers after running different values of the learning rate. As observed, the lower the learning rate is, the more chance drivers have to explore the network because the probability of selecting an option does not increase/decrease that fast. This implies that drivers try more travel options before sticking to their 'best' one. On the contrary, if the learning rate is high, drivers rapidly converge to an option (even if this option is not their 'best' one) and do not have the chance to try other alternative options. The difference shown in Figure 6.31 may get worse if more travel options are provided to drivers.

To sum up, the following conclusions can be extracted from the sensitivity analysis: (1) High learning rates mean that drivers find 'good' options faster (not

necessary the 'best' options) and rapidly stick to them and this implies a less exploration phase. (2) Low learning rates mean that drivers take time to learn and find the 'best' travel option and this implies that more options are used (more exploration phase).

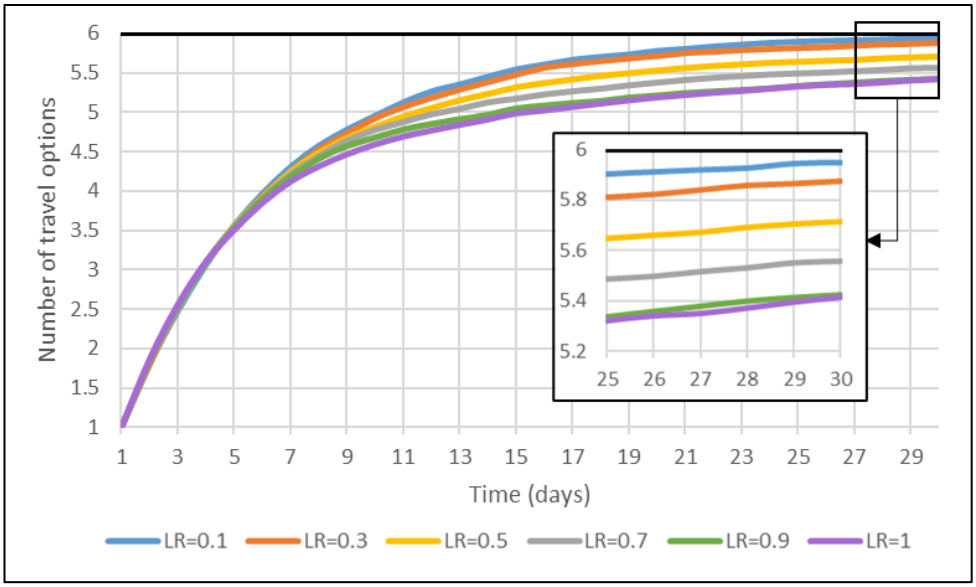

Figure 6.31. Average cumulative number of travel options (10-sim result) that drivers have used on average after using different values of the learning rates.

6.10. Comparison to previous methodologies and contribution

This section compares the methodology proposed in this chapter to the ones presented in the literature. Table 6.6 explains how the new improvements fill the gaps of previous models. The contributions to the knowledge are therefore also included in this table.

Table 6.6. Comparison of the main drawbacks of previous methodologies and the ones proposed in this Chapter 6.

Drawbacks of previous models	Solution of the proposed model
Expected travel cost. The expected travel cost calculation in Wei *et al.* (2014) considers a weighted average of travel costs of ALL routes for an OD pair.	**Section 6.4.** This model proposes an improved formulation to calculate the expected travel cost that only considers routes with the same departure times.
Memory and bad experiences. All travel experiences are equally important in previous models (Ozbay, Datta and Kachroo, 2001; Wei, Ma and Jia, 2014). Only the memory factor reduces the importance of previous travel experiences.	**Section 6.4.2.** This model introduces a new approach that considers the importance of bad experiences vs good ones. The section describes a novel method to include these new features on previous models. The model also implements the idea that bad experiences wear off more slowly than good ones. It is done by adding a novel approach that considers the bad-memory decay over time.
Updating probability vector. Previous models (Ozbay, Datta and Kachroo, 2001) that also consider departure time choices do not differentiate between options with different departure times. For example, if stimulus is negative, the probability of selecting the chosen option is decreased and the rest of options increased. However, there can be other options with different departure times that should not be increased because in reality drivers are less likely to choose it.	**Section 6.6.** A new and more realistic approach is proposed that classifies travel options by favourable and unfavourable in order to update the probability of selecting options for the next day. This allows the possibility of not considering unchosen options as a fixed block of options whose probability is increased/decreased. Travel options are considered individually, allowing a more flexible approach.

Continuous in the next page

From the previous page

Drawbacks of previous models	Solution of the proposed model
Option of 'not travelling by car' on a day. Previous reviewed RL models of Section 6.1.3 do not include the option of allowing drivers not to travel on a day. However, this option acquires importance especially after disruptive events and models should allow drivers to decide between cancelling the trip or even use another transport mode if it is available.	**Section 6.8.** This model adds a new feature as it incorporates an additional option that allows drivers not to travel by car and use other transport modes or cancel their trip. Although the approach proposed in Section 6.9 is not a very sophisticated one, it provides the first step to build a multi-modal transport model in which drivers can cancel their trips if alternative transport modes do not provide good services.
Level of resolution. Previous models apply their reinforcement-learning model using a macroscopic traffic simulator (Ozbay, Datta and Kachroo, 2001; Wei, Ma and Jia, 2014; de Oliveira Ramos and Grunitzki, 2015) or a microscopic traffic simulator (Wahba and Shalaby, 2005).	**Previous chapter 5**. To the best of the author's knowledge, this is the first reinforcement-learning model that simulates departure time and route choices and is applied on a mesoscopic traffic simulator.

6.11. Limitations and further work

This section presents Table 6.7 which includes the limitations of the proposed model and some key areas of further research.

Table 6.7. Limitations and areas of improvement of the reinforcement-learning model

Limitation	Areas of improvement
Day-to-day learning model. Drivers acquire knowledge about the environment after repeatedly making travel decisions. This implies that drivers have to travel on an everyday basis to learn from their decisions. The model is ideal to simulate how drivers commute and make day-to-day travel decisions. However, although this model can include leisure-based activities, it might be not very realistic as people do not require travelling repeatedly every day for these purposes.	New improvements should study the possibility of including leisure-based activities that are not usually undertaken on an everyday basis by each driver. This can be done by considering that, instead of learning between days, drivers can learn between "X" days that are the days that drivers undertake the activities.
Initial path set generation. The path set generation always starts with the K-shortest free-flow paths for each OD pair. However, for instance on an urban network, there could be too much overlap between these K-shortest paths. This means that, if something wrong happens on the network, drivers will not know enough alternative routes to get to their destination.	An improved path set generation could be implemented that finds the K-shortest paths but penalises those paths that share some links.
Learning rate and heterogeneity of drivers. A static learning rate for each driver may not reflect how drivers learn in real life. High values of learning rate make driver converge faster to some travel options that may not be the 'best' one. On the contrary, lower values of learning rates make drivers slow down the convergence process.	Further research should be done in order to understand how fast/slow drivers stick (converge) to certain travel options. A more dynamic approach should be considered in which drivers can learn faster/slower at different times and therefore try more/less travel options. Different values of learning rates should also be assigned to different types of drivers to show the heterogeneity of drivers.

Continuous in the next page

From the previous page

Limitation	Areas of improvement
Exploration vs Exploitation. Travel options that are not chosen initially, are less likely to be chosen over time, in the absence of sufficient exploration. Sometimes these options are even never used. This was also identified by Duffy (2006).	Make sure that all travel options are used at least once. This can be done extending the exploration phase of the ε-greedy approach or assigning a lower learning rate during the pre-disruptive stage.
Multi-modal transport model. The extra option of 'not travelling by car' added in this model requires the understanding of existing alternative transport modes. The approach proposed in Section 6.9 is not the most sophisticated one as it requires data that is not easily available.	Surveys could be done in order to understand drivers' satisfaction to the use of alternative transport modes available in the area. Alternatively, a multi-modal approach could be added to the current model so that it can influence drivers' decision of 'not travelling by car' and use another transport modes.
Drivers' information. The proposed model considers that drivers have only access to travel information based on their previous experience. External travel information should be provided in order to allow drivers to make more informed travel decisions.	External travel information such as the one provided by GPS navigation, radio, social media could be used to update the probability of selecting travel options on each day. There is still room for improvements in the direction of managing traffic. Incentives can be given to drivers that select those options that are globally more efficient rather than just minimising the individual travel cost of each driver.
Calibration and validation. The model needs to be calibrated to the traffic conditions that are applied and validated using real traffic data in order to be applicable to real life operations. The lack of time has made this process impossible to complete.	Future work should focus on gathering traffic data to calibrate the model and validate the results.

6.12. Conclusions

This chapter aims to answer the following research questions: RQ6 "What is the current state-of-the-art on reinforcement-learning traffic models and their application to disrupted traffic networks?". RQ7 "How can the updating probability scheme of selecting travel options of previous RL traffic models be improved, taking into account departure time differences between travel options?". RQ8 "How can the RL traffic model incorporate the possibility of cancel a trip or use alternative transport modes if disruptive events occur?". RQ9 "To what extend can bad memories of previous trips affect drivers' travel decisions of future trips and how can it be implemented in the formulation of the RL traffic model". RQ10 "What is the impact of the learning rate parameter on the global network performance?".

This chapter presents an improved reinforcement-learning traffic model that aims to simulate the drivers' decision making process. The model described in this chapter uses a reinforcement-learning technique that allows drivers to make their own travel decisions based on previous travel experiences. Drivers may choose different departure time and route options and learn which choices are the 'best' for them in minimising their travel cost. A renewed formulation for the expected and perceived travel cost is formulated. It also incorporates a new feature that quantifies the importance of bad memories vs good ones and their decay over time. An additional option is also added to this model that considers the possibility of cancelling the trip or even use an alternative transport mode. A new updating probability scheme that differentiates between favourable and unfavourable travel options and updates the probabilities of selecting travel options for each driver is proposed in this chapter. All these novel features constitute part of the improvements that previous RL traffic models were demanding and they will help to provide results that are a step closer to reality.

The departure time and route choice model is applied to the Sioux Falls transport network (South Dakota, US), illustrating the concepts introduced in this chapter. Results from the example include individual driver's travel decisions and global average travel costs. A sensitivity analysis of the learning rate parameter is also undertaken, showing the meaning of high and low learning rates. Limitations and

potential areas of further research show the need to continue betting on these artificial intelligence models to simulate drivers' behaviour.

CHAPTER 7

Extending the reinforcement-learning model to include on-board travel decisions and pre-departure and in-journey travel information

7.1. Introduction

The model presented in the previous chapter introduced an improved reinforcement-learning model that was applied to the area of transport modelling. It focused on the pre-disruption stage where drivers had no previous knowledge about traffic conditions in the network and during this phase they were building up their own travel experience. Through reinforcement learning, within the model drivers made decisions on route and departure time based on their previous travel experience and learnt from their mistakes. However, neither the model of Chapter 6 nor the reviewed RL traffic models (Ozbay, Datta and Kachroo, 2002; Wahba and Shalaby, 2005; Wei, Ma and Jia, 2014; de Oliveira Ramos and Grunitzki, 2015) describe what happens to drivers' behaviour when a disruptive event causes the closure of certain roads. If drivers face disruption, the model must reflect how drivers adjust to unexpected events when they encounter disruption for the first time. Apart from this, another important aspect that previous RL traffic models do not include is the provision of real-time travel information to drivers. This provision of information is potentially highly beneficial under unexpected disruptive events such as incidents, road closures, etc. As previous RL traffic models have not considered the impact of disruptive events on drivers' behaviour, there has been no need to incorporate additional traffic information. Advanced Traveller Information Systems (ATIS) and Road Traffic

Information (RTI), key components of the Intelligent Transportation Systems (ITS), are designed to assist drivers in making more informed travel decisions. This additional information is likely to enable drivers to choose more efficiently among available routes and departure times, reducing congestion and travel times. As Tavares and Bazzan (2012) concluded, both previous travel experience and additional information play an important role in decisions made by drivers.

The main aim of this chapter is to improve the RL traffic model presented in Chapter 6 by incorporating on-board travel decisions and adding the provision of external traffic information. Section 7.2 presents a framework that allows drivers to make on-board travel decisions. Section 7.3 introduces types of external travel information that is provided to drivers and the following Sections 7.4, 7.5 and 7.6 describe more in detail pre-trip and en-route information considered in the model. Section 7.7 applies the model to the Sioux Falls transport network (South Dakota, US) in order to illustrate the concepts explained in this chapter. Section 7.8 describes the drawbacks of previous models and highlights the contribution that this model makes to knowledge. Finally, Section 7.9 and 7.10 describe some limitations of the model, further work that can be done in order to improve the current model and some conclusions.

7.2. On-board travel decisions with no external information

Drivers have to make decisions mid-journey. An unexpected congestion or a road closure may make drivers decide to take another route. But, how do drivers make the decision of changing routes? What triggers the re-route decision? Which route do drivers choose if they opt for rerouting? The following section presents a framework that allows drivers to make on-board decisions. Figure 7.1 includes a flowchart that summarises the contents of the rest of this section. When drivers arrive at an intersection, they evaluate the conditions (described later on in this section) that may (or may not) trigger the on-board decision-making process. If drivers decide to re-route, the model differentiates between a road closure and a non-closure. If a road segment is closed to traffic, driver can decide between following the diversion route that is set in place for that closure or find alternative routes that he/she has already used in a previous trip. Following a deterministic approach, the modeller can decide

the percentage of drivers that prefer to use diversion routes under these circumstances. However, in order to reduce the number of variables, the model assumes that all drivers will follow diversion routes if these are set in place after road closures. If the road is not closed to traffic, drivers can choose any alternative route that has been used by them in the past. The model introduces an algorithm that determines the route that drivers prefer to follow based on previously experienced travel times (Section 7.2.2). The model also allows drivers to decide if they want to abandon the trip if certain conditions are satisfied (Section 7.2.3).

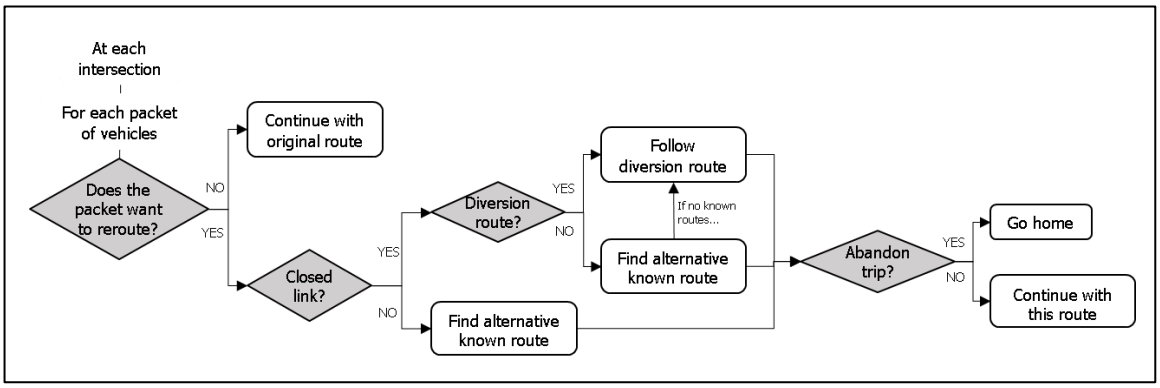

Figure 7.1. Flowchart of the on-board drivers' decision algorithm

The on-board decisions that drivers make due to disruptive events may also influence future travel decisions. That is why the option probability functions presented in Section 6.6 of Chapter 6 are also reformulated in Section 7.2.5 in order to consider the impact of on-board travel decisions. This is inspired by the similar idea proposed by Sutton and Barto (1981) that penalises bad intermediate actions on the original Bush-Mosteller model (1951) of reinforcement learning.

7.2.1. Triggering on-route drivers' decisions

The model allows drivers to make re-routing decisions when they face mid-trip disruptions. Note that when drivers have no external information, they need to make the re-routing decision based on current traffic conditions that they are experiencing and on the memory they have from previous trips.

In this model, two conditions are proposed to allow driver to decide if they remain on their chosen route or they re-route. If any of these two conditions are met,

it can trigger the on-board decision-making process of drivers. At each intersection, drivers check if any of the following two conditions are met and therefore, make the on-board decision.

- ✓ CONDITION 1: The next link is closed

  As drivers have no additional external information, they cannot know if the next road segment is closed or open. Therefore, if they face a road that is closed, they have to reroute.

- ✓ CONDITION 2: Busy road segment and willingness to reroute

  It is assumed that drivers can observe if a road is busy or not by looking at the density of vehicles ahead. If the density of vehicles on that road exceeds a user-defined threshold, then drivers have the chance to re-route (Equation (7.1)). However, not all drivers are aware of the density condition or they might be not willing to re-route. Therefore, in order to consider this heterogeneity of drivers, an additional variable called *patience level* shows how patient a driver is and it indicates the probability of staying on the same route or changing to another one. The more patient a driver is (high patience value), the higher the probability of staying on the chosen route. On the contrary, if a driver has a low patience value then this driver will have a higher probability of changing to another route.

  The patience level of drivers can also be altered if they face more than one busy link on the same day. The tiredness of encountering congested links and switching routes can make drivers to stick to certain routes even if these are busy. In other words, drivers have a limited number of on-board decisions. This restriction has been imposed in order to limit those drivers who would otherwise switch routes all the time during congested conditions.

$$\frac{k_l}{k_{max,l}} > \lambda \tag{7.1}$$

And

$$\vartheta_h > \left[\Omega_h + \frac{J_h}{\max J_h} \cdot (1 - \Omega_h)\right] \tag{7.2}$$

Where,

l, the link number that packet h of drivers wants to use.

k_l, number of vehicles per km on link l.

$k_{max,l}$, maximum number of vehicles per km on link l.

λ, user-defined threshold that is defined for each driver. It limits the maximum number of vehicles that can be on a road without triggering on-board decisions. It can take a value between 0 and 1. It can also take different values for each driver.

ϑ_h, a random value for each packet h of drivers. These values follow a uniform distribution between 0 and 1.

Ω_h, patience level of a packet h of vehicles. It can take a value between 0 and 1 and it is assigned to each packet of drivers following a pre-defined probability distribution.

J_h, number of disrupted links that driver h has experienced on the same day.

$\max J_h$, user-defined maximum number of disrupted links that limits the number of re-routes this driver can take.

The right side of the Equation (7.2) limits the willingness of a packet of drivers h to change route. In order to know if a packet of drivers is willing to reroute, a random value (ϑ_d) is generated for each packet h. If the random value is lower than the willingness to reroute, this packet of driver sticks to the same route. If the random value is higher, then drivers change route only if Equation (7.1) is also satisfied. Every time drivers face a disrupted road segment, the willingness to reroute is increased and therefore drivers are less likely to reroute when they face another disruption. A graphical example of how the willingness to reroute changes when more disrupted road segments are faced is included in Figure 7.2. Note that both Equations (7.1) and (7.2) must be satisfied to fully meet condition 2.

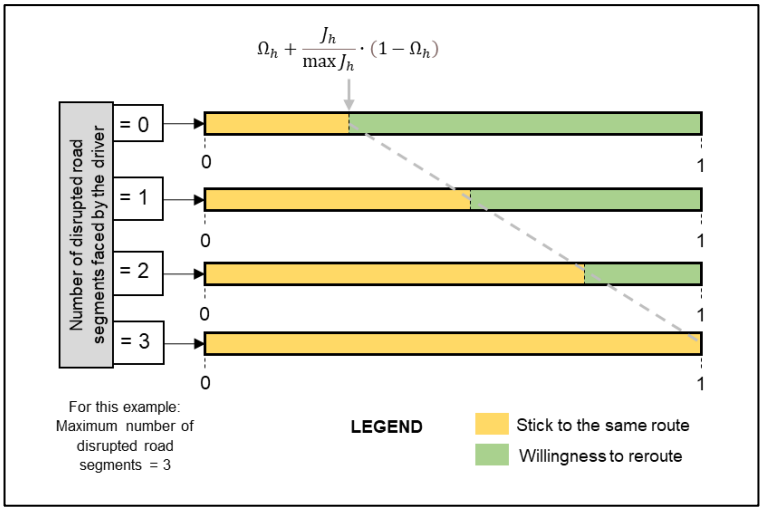

Figure 7.2. Example of how the willingness to reroute changes when more disrupted road segments are faced.

7.2.2. Route choice algorithm

This subsection describes the algorithm that is used to find alternative routes after facing a disruption. The algorithm works differently depending on whether the disrupted link is closed or busy. If the link is closed (condition 1 of previous Section 7.2.1 is satisfied), it is assumed that a diversion route is set in place. This new route is obtained as the shortest travel distance between the nodes that form the disrupted link. In this case, drivers have to follow the diversion route until it encounters the original route that this driver wanted to follow. If the link is busy (condition 2 of previous Section 7.2.1 is satisfied), an algorithm finds a previously used route that avoids the disrupted link (if it is possible). A full description of the algorithm is included in Figure 7.3 with an example to complement the explanation. The advantage of this algorithm is that it allows drivers to go back to previous nodes of the original route and find alternative paths from these nodes avoiding the disrupted links. A list of alternative routes is generated and the travel time of all these routes is calculated based on previous travel experience. The route with minimum travel time is the one selected by each packet of drivers.

Note that if the algorithm does not find an alternative route, it means that drivers do not know alternative routes because they have not used them in the past. In this case, drivers would have to choose between sticking to the original route even

if the link is busy or taking the risk, explore the network and find a way to reach the destination. In this model, if drivers do not know alternative routes, drivers are forced to stick to the original route. Future version of this model should include an algorithm that simulates how drivers take the decision between sticking on the same route or explore the network. The process of exploring and creating a new route without previous experience also needs to be implemented in future versions of the model.

Algorithm to find a new route based on previous experience

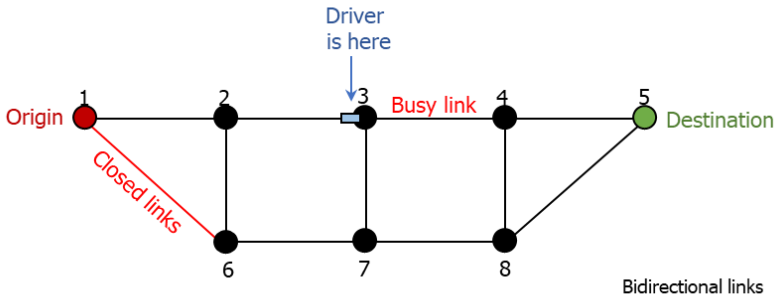

Procedure	Example
1. Find the current route	Route = Nodes [1 2 3 4 5]
2. Identify the problematic link	Problematic link => Nodes [3 4]
3. Find the node where the driver is located.	Current node = 3
4. Find a new partial route from the node where the driver is located until the destination node (avoiding the problematic link)	
4.1. For all known routes (based on previous experience), find those routes that contain the current node where the driver is located	Possible subroute 1 = [3 7 8 4 5] Possible subroute 2 = [3 7 8 5]
4.2. Exclude those routes that contain the problematic link	-
5. Find other routes that include going back certain nodes (following the same path) and find from that position known routes to the destination	
5.1. Go back one node from current route	Go-back route = [3 **2** …]
5.2. Repeat step 4 from this new node in order to find more partial routes	Possible subroute 3 = [3 **2** 6 7 8 4 5] Possible subroute 4 = [3 **2** 6 7 8 5]
5.3. Repeat steps 5.1. and 5.2., going back more nodes (until the origin)	Possible subroute 5 = [3 **2** **1** 6 7 8 4 5] Possible subroute 6 = [3 **2** **1** 6 7 8 5]
6. Remove those subroutes that contain any closed link	Remove subroutes 5 and 6 (closed links 1-6)
7. Obtain the travel time (based on previous experience) of each possible subroute.	Subroute 1 → TT= 20 min Subroute 2 → TT= 18 min Subroute 3 → TT= 30min Subroute 4 → TT= 28 min
8. Select the subroute with the minimal travel time	Subroute 2 = [3 7 8 5]
9. Complete the route by adding the first part of the original route	Selected route = [1 2 3 7 8 5]
NOTE: If there are not known routes available, then stick with original route	

Figure 7.3. Algorithm that finds a new route based on previous driver's experience and the application to an example.

7.2.3. Abandon trip and return home

The model adds the feature of allowing drivers to abandon their trip and go back to the origin node if some conditions are met. This important feature needs to be considered especially when dealing with disrupted conditions where drivers have to reroute. Previous RL traffic models do not incorporate this feature and in such cases, drivers are forced to use any of the pre-defined routes even if it takes too much time to get to the destination. The benefit of adding this new feature is two-fold: first, it reflects how drivers would act under these circumstances and secondly, it releases traffic from some congested areas as some drivers would abandon their trip and go home under extreme circumstances.

Drivers can decide to abandon their trip if any the following conditions are met. Condition (1): if drivers cannot find any alternative known route to follow after the closure of a road segment and there is no diversion route place set in place; and/or Condition (2): if the expected travel time of the new route is too high. This second condition is mathematically expressed in Equation (7.3). It means that if the expected arrival time calculated for each alternative option is later than the starting time of the activity, drivers abandon their trip. The modeller can also add an extra additional late arrival value, to be more flexible and allow drivers to arrive later.

$$EAT_{hz} > ST + EL \tag{7.3}$$

Where,

EAT_{hz}, is the arrival time that packet h of drivers expects after choosing new travel option z.

ST, is the starting time of the activity.

EL, is the user-defined extra time that allows drivers to arrive later than the starting time of the activity.

The expected arrival time (EAT_{hz}) is calculated in Equation (7.4) as the sum of the current time that is being analysed and the expected travel time of the new selected option. The expected travel time is calculated as a weighted average of the travel time of all links that form the route as shown in Equation (7.5).

$$EAT_{hz} = CT + ETT_{route,h} \tag{7.4}$$

Where,

CT, current time that is being analysed (e.g. 8:04am).

$ETT_{route,h}$, is the travel time of the new route that the packet h of drivers expects. This can be calculated as shown in Equation (7.5).

$$ETT_{route,h} = \sum_{l}^{all\ links\ route} ett_{lh} \tag{7.5}$$

Where,

l, the link number.

ett_{lh}, travel time that packet h of drivers expects from link l, which is calculated as shown in Equation (7.6).

$$ett_{lh} = \frac{\sum_{j=1}^{t}(\varphi_j \cdot tt_{lhj})}{\sum_{j=1}^{t}\varphi_j} \tag{7.6}$$

Where,

tt_{lhj}, is the travel time on link l that packet h of drivers have experienced on day j. If this packet of drivers has never used this link, the travel time considered is the free-flow travel time.

φ_j, represents the memory level of travellers ($0 < \varphi \leq 1$). Same variable explained in Section 6.4.1 of Chapter 6.

t, is the current day that is being analysed.

When drivers decide to abandon their trip and return to the origin node, the model forces drivers to follow the same path that they have originally selected to use for that day but in the opposite direction. The model also assumes that they cannot take more on-board decisions on their way home. This tries to avoid drivers make unnecessary decisions when they already know they are cancelling the trip and going home.

The modeller can decide whether this 'abandon trip' module is considered or not in the model. If it is not considered, then drivers cannot abandon trip and they are forced to stick with the original route even though it is busy.

7.2.4. Isolated nodes: cancelling trips

The unexpected closure of some roads due to hazard impacts might cause the isolation of some nodes on the network. Drivers that do not have external information cannot know *a priori* which nodes are isolated. In these cases, drivers might be stuck on the network trying to find alternative paths in the model. In order to avoid this situation, drivers are forced to make the decision of cancelling the trip at the beginning of each day. Therefore, the model assumes that all drivers know if any node is isolated, so that they can cancel the trip if they cannot leave the origin node or they cannot get to the destination node.

7.2.5. Impact on future decisions: updating option probabilities

Previous sections 7.2.1 to 7.2.4 have introduced a method to allow drivers to make on-board decisions when no external travel information is provided. This means that if they face road closures or busy roads they can decide to follow an alternative route until they get to their destination. However, these multi-day disruptions may also have an impact on future travel decisions. As an example, if drivers face the same road closure day after day, they will be less likely to choose any route that contains that closed road in the following days until further notice of the road opening. This additional aspect is also taken into account in the improved formulation presented in this section. It updates the probabilities of selecting travel options for future days considering on-board decisions.

The previous Section 6.6 of Chapter 6 describes the formulation that is used to update the drivers' probability of selecting travel options for the next day. However, this formulation does not include the influence of any on-board travel decision. For that reason, there is a need to update the formulation in order to incorporate the consequences of on-board decisions.

Following the same structure expressed in Chapter 6, the formulation used to update the option probabilities is included in Table 7.1. Equation (7.7) and (7.8) are used if the sign of the stimulus value is positive and Equation (7.9) and (7.10) if the sign of the stimulus value is negative. The difference compared to the previous formulation included in Table 6.3 is the addition of a term that reduces the probability of selecting those options that contain disrupted routes. As no external travel

information is provided, this reduction is only applied to the disruptions that a packet of driver faces on day t and it impacts the probabilities of choosing travel options for the day $t+1$. This means that if no disrupted option is encountered on a day, then the probability reduction is not applied to any travel option. Mathematically, these terms are preceded by the binary variable F in equations of Table 7.1, which allows the modeller to decide if this new feature of reducing the probability of choosing disrupted options is used or not. If $F = 0$, the formulation of Table 7.1 is exactly the same as the one described in Table 6.3 of Chapter 6 and therefore this additional feature is not used. One of the variables that quantifies the probability reduction of selecting those options that contain at least a disrupted road segment is d_z. Depending on the number of consecutive days that this packet of drivers has faced the same disruption, the variable takes different values ranging from 0 (no reduction) to 1 (maximum reduction) – see Equation (7.14) after Table 7.1. It is assumed that drivers do not know when the disruption will be cleared up unless they face the road segment again and see that is open. A more detailed explanation of these additional terms is included after Table 7.1. Note that, from now on, the chosen option m is the revised option (if packet has re-routed) and not the originally option selected by the packet of drivers.

7.2.5.1. Positive stimulus

As already explained in Section 6.6.1 of Chapter 6, a positive stimulus ($S_{hmt} \geq 0$) means that drivers are satisfied with the selected travel decision for that day and therefore, they are more likely to repeat the same option the next day. The previous formulation [Equations (6.22) and (6.23)] increases the driver's probability of selecting the chosen option again for the next day and decreases the probability of selecting unfavourable options. However, in order to account for the disrupted options due to on-board travel decisions, an updated formulation is presented in Table 7.1. A graphical example of the idea of how this formulation works is included in Figure 7.4. If stimulus is positive, the probability of selecting again the chosen option is increased and the probability of selecting unfavourable options or disrupted options is decreased.

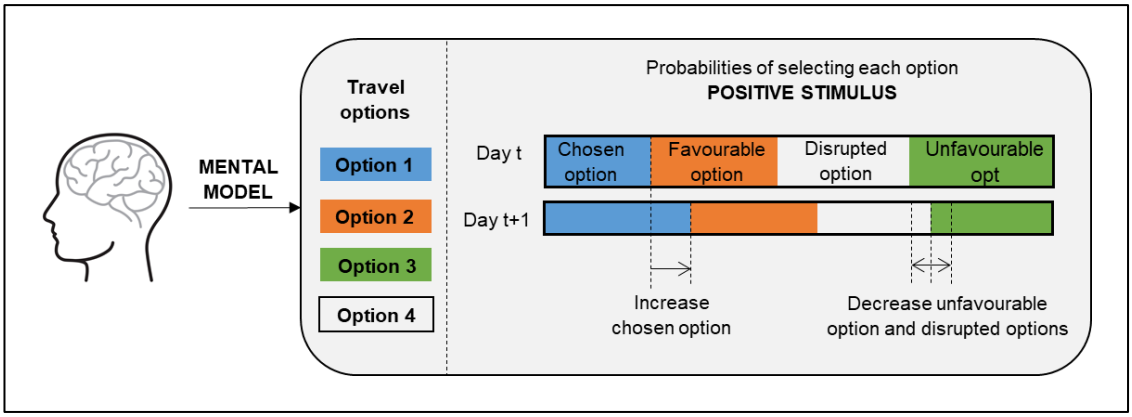

Figure 7.4. Graphical example of the improved option probability updating process when stimulus is positive.

Equation (7.7) in Table 7.1 updates the probability of choosing the option m for the next day ($p_{m(t+1)}$). The new value is calculated by adding to the previous probability (p_{mt}) an additional value that comes from the probabilities of the unfavourable options and disrupted options. If an option is favourable but it contains a link that is disrupted, it is considered as a disrupted option.

Equation (7.8) in Table 7.1 updates the probability of choosing those options that have not been selected by the packet of drivers on day t ($p_{z(t+1)}$). If the option is favourable, the probability remains the same as the previous day. If the option is unfavourable or it is a disrupted option, then the probability of selecting these options the next day is reduced. The quantity by which each option is reduced is directly proportional to the value of the probability of each option. This means that if an option has more probability of being selected than another one, the reduction will be higher on that option.

7.2.5.2. Negative stimulus

As described in Section 6.6.2 of Chapter 6, a negative stimulus ($S_{hmt} < 0$) means that drivers are not satisfied with the selected travel decision for that day and therefore, they are less likely to repeat the same option the next day. The previous formulation [Equations (6.24) and (6.25)] reduces the probability of selecting again the chosen option and unfavourable options for the next day and increases the probability of selecting favourable travel options. However, an updated formulation that is used to update probabilities when stimulus is negative is presented in this section. This new

formula considers disrupted options as unfavourable options, so that the probability of selecting these options is not increased.

In this sense, a travel option z that is not selected by the packet of drivers h on day t is considered unfavourable in the following cases:

c) Driver that chooses option m on day t arrives earlier than the PATI and this alternative travel option z that is being analysed has the same route but earlier departure time than option m.

d) Driver that chooses option m arrives later than the PATI and this alternative travel option z has the same route but later departure time than option m.

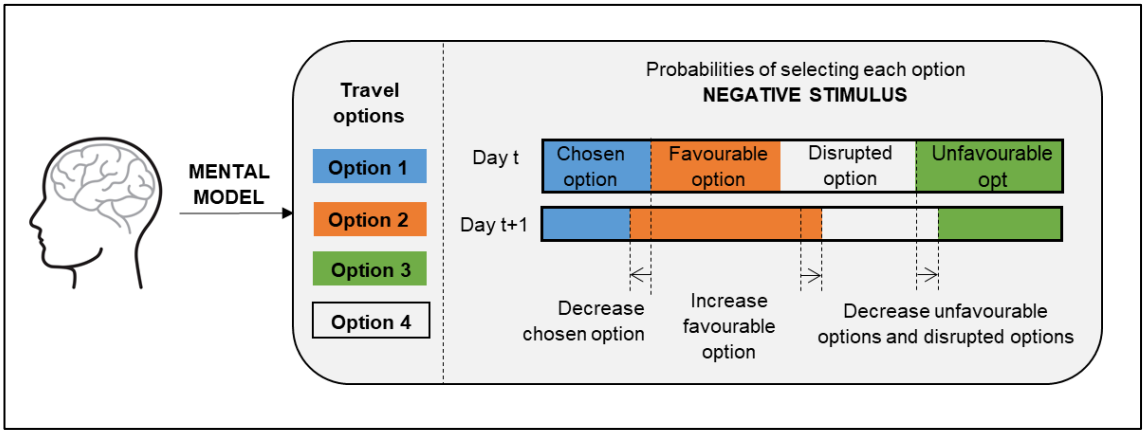

Figure 7.5. Graphical example of the improved option probability updating process when stimulus is negative.

The graphical example shown in Figure 7.5 explains how the proposed formula works. The probability of selecting the chosen option, disrupted options and unfavourable options is decreased, whereas the probability of selecting favourable options is increased. The formulation for the chosen option and the rest of options is included in Equations (7.9) and (7.10) of the same table.

Equation (7.9) updates the probability of choosing the option m for the next day ($p_{m(t+1)}$). The new value is calculated reducing the previous probability (p_{mt}) a certain value that depends on the stimulus value of the driver.

Equation (7.10) updates the probability of choosing those options that have not been selected by the packet of drivers on day t. In order to make it easier for the reader, a breakdown of this equation is included in Figure 7.6. The equation is divided

into three terms, exactly the same terms that were explained in the previous formulation in Chapter 6. The first one corresponds to the probability value of the previous day. The second and third ones are either-or terms that depend on the number of unfavourable options. Within the second term, additional terms are added compared to the previous formulation. These are the ones related to disrupted options. The probability of selecting favourable options is increased except those favourable options that are disrupted. The probability of selecting unfavourable options and disrupted options (even if these are favourable) is decreased. The last term is included just in case there are no favourable options so that all the rest of options are increased even if they are unfavourable or disrupted options.

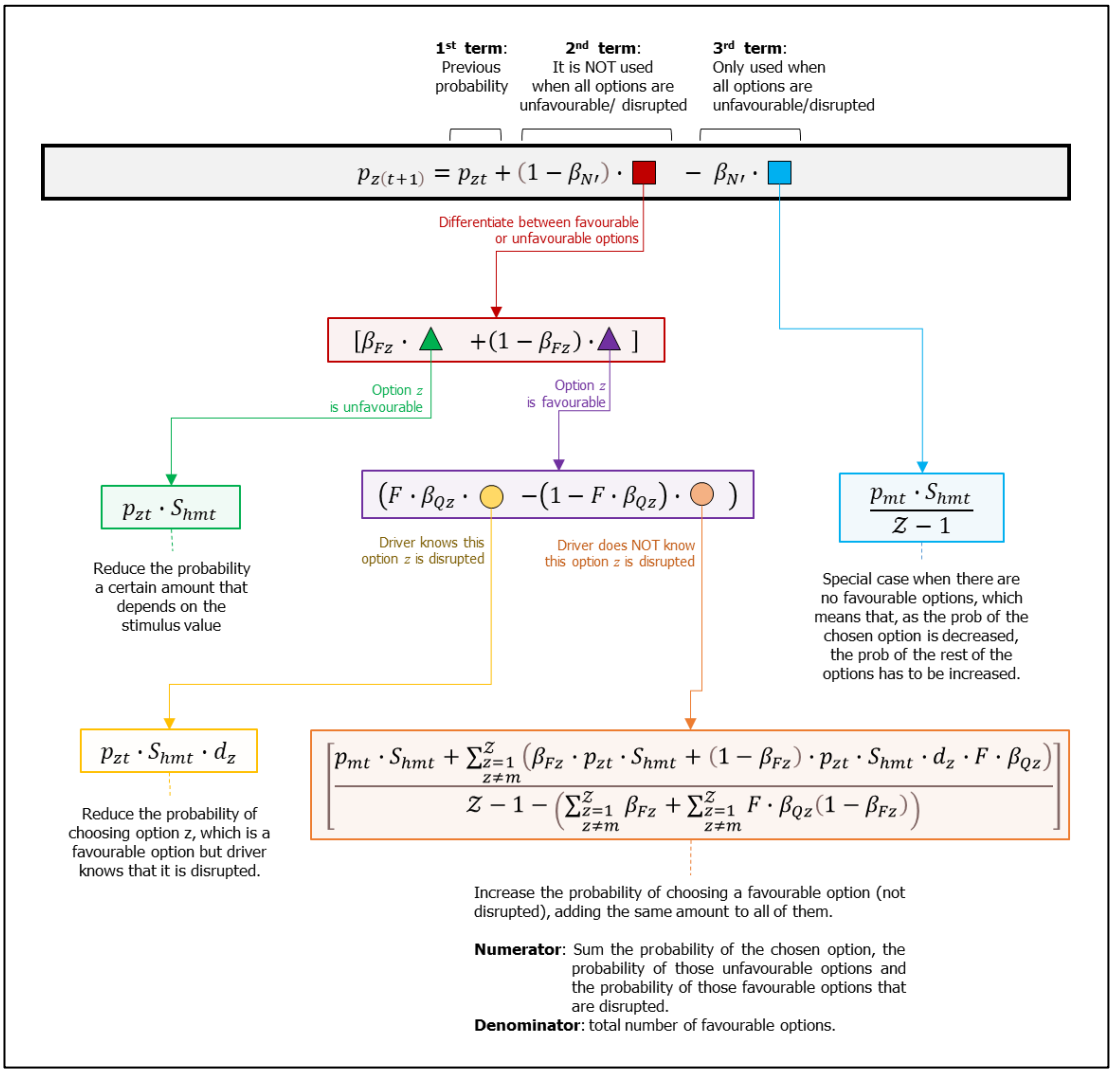

Figure 7.6. Breakdown of Equation (7.10) that updates the probability of selecting travel options that are not chosen on day t when the stimulus is negative.

Table 7.1. Option probability updating functions when stimulus is positive and negative.

		Formulation	Equation
Positive stimulus ($S_{hmt} \geq 0$)	Chosen option m on day t	$p_{m(t+1)} = p_{mt} + \left(1 - p_{mt} - \sum_{z=1}^{\mathcal{Z}} \left[\left(1 - F \cdot \beta_{Qz}\right) \cdot p_{zt} \cdot \beta_z\right]\right) \cdot S_{hmt}$	(7.7)
	Rest of options z	$p_{z(t+1)} = p_{zt} - \left[(1 - \beta_z) + \beta_z \cdot \beta_{Qz} \cdot F\right] \cdot \left[\frac{(1 - \beta_z) \cdot p_{zt} + \beta_z \cdot F \cdot \beta_{Qz} \cdot d_z \cdot p_{zt}}{\sum_{\substack{z=1 \\ z \neq m}}^{\mathcal{Z}} \left[(1 - \beta_z) \cdot p_{zt} + \beta_z \cdot F \cdot \beta_{Qz} \cdot d_z \cdot p_{zt}\right]}\right] \cdot \left[\left(1 - p_{mt} - \sum_{z=1}^{\mathcal{Z}} \left[\left(1 - F \cdot \beta_{Qz}\right) \cdot p_{zt} \cdot \beta_z\right]\right) \cdot S_{hmt}\right]$	(7.8)
Negative Stimulus ($S_{hmt} < 0$)	Chosen option m on day t	$p_{m(t+1)} = p_{mt} + p_{mt} \cdot S_{hmt}$	(7.9)
	Rest of options z	$p_{z(t+1)} = p_{zt} + (1 - \beta_{N'}) \cdot \left[\beta_{Fz} \cdot p_{zt} \cdot S_{hmt} + (1 - \beta_{Fz}) \cdot \left(F \cdot \beta_{Qz} \cdot p_{zt} \cdot S_{hmt} \cdot d_z - \left(1 - F \cdot \beta_{Qz}\right) \cdot \left[\frac{p_{mt} \cdot S_{hmt} + \sum_{\substack{z=1 \\ z \neq m}}^{\mathcal{Z}} \left(\beta_{Fz} \cdot p_{zt} \cdot S_{hmt} + (1 - \beta_{Fz}) \cdot p_{zt} \cdot S_{hmt} \cdot d_z \cdot F \cdot \beta_{Qz}\right)}{\mathcal{Z} - 1 - \left(\sum_{\substack{z=1 \\ z \neq m}}^{\mathcal{Z}} \beta_{Fz} + \sum_{\substack{z=1 \\ z \neq m}}^{\mathcal{Z}} F \cdot \beta_{Qz}(1 - \beta_{Fz})\right)}\right]\right)\right] - \beta_{N'} \cdot \frac{p_{mt} \cdot S_{hmt}}{\mathcal{Z} - 1}$	(7.10)

$z \in \mathcal{Z}, \quad z \neq m$

Where:

z, travel option that is not chosen on day t.

m, travel option that is chosen on day t (diverted option if packet of drivers has rerouted).

$\mathcal{Z}$, total number of travel options.

p_{mt}, is the probability of selecting option m on day t.

p_{zt}, is the probability of selecting another option z on day t.

$p_{m(t+1)}$, is the new probability of selecting the travel option m on day $t+1$.

$p_{z(t+1)}$, is the new probability of selecting the travel option z on day $t+1$.

S_{hmt}, stimulus value of packet of drivers h after choosing option m on day t.

β_z, binary variable (0-1) that indicates whether option z is favourable ($\beta_z = 1$) or unfavourable ($\beta_z = 0$) on day t when stimulus is positive.

$$\beta_z = \begin{cases} 1, & if\ AT_{hm} < ET_h \ \ and \ \ RU_z = RU_m \ \ and \ \ DT_z > DT_m \\ 1, & if\ AT_{hm} > LT_h \ \ and \ \ RU_z = RU_m \ \ and \ \ DT_z < DT_m \\ 0, & otherwise \end{cases} \tag{7.11}$$

$$z \in \mathcal{Z}, \quad z \neq m$$

RU_z, path/route of option z at day t.

RU_m, path/route of chosen option m at day t.

DT_z, departure time of option z at day t.

DT_m, departure time of chosen option m at day t.

ET_h, earliest limit of the preferred arrival time interval (PATI).

LT_h, latest limit of the preferred arrival time interval (PATI).

AT_{hm}, arrival time of driver h choosing option m.

β_{Fz}, binary variable (0-1) that indicates if an option z is favourable ($\beta_{Fz} = 0$) or unfavourable ($\beta_{Fz} = 1$) when the stimulus is negative.

$$\beta_{Fz} = \begin{cases} 1, & if\ AT_{hm} < ET_h \ \ and \ \ RU_z = RU_m \ \ and \ \ DT_z < DT_m \\ 1, & if\ AT_{hm} > LT_h \ \ and \ \ RU_z = RU_m \ \ and \ \ DT_z > DT_m \\ 0, & otherwise \end{cases} \tag{7.12}$$

RU_z, path/route of option z at day t.

RU_m, path/route of chosen option m at day t.

DT_z, departure time of option z at day t.

DT_m, departure time of chosen option m at day t.

ET_h, earliest limit of the preferred arrival time interval (PATI).

LT_h, latest limit of the preferred arrival time interval (PATI).

AT_{hm}, arrival time of driver h choosing option m.

F, binary variable (0-1) that indicates the presence or absence of the new feature presented in this chapter that reduces the probability of selecting those disrupted options. It can take a value of 1 ($F = 1$) if the reduction of the probability is required or a value of 0 ($F = 0$) if it is not required. Note that if $F = 0$, the formulation of Table 7.1 is exactly the same as the one described in Table 6.3 of Chapter 6.

β_{Qz}, binary variable (0-1) that takes a value of 1 ($\beta_{Qz} = 1$) if a packet of drivers h is aware of the disrupted route of option z. Driver knows of this disrupted route because he/she has faced a disrupted link that is included in the route; and it takes the value of 0 ($\beta_{Qz} = 0$) if the packet of drivers does not know that this route is disrupted.

$\beta_{N'}$, binary variable (0-1) that takes the value of 1 ($\beta_{N'} = 1$) if all unselected options are unfavourable/disrupted, or 0 ($\beta_{N'} = 0$) otherwise. This is done in order to avoid having a denominator with a value less than 1. If $\beta_{N'} = 1$, the second term of the formula cannot be computed in the formulation and only the third term is be calculated.

$$\beta_{N'} = \begin{cases} 1, & if \quad Z - 1 - \left(\sum_{\substack{z=1 \\ z \neq m}}^{Z} \beta_{Fz} + \sum_{\substack{z=1 \\ z \neq m}}^{Z} F \cdot \beta_{Qz}(1 - \beta_{Fz}) \right) < 1 \\ 0, & otherwise \end{cases} \tag{7.13}$$

d_z, variable that reduces the probability of selecting those options that contain at least a disrupted link. This variable is represented by a function that is shown in Figure 7.7. It can take values between 0 (drivers does not reduce the probability of selecting disrupted options) and 1 (drivers avoid these disrupted options and reduce the probability of selecting these options to zero). Mathematically, it is expressed in Equation (7.14).

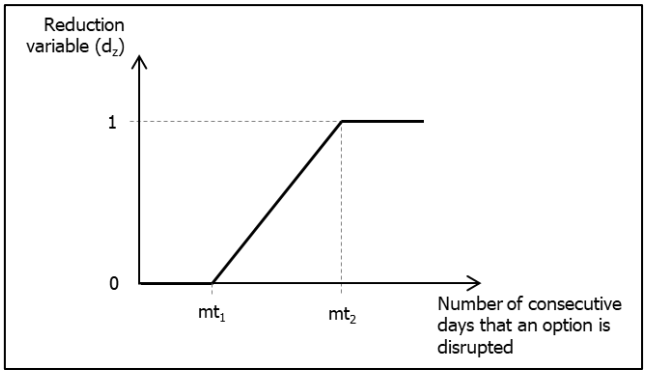

Figure 7.7. Function of the reduction variable d_z

$$d_z = \begin{cases} 0 & if \quad ct < mt_1 \\ \dfrac{ct - mt_1}{mt_2 - mt_1} & if \quad mt_1 < ct < mt_2 \\ 1 & if \quad ct \geq mt_2 \end{cases} \tag{7.14}$$

Being,

ct, the number of consecutive days that an option is disrupted.

mt_1, the maximum number of consecutive days that a driver can face a disrupted route without reducing the probability of being selected. This is a user-defined value.

mt_2, the minimum number of consecutive days that a driver can face a disrupted route without reducing completely to zero the probability of being selected. This is also a user-defined value.

Note that the value of mt_1 and mt_2 can vary between drivers.

It is important to mention that the equations of Table 7.1 can be reduced to simpler equations considered in previous chapters if some conditions are satisfied. If the new feature of reducing the probability of selecting disrupted options is not considered ($F = 0$), equations of Table 7.1 are the same as the equations of Table 6.3 included in previous Chapter 6. Additionally, if travel options are not divided into favourable and unfavourable ($\beta_N, = 1$ and $\beta_z = 0$), Equations (7.7) to (7.9) are the same as the ones considered in the original formulation developed by Wei *et al.* (2014). The last Equation (7.10) (negative stimulus) is slightly different because the proposed model increases the probability of choosing the unselected favourable options by adding the

same quantity to these unselected options whereas the formulation of Wei *et al.* (2014) adds the quantity that is proportional to the previous probability. However, this has been reformulated because if all unselected options have a previous probability of zero, then the model proposed by Wei *et al.* (2014) could not increase the probability of these options. This problem is solved with the proposed model.

7.3. Provision of external information to drivers

The interaction between information and communication technologies (ICT) and human travel behaviour is an area that has received considerable attention in recent years (Emmerink *et al.*, 1996; Dia, Harney and Boyle, 2001; Bekhor, Ben-Akive and Ramming, 2002; Koski, 2002; Parvaneh, Arentze and Timmermans, 2010; de Abreu e Silva, de Oña and Gasparovic, 2017; Wang, He and Leung, 2018; Jamal and Habib, 2020). Advanced Traveller Information Systems (ATIS) and Road Traffic Information (RTI), key components of Intelligent Transportation Systems (ITS), are designed to assist drivers in making more informed travel decisions. It has the potential to reduce congestion, improve network performance and reduce environmental impacts. The additional information is likely to enable drivers to choose more efficiently among available routes and departure times, reducing congestion and travel times.

As mentioned in Chapter 2 and 6, previous RL traffic models do not provide external travel information to drivers. The importance of advanced and on-route travel information is vital in a world that is becoming more and more dependent of technological systems. Results from RL models would be misleading if external information is not provided to drivers.

The model proposed in this thesis goes a step beyond previous RL traffic models and introduces the possibility of adding external travel information to drivers. The ATIS-supplied information considered in this model can take place at two main instances: at the origin of the trip (pre-trip information) or on-route (GPS navigation or Variable Message Signs VMS). The following sections of this chapter describe more in detail how this new information is implemented in the model and the type of information that is provided. The modeller needs to define the information that is assigned to each packet of drivers. The model assumes that if a packet of drivers

receives external travel information, they rely on this information and they will follow it.

7.4. Pre-trip information

Pre-trip information is the travel information that is provided to drivers at origins before undertaking their trips. This information is disseminated through television, radio, computer online services, mobile phones, etc. With this information, drivers can make more efficient travel decisions by changing departure time, route, destination, or even cancel the trip. However, the current version of the model only allows drivers to change route and cancel the trip. This information is especially important when several road sections are closed to traffic and drivers need to find alternative routes to get to their destination. Therefore, pre-trip information can help drivers to reduce the risk of arriving late to the destination by avoiding road closures.

7.4.1. Type of pre-trip information and implementation

The pre-trip information that is provided in this model informs at the start of the trip which links are closed or partially closed. If drivers receive this information, they become aware of which links are closed but they do not look for information advising them of the best route available. Drivers assess possible routes based on their previous experience. The model assumes that if a link is closed, a diversion route is set in place avoiding that closure. If a link is partially closed, there is no diversion route set in place because the link is still open to traffic.

As explained in Section 6.2 of the previous chapter, drivers have in mind a probability associated with the selection of each travel option on each day. If they receive updated information about road closures, these probabilities might be altered temporally. The new updated probabilities are the ones that need to be obtained in order to allow drivers to select a travel option on each day. Figure 7.8 shows how the addition of new pre-trip information is incorporated into the framework of drivers' decision-making process explained in the previous Section 6.2.1 of Chapter 6. The following paragraphs explain the process that has been implemented in this model to calculate the new updated probability based on pre-trip information.

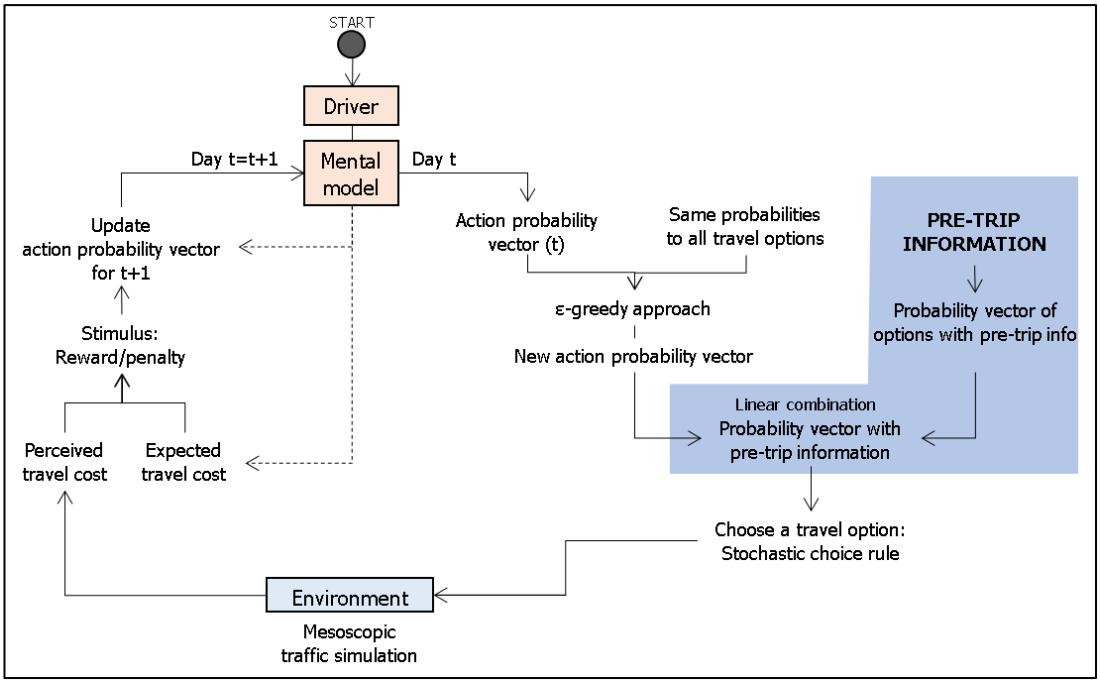

Figure 7.8. Addition of pre-trip information in the drivers' decision-making process framework

The temporal probability of choosing a travel option is expressed in Equation (7.15). It is calculated as a linear combination between the probability obtained from the mental model of each driver and the probability associated with the updated pre-trip information. Note that a constant value (ξ) between 0 and 1 weights the importance of new information versus previous travel information that is obtained from previous experience. The extreme value of $\xi = 0$ indicates that drivers prefer to use the updated information rather than the information that they have learnt from previous travel experiences. If it takes a value of $\xi = 1$ means that drivers prefer not to follow pre-trip information and instead they follow the information they have experienced from previous days. Note that the probability vector that is used to update the probabilities for the next day (see Figure 7.8) is the one that each driver has on their mental model ($p_{z,mental}$) and not the new temporal probability vector ($p_{z,new}$) obtained from the addition of pre-trip information. It is important to emphasise that this new probability is just to choose the travel option for the day in question.

$$p_{z,new} = \xi \cdot p_{z,mental} + (1 - \xi) \cdot p_{z,pretrip} \quad (7.15)$$

Where:

$p_{z,new}$, is the new probability that is obtained as a combination of the $p_{z,mental}$ and the $p_{z,pretrip}$.

$p_{z,mental}$, is the probability that the driver has in his or her mind that comes from the learning-based decisions taken in other days.

$p_{z,pretrip}$, is the probability that is assigned to the options based on the pre-trip information received.

ξ, user-defined value (between 0 and 1) that quantifies how the new pre-trip information is altering the mental probabilities of selecting travel options.

Note that the option probability vector ($p_{z,mental}$) that drivers build through experience in their minds is already explained in previous Chapter 6. However, the procedure to obtain the probability of selecting travel options associated with the new pre-trip information ($p_{z,pretrip}$) is not described yet. The method proposed in this model is based on the idea that the travel option that has the minimum travel cost is more likely to be chosen by drivers. This means that the travel cost of all possible options needs to be calculated and then the model has to assign a probability that is inversely proportional to the travel cost. A more detailed explanation is described in the following steps:

1) For each driver that receives pre-trip information, identify all possible known routes that this driver could choose on that day. Routes that contain roads that are closed should also include the diversion routes.
2) For each possible option, calculate the expected travel cost based on the travel experience of previous days. The procedure is the same as the one explained in Section 6.4 of Chapter 6. If a link has never been used, the travel time of that link is assumed to be the free-flow travel time. If a link is closed, a diversion route will be set in place and the travel time of the whole route will be calculated. However, if a link is partially closed, as there is no diversion route set in place because drivers can still use the link, a penalty has been

applied to the link that is disrupted. The travel time of a disrupted link (not totally closed) is obtained following Equation (7.16). The undisrupted travel time is penalised depending on a user-defined penalty value and the remaining capacity of that link. The more remaining capacity the link has, the less penalty is applied to the link.

$$tt_{withpenalty} = tt_l * (1 + penalty * (1 - CR_l)) \quad (7.16)$$

Where,

$tt_{withpenalty}$, is the travel time of link l after being penalised due to the capacity reduction.

tt_l, is the travel time of link l.

$penalty$, is a user-defined value that penalises the undisrupted travel time of a link. It can take a value between 0 and 1.

CR_l, is the remaining capacity of a disrupted link. It varies between 0 and 1.

3) Re-scale between the range of 0-1 using an inverse cross-multiplication as shown in Equation (7.17). The lowest travel cost value takes the highest value (1) and higher values of travel cost get values lower than 1.

$$V_z = \frac{\min(c_z) \cdot 1}{c_z} \quad \forall z \quad (7.17)$$

Where,

V_z is the new value of the travel cost in the range of 0-1.

c_z is the travel cost of travel option z.

4) Obtain the probability of choosing travel options associated with the new pre-trip information ($p_{z,pretrip}$).

$$p_{z,pretrip} = \frac{V_z}{\sum V_z} \quad (7.18)$$

7.5. External on-board information: GPS navigation

GPS (Global Positioning Systems) are those systems that provide full car navigation with route information, providing turn-by-turn directions to drivers. These navigation

systems are now a common part of driving and the influence of these systems on drivers' behaviour and network performance cannot be avoided. Previous reviewed RL traffic models do not incorporate this type of on-board information. The aim of this section is to go a step further and include external GPS information in the drivers' decision-making process. That is the reason why this model has also included GPS navigation as a way of providing information about the shortest route that drivers can take.

This model allows drivers to use GPS information as a (1) route planning or as (2) an on-route decision. The former is done before departure and provides the shortest travel time route at the beginning of each trip. On the contrary, the latter provides the shortest travel time route at each intersection so that drivers can change route on their way until they get to the destination.

7.5.1. Shortest travel time route

The information that GPS provides in this model is the route that has the shortest travel time from an origin to a destination based on current traffic conditions. When a driver is about to make a decision, current traffic conditions are obtained based on a macroscopic level. The total number of vehicles is known on all links and at all times. Travel time on each link can be calculated based on the BPR function (Bureau of Public Roads, 1964) that is shown in Equation (7.19). The Dijkstra algorithm (Dijkstra, 1959) is used to find the shortest path between a node and a destination. Drivers revise their route whenever they approach an intersection and if the route is different from the previous one, they change routes. An alternative approach would be to sample the travel times on each link in the model and use this information to estimate the shortest path between two places.

$$tt_l = tt_O \cdot \left[1 + a \cdot \left(\frac{q_l}{q_{lmax}}\right)^b\right] \tag{7.19}$$

Where,

tt_O, free-flow travel time.

tt_l, travel time of link l.

q_l, traffic volume on a link l.

q_{lmax}, capacity of the link l.

α, BPR coefficient, often set at 0.15.

β, BPR coefficient, often set to 4.

Note that the shortest travel time route is calculated at all intersections for all drivers that arrive at intersections and use GPS information. This means that on an urban environment where drivers find intersections very often, the computational time of the Dijkstra algorithm can be very high because it has to be run a lot of times. For instance, a driver may approach intersections every minute in an urban area. However, the shortest path may not change between minutes and there is no need to update the shortest route for all drivers at every single minute. For that reason, and in order to speed up the computational time of the global model, the shortest path algorithm is only called every fixed amount of time. This means that if the modeller decides to set the updating time to 3 minutes (for example) the shortest route will not be updated within 3 minutes even if they approach an intersection. The modeller is the one that decides the amount of time between updates. If the updating time is set to 0, it means that there is no limit of updates and the shortest route algorithm will be run at every intersection.

As drivers receive real-time information about the travel time of the shortest route to get to their destination, the model allows drivers to cancel their trip if the expected arrival time is much later than the starting time of the activity. The equation that is used is the same Equation (7.3) described in Section 7.2.3, but with the difference that the expected arrival time is calculated using the information that is provided by the GPS.

7.5.2. Updating the expected travel cost formula

If drivers receive the shortest route from the GPS information, they know the travel time that is expected based on current traffic conditions. Therefore, the expected travel cost should also incorporate the information that the GPS provides. The previous formulation (Equation (6.12)) presented in Section 6.4 of Chapter 6 does not include any external information that driver may receive via GPS. The formulation presented in the following Equation (7.20) is exactly the same formulation as the Equation (6.12) but adding the additional terms that include the expected travel cost of the GPS route (shown in bold and green colour).

$$A_{ht} = \begin{cases} 0 & if\ t = 1 \\ \dfrac{\sum_{j=1}^{t-1}\left[\varphi_j \cdot \left(\sum_{z=1}^{Z} B_{hzj} \cdot C_{hzj}\right)\right] + \boldsymbol{\varphi_t \cdot g_h \cdot E[C_{hzt}]}}{\sum_{j=1}^{t-1}\left[\varphi_j \cdot \sum_{z=1}^{Z} B_{hzj}\right] + \boldsymbol{\varphi_t \cdot g_h}} & if \sum_{j=1}^{t-1}\sum_{z=1}^{Z} s_{hzj} = \\ \dfrac{\sum_{j=1}^{t-1}\left[\varphi_j \cdot \left(\sum_{z=1}^{Z} B_{hzj} \cdot s_{hzj} \cdot C_{hzj}\right)\right] + \boldsymbol{\varphi_t \cdot g_h \cdot E[C_{hzt}]}}{\sum_{j=1}^{t-1}\left[\varphi_j \cdot \sum_{z=1}^{Z}\left(B_{hzj} \cdot s_{hzj}\right)\right] + \boldsymbol{\varphi_t \cdot g_h}} & otherwise \end{cases} \quad (7.20)$$

Where,

φ_t, is the memory level of travellers on day t ($0 < \varphi_t \leq 1$).

g_h, is a binary variable that takes a value of 1 if packet of drivers h receives GPS information or 0 if packet h does not receive that information.

$E[C_{hzt}]$, is the estimated travel cost of option z that packet of drivers h receives from the GPS systems on day t. It is calculated using the same expression of the travel cost function of Section 6.3 of Chapter 6 but considering the estimated travel time provided by GPS systems.

The rest of the variables are the same as the ones described in Section 6.4 of Chapter 6.

7.6. External on-board information: Variable Message Signs (VMS)

Variable Message Signs (VMS) are one of the components of the Advanced Traveller Information System (ATIS) that are used to disseminate non-personalised real-time traffic information to drivers who are already travelling on the network. This model also incorporates this type of information and the locations of the VMS are pre-defined by the modeller. There can only be one VMS per link and not all links need to have VMS.

Two types of information can be disseminated via VMS: (1) information used to manage incidents on the network and (2) general driver information. As prescribed in Schedule 15 of the "The Traffic Signs Regulations and General Directions order" in United Kingdom (HM Government, 2002), the information that can be shown on a VMS should contain the following information:

- Problem and location of a disruptive event.
- Effect (e.g. Long delays, Delay information, Travel time information).
- Guidance (e.g. use M8).

The VMS considered in this model only displays generic information about closed roads, busy roads when the density of vehicles on a link is higher than a pre-defined value ($k_l > k_{Q,VMS}$) or those roads whose capacity is lower than a certain pre-defined value ($Q_{limit\,VMS}$). These are the links that drivers will try to avoid. This is especially important because, in the scenario of a disruption, drivers that have no pre-trip or GPS information can follow the information that is provided by the VMS and avoid the congestion caused by those disrupted links.

The information displayed on a VMS can also make drivers decide about changing routes. Previous Section 7.2 proposed two conditions to trigger the procedure to make new on-board decisions. However, as VMS information can also trigger new travel decisions, this additional condition should also be taken into account. The procedure that selects the new route is the same as the one explained in Section 7.2.2.

7.6.1. VMS activation: range of coverage

Each VMS displays the information of roads that are located within a range of coverage. Incidents that happen out of this range are not displayed on the signs. This model has proposed a method that limits the range of coverage of each VMS. These limits are defined by two conditions and the more restrictive condition sets the limit of the coverage. The first condition is defined by the number of consecutive road segments. For example, if this is set to 2 consecutive links, all that happens within these links is displayed on the VMS. However, as the length of these consecutive links can be too short at certain locations, a second condition is added and is defined as the maximum length of these consecutive links. Following the previous example, if the length of these 2 consecutive links is below a pre-defined maximum length (e.g. 10km), all that happens on those consecutive links whose total length is below that defined value is displayed on the VMS. Therefore, the range of coverage of each VMS is limited to a pre-defined number of consecutive links unless the sum of their length is less than a defined value, in which case all consecutive links included within that length will be displayed on the sign. In order to clarify this idea, a simple example is described below. It is assumed that the VMS shown in Figure 7.9 can only display what happens on the two consecutive links as mentioned in the first condition. The

second condition is defined by a pre-defined length, which in this case it is assumed to be 10 km for example. The sum of the length of the two consecutive links following the VMS is less than the pre-defined length of the second condition. This means that the VMS can show the information of all consecutive links located in a radius of 10 km. If the length of the two consecutive links were higher than 10km, then the VMS would display only the information of these two consecutive links.

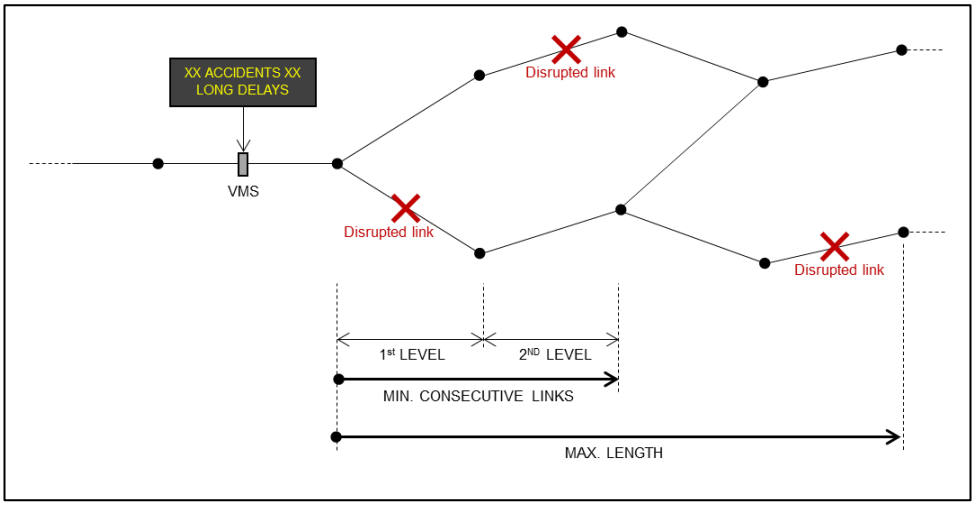

Figure 7.9. Example of the range of coverage of a VMS.

7.7. Illustrative example

In this section, the post-disruption model proposed in this chapter is applied to the same transport network used in Chapter 6, the Sioux Falls Network (South Dakota, US). The aim of this example is to illustrate how the addition of external travel information after disruptive events can impact the performance of the whole network. The provision of additional information can help drivers make more informed travel decisions and choose those routes without disruptions. On-board drivers' decisions are also allowed. In this example, no optimisation is involved and the effectiveness of a single repair strategy is assessed by measuring the performance of the whole system after repairs. Results show the evolution of total travel costs over time under the provision of different levels of external traffic information to drivers.

7.7.1. Road network, traffic demand data and disruptive scenario

The Sioux Falls network used in this example is exactly the same network used in Chapter 4 and 6. It consists of 24 nodes and 76 links as shown in Figure 7.10 and whose characteristics are presented in Table A.1 and Table A.2 of the Appendix 1.

Traffic demand, which is extracted from the work done by Martinez-Pastor (2017), considers a total number of 4840 trips per hour – see the OD matrix in Table A.3 in Appendix 1. In this example, it is assume a maximum set of initial routes for each OD pair of 2 and it is expected that drivers choose between 3 possible departure times (8am, 8:15am or 8:30am). For this reason, the peak period modelled in this example is adapted to these 3 departure times and therefore the period of demand that is analysed is between 8am and 8:45am. This means that the total number of trips is proportionally 3636 trips for that time period. A warm-up and cool-down 30-min period are also simulated with a proportional number of trips for that amount of time. Vehicles are grouped into packets of 10 vehicles.

The disruptive scenario considered in this example is the one obtained on the example included in Section 4.4.2 of Chapter 4. Seven bridges (B3, B4, B5, B6, B7, B8 and B10) have been identified as damaged. The repair strategy proposed for this example is the same as the one considered in Table 4.2 of Chapter 4. The simulation time is 55 days. The disruption occurs at day 26. The pre-disrupted state is from day 1 to day 25. During this period, drivers are learning based on their day-to-day travel experience. It is assumed that after 25 days, drivers achieve an stable state which means that the overall travel cost is not further reduced.

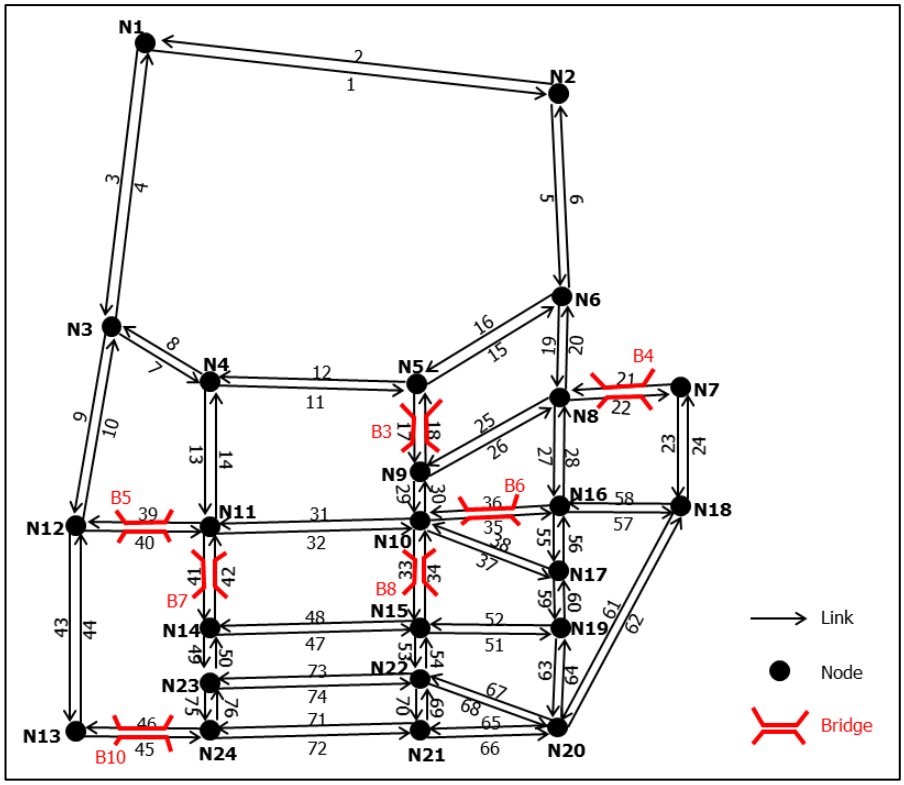

Figure 7.10. Location of the damaged bridges on the Sioux Falls network.

Regarding the external information that drivers receive, the existing literature does not show the type of traffic information that drivers use on the Sioux Falls network while travelling to their destination. Given the lack of data, it was assumed 6 cases representing different situations where drivers use different types of information. Case 1 is the first hypothetical situation when drivers do not receive any external travel information. Case 2 introduces pre-trip information of disrupted roads as shown in Section 7.4. Case 3 and Case 4 incorporate the GPS information providing route planning and on-route guidance respectively as shown in Section 7.5. Case 5 shows the impact of VMS information. Finally, Case 6 combines all types of information. Table 7.2 summarises all these described cases. The value of the rest of the parameters used in this example is included in Table 7.3. These values have been selected at the author's judgement.

Table 7.2. Cases that distribute external information among drivers

	Distribution of drivers and information
CASE 1	100% of drivers with no external information
CASE 2	50% of drivers with no external information 50% of drivers with pre-trip information
CASE 3	50% of drivers with no external information 50% of drivers with GPS planning (before departure)
CASE 4	50% of drivers with no external information 50% of drivers with GPS on-route
CASE 5	100% of drivers with no external information All drivers can receive information via VMS
CASE 6	40% of drivers with no external information 20% of drivers with pre-trip information 20% of drivers with GPS planning (before departure) 20% of drivers with GPS on-route

Table 7.3. Values of the variables considered in this example

Variable	**Value**	**Variable**	**Value**
# routes per OD	2	# departure times	3
Travel cost function		**General**	
$\boldsymbol{\beta_1 = \beta_2 = \beta_3 = \beta_4}$	1	Vehicles/packet	10
Memory function (Section 6.4)		Simulation time	55 days
Linear function		ε-greedy approach	None
$\boldsymbol{B_{max}}$	3	Pre-disruptive time	25 days
$\boldsymbol{b_1}$	10min	Post-disruptive time	30 days
$\boldsymbol{b_2}$	30min	Learning rate	0.4
$\boldsymbol{\theta}$	Uniform distribution [0,90]	# of simulations	10
Option of not travelling (Section 6.8)			
$\boldsymbol{y_{RC}}$	0.8	acc_a	Probability distribution of Figure 6.21.
$\boldsymbol{t_{RC}}$	10 min	$freq_a$	Uniform distribution [-1,1]
$\boldsymbol{U_s}$	0.8	$comf$	Uniform distribution [-1,1]
$\boldsymbol{U_f}$	0 days	g	3 days
$\boldsymbol{t_{min}(freq_a)}$	10 min	$AA = BB = CC = DD$	1
$\boldsymbol{t_{max}(freq_a)}$	1h	$\boldsymbol{HH = JJ = LL}$	0.333
Preferred arrival time interval (PATI) (Section 6.2.2)			
Activity starting time	9am	Activity	WORK
PATI 1 (time before activity starts)	Between 20 and 10 min	Distribution of drivers that prefer PATI 1	50%
PATI 2 (time before activity starts)	Between 10 and 5 min	Distribution of drivers that prefer PATI 2	50%
Repair module (Chapter 4)			
Base damage (D)	10 res-day	Repair teams	13 units
Angle of productivity-repairs graph	45 degrees	Saturation level repair teams	5 units

Continuous in the next page

From the previous page

On-board decisions (Section 7.2)			
Variable $\boldsymbol{\lambda}$	0.9	Ω_h, patience level of vehicles	Uniform probability distribution [0,1]
$\boldsymbol{maxJ_h}$	3 links	EL	30 min
$\boldsymbol{mt_1}$	1 day	mt_2	3 days
External information (Section 7.3 to 7.6)			
$\boldsymbol{\xi}$ (Equation (7.15))	0.2	$penalty$ (Equation (7.16))	0.5
GPS update route	0 min	-	-
VMS: number of consecutive roads	2	VMS: length of consecutive links	10 km
$\boldsymbol{Q_{limit\,VMS}}$	20%	$k_{Q,VMS}$	90%
Links with VMS:		1, 2, 5, 6, 9, 10, 11, 12, 31, 32, 47, 48, 61, 62	

7.7.2. Results and discussion

7.7.2.1. Aggregated results: total travel time with external information

This section describes the results obtained after running the model through a series of cases. Each case shows a different provision of travel information to users. Results will show the impact of the addition of external travel information on the general network performance. Figure 7.11 (A and B) shows the evolution of total travel time and total number of completed trips before and after the disruptive event. In this example, a completed trip means that a driver arrives to the destination. Each line represents the results of a particular distribution of travel information through users. For each case (see Table 7.2 of cases), 10 simulations have been run in order to consider the stochastic nature of the model. The average value of these 10 simulations of each particular case is represented by each line of the graph. The model is performed on a computer with 8 GB memory and a quad-core 3.3 GHz Intel i5-3550 processor. Parallel computing have been used to run these 10 simulations and it took on average 40 min to run each pack of 10 simulations.

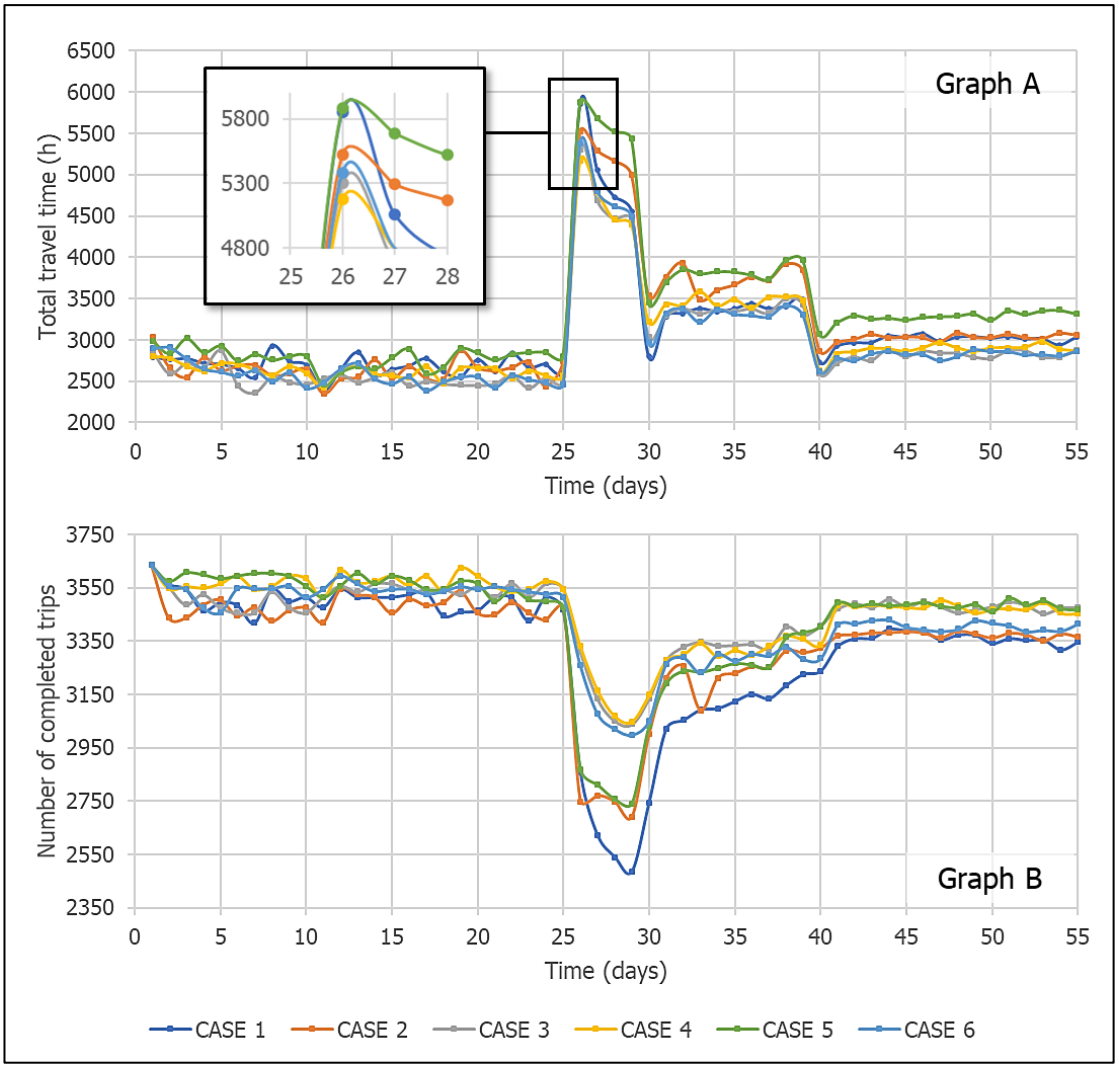

Figure 7.11. Evolution of total travel time and number of trips over time before and after the disruptive event. Each line shows the mean of 10 simulations. Each case represents a different distribution of travel information (see Table 7.2 of cases). Learning rate=0.4.

From day 1 to day 25, there is a period of no disruption. This is the pre-disruption stage described more in detail in Chapter 6. During this time, drivers are trying different travel options and storing the information (travel time, arrival time, etc.) after each journey. In this example, after 10 days, drivers reach a stable state in which they have chosen their preferred travel option and travel time is not further reduced as observed in Graph A. This pre-disruptive stage is only used to allow drivers to experience and learn from their mistakes and find the 'best' option for them. As it is observed, during this period of no disruption, the information that is provided to

drivers does not make a significant difference in terms of travel time and completed trips on the considered cases.

The disruption occurs on day 26. There is an increase on the total travel time and a reduction on the number of completed trips in all considered cases. Case 1, Case 2 and Case 5 produce the highest increase in travel time and the highest reduction in the number of completed trips the day after the disruption. Case 3 and Case 4 also achieve a high value of travel time but less than the previous cases. Case 6, which is a mixture of external travel information and drivers with only their previous travel experience, has the lowest increase in travel time after the disruption and one of the lowest reduction in terms of completed trips. From the 26th day to the 42nd day, repairs are still taking place and this is observed in high values of travel time and low values of completed trips. After day 42, a stable state is observed in which drivers get back to normal. However, as shown in Figure 7.11-A, the post-disruption total travel time is not the same as the pre-disruption one. The same happens with the number of completed trips.

At this point, it is interesting to analyse and understand the reasons and mechanisms by which these results have been obtained and the limitations of the model application. In order to do so, the reader needs to understand how drivers evolve and adapt to the situation during and after disruption. When drivers receive information about road closures, they retain that information in their memories when considering how to travel on the next days which, in that case, they will use this information to make more informed decisions. The post-disruption stage shows that Case 3 and Case 4 achieves lower values of travel time (and higher values of completed trips) faster than other cases in which drivers who do not receive external information and need more time to adapt to these network changes.

In this particular example, there is not a significant difference in travel time between knowing which links are closed (Case2) and not using any external information (Case1). The reason is due to the module that obtains the initial subset of routes that each driver knows. In this example, only two routes are known from the beginning. This module that obtains the initial subset of routes is not very sophisticated as described in the model limitations (Section 6.11 of Chapter 6) and the calculated routes may share a number of links between them. If a driver knows

the links that are closed and these links are located on both routes, then this driver cannot choose an alternative undisrupted route. In this case and due to the way that the model is implemented, this driver has to follow the diversion route which is exactly the same route as the one that the driver with no external information would follow. This problem disappear if the initial subset of routes does not share any links.

As observed in Figure 7.11-A, the pre-disruption phase (from day 1 to day 25) shows some fluctuations in the graph while the final phase of the post disruption presents a smoother transition. This is because the pre-disruption phase has not been obtained from 10 simulations and instead only 1 simulation has been calculated. The reason is based on the fact that the 10 simulations of the post-disruption phase must have the same initial pre-disruption data in order to compare the results. That is why a single simulation of the pre disruption is calculated and it is used as a starting point. The 10 simulations of the post disruption phase are calculated based on that initial data. In the graph, the average of these post-disruption 10 simulations is shown and for that reason, a smoother transition is observed between days.

It is also observed that the number of completed trips decreases one or two days after the disruptive event on day 26. The reason for this is because drivers who experience the first day of the disruption do not arrive at the scheduled time to undertake the activity and this makes drivers increase the probability of not travelling by car the next day.

During the disruption phase as capacity is limited, cancelled trips are expected. However, as observed in Graph B of Figure 7.11, some drivers have chosen the option of 'not travelling by car' during the pre-disruption phase and in the post-disruption phase. The reason for this are explained in the formulation. Equation (6.32) (see Section 6.8 of Chapter 6) calculates the new probability of choosing the option of 'not travelling by car' using parameters that have not been calibrated/validated. This means that, if a driver arrives late to the activity, the new probability of choosing the option of not travelling by car on the following day increases, and the size of this increase depends on the values of selected parameters which have not been calibrated with real-life data. In order to demonstrate the sensitivity of the model to selected values of AA, BB, CC, DD of Equation (6.32), Figure 7.12 shows the impact of these variables on the number of completed trips. These user-defined variables,

which are described in detail in Section 6.8 of Chapter 6, are used as weighting factors of the terms included in the calculation of the new probability of choosing the option of 'not travelling by car'. The extreme values indicate that if $AA = BB = CC = DD = 0$, the probability of choosing this non-travel option is zero for all drivers and that is the reason why all trips are completed during the pre-disruption stage and after the disruption phase., but not during the disruption phase. On the other hand, if $AA = BB = CC = DD = 1$, all terms that are calculated on the formula and the probability of choosing the option of 'not travelling by car' may not be zero. That is why some drivers choose the option of 'not travelling by car'. Further work should include the calibration and validation of these parameters with real-life data.

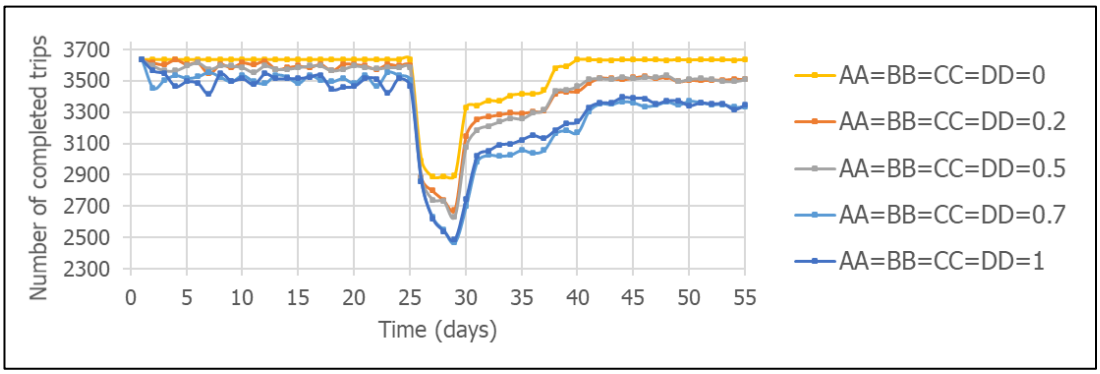

Figure 7.12. Impact of parameters (AA, BB, CC, DD) of Equation (6.32) on the number of completed trips. Only for case 1 (no external information). Parameters of Table 7.3.

From a global point of view, it is interesting to know the difference between the types of external information provided to users based on a resilience measure. This is be the information that will be used in the global optimisation problem considered in Chapter 3. In this section, the resilience measure is calculated as the area under the 'total travel time' curve (Figure 7.11-A) and under the 'completed trips' curve (of Figure 7.11-B) from the day of the disruption. For the specific Graph A, the higher the value of the area, the more travel time drivers have experienced to get to their destination. This means that lower values of the area provides a better adaptation of drivers to the disrupted network and posterior repairs in terms of travel time. For the graph B, the higher the area under the curve is, the more trips have been completed. In order to study the effectiveness of providing external travel information to drivers, both areas have been taken into account. External information

is important to reduce travel time but it can also be used to alert drivers of potential road closures so that they can complete their trips effectively.

Figure 7.13 shows the confrontation of the two objectives and the values taken by the different studied cases. As observed, drivers who have no external information (Case1) get a low value of the area in terms of travel time. However, the lack of information of those roads that are closed is translated in a reduction of the number of completed trips. This situation improves if the information about road closures is delivered to drivers (Case 2, pre-trip information in this model). In this case, drivers are aware of all road closures so that they can choose the undisrupted route. The number of completed trips increases compared to the number of completed trips when no information is available, although travel time increases slightly. When drivers also receive information about the shortest routes via GPS navigation (Cases 3 and 4), there is a reduction in travel time and more trips are completed compared to the previous cases. However, if the information about the location of the road closures is only provided via VMS (Case 5), the total travel time is not reduced compared to the previous cases but the number of completed trips is higher than case 1 and case 2. The reason for not observing a reduction also in terms of travel time is due to two possible options: 1) The number of damaged roads compared to the size of the network is high which means that drivers do not have a lot of alternative undisrupted routes to choose. 2) Probably also related to the previous reason, when VMS informs drivers of which roads are disrupted, drivers tend to choose alternative routes that avoid the critical road segments. This can be a counter-productive situation as disrupted routes may not be chosen by anyone and may be free of congestion, whereas the alternative routes, which were uncongested, become congested. As a result, total travel time increases. The last Case 6 corresponds to the case that includes all types of information together. It is observed an improvement in terms of travel time and completed trips compared to the case with no provision of external information.

The results shown in this section evidence the importance of including the provision external information to road users on traffic models. This information can help drivers make better travel decisions, especially when multiple road closures are produced. Although the traffic information provided by this model to road users is

simplified (adapted to a simple model), there is still evidence of a global improvement in the network performance. Therefore, the addition of the module that provides external information to drivers can be a significant improvement compared to the previous RL traffic models that did not include the dissemination of any type of external information.

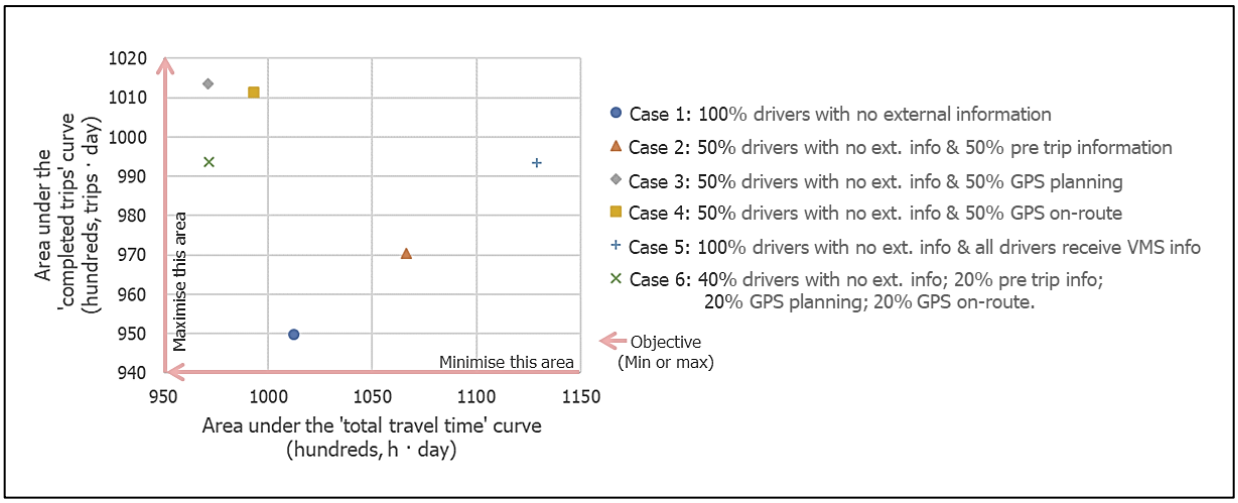

Figure 7.13. Bi-objective graph that compares all 6 cases of information provision considered in the model in terms of the area under the 'total travel time' curve and 'completed trips' curve. Data used from Figure 7.11, from day 26th to 55th.

7.8. Comparison to previous methodologies and contribution

This section compares the methodology proposed in this chapter to the ones presented in the literature. Table 7.4 explains how the new improvements fill the gaps of previous models. The contributions to the knowledge are therefore also included in this table.

Table 7.4. Comparison of the main drawbacks of previous methodologies and the one proposed in this Chapter 7.

Drawbacks of previous models	Solution of the proposed model
No on-board decisions are allowed. Previous RL traffic models (Ozbay, Datta and Kachroo, 2001; Wei, Ma and Jia, 2014; de Oliveira Ramos and Grunitzki, 2015) were not applied to disrupted scenarios, which meant that drivers did not need to make on-route decisions.	**Section 7.2.1.** This model incorporates the novelty of adding on-board travel decisions on RL traffic models. This is important especially when disruptions occur. If a link is busy or closed, the model allows drivers to decide and change routes on their way to the destination. **Section 7.2.2.** The model also includes a new algorithm that is used to find the alternative routes that drivers would choose after facing a disruption.
Drivers were forced to finish their trip. All reviewed RL traffic models did not allow drivers to abandon their trip in the middle of a journey. If drivers were on their way, they were forced to use the chosen route and arrive to the destination.	**Section 7.2.3.** A new feature allows drivers to decide to abandon their trip and return home if they face a severe disruption. This feature can release traffic from some congested areas as some drivers abandon their trip and avoid reaching more disrupted areas.
Option probability updating functions. Previous functions only updated the drivers' probability of choosing options for the next day. However, these updating schemes might change if disruptions occurred. Previous functions did not penalise any travel option that contained a link that was disrupted.	**Section 7.2.5.** This model modifies the updating functions described in Chapter 6 by introducing additional and novel factors that account for the influence of any on-board travel decision taken by each driver.
No external travel information was provided. Previous reviewed RL traffic models did not provide external travel information to drivers.	**Section 7.3 to 7.6.** The model introduces the possibility of adding external travel information to drivers. To the best of the author's knowledge, this is the first RL traffic model that incorporates this new feature.

7.9. Limitations and further work

This section presents Table 7.5 which includes the limitations of the proposed model and some key areas of further research.

Table 7.5. Limitations and areas of improvement of post-disruption model proposed in this Chapter 7.

Limitation	Areas of improvement
Lack of data to calibrate/validate results. It has not been found a previous study that indicates a percentage of drivers that uses on a daily basis pre-trip and/or on-board information on particular areas. Without this information, the alternative option is to estimate an approximate distribution of information between drivers. Results from the current model should be analysed, taking into consideration this assumption.	Future work should study how many drivers use pre-trip information or on-board information on their day-to-day journeys on specific areas.
Drivers' usage of information. This proposed model assigns a certain external information to drivers and it assumes that they follow the information every day. However, if drivers achieve a repetitive behaviour, they may ignore (or do not plug in) the information provided through radio or GPS. If they face a disruption, they will turn on the devices to follow instructions. This means that drivers do not necessarily follow the information every day.	A dynamic usage of the information is proposed as a future improvement of the model. It implies the introduction of a new term 'habit' and the conditions that are required to become a habit. If conditions are met, drivers may ignore information such as the shortest route and follow the route that they have chosen on their every day basis.

Continuous in the next page

From the previous page

Limitation	Areas of improvement
Diversion routes. The method proposed in Section 7.4, which obtains the probability of choosing a travel option after receiving pre-trip information, assumes that drivers know the diversion route set in place for each road closure. In reality, this is not known until drivers reach the location of the closure (unless they search more information on the media). Also, in this model, diversion routes are automatically obtained as the shortest path between the initial node and the final node of the closed link. In reality the modeller should decide the path of the diversion route.	Further work needs to be done in order to avoid the assumption that all drivers know the diversion route set in place even before reaching the closure. It is also proposed a modification of part of the code so that it allows the modeller to set manually a diversion route.
Information provided by the VMS. The current model only provides generic information about the roads that are closed. However, in reality, VMS are also designed to provide alternative undisrupted routes to drivers.	An improvement of the information that is provided by the VMS is proposed for future versions of the model. It should also include alternative route suggestions so that drivers can decide whether they prefer to choose the suggested route or follow the original path. This can also be used by traffic controllers to improve the network performance by suggesting alternative diversion routes.
Information provided by the GPS navigation. The model only provides the shortest route between the origin and destination nodes.	Future versions of the model should also incorporate other types of routes, such as longer routes that avoid congested areas, and analyse the impact of them on the network performance. Smartphone apps could also boost the usage of these routes by offering vouchers or points to those drivers who are willing to use these alternative paths.

Continuous in the next page

From the previous page

Limitation	Areas of improvement
Unknown routes. The current model does not allow drivers to explore the network in order to find new unknown routes. In this model, drivers can only follow known routes, diversion routes or new routes that are provided by new external information.	A method to improve the current route choice algorithm (Section 7.2.2) by allowing also drivers to explore the network and find new routes. In this case they need to decide if they want to take the risk and explore the network or they prefer to use their known routes. An algorithm that simulates how drivers explore the network should also be implemented.
Acquire knowledge from past disruptive events. During the pre-disruption phase, drivers are acquiring knowledge about the network in a scenario without disruptions. However, drivers should also learn from disruptive events and find possible alternative routes before facing a real disruptive event in the simulation. If they do not practice and learn from other hypothetical disruptive events, they may not be fully prepared and their reaction may be inefficient.	Future applications of the model should include disruptive events during the learning phase, before the real disruptive event happens. This allow drivers to remember these previous disruptive events and the routes they took to overcome these past situations.

7.10. Conclusions

The content of this chapter answers the following research questions: RQ11 "How can the on-board drivers' decision-making process be modelled and implemented on the traffic simulator?". RQ12 "How can the consequences of an on-board decision after a disruptive event impact future travel decisions and how can it be implemented on a RL traffic model?" Or, in other words, "how can the functions that update the option probabilities of the RL traffic model be reformulated in order to incorporate the consequences of on-board travel decisions?". RQ13 "To what extent does providing information (pre-trip information, GPS navigation, Variable Message Signs, etc.) to drivers improve the recovery of transport networks?".

This chapter presents some improvements to the previous version of the RL traffic model (included in Chapter 6). This updated model goes a step beyond previous RL models and introduces the possibility of making on-board travel decisions and also adds the provision of external travel information to drivers. A framework that simulates the on-board decisions that drivers make when they face a disrupted road segment is developed. A new route choice algorithm is also implemented in order to find alternative undisrupted routes when drivers decide to re-route. Probability functions are also reformulated in order to consider the impact of on-board travel decisions. External travel information, pre-trip (radio) and on-route (GPS and VMS) are also incorporated for the first time into a RL traffic model. A new method that updates the option probability vector of each driver due to the provision of pre-trip information is also implemented. It is also included a procedure that calculates the probability of choosing travel options associated with the pre-trip information.

The updated model is applied to the Sioux Falls transport network (South Dakota, US), illustrating the concepts introduced in this chapter. Six cases that represent different distributions of external travel information that are provided to drivers are considered. In order to be able to compare the different cases, the results of the model are analysed based on two performance indicators: total travel time and number of completed trips. Results evidence the importance of including the provision of external information to road users. The information can help drivers make better travel decisions, especially when multiple road closures exist. A global improvement on the network performance is observed when information is provided. There is a noticeable benefit of including external information compared to previous RL traffic models that did not include this information. Among the benefits, a reduction in total travel time and an increase in the total number of completed trips after disruptive events. Limitations and potential improvements, which are included at the end of the chapter, highlight the importance of continue researching and improving current RL traffic models with the aim of bringing current results a step closer to reality.

CHAPTER 8

Application of the road recovery model to a disrupted network in the north of Scotland

8.1. Introduction

To demonstrate the applicability of the methodologies presented in this thesis, the proposed road recovery model was applied to a real network. In particular, a portion of the Scottish road network was considered. The selected region is located in the North of the county and it has been chosen as a case study due to the peculiarities of the network and the area: its susceptibility to landslide activity (Postance *et al.*, 2017) and its sparse network makes this region ideal to be considered as the application of the recovery model. The impact of hazardous events (especially landslides in this area) on the road network may produce the closure of some routes, which may isolate some remote areas of Scotland and communities may have limited alternative transport routes available. Congestion or closures may lead to increases in business costs, as drivers have to find other routes (if available) and spend more time travelling. According to a research commissioned by Highlands and Islands Enterprise (HIE) about the transport connectivity and economy of the Scottish regions, road closures produce longer journey times, additional delays, costs for businesses, impact on the tourist market as fewer people are willing to travel with disruptions, among other consequences (Ekosgen, 2016). Climate change models for Scotland predict an increase in the intensity of heavy rainfall events in summer and winter. Also overall summers are projected to become drier and winters wetter (UK Met Office, 2018). This means that the risk of landslides and flooding is likely to increase in the future. The model presented in this thesis can help transport

authorities and operators to find a list of repair strategies that leads to a (near-) optimal recovery of disrupted road networks.

Previous recovery models have been applied to real networks as is shown in the list of networks presented in Table A.4 of Appendix 4. However, to the best of the author's knowledge, the use of a reinforcement learning approach to simulate drivers' behaviour on a recovery model has never been applied to real networks. The application of the model that is described in this chapter presents a real challenge from a computational and technical point of view as a large number of road segments and individual drivers' travel decisions are simulated.

The rest of the chapter is organised as follows. Section 8.2 presents the formulation of the problem and describes a summary of the methodology used to find the optimal repair strategies. Section 8.3 and 8.4 explain a detailed description of the road network and travel demand. Section 8.5 generates the landslide damage scenario. Section 8.6 indicates the level of external information that is provided to each driver. Section 8.7 summarises the variables involved in the model and Section 8.8 justifies the number of simulations that the model is run. Finally, section 8.9 presents the results of the model and Section 8.10 and 8.11 describes some limitations, future work and conclusions.

8.2. Problem formulation and methodology

The aim of this chapter is to apply the proposed model to a damaged Scottish road network and find the optimal (or near-optimal) repair strategies that maximise the performance of the system. Two objective functions were applied in this model (see Section 3.4 of Chapter 3): total travel cost and network connectivity. Total travel cost was measured as the sum of the time that each driver spent to get to their destination including the penalties for early/late arrivals as described in Section 6.3. This metric includes the total travel costs of all vehicles that departed during the peak period 8:00-9:00am, excluding those vehicles that decided to return home in the middle of a trip. These excluded vehicles were counted under the connectivity metric. The network connectivity metric that was used in this case study only considered the demand side of the formulation proposed in Equation (3.17). The reason for not

including the supply side of the formula was due to the high computational time that was required to check if each node pair of the network was connected. Therefore, network connectivity metric quantified the fraction of demand that was satisfied, which means those vehicles that successfully arrived at their destination.

The repair strategy (decision vector) that the optimisation model needs to find is the same as the one included in Equation (3.2) of Section 3.3.2 of Chapter 3. As a reminder, the repair strategy was defined as a combination of two main decisions: the identification of a priority order of repairs and the allocation of repair resources to damaged locations. The multi-objective optimisation algorithm that was used in this model was the Non-dominated Sorting Genetic Algorithm (NSGA-II) (Deb *et al.*, 2000), which was already presented in Section 3.5 of Chapter 3.

The proposed methodology is included in Figure 8.1. It divides the model into 5 parts: preliminary data, pre-disruption phase, damage scenario simulation, post-disruption phase and optimisation model. Each part was run in a sequential order, meaning that one section could not be run before another section because it needed the outputs of the previous one to start the simulation.

The first part dealt with the input data of the model. On the supply side, physical characteristics of the model included the location of nodes and links, link capacity and free-flow speed, type of road segment and length. On the demand side, travel demand data obtained from the National Trip End Model (NTEM) was used. Further details are below.

All this information was sent to the next part which was the calculation of the pre-disruption database. In this section, there was no disruption yet and drivers were trying travel options in order to find and select their option with minimum travel cost. In this sense, drivers were learning based on their travel experience. In this model, this process lasted from Day 1 to Day 27 of the simulation. Due to the stochastic nature of the RL traffic model, several simulations of the pre-disruption stage were obtained and the closest to the average behaviour of these was selected. This was considered as the common drivers' behaviour during the pre-disruption stage of all future repair strategies. Therefore, all repair strategies shared the same drivers' pre-

disruption behaviour, so that it did not interference on the effectiveness of each repair strategy.

After that, damage was simulated on the Scottish road network. Based on the methodology proposed in Chapter 4, several road segments were identified as damaged on Day 28. Minor, moderate, severe and collapse states were also assigned to these damaged road segments based on pre-defined probability distributions. Damage was defined in this model as a reduction of road capacity. Therefore, the information that was provided to the next part of the sub-model was a capacity-reduced damaged network.

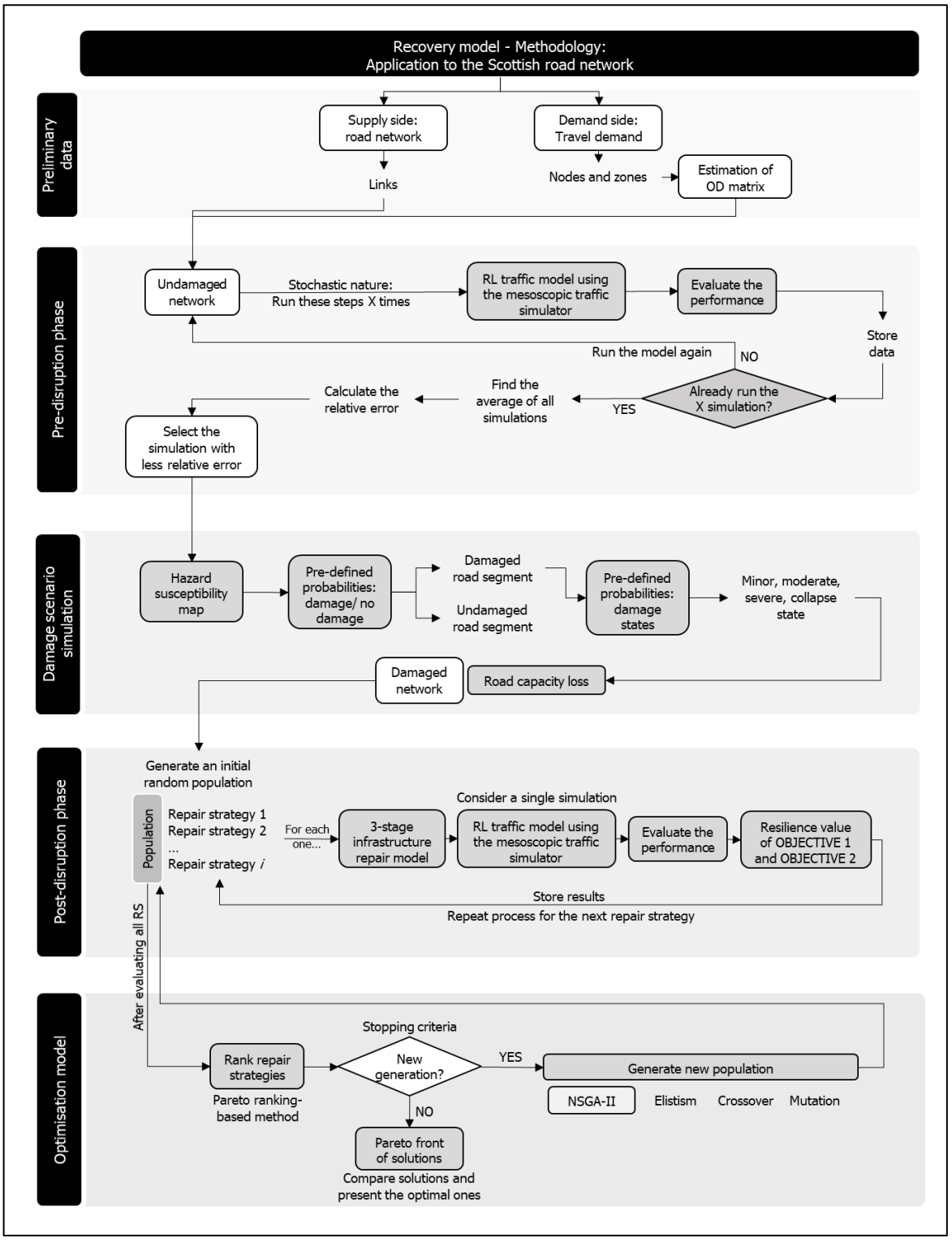

Figure 8.1. Methodology of the proposed recovery model applied to the Scottish case.

The next part entailed the post-disruption phase in which the effectiveness of repair strategies were obtained after running the model for 20 simulated days. Initially, a population of 20 repair strategies was generated. For each strategy, a resource allocation plan and a capacity recovery schedule was generated from the infrastructure repair model (see Section 4.3 of Chapter 4). The impact of these road changes on drivers' behaviour was simulated using the improved RL traffic model (Chapter 6 and 7) and the movement of vehicles through the network was simulated using the proposed mesoscopic traffic simulator (Chapter 5). Then, the performance of the network after 20 days was analysed and resilience values were obtained for both objective functions. The process was repeated for each repair strategy considered in the population of repair strategies.

After evaluating all repair strategies, the next part included the optimisation model. All repair strategies were ranked from best option to worst option as described in Section 3.5 of Chapter 3. A new generation of repair strategies (new population) was obtained using the mechanisms (elitism, crossover, mutation) provided by the NSGA-II. The process of evaluation of the post-disruption phase of the new generation was repeated. This loop terminated when a stopping criteria was reached so that no further generation of repair strategies was carried out and therefore, the (near-) optimal Pareto front of solutions was provided. In this case, the stopping criteria was reached if: (1) a certain number of generations were run (in this case the limit is 60 which was set due to computational reasons), or (2) the difference between the Pareto front of solutions of one generation and the following was not improved. The following sections explain more in detail some of these steps that have been briefly described here.

8.3. Supply side: network description

The Scottish road network was modelled as a graph where intersections were represented by 396 nodes and roads by 978 links. The network topology and attributes were obtained from Ordnance Survey (OS) data (Ordnance Survey, 2019). The GIS file from OS data contained information about the characteristics (e.g. length, width, road class, etc.) of all Scottish roads. Only motorways, A roads and B roads were considered in this network. The capacity of each road was estimated based on

the methods proposed by the Design Manual for Roads and Bridges (DMRB) for urban roads DMRB TA 79/99 (Highways Agency, 1999) and for rural roads DMRB 46/97 (Highways Agency, 1997). The procedure that was followed to calculate road capacities is included in Appendix 5. The desired speed of each road is also included in Appendix 5. Figure 8.2 shows the considered road network.

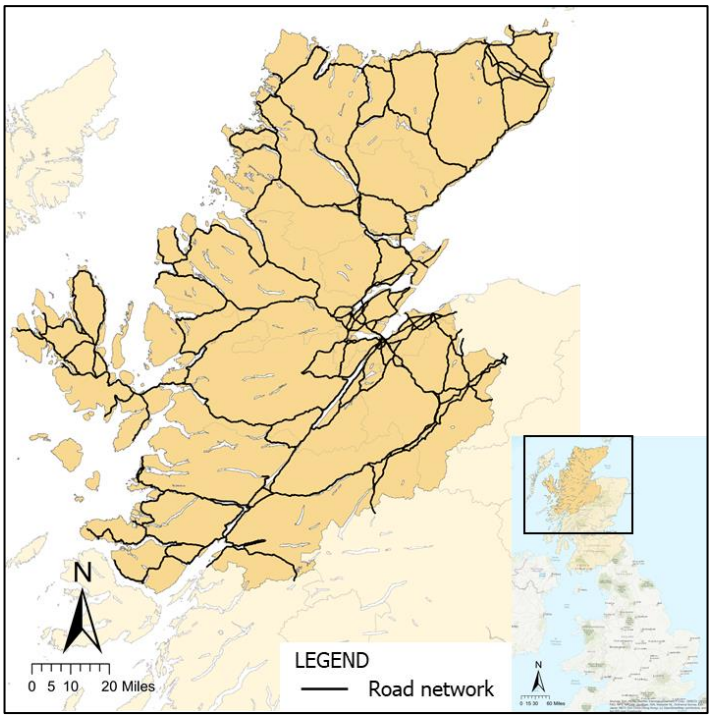

Figure 8.2. Area of study including the road network. Contains OS data © Crown copyright and database right 2020. Ordnance Survey (Educational Service Provider Licence Number 100025252).

There are some nodes that are more important than others because they provide Health and Social Care Services, ferry services, airport services, etc. Appendix 3 includes the maps of some of these services: the location of the NHS Highland hospitals (Figure A.6), location of ferry services (Figure A.7) and location of main airports (Figure A.8). According to Equation (3.17), the connectivity metric considered in this model can give higher importance to certain destination nodes. In this case, only those nodes that located hospitals and airports acquired higher importance.

The external information provided by the Variable Message Signs were also considered in this model. The locations of these VMS are included in the map of Figure A.9 in Appendix 3.

8.4. Travel demand

This section describes the process of estimating travel demand between the defined zones in Scotland. The output of this section is an estimation of the origin-destination matrix which indicates the number of trips between each pair of zones.

8.4.1. Estimation of the origin-destination (OD) matrix

8.4.1.1. NTEM Trip generation and zone characterisation

The trip generation process calculated the number of trips produced from or attracted to a zone, based on socio-economic characteristics of that zone. The number of trip productions and attractions were obtained from the National Trip End Model (NTEM) accessed through TEMPRO (Department for Transport, 2017).

NTEM divided Scotland into 499 zones (National Records of Scotland, 2011). The study area was formed from 24 NTEM zones located in the North of Scotland; the remainder of Scotland was divided into 4 external zones as follows: Zone 1: Argyll and Bute; Zone 2: Aberdeen(shire); Zone 3: South Scotland; and Zone 4: West Aberdeenshire/South Moray, based on aggregations of NTEM zones. Western Isles, Orkney and Shetland were excluded from model. Each trip departed/arrived from/to a geometric centroid of each zone, which represented the 'centre of activity'. A graphical representation of these centroids is included in Figure 8.3. These centroids were connected to the transport network through centroid connectors, which represented local roads with infinite capacity. It was assumed that vehicles travelled at a speed of 32km/h on centroid connectors and the time that drivers spent travelling on them was also computed on the travel cost formulation [Equation (6.4)]. Only one centroid connector per zone was used and this was obtained connecting the centroid to the nearest node of the road network.

The number of trips that the NTEM provided (produced and attracted at each zone) were for the AM period (7:00 – 10:00 am weekday). The base year considered for the extraction of trips from TEMPro software was 2019. Only cars were considered and buses or HGVs were excluded from the study. Six purpose-based categories of trips were considered: work, employers business, education, shopping, personal business and others (that include recreational/social purposes).

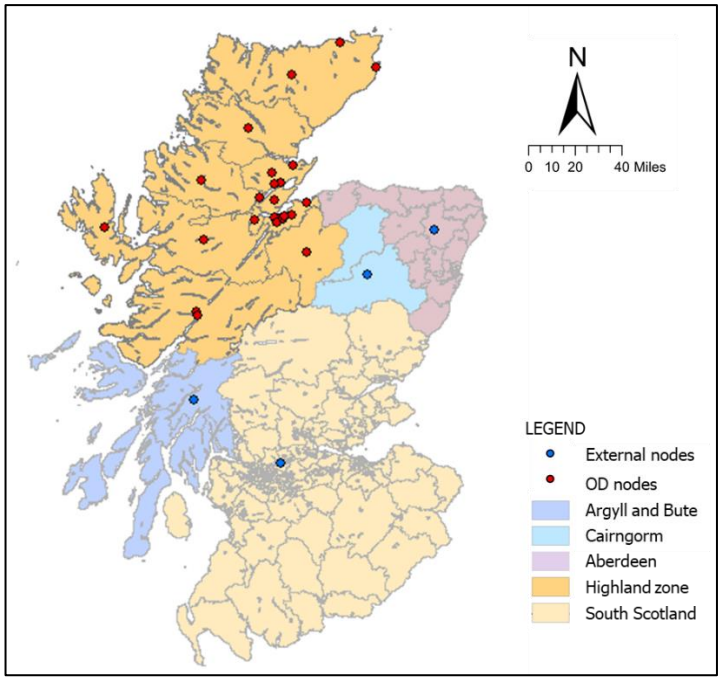

Figure 8.3. NTEM distribution of zones. The initial distribution of 24 internal zones in the Highland zone and 4 external zones and their corresponding centroids. Contains OS data © Crown copyright and database right 2020. Ordnance Survey (Educational Service Provider Licence Number 100025252).

8.4.1.2. Trip distribution: Gravity model

In order to obtain the distribution of trips between zones, a gravity distribution model (Ortuzar and Willumsen, 2011) was applied to the NTEM data using the commercial transport planning software TransCAD (Caliper Corporation, 2008). The aim of using a trip distribution model was to obtain an Origin-Destination matrix, which indicated the number of trips going from each origin to each destination. The gravity model assumed that the number of trips produced at an origin and attracted to a destination were directly proportional to the total trip productions at the origin and the total trip attractions at the destinations and inversely proportional to the travel cost between the origin and destination. The output from this distribution model was the morning peak period Origin-Destination Matrix (7:00 – 10:00 am hours).

$$OD_{ij} =\propto \ OP_i \ \ DA_j \ \ f(c_{ij}) \tag{8.1}$$

Where,

OD_{ij}, is the trips produced in an origin zone i and destination zone j.

$\propto$, is the proportionality factor.

OP_i, are the total trip production at zone i.

DA_j, are the total trip attraction at zone j.

$f(c_{ij})$, is the deterrence (travel cost) function between any pair of zones i and j. The deterrence function considered in this model is the one included in Equation (8.2).

$$f(c_{ij}) = e^{-\tau \cdot tt_O} \tag{8.2}$$

Where,

τ, is the travel deterrence parameters obtained from the Guidance on Accessibility Planning in Local Transport Plans, Technical Annex 6 (Department for Transport, no date). It depends on trip purposes (Work $\tau = 0.036$; Employers business $\tau = 0.013$; Education $\tau = 0.042$; Shopping $\tau = 0.085$; Personal Business $\tau = 0.042$; Others $\tau = 0.030$).

tt_O, is the free-flow travel time.

8.4.1.3. OD matrix disaggregation

The NTEM provided a low resolution zoning system, as observed in previous Figure 8.3. Some zones covered very large areas and therefore the assumption that the centre of activities were located in the centroid of each zone was not valid. This could lead to an inaccurate simulation that was a poor representation of reality. Thus it was decided to improve the resolution of the model by disaggregating NTEM internal zones into smaller zones based on Datazone geography. The process of matrix disaggregation was done using a built-in function in TransCAD (Caliper Corporation, 2008). Origin trips of NTEM zones were assigned to the smaller zones assuming that they were proportional to the residential population at datazone level. Likewise, for the internal zone destination disaggregation, the destination trips of NTEM zones were assigned to the smaller zones assuming that they were proportional to the employment at the datazone level. It is expressed mathematically as shown in Equation (8.3). The data used to undertake the disaggregation was extracted from the Scotland's Census 2011 (Scottish Government, 2011), code *DT604SCdz*, and all

people aged 16 to 74 in employment were included in the analysis. Additionally, a manual screening was done in order to cluster Datazone centroids that were located in close proximity to one another. Only one selected centroid represented all datazones in the cluster. This clustering process benefited the model by speeding up the computational time required to run the model (fewer OD pairs were modelled). The resulting group of centroids considered in the model and the comparison to the previous centroids of the NTEM zone level is included in Figure 8.4.

$$TR_{DZi} = TR_{NTEM} \cdot \not{f} \tag{8.3}$$

Where,

TR_{DZi}, is the number of trips that were assigned to the smaller zone i (datazone level).

TR_{NTEM}, are the aggregated number of trips on the NTEM zone level.

$\not{f}$, is the factor that converts aggregated trips to disaggregated trips. It is calculated using the following equation:

$$\not{f} = \begin{cases} \dfrac{RS_{DZ}}{TP_{NTEM}}, & for\ origin\ disaggregation \\ \dfrac{EP_{DZ}}{EP_{NTEM}}, & for\ destination\ disaggregation \end{cases} \tag{8.4}$$

Where,

RS_{DZ}, is the residential population at datazone level.

TP_{NTEM}, is the aggregated residential population at NTEM zone level.

EP_{DZ}, is the employment at datazone level.

EP_{NTEM}, is the aggregated employment at NTEM zone level.

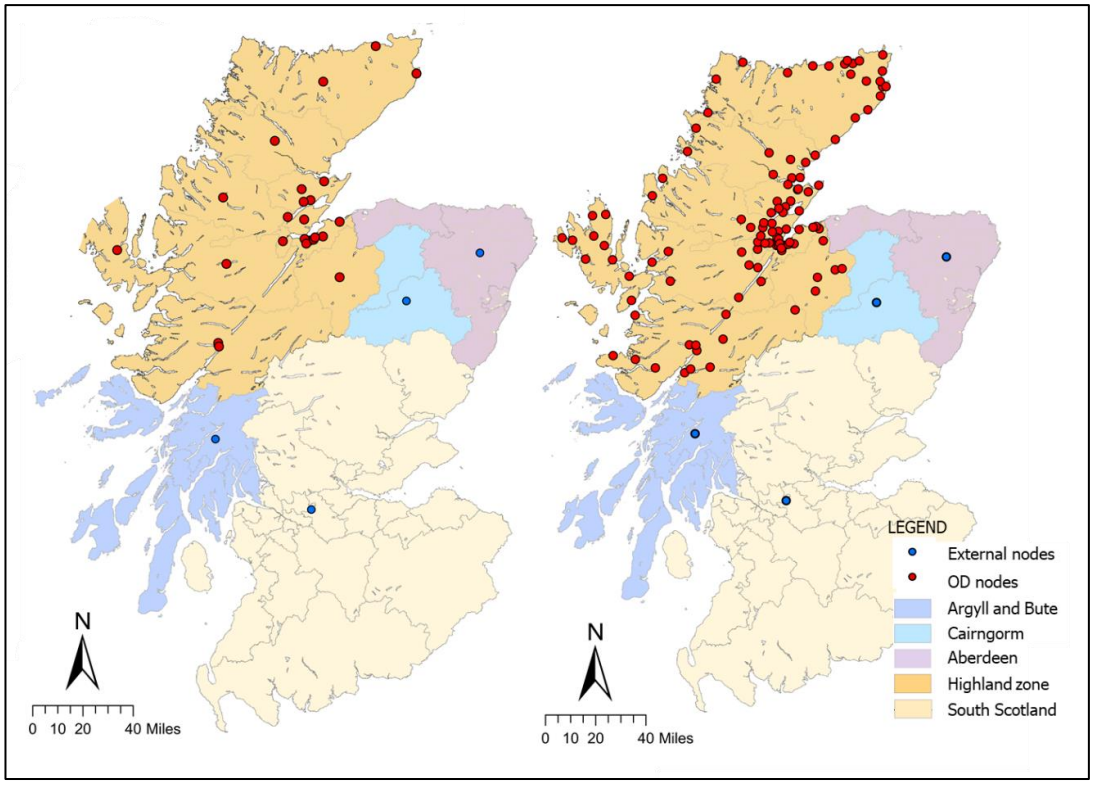

Figure 8.4. On the left, the initial distribution of 28 OD nodes (centroids). On the right, the final distribution of 113 OD nodes after matrix disaggregation. Contains OS data © Crown copyright and database right 2020. Ordnance Survey (Educational Service Provider Licence Number 100025252).

8.4.1.4. OD matrix transformations

The OD Trip Matrix obtained applied to the time period 7:00 – 10:00 am. However, the study period considered in this model was an hourly peak period (8:00 – 9:00 am weekday) which meant that the three-hour period had to be transformed into a hourly period. The following Equation (8.5) was used to reduce the number of trips to the hourly period. The PF is the peak 3-hour factor that was used to consider a non-uniform distribution within the 3 hour period, representing the busiest hour of the 3 hour period. The number of trips were rounded to the nearest whole number after applying Equation (8.5). A warm-up period (from 7:30 to 8:00 am) and cool-down period (from 9:00 to 9:30 am) were also considered in order to avoid having an empty network (without vehicles) at the beginning/end of the simulation.

$$t_{ij} = \frac{T_{ij}}{3 \times PF} \tag{8.5}$$

Where,

t_{ij}, is the hourly demand between zones i and j (veh/h).

T_{ij}, is the total demand between zones i and j in period 7:00-10:00am hours.

PF, is the peak 3-hour factor. It was assumed to be 0.85.

After the reduction to the hourly period, the following trips were excluded from the analysis: (1) Trips between external zones were omitted; (2) Trips within the same zone (internal trips) were excluded; (3) If the number of trips between an OD pair after the reduction to the hourly period was less than 1, these trips were omitted.

8.4.1.5. Final OD results

A total number of 15741 trips were considered for the hourly period 8:00 – 9:00am in the final OD matrix. Trips were grouped into 113 OD pairs. Figure 8.5 shows the final distribution of centroids and the trips that were produced/attracted at each zone. Drivers were allowed to choose between two departure times: at 8:00am or at 8:30 am.

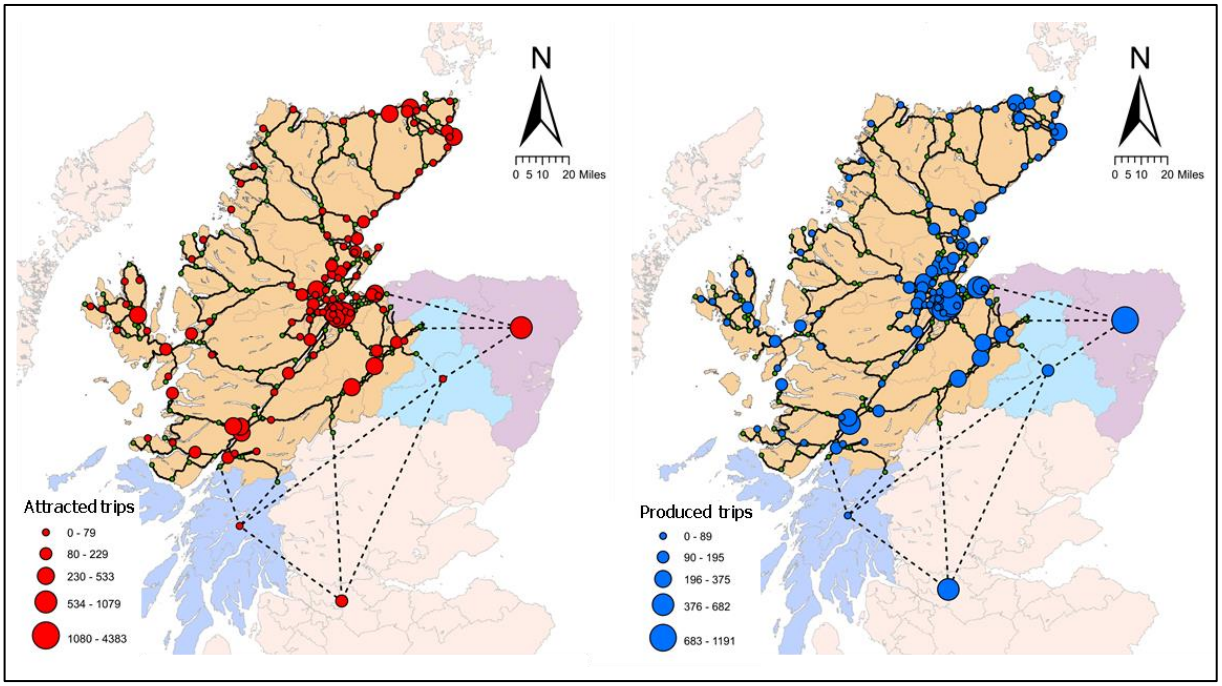

Figure 8.5. On the left, the number of trips that are attracted at each zone. On the right, the number of trips that are produced at each zone. Contains OS data © Crown copyright and database right 2020. Ordnance Survey (Educational Service Provider Licence Number 100025252).

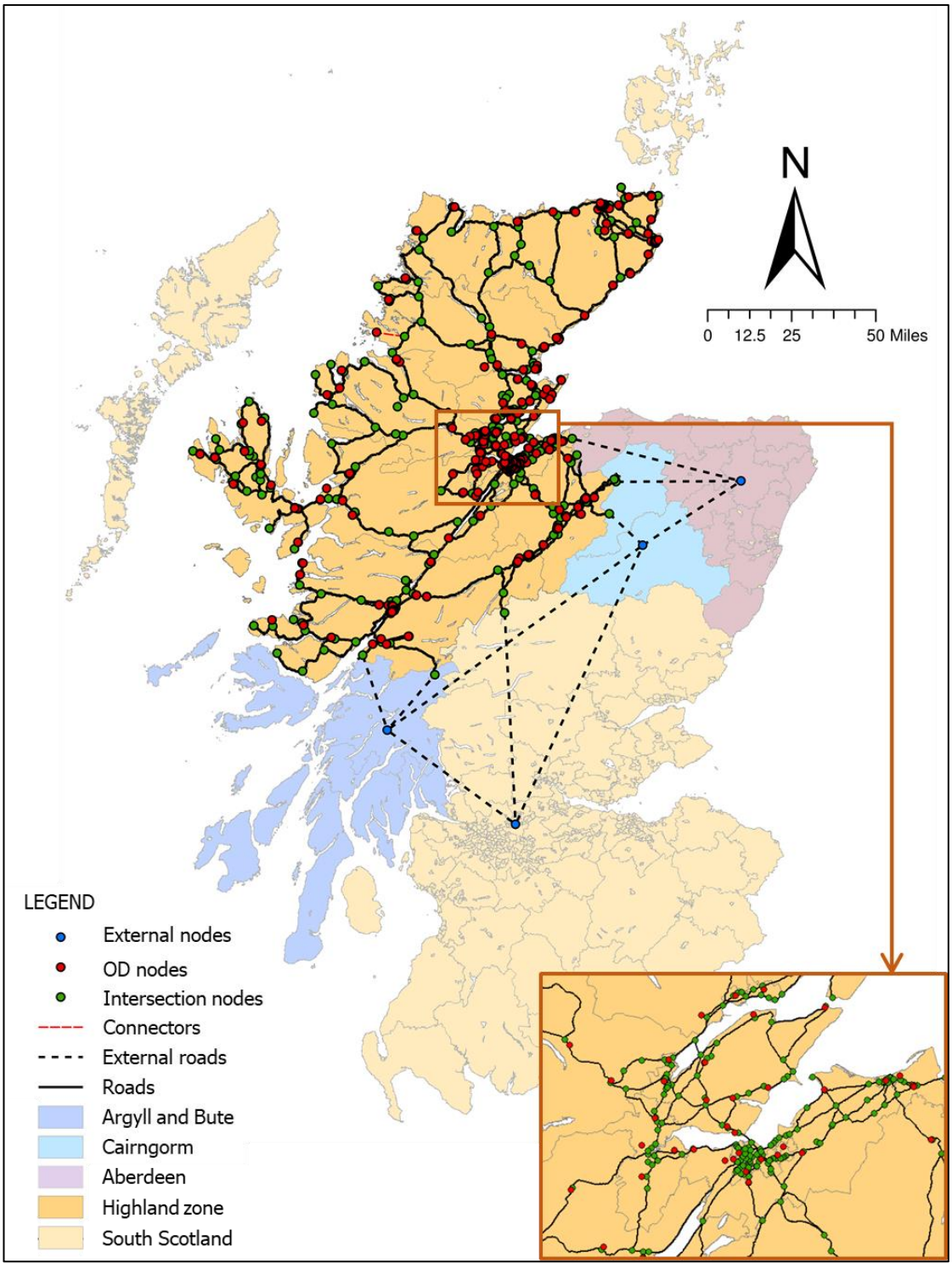

Figure 8.6. Map of Scotland showing the considered road network, centroids of datazones and external zones. Contains OS data © Crown copyright and database right 2020. Ordnance Survey (Educational Service Provider Licence Number 100025252).

8.4.2. OD data analysis and modelling implications

8.4.2.1. Number of vehicles per packet

In order to speed up the simulation process, vehicles that departed at the same time from the same origin and arrived at the same destination were grouped into packets. The simulation time grows exponentially with the number of packets. The drawback of grouping vehicles was the following: the more vehicles per packet, the less individual travel decisions were simulated, which meant that less level of detail was modelled.

The question that raised was: What was the optimal number of vehicles that could be grouped into packets in order to get a maximum computational time reduction while keeping a reasonable resolution of the model? A distribution of the number of vehicles that contained each OD pair is shown in Figure 8.7, graph on the left. It shows that more than 44% of all OD pairs contained fewer than 5 vehicles travelling between each pair. This meant that having more than 5 vehicles per packets would not get any reduction in the number of simulated packets on those OD pairs. If this idea was extrapolated to all OD pairs, the graph on the right of Figure 8.7 was obtained and it showed the number of vehicles per packets and the total number of packets that the model had to simulate. If only 1 vehicle per packet was considered, the model needed to simulate the total number of 15741 vehicles. The more vehicles added to each packet, the fewer number of packets were simulated. However, the reduction in the number of packets was negligible when the number of vehicles per packet was higher than 25 or 30. For this particular case study, the selected number of vehicles per packet was set to 25. If there were fewer than 25 vehicles in an OD pair, then the packet size would contain the corresponding number of vehicles.

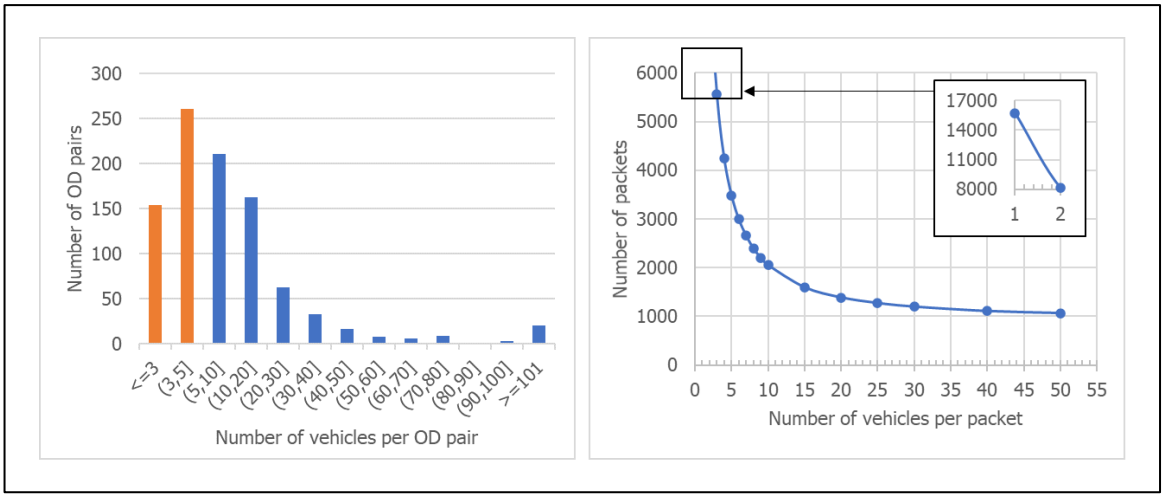

Figure 8.7. On the left, the distribution of the number of vehicles on each OD pair. On the right, the number of packet that the model needs to run depending on the number of vehicles per packet considered.

8.4.2.1. Activity starting time

Travel demand described in the previous Section 8.4.1 could include any trip around Scotland. Travel distance between OD pairs might vary from just a few kms to hundreds of them as observed in Figure 8.8. This meant that travel time could range from minutes to hours. If the earliest departure time of vehicles was at 8:00am (see Section 8.4.1.5) and the travel time of some vehicles was in the order of hours, it would not be appropriate to consider only one activity starting time (at 9:00am) for all OD trips. Therefore, the model considered 4 different activity starting times (9:00am, 10:00am, 11:00am and 12:00noon) so that it could be assigned to drivers depending on the distance they had to their destination (OD pair). The expected travel time was obtained assuming a constant average travel speed of 70km/h and the shortest path to all destinations was obtained. If the travel distance of an OD pair was less than 70km, the activity starting time would be at 9am. If the distance was between 70km and 140km, the starting time would be at 10am. If the distance was between 140km and 210km, the starting time would be at 11am. And if it was further than 210km, the starting time would be at 12noon. Note that the model was run until the last vehicle arrived to its destination.

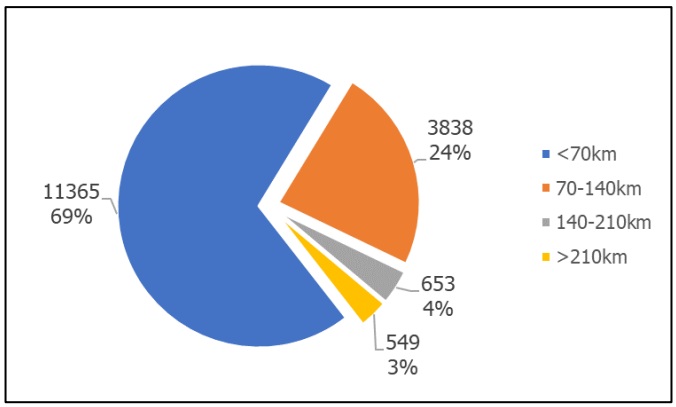

Figure 8.8. Distribution of trips in terms of travel distance (considering the shortest path to their destination).

8.5. Disruption scenario. Landslide-damaged roads

The aim of this section is to create a damage scenario that simulates damage caused to multiple road segments as a result of a severe weather event. The potential scenario considered in this case study focused on the impact of a series of landslides that occurred in different areas of the study network. A large part of the UK's strategic transport network is located in places considered highly susceptible to landslides (Postance, 2017). The impact of landslides affecting the road network in the north of Scotland can be significant as the number of alternative roads that drivers can choose, avoiding the damaged roads, is limited at certain locations. These problems can get worse as climate change models for Scotland predict an increase in precipitation in winter (UK Met Office, 2018), which means that more landslides and floods are likely to occur in the future.

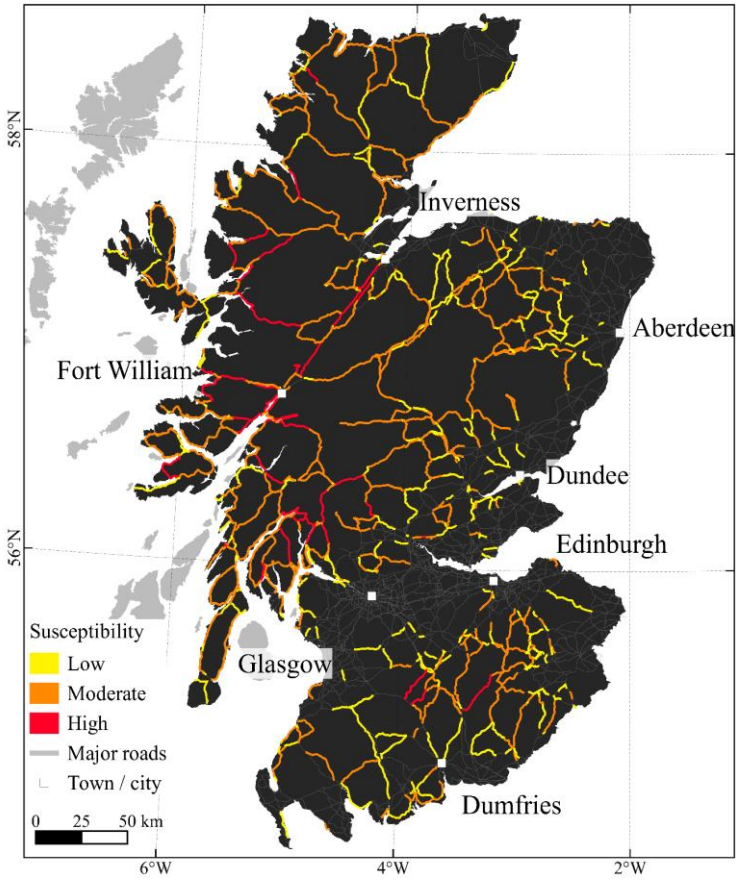

Figure 8.9. Susceptible road segments on the major Scottish road network. Map extracted from the work done by Postance (2017).

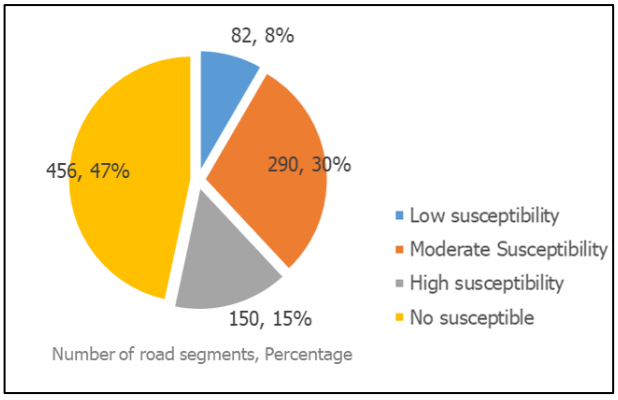

Figure 8.10. Number of road segments classified according to their susceptibility level. Information extracted from the map of Figure 8.9.

The framework presented in Chapter 4 was used to generate the damage scenario. A road segment susceptibility map (Figure 8.9) was extracted from the work

done by Postance (2017). The map was obtained from the intersection of a landslide susceptibility map, which identified areas predisposed to landslides, and the Scottish major road network. It showed which road segments were more susceptible to be damaged by landslides. The susceptibility was represented by four categorical classes: not susceptible, low susceptibility, medium susceptibility and high susceptibility. As no more data was available, the damage probability associated with each level of susceptibility of each road segment was defined by the modeller. As described in Chapter 4, the level of susceptibility might indicate the likelihood that a road segment was affected by this hazard. This meant that if an area was highly susceptible to a certain hazard, road segments that were located in that area would be more likely to be affected by this hazard. Therefore, the probability of being damaged was higher. Based on this idea, Figure 8.11 shows the damage probability associated with each susceptibility level considered in this model. Initially, these values were assumed by the author, but if further data were available, these limits could change. These probability values indicated that, for a large enough sample, the X% (value of the vertical axis in Figure 8.11) of those road segments of the corresponding susceptibility level were considered as damaged. Note that the susceptibility level assigned to centroid connectors was zero.

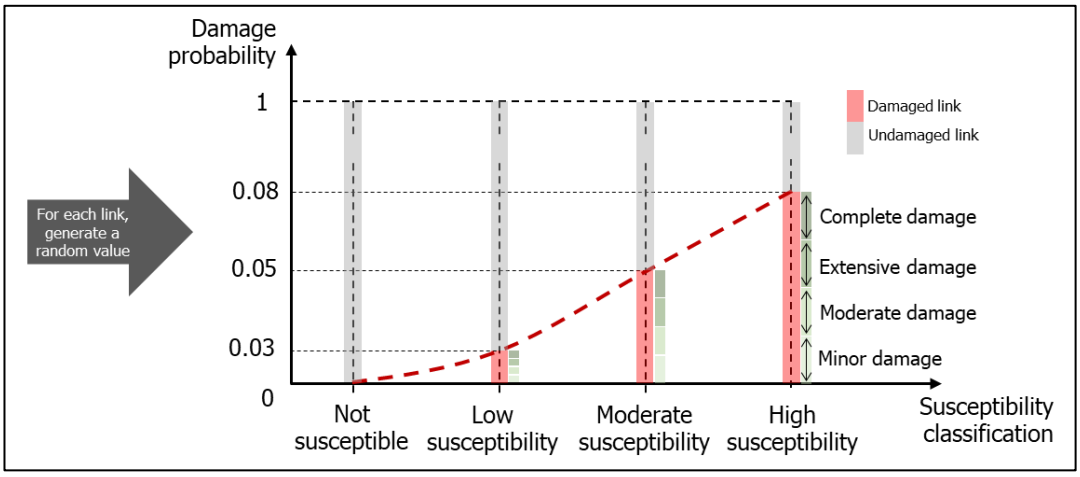

Figure 8.11. 'Hazard susceptibility vs. damage probability' graph. It shows the probability limits assumed for this example.

Based on the stochastic method presented in Equations (4.1), (4.2) and (4.3) of Chapter 4, several road segments were identified as damaged and a categorical

damage state was assigned. The process of selecting which road segments were damaged was as follows: (1) Generate a random value for each road segment following a uniform probability distribution; (2) Depending on the susceptibility level of each road segment and considering a user-defined damage probability, it was classified as damaged road segment (if the random value was above the probability associated) or undamaged road segment (if the random value was below the probability associated with that susceptibility level). This model assumed that if a road segment was damaged, the probability of having a minor, moderate, extreme or complete damage was selected according to a uniform distribution.

A total number of 8 bidirectional road segments (16 in total) were considered as damaged: DL1, DL2, DL3, DL4, DL5, DL6, DL7 and DL8. The following damage value function, which was described in Chapter 4 and included in Table 8.1, converted the categorical damage state to a numerical value of that damage. For simplicity, a linear function was assumed in this case study although in the real world it might be closer to a non-linear function in which the damage value of 'complete damage' would be higher than 4 times the minor damage. The location of these damaged road segments is included in Figure 8.12. It was assumed that damage was produced on day 28 of the simulation.

Table 8.1. Disruption scenario: affected links, damage state, quantification and road capacity

Road segments[2]	Damage state	Damage value (res-day)	Post-disruption road capacity (% original capacity)[1]	Minimum repair teams to start repairs
Rest	No damage	0*D	100%	-
DL3, DL6	Minor damage	1*D	50%	1
DL5	Moderate damage	2*D	0%	1
DL2, DL4, DL7	Severe damage	3*D	0%	2
DL1, DL8	Complete damage	4*D	0%	3

Being base damage D = 10 res-day for this particular example

[1] Reference: Padgett and DesRoches (2007)

[2] One-way road segment

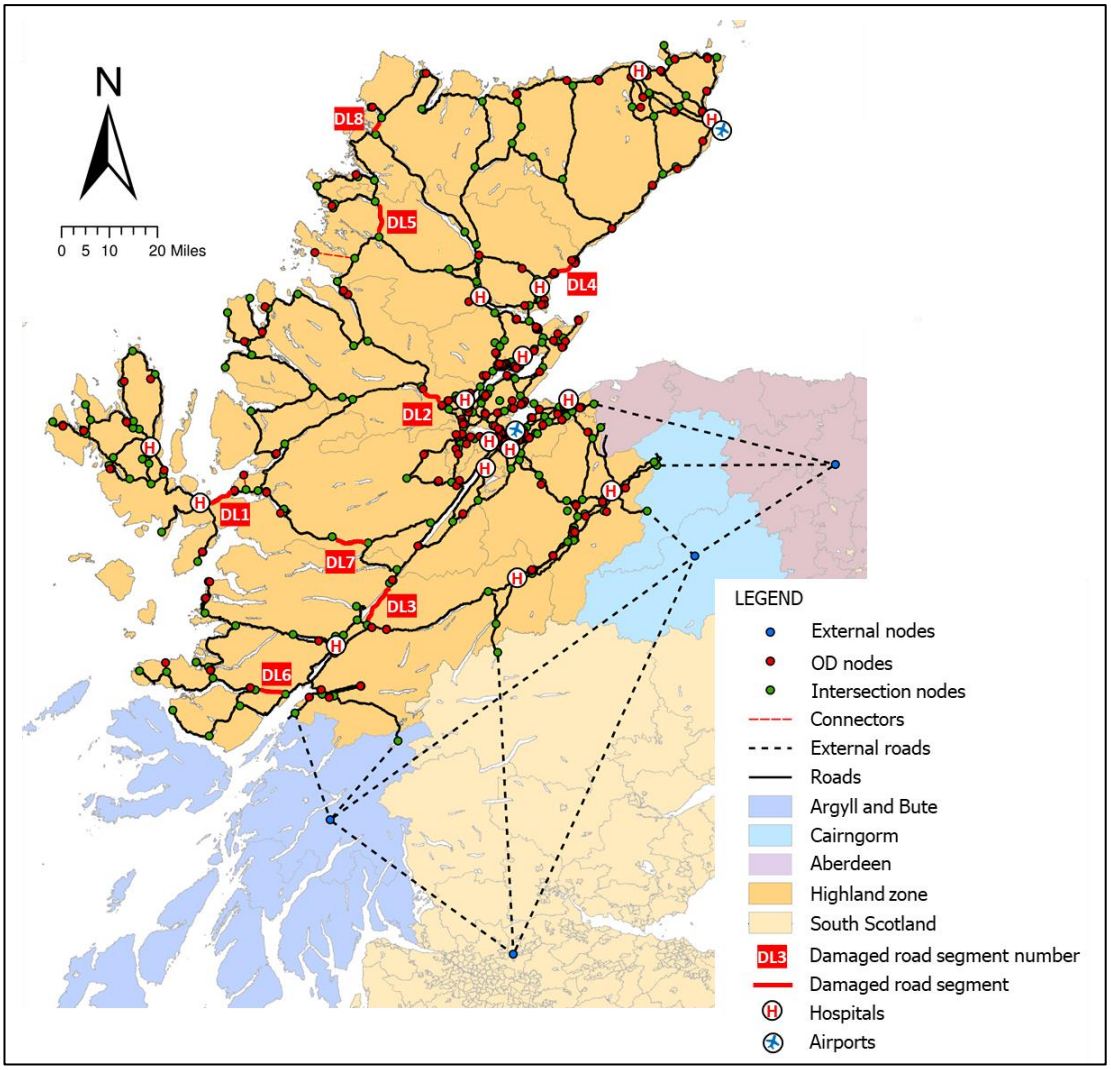

Figure 8.12. Location of the damaged road segments considered in this model application. Contains OS data © Crown copyright and database right 2020. Ordnance Survey (Educational Service Provider Licence Number 100025252).

8.6. External travel information

No previous studies have been found that evidence the percentage of drivers that use no travel information, pre-trip information or GPS navigation systems on their day-to-day journeys. This lack of information made the author assume a distribution of external information among drivers. In this model it was assumed that 25% of drivers did not receive any external information and they made travel decisions based on their own travel experience. Another 25% of drivers received pre-trip information which meant that they could know before travelling which road segments were closed. Another 25% of drivers checked the shortest travel time route before departure. And

the rest 25% of drivers used GPS navigation during their journey. Additionally, all drivers received the information that was provided via VMS at certain locations.

8.7. Summary of variables

The following Table 8.2 summarises all input variables and their values that were used in this model.

Table 8.2. Values of the variables considered in this example

Variable	Value	Variable	Value
# routes per OD	3	# departure times	2
Travel cost function		**General**	
$\boldsymbol{\beta_1 = \beta_2 = \beta_3 = \beta_4}$	1	Vehicles/packet	20
Memory function (Section 6.4)		Simulation time	47 days
Linear function		ε-greedy approach	None
$\boldsymbol{B_{max}}$	3	Pre-disruptive time	27 days
$\boldsymbol{b_1}$	10min	Post-disruptive time	20 days
$\boldsymbol{b_2}$	30min	Learning rate	0.4
$\boldsymbol{\theta}$	Uniform distribution [0,90]	# of simulations	VAR
Option of not travelling (Section 6.9)			
$\boldsymbol{y_{RC}}$	0.8	acc_a	Probability distribution of Figure 6.21.
$\boldsymbol{t_{RC}}$	10 min	$freq_a$	Uniform distribution [-1,1]
$\boldsymbol{U_s}$	0.8	$comf$	Uniform distribution [-1,1]
$\boldsymbol{U_f}$	0 days	g	3 days
$\boldsymbol{HH = JJ = LL}$	0.333	$AA = CC$	0.02
$\boldsymbol{t_{min}(freq_a)}$	10 min	$BB = DD$	1
$\boldsymbol{t_{max}(freq_a)}$	1h		
Preferred arrival time interval (PATI) (Section 6.2.2)			
Activity starting time	VAR	Activity	WORK
PATI 1 (time before activity starts)	Between 20 and 10 min	Distribution of drivers that prefer PATI 1	50%
PATI 2 (time before activity starts)	Between 10 and 5 min	Distribution of drivers that prefer PATI 2	50%
Disruption scenario (Section 4.2)			
$\boldsymbol{a}$ (Section 4.2.1)	0.08	c (Section 4.2.1)	0.03
$\boldsymbol{b}$ (Section 4.2.1)	0.05		
Repair module (Chapter 4)			
Base damage (D)	10 res-day	Repair teams	16 units
Angle of productivity-repairs graph	45 degrees	Saturation level repair teams	5 units
On-board decisions (Section 7.2)			
Variable $\boldsymbol{\lambda}$	0.9	Ω_h, patience level of vehicles	Uniform probability distribution [0,1]
$\boldsymbol{maxJ_h}$	3 links	EL (Equation (7.3))	2h
$\boldsymbol{mt_1}$	1 day	mt_2	3 days
Distribution of information between drivers			
Drivers with no external information	25%	Drivers with pre-trip information	25%
Drivers with GPS planning information	25%	Drivers with GPS en-route information	25%

Continuous in the next page

From the previous page

External information (Section 7.3 to 7.6)			
ξ (Equation (7.15))	0.2	$penalty$ (Equation (7.16))	0.5
GPS update route	10 min		
VMS: number of consecutive roads	2	VMS: length of consecutive links	10 km
$Q_{limit\ VMS}$	20%	$k_{Q,VMS}$	90%
Link IDs with VMS:		39, 40, 69, 70, 163, 164, 183, 184, 291, 292, 293 , 294, 305, 306, 365, 366, 441, 442, 463, 464, 483, 484, 555, 556, 710, 711, 713, 714, 811, 812, 847, 848, 853, 854, 855, 856	

8.8. Stochasticity of the model: single vs. multiple simulations

One of the characteristics of the RL traffic model is the randomness involved in the drivers' decision-making process (apart from the randomness included in network failures, external events and restoration actions of the recovery model). The impact of each repair strategy on drivers' behaviour needs to be modelled several times in order to get accurate results. This can be a real challenge from the point of view of the computational time. Running the whole model several times for the same repair strategy requires computer time and efforts. In this case, the model was performed on a computer with 8 GB memory and a quad-core 3.3 GHz Intel i5-3550 processor. To run one simulation of a repair strategy it took approximately 1.5 hours, which meant that for 10 simulations of the same repair strategy it would take 15 hours. With parallel computing, computational time could be reduced to even minutes if multiple computers were used at the same time, but more data was stored for each repair strategy. As observed, the computational effort that required the modelling of multiple simulations of a single repair strategy was high. Therefore, the aim of this section is to analyse the difference between modelling a single simulation and multiple simulations for the same repair strategy and observe whether this extra computational time of running multiple simulations (1.5h vs. 15h) is worthwhile or not.

The network and travel data used in this example was the same as the one described in previous sections of this chapter. Two random repair strategies were chosen to be analysed and the effectiveness of each one was obtained. The pre-disruption phase was obtained after running the model on an undamaged network. This phase shared results for both repair strategies to ensure that it did not interfere with the effectiveness of each strategy. The model was run ten times for each repair

strategy. Figure 8.13 shows the impact of each strategy on the total travel cost, considering 10 simulations for each one and the mean of all simulations.

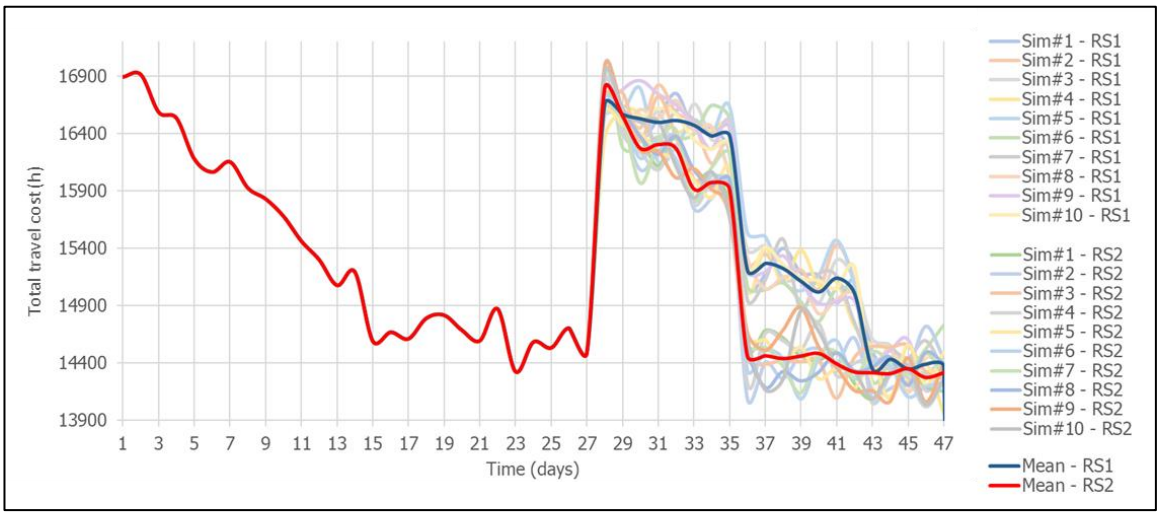

Figure 8.13. Total travel cost comparison between two random repair strategies. The pre-disruption stage was the same for both strategies. Only the post-disruption stage changes based on the effectiveness of each repair strategy. Notation: RS=Repair strategy. Sim=Simulation.

The effectiveness of each repair strategy was measured using the resilience metric described in Section 3.4 of Chapter 3. It calculated the area under the total travel cost curves of the post-disruption phase. The mean of 10 simulations was used to compare the effectiveness of repair strategies #1 and #2. The difference in mean resilience between the two repair strategies was 7242 h·day, which is graphically shown as the area between the mean curves on Figure 8.13.

On the other side, the effectiveness of each single simulation was compared to the mean value of the same repair strategy. Results of the comparison are shown in Figure 8.14 and it indicates the differences in terms of resilience values of each simulation compared to the mean values of the same repair strategy. As observed, the maximum difference is found in simulation #6 of repair strategy 1 with a resilience value of 911h·day. This corresponds to a relative error lower than 0.3%, which is negligible. The standard deviation of resilience for repair strategy 1 is 571 h·day and for repair strategy 2 is 439 h·day.

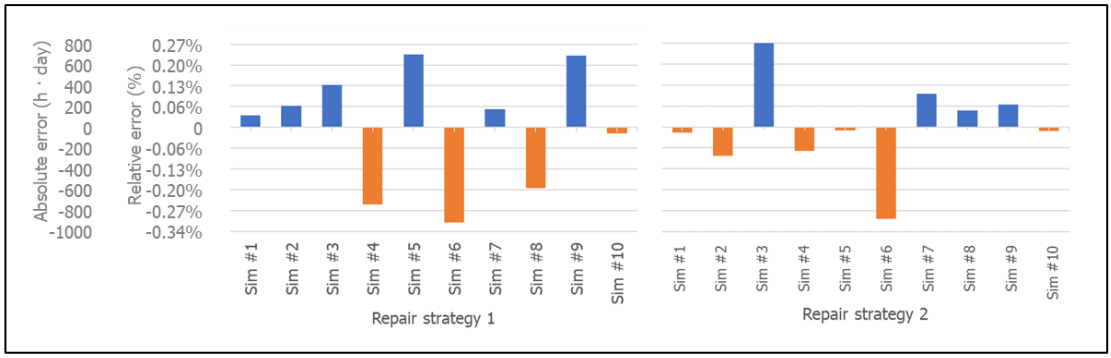

Figure 8.14. Differences of resilience values in terms of total travel cost of each simulation compared to the mean of the same repair strategy.

Additionally, the differences between the effectiveness of individual simulations of each repair strategy is included in Figure 8.15. Each bar considered the difference of resilience values of total travel cost between a single simulation of repair strategy #1 and a single simulation of repair strategy #2. The black dotted line represents the difference between the mean values of both strategies and both red lines showed one standard deviation (687 h·day) from the mean. Pairwise comparison between individual simulations from each repair strategy shows the difference ranges from ~5500 h·day to ~8750 h·day. The maximum difference from the mean was obtained when simulation #6 of RS1 was compared to simulation #3 of RS2. The obtained value was 5517 h·day, which compared to the mean value (7242 h·day) gave a maximum relative error of 23.8%.

After observing the results from this section, it was concluded that, for the purpose of this case study, it was not worth executing the model for 10 simulations because the computational time increased by 4 or 5 times while the differences between simulations and their mean value for this particular case were negligible (~±0.3%). However, the main difference between considering n=1 or n=10 simulations per repair strategy may be the final ranking of 'best' repair strategies that results from the simulation. Similar repair strategies may be in different positions in the ranking depending on whether n=1 or n=10. However, in any case, these small changes would not alter the final Pareto front of solutions. Therefore, for the rest of the chapter, a single simulation per repair strategy is considered, taking into account the potential error that this assumption might entail.

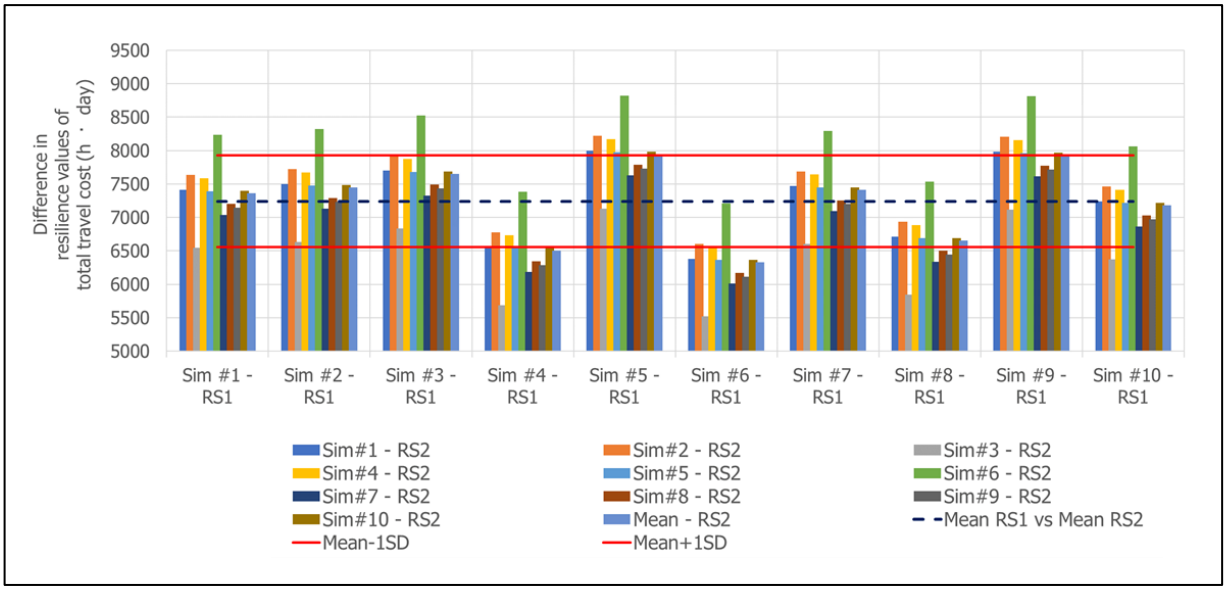

Figure 8.15. Differences in terms of resilience values between any simulation of the repair strategy 1 and any simulation of repair strategy 2. The dotted line represents the difference between the mean values of repair strategy 1 and the mean values of repair strategy 2. Notation: RS=Repair strategy. Sim=Simulation. SD=Standard Deviation.

8.9. Results and discussion

8.9.1. Pre-disruption stage

During the first 27 days of the simulation, there was no disruption involved and drivers were trying travel options in order to find and select their option with minimum travel cost. Drivers were learning based on their previous travel experience. The travel decision they made on a day was influenced by their decisions in previous days. As observed, in the long run and assuming that there are no changes in overall demand and the network, drivers will tend towards the alternative which they are satisfied with.

Due to the stochastic nature of the model, the pre-disruption stage model (see Chapter 6) was run several times in order to show the randomness involved in the drivers' decision-making process. Figure 8.16 shows 22 simulations of the pre-disruption phase. The mean value of each day was also calculated. The model needed to be run until the conditions stabilised, which was when drivers found their preferred travel option. In this case, it was considered that conditions were stabilised when the difference in terms of total travel cost of 4 consecutive days measured on the mean

curve was less than 50h, which was a negligible value compared to the total travel cost that was obtained on a single day. After 27 days travel cost stabilised, which meant that most drivers already selected their satisfactory travel option.

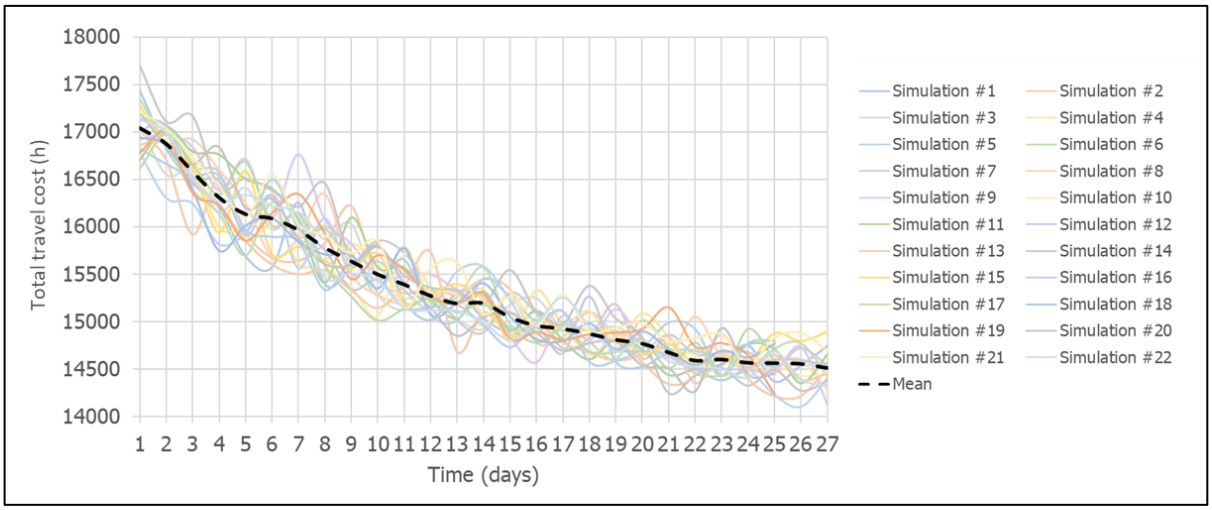

Figure 8.16. Multiple simulations (22 + mean values) of the pre-disruption phase.

The travel choices that drivers made on Day 27 was used as input to the post-disruption stage. The problem was that the evaluation of the effectiveness of each repair strategy needed to be done using only one simulation of the pre-disruption stage. Otherwise, if different simulations were used for each repair strategy, it might influence the effectiveness of each strategy because the starting database for each driver might be different. Therefore, only a single simulation needed to be chosen for all repair strategies. But, which pre-disruption data should be considered among all 22 simulations? The mean value of all of them could not be chosen because it was not a simulation obtained from the model. In this case, the closest simulation to the mean value was selected as data for the post-disruption stage because it was close to the average behaviour of all simulations. The procedure that was used to select the closest simulation is detailed as follows: (1) Obtain the relative error of the total travel cost on each simulation compared to the mean on each day using Equation (8.6); (2) Sum all relative errors (positive and negatives) of a single simulation for all days; (3) Identify the simulation with the minimum sum of relative errors. Figure 8.17 shows the sum of relative errors of all simulations. The lower the error associated with a simulation, the closer to the mean curve it is. The sum of relative errors is

indicated in a bar at the top of the figure. The closest simulation to the mean is simulation#3, which had a sum of errors of 22.1% after 27 days. Therefore, this was the one that was selected for the post-disruption stage.

$$RE(\%) = \frac{TTC_{ts} - \overline{TTC}_{t,22}}{\overline{TTC}_{t,22}} \cdot 100 \tag{8.6}$$

Where,

TTC_{ts}, is the value of the total travel cost of simulation s on day t.

$\overline{TTC}_{t,22}$, is the mean value of the total travel cost of 22 simulations on day t.

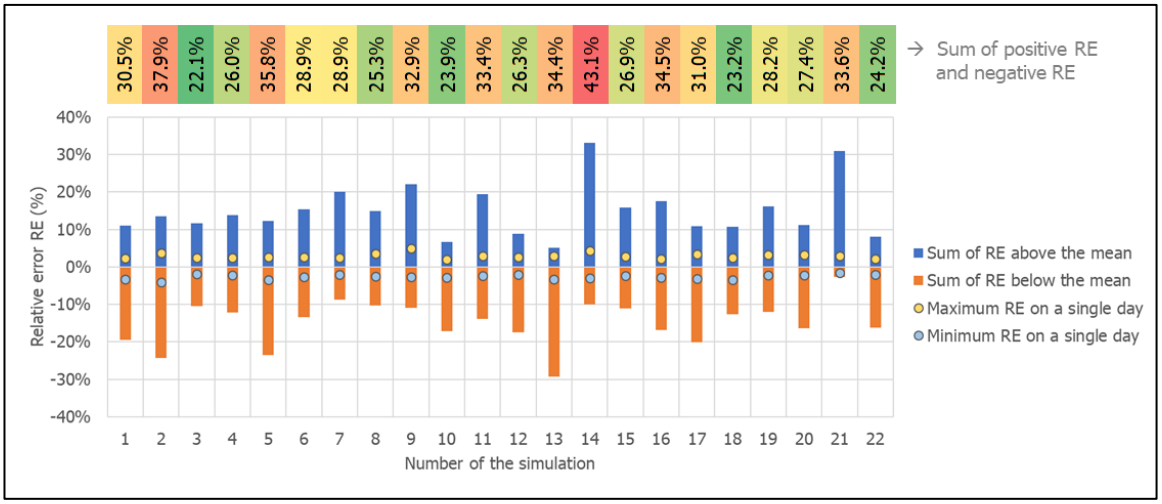

Figure 8.17. Sum of the relative error of each simulation in relation to the mean.

8.9.2. Post-disruption stage.

On Day 28, the hypothetical hazardous event damaged the road network producing a capacity reduction on certain road segments as described in previous Section 8.5. Results from the post-disruption phase showed how drivers reacted to these network changes and the effectiveness of the implemented repair strategies was evaluated. The starting data on this post-disruption phase was the same for all simulations so that it did not interfere with the effectiveness of each repair strategy.

After running all repair strategies considered in the optimisation model (a total of 1200 repair strategies), Figure 8.18 shows the evolution of the impact of all repair strategies on the total travel cost and network connectivity. There was considerable

variability in the impact produced by the different strategies which demonstrates the diversity of repair strategies analysed in the model.

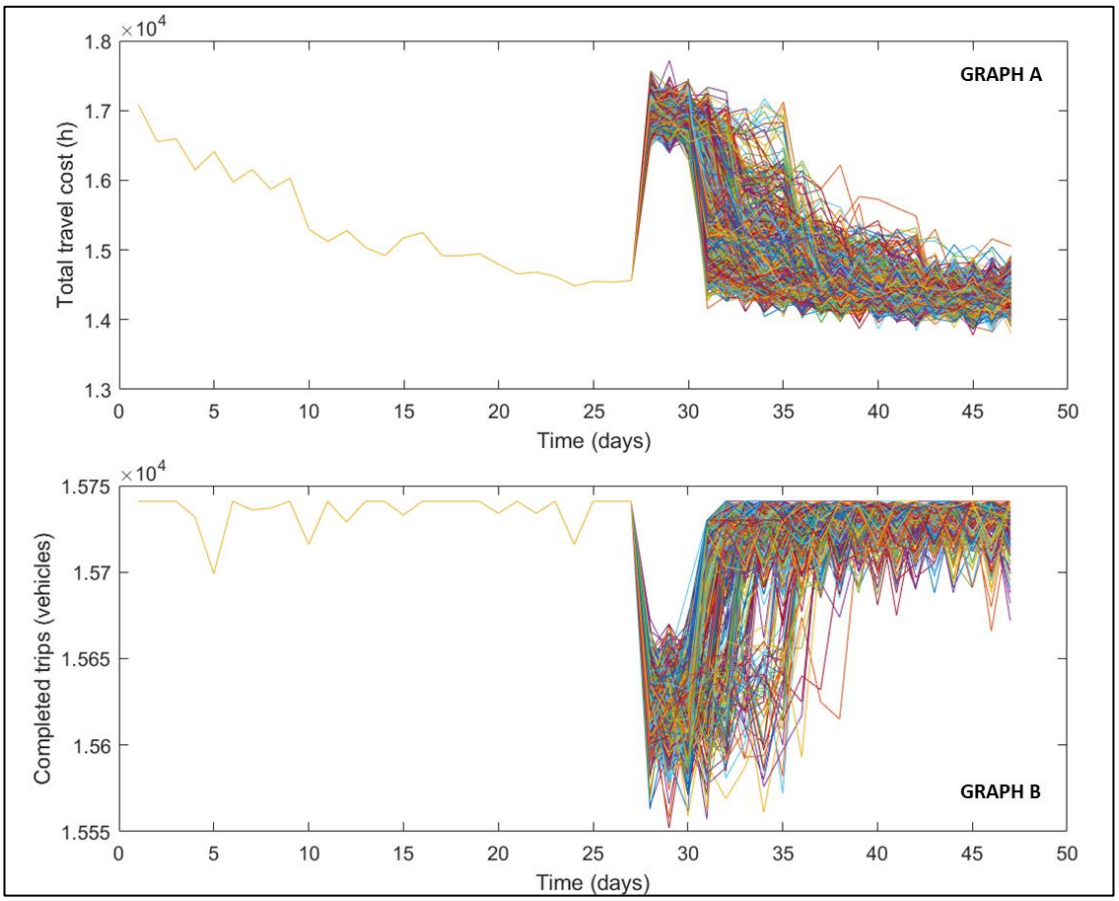

Figure 8.18. Evolution of the total travel cost and network connectivity measured as the number of completed trips of all repair strategies. Pre-disruption phase: from day 1 to day 27. Post-disruption phase: from day 28 to day 47. A total of 1200 repair strategies.

A directed graph of the Scottish network showed in Figure 8.19 was created by a built-in function in MATLAB (The MathWorks Inc., 2018). This figure superimposed the road network implemented in MATLAB and the Scottish map so that readers can relate the road network to real locations. Figure 8.20 used this directed graph to show the impact of road closures on the flow of vehicles on Day 27 (pre-disruption) and on Day 28 (post-disruption). The first row of graphs represents the relation between the flow of vehicles and road capacity. The second row of graphs shows the flow on each link. As observed, the first impact of the disruption is the increase in the volume of vehicles on alternative routes due to the closure of some

other roads. In particular, the area near Inverness and Lairg (near DL2) shows at major increase in flow values.

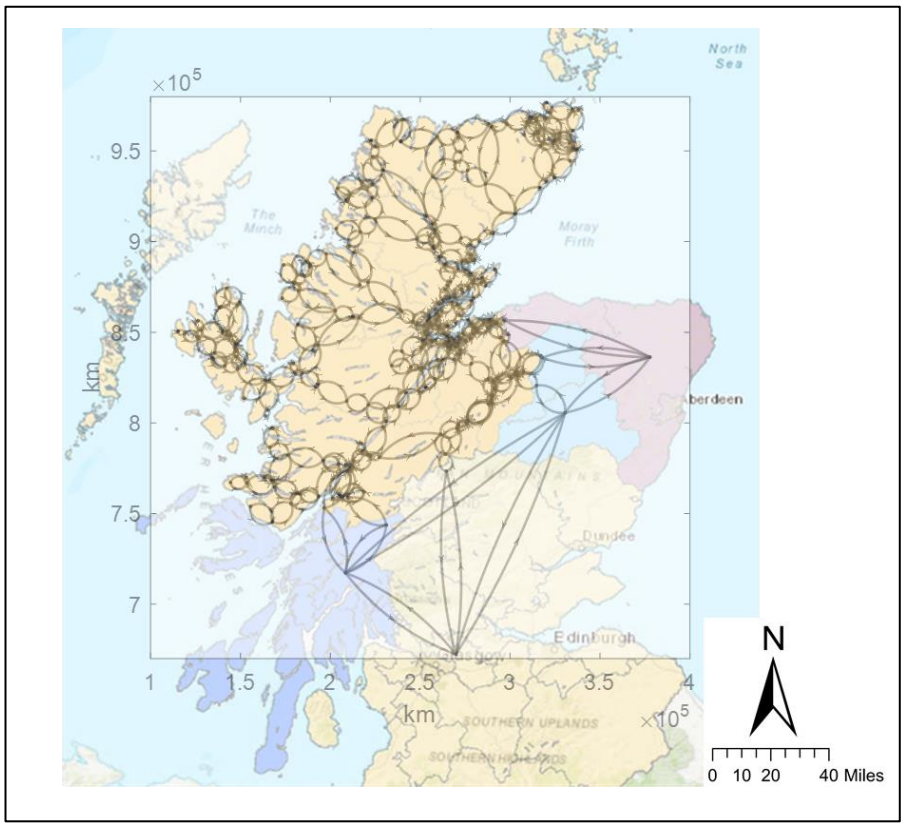

Figure 8.19. Scottish road network extracted from a built-in function (*digraph*) of MATLAB (The MathWorks Inc., 2018). This function represents roads as directed graphs between two nodes using a curved line. The real distance is included in MATLAB as an input. The map that shows the Scottish areas is not provided by MATLAB and is included in order to help readers to identify the location of roads on the Scottish area. Contains OS data © Crown copyright and database right 2020. Ordnance Survey (Educational Service Provider Licence Number 100025252).

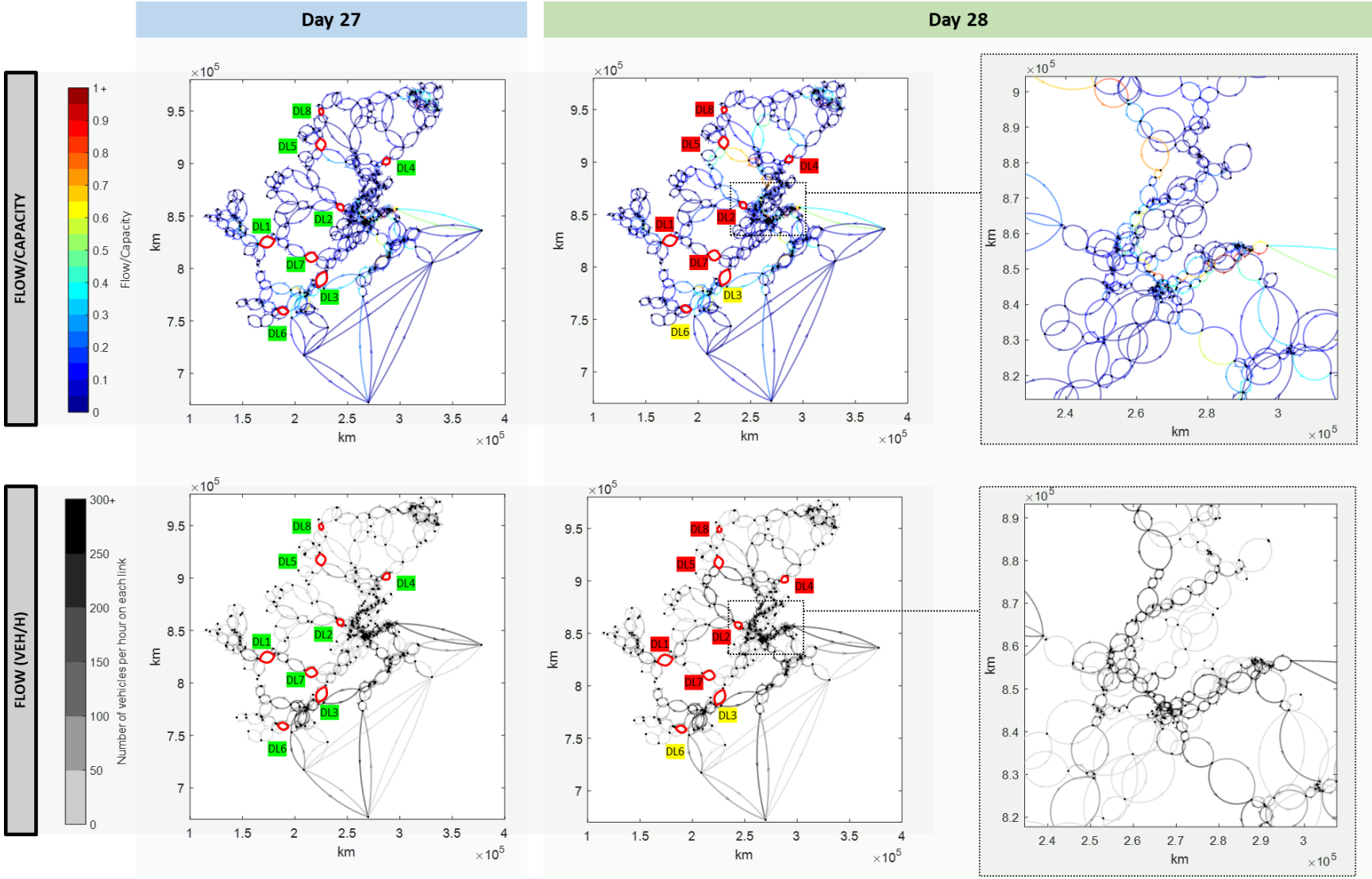

Figure 8.20. Scottish road network map showing the relation flow/capacity and flow on Day 27 (before the disruption) and on Day 28 (after the disruption) during the peak period bet ween 8am and 9am. In red lines, the damaged road segments.
DLx road segment open to traffic; DLx partially open to traffic; DLx totally closed to traffic.

8.9.3. Optimisation results

The model was performed on a computer with 8 GB memory and a quad-core 3.3 GHz Intel i5-3550 processor. For each repair strategy, the model took ~1.5-2h on average to run one simulation. A total number of 1200 repair strategies were simulated on the optimisation model. In order to speed up the running process, parallel computing was used so that two simulations were run at the same time. Two laptops were used, with the same characteristics that are indicated at the beginning of this paragraph. This reduced the computational time to half of the original amount of time. Therefore, the model needed ~1200 hours (~50 days) to run the whole optimisation problem.

Results from the optimisation model are included in Figure 8.21. It shows the value of the two conflicting objectives in each repair strategy. It also includes the Pareto front of solutions of generations 1, 10, 20, 30, 40, 50 and 60. Due to computational time limitations, only 60 generations were run. The evolution of the front of solutions after each generation shows a clear trend towards at decrease in total travel cost and the increase in network connectivity. A great improvement is observed in the search for optimal solutions between generation 1 and 10, while among the rest of generations this improvement is smaller. The reason behind this is that the initial population of repair strategies is generated randomly which means that there is more variability in the range of solutions. However, while the optimisation process is getting closer to the last generations, the repair strategies are more similar between them which means that there is less variability on the solutions and therefore huge improvements are not expected. A small improvement in the front of solutions is still observed between generations 50 and 60, which may indicate that the model has not reached the most optimal front of solutions. As the aim of the chapter was to demonstrate the applicability of the model to a real road network, it was decided that the value of running further generations of the model to obtain a solution closer to the optimal was marginal.

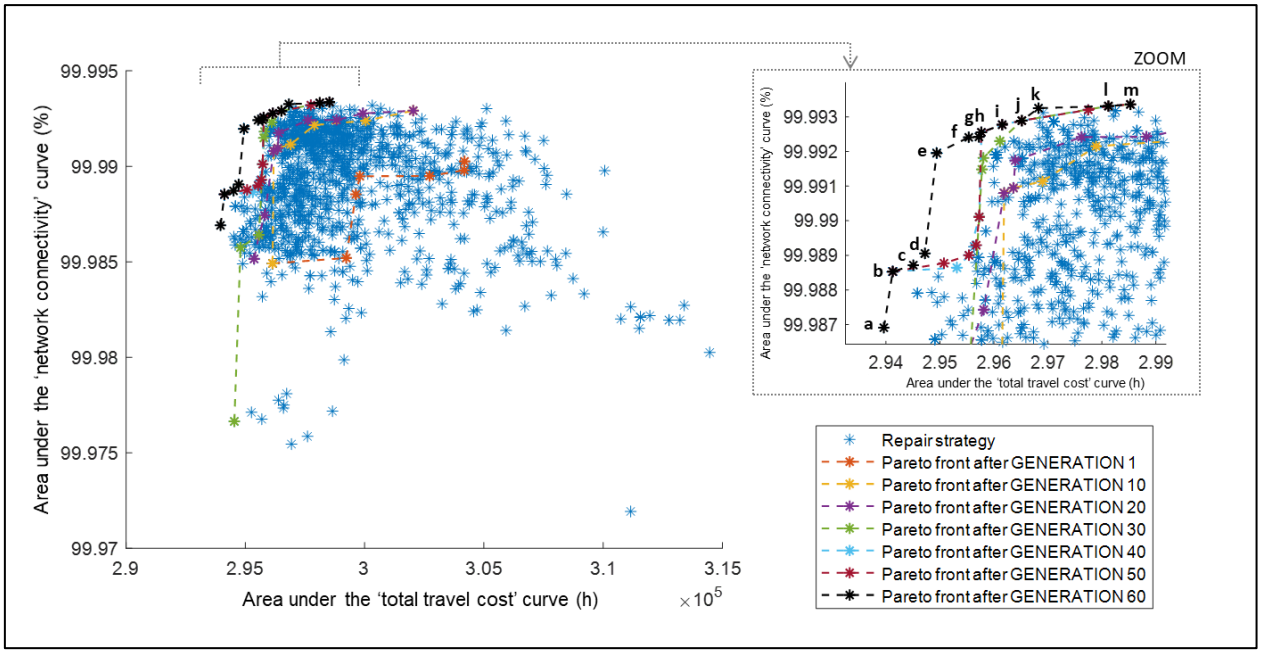

Figure 8.21. Bi-objective graph with all repair strategies and the Pareto front of solutions for 60 generations

After 60 generations, the Pareto front of solutions showed 13 potential (near-) optimal solutions (from "a" to "m" in Figure 8.21). The priority order of repairs and the repair teams assigned to each damaged location of the final 13 repair strategies is included in Table 8.3 and Table 8.4. Results show the similarity between some repair strategies. There is a clear trend towards repairing DL2 in the first place, DL4 in the second place, DL8 in the seventh place and DL6 in the last place. The order of repairs for the rest of damaged locations varies depending on the considered repair strategy. Regarding the allocation of repair teams (Table 8.4), most of them assign a value of "5" which was the maximum value that could be allocated to a damaged road segment (see "Saturation level repair teams" on the summary of variables in Section 8.7).

Table 8.3. Priority order of repairs of all optimal repair strategies after the 60th generation. The number "1" indicates the highest priority value and "8" the lowest priority value.

Damaged road segments	Repair strategy a	Repair strategy b	Repair strategy c	Repair strategy d	Repair strategy e	Repair strategy f	Repair strategy g	Repair strategy h	Repair strategy i	Repair strategy j	Repair strategy k	Repair strategy l	Repair strategy m
DL1	5	5	5	5	4	3	4	3	3	3	2	2	5
DL2	1	1	1	1	1	1	1	1	1	4	1	3	4
DL3	7	6	6	3	6	6	6	6	6	6	5	6	3
DL4	3	2	2	2	2	2	2	2	2	2	3	1	1
DL5	2	3	3	6	5	5	7	5	5	5	6	5	6
DL6	8	8	8	8	8	8	8	8	8	8	8	8	8
DL7	4	4	4	4	3	4	3	4	4	1	4	4	2
DL8	6	7	7	7	7	7	5	7	7	7	7	7	7

Table 8.4. Assigned resources to each damaged road segment on the optimal repair strategies after the 60th generation. The value (e.g. "5") indicates the number of repair teams that are allocated on each damaged location.

Damaged road segments	Repair strategy a	Repair strategy b	Repair strategy c	Repair strategy d	Repair strategy e	Repair strategy f	Repair strategy g	Repair strategy h	Repair strategy i	Repair strategy j	Repair strategy k	Repair strategy l	Repair strategy m
DL1	5	5	5	5	5	5	5	5	5	5	5	5	5
DL2	5	5	5	5	5	5	5	5	5	5	5	5	5
DL3	3	3	1	3	3	3	3	3	3	3	3	1	1
DL4	5	5	5	5	5	5	5	5	5	4	5	4	4
DL5	3	5	5	3	5	5	5	5	5	5	3	5	3
DL6	4	4	3	4	3	3	3	5	3	3	3	3	4
DL7	5	5	5	5	5	5	5	5	5	4	5	5	5
DL8	5	3	3	3	3	3	3	3	3	5	3	3	3

The impact of these repair strategies on the performance of the system is observed in Figure 8.22. It shows the evolution of total travel cost and network connectivity over time of these 13 repair strategies. Regarding the total travel cost (graph A) and as stated above, drivers are getting information about daily traffic conditions (creating on their own experience) during the first 27 days and therefore, they are improving their departure time and route choices through a learning process. Only when the overall performance is stable, is it assumed that drivers have found a satisfactory travel option. On Day 28, the closure of some roads produces an increase in the average travel cost as drivers have to adapt to new network conditions and take longer routes to reach their destinations.

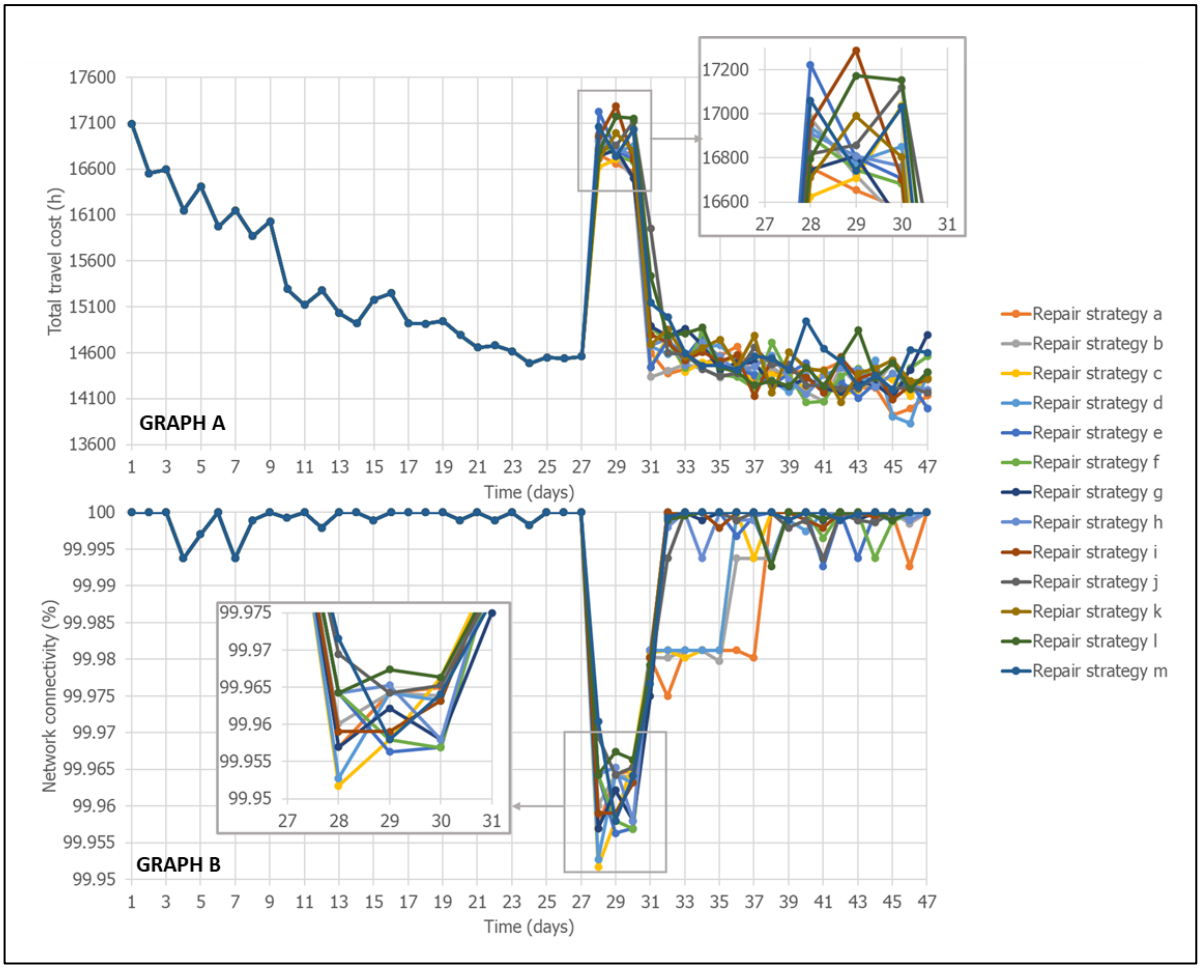

Figure 8.22. Evolution of the total travel cost (graph A) and network connectivity (graph B) of all optimal front of repair strategies after the 60th generation.

The differences between of selected (near-) optimal repair strategies in terms of total travel cost are small. All of them follow the same pattern with a peak value on days 28, 29 and 30 and lower values the rest of the days. The highest impact after the closure of these road segments on Day 28 appears on repair strategies *e, i, j, k, l, m* and lower impact on repair strategies *a, b, c, d*. The graph also shows that the performance in terms of travel cost achieves a lower value at the end of the simulation compared to the pre-disruption value. This suggests that, during the pre-disruption phase, drivers stick to certain travel options that are not necessarily the optimal for them. However, once a disruption occurs, drivers are forced to try alternative routes and they find that these travel options are better in terms of travel cost than the pre-disruptive ones and therefore, the overall network cost is reduced. Regarding the

evolution of the network connectivity in Graph B of Figure 8.22, repair strategies *a, b, c* and *d* have the lowest values of connectivity among the front of optimal solutions after the 60th generation, but lowest total travel cost as well. Note that option *c* is mostly hidden by option *d.*

The road opening plan that is extracted from each repair strategy is included in Figure 8.23. It shows when each damaged road segment is totally closed (0% of original capacity), partially open (50% of the original capacity) and totally open (100% of the original capacity). A summary of Figure 8.23 is included in Table 8.5. It shows the day when each road segment totally opens to traffic (full capacity) after repairs.

Some of the main differences between repair strategies in terms of opening-closing dates are described as follows. It is observed that some strategies repair DL1 later than others. This road segment connects the Isle of Skye to the rest of the Scottish network and if this link is not connected, drivers cannot leave/enter the island by car. Repair strategies *a, b, c* and *d* partially open DL1 on days 36-38, while the rest of strategies partially open this road segment on day 32. This is reflected in a lower value of connectivity on these repair strategies *a, b, c* and *d* as there are 4-6 days that drivers cannot leave/enter the island.

It is also observed that only two strategies (*a* and *j*) repair the whole network within the simulation period (<47 days). The rest of strategies need more days to fully open damaged road segment DL8.

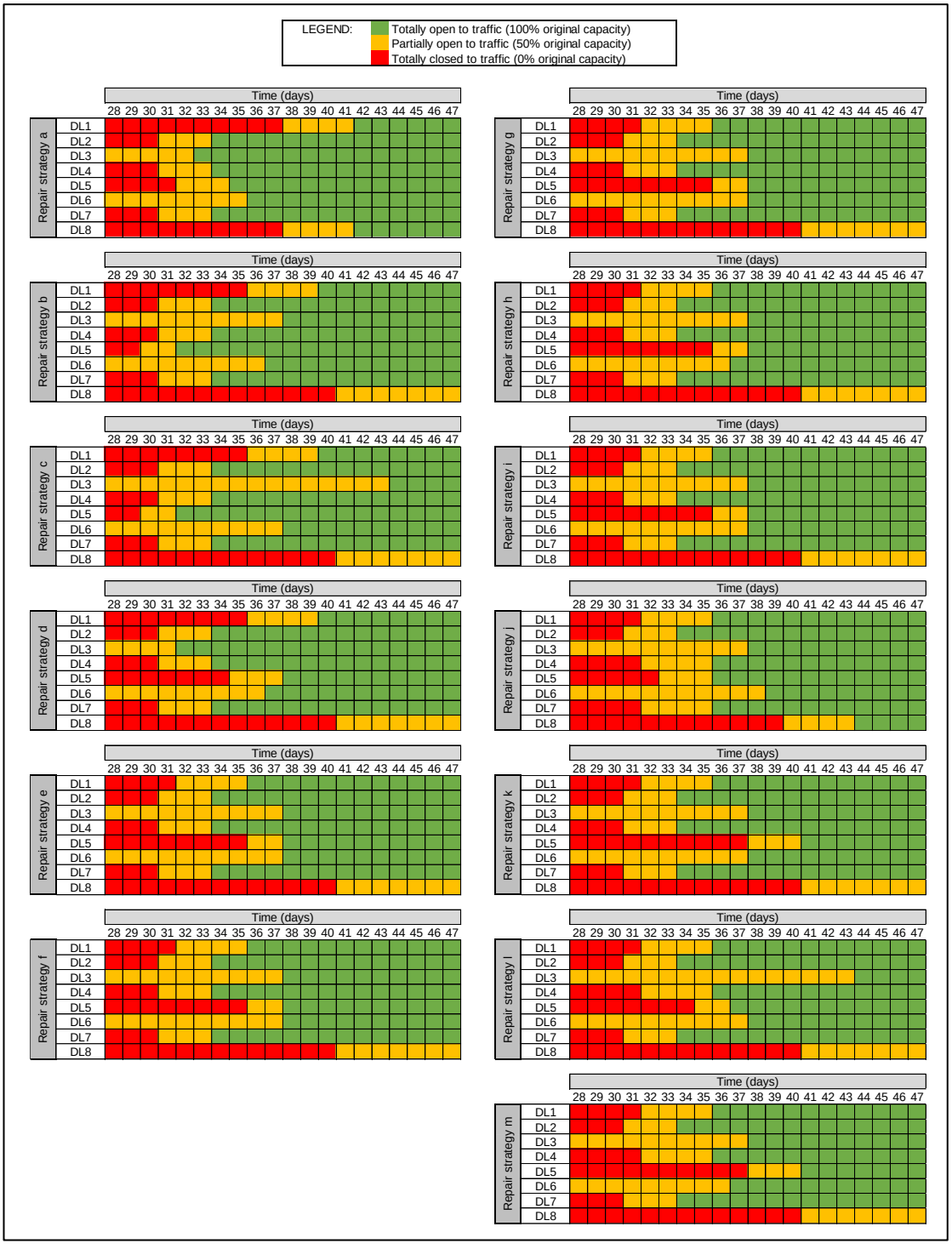

Figure 8.23. Opening-closing dates of damaged road segments based on the optimal repair strategies obtained after the 60th generation.

Table 8.5. Opening day of damaged road segments (full capacity) on the optimal repair strategies after the 60th generation. Note that these road segments are closed on the 28th day. The term ">47" indicates that the damaged road segment is not fully open to traffic on day 47, which is the last day of the simulation.

Damaged road segments	Repair strategy a	Repair strategy b	Repair strategy c	Repair strategy d	Repair strategy e	Repair strategy f	Repair strategy g	Repair strategy h	Repair strategy i	Repair strategy j	Repair strategy k	Repair strategy l	Repair strategy m
DL1	42	40	40	40	36	36	36	36	36	36	36	36	36
DL2	34	34	34	34	34	34	34	34	34	34	34	34	34
DL3	33	38	44	32	38	38	38	38	38	38	38	44	38
DL4	34	34	34	34	34	34	34	34	34	36	34	36	36
DL5	35	32	32	38	38	38	38	38	38	36	41	37	41
DL6	36	37	38	37	38	38	38	37	38	39	38	38	37
DL7	34	34	34	34	34	34	34	34	34	36	34	34	34
DL8	42	>47	>47	>47	>47	>47	>47	>47	>47	44	>47	>47	>47

The following Figure 8.24 and Figure 8.25 show the evolution of flows during 3 days (Day 30, 31 and 32) as a result of applying repair strategies *a* and *m*, which are the most different strategies of the Pareto front of solutions (see Figure 8.21). As observed, there is no significant difference between these two repair strategies on Day 30. However, on Day 31, some road segments located near DL4 and DL5 still have higher flow of vehicles (in the order of 100veh/h) after applying repair strategy *m* compared to repair strategy *a* (less than 40veh/h). The reason is due to the repairs that were undertaken in DL4. In repair strategy *a*, DL4 was already (partially) open to traffic on Day 31, while in repair strategy *m*, DL4 was still closed to traffic which forced drivers to use these other road segments. In terms of total travel cost, drivers needed to follow a longer route compared to repair strategy *a* and this was already shown in Figure 8.21, when a higher value of total travel cost was observed in repair strategy *m* compared to the lower value of repair strategy *a*. In terms of connectivity, if diversion route is very long then some drivers may cancel the trip resulting in decrease in connectivity. This means that when a solution involves a long diversion route then there may be a significant trade-off between increasing connectivity (what is being connected) and increasing total travel time.

To sum up the results of this section, a Pareto front of 13 repair strategies were found. These solutions contained strategies with lower total travel cost values and higher connectivity values (e.g. the extreme repair strategy *a* of the Pareto front) and strategies with higher total travel cost values but lower connectivity values (e.g.

the extreme repair strategy *m* of the Pareto front). Regarding the opening-closing dates of damaged road segments, only two strategies (*a* and *j*) repaired the whole network within the simulation period (<47 days) while the rest of strategies needed more days to fully open damaged road segment DL8. It is ultimately a question for the decision-maker as to what specific strategy is chosen.

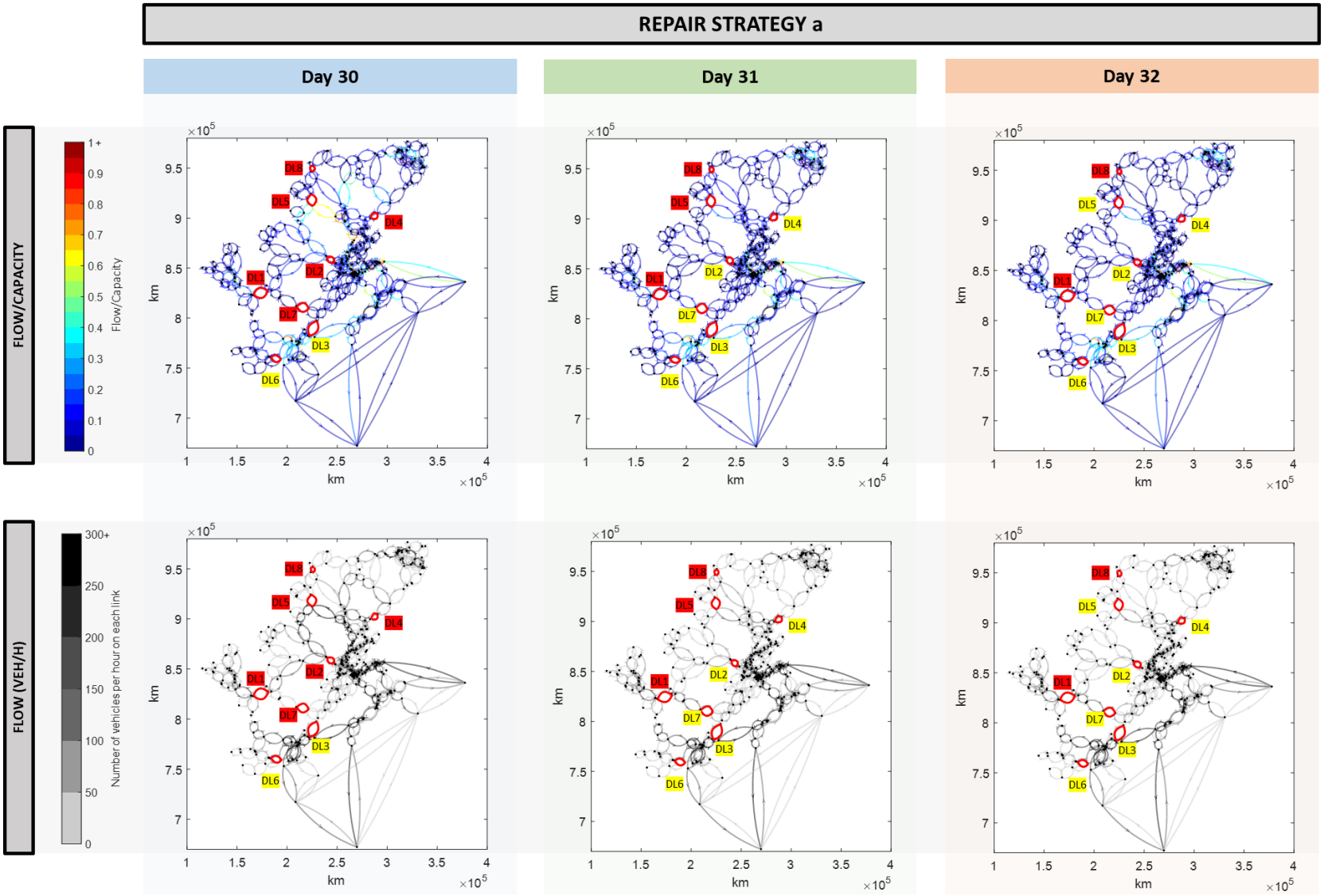

Figure 8.24. Scottish road network map showing the relation volume/capacity and flow on days 30, 31 and 32 during the peak period between 8am and 9am of REPAIR STRATEGY a. In red lines, the damaged road segments.
DLx road segment open to traffic; DLx partially open to traffic; DLx totally closed to traffic.

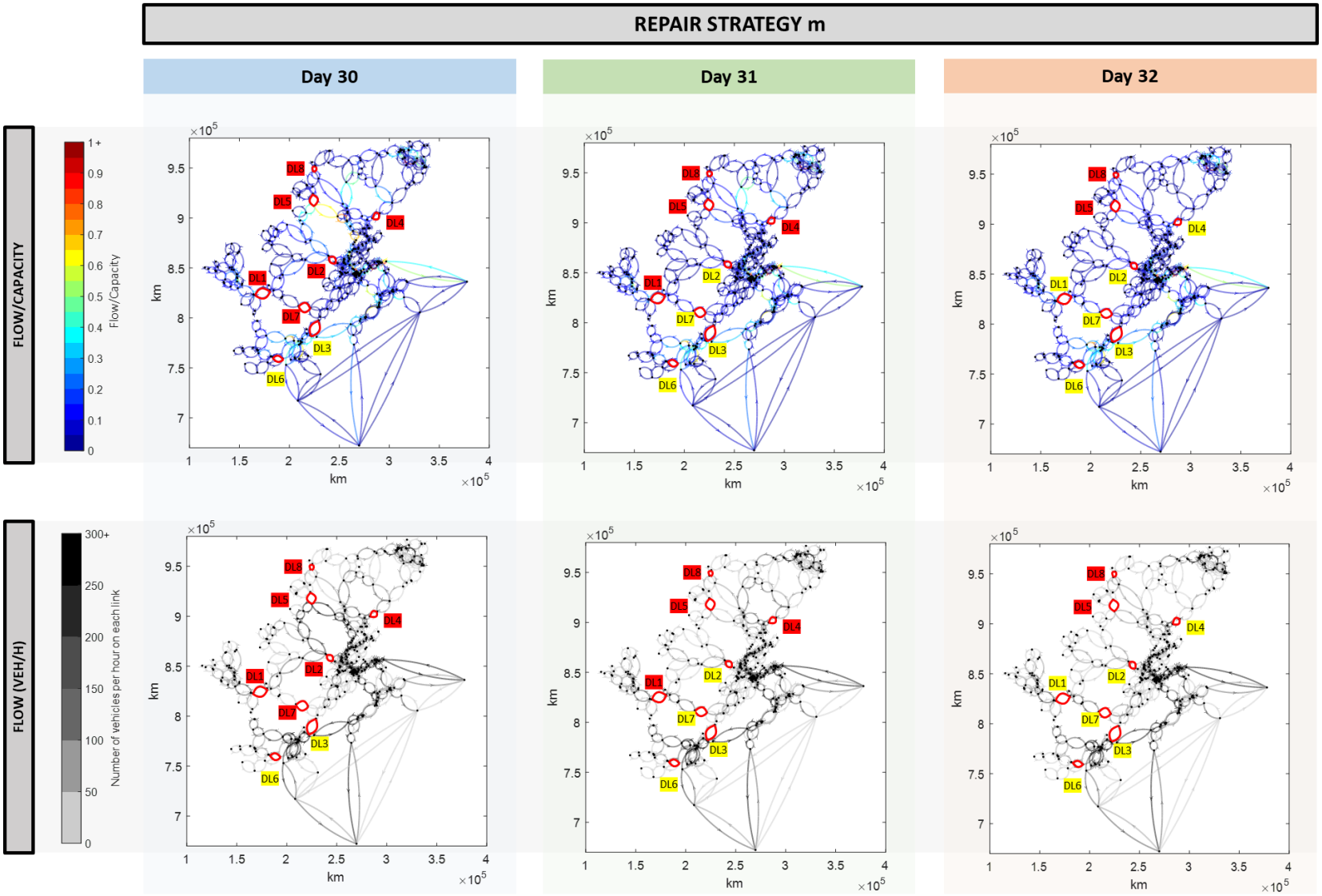

Figure 8.25. Scottish road network map showing the relation volume/capacity and flow on days 30, 31 and 32 during the peak period between 8am and 9am of REPAIR STRATEGY m. In red lines, the damaged road segments.
DLx road segment open to traffic; DLx partially open to traffic; DLx totally closed to traffic.

8.10. Calibration and validation of model parameters

The model proposed in this thesis includes a number of parameters that should be appropriately determined to reproduce the traffic flow characteristics and travel behaviour with the highest accuracy. Before employing the model in practice, it is important to calibrate it against real traffic data. There are several methods to calibrate the model but the most common approach is to minimise the difference between the model estimation and the real traffic data using some optimisation tools (Spiliopoulou *et al.*, 2015). Due to time limitations, the model applied in this chapter has not been calibrated and validated using real traffic data. Therefore, the aim of this section is to describe the procedure that should have been carried out.

The parameter estimation problem can be formulated as a nonlinear least-squares optimisation problem, which minimises the difference between model calculations and real traffic data. The measurable model output and the real measured traffic data consists of flows and mean speeds at certain network locations where data can be obtained. The procedure that can be used to obtain the optimal model parameters is included in Figure 8.26. Initially, the parameters of the model are assigned a random value. Then the model is simulated and the results (flow and speed) from the simulation are compared to the collected real traffic data. As mentioned before, a nonlinear least-squares error formulation is used to quantify the difference between model outputs and real data. This formulation is included in Equation (8.7).

$$Y = \sqrt{\frac{1}{t} \cdot \sum_{t=1}^{t_1-1} [x(t) - x'(t)]^2} \tag{8.7}$$

Where,

t, time (days).

t_1, User-defined time horizon.

$x(t)$, results from the model simulation (e.g. traffic flow, speed).

$x'(t)$, collected real traffic data (e.g. traffic flow, speed).

Y, difference between model simulation and real traffic data.

Then, if the error is below the desired user-defined value, the model parameters are the optimal for that specific case. If it is not, then the selected optimisation algorithm has to find new model parameters and repeat the exact process. Furhter research needs to be done in order to select the appropiate optimisation algorithm.

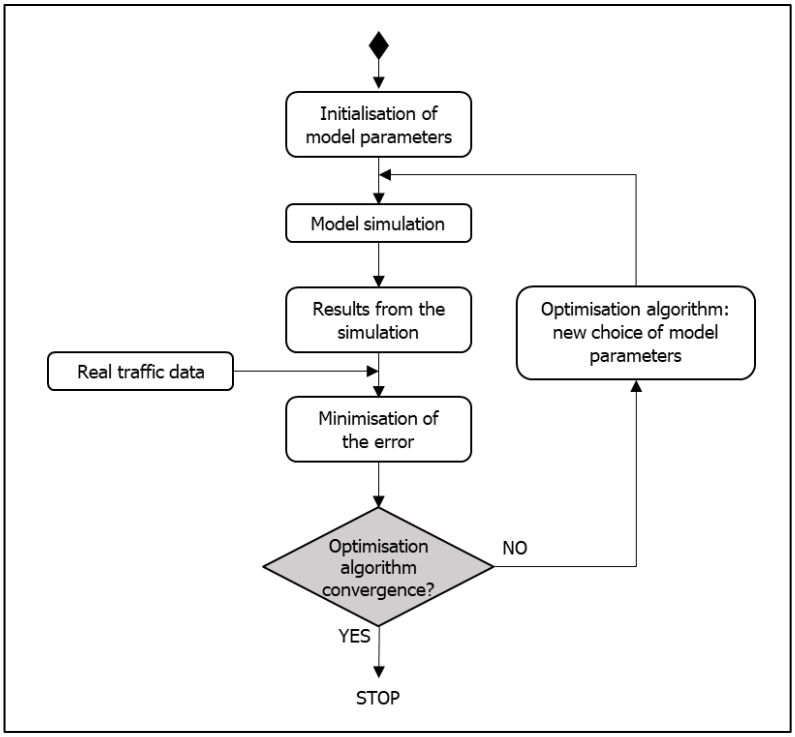

Figure 8.26. Model calibration procedure

8.11. Model limitations and future work

This section discusses potential limitations of the model application to a real case study. Note that these limitations are additional to those already indicated in the corresponding chapters that describe the model. Future work that aims to overcome these limitations is also included in this section.

(1) *Computational cost*. The model takes a significant amount of time to evaluate the consequences of a single repair strategy. Some of the reasons are explained as follows:

a. There is a large number of nodes, links and OD pairs that needs to be simulated for the Scottish case.

b. Large amount of pre-disruption data. This data is used by the post-disruption phase and contains all information that vehicles have been storing during the first 27 days (travel decisions, travel times, expected travel costs, stimulus values, probabilities associated with the selection of each option, on-board decisions, etc.). For this particular case, these files can reach almost 1GB of size, which means that the model has to access this file every time it needs data from the pre-disruption phase. The size of these files is proportional to the number of days that is being analysed, the number of OD pairs and the number of packets of vehicles. The bigger the size of these files, the more time the model takes to run. Also, the more vehicles on the network, the more time is required to get stable conditions and therefore, more days are needed on the pre-disruption phase.
c. Modules, such as the one that finds the shortest path between two nodes, requires analysing all nodes and links. In particular, the Dijkstra algorithm (1959) creates a tree of shortest paths from the starting node, the source, to all other points in the graph. Every time a packet of drivers use GPS navigation, the algorithm is run at each intersection or after a pre-defined amount of time. If there is a large number of nodes and links and drivers who use GPS systems, the computational time of the algorithm will be high.
d. The simulation of the warm-up and cool-down periods follows the same algorithm as the one that models drivers' behaviour during the peak period. It also consumes a lot of time and then the results do not have much use apart from filling the network of vehicles at the beginning and at the end of the simulation.

Future work needs to focus on improving the efficiency of the model so that it can be run faster. It can be done by: (a) Reducing the pre-disruption data that is transferred to the post-disruption phase so that the memory access cost is reduced; (b) Improving the efficiency of the mesoscopic traffic simulator algorithm as it has already mentioned in previous Chapter 5 so that the computational cost is reduced; (c) Research alternative algorithms that find the shortest route between two nodes

and analyse which one is more efficient in terms of computational cost. Recent reviews show the potential of alternative shortest path algorithms (Magzhan and Jani, 2013; Latuconsina and Purboyo, 2017; Lewis, 2020). The model can also be examined in order to see if the Dijkstra algorithm can be run fewer times and therefore reduce the running time; (d) The optimisation model does not need to be calculated for 60 generations as there is not a huge improvement on the last generations. Instead, the model could have stopped before as no further improvements would have been achieved.

(2) *Warm-up/Cool-down periods*. Apart from the computational cost mentioned in the previous point, these periods have been limited to 15 min before the simulation of the peak period and 30 min after. This means that after these 30 min, no more vehicles are entering the network. However, some vehicles are still travelling after this time (journey times can be even higher than 2hours). The model should have kept loading the network with inter-peak flow during the cool-down period until all vehicles entering the network during the period 8:00-9:00am reached their destination. However, due to computational costs, these periods were not extended and it was recognised as a limitation of this application of the model. This may have influenced the modelling results as the lack of vehicles of the network may have produced a reduction of journey times on those vehicles that were travelling with an "empty" network.

Future work should study other ways of incorporating the warm-up/cool down periods without running the RL traffic model for these vehicles. It also removes the need to store drivers' travel information between days. An option could be the assignment of vehicles of the warm-up/cool-down period using a user-equilibrium model so that it would speed up the running time. Another option to reduce the computational time is to stop the model when drivers that depart at the peak period arrive at their destinations. This means that the model does not simulate the movement of more vehicles of the cool-down period, even if these vehicles have not arrived yet to their destinations.

(3) *Multi-modal approach*. As already mentioned in Section 6.11 of Chapter 6, adding the extra option of 'not travelling by car' requires the understanding of existing alternative transport modes on the region. This requires data that is not easily

available and that is the reason why random probability distributions have been used to define the accessibility of certain nodes to alternative transport modes and the frequency of service. For this particular case, data from other transport modes such as buses and trains should be gathered and analysed. However, as the aim at this stage was not to develop a multi-modal approach, this work is out of the scope of this thesis. Future work should focus on incorporating a more sophisticated multi-model approach to the current model or collect data so that it can be used in the application to the case study.

(4) *Distribution of external travel information to drivers*. The author has not found previous studies that evidence the percentage of drivers that use pre-trip information or GPS navigation systems on their day-to-day journeys. Future work should study the drivers' usage of external travel information on Scottish regions via surveys.

(5) *Calibration/Validation.* The model needs to be calibrated to the traffic conditions that are applied and validated using real traffic data in order to be applicable to real life operations. The lack of time and available traffic data has made this process uncompleted. Future work should focus on gathering traffic data to calibrate the model and validate the results.

Other areas of future work should focus on the following points:

(a) *Role play scenario.* As this is first time that a RL traffic recovery model is applied to the Scottish road network, there is no benchmark to compare with. Alternatively, a role play scenario can be used to measure the effectiveness of the model. The same scenario simulated in this chapter can be provided to a transport asset manager and ask them to decide how to repair the network under such conditions. A comparison between the repair strategy proposed by the asset manager and the one that is provided in this model can be done. It may show that asset managers' decisions are (or not) near the optimal.

(b) *Past scenario simulation*. Similarly to the previous point, data from previous multi-day damage scenarios can be simulated (if enough data is available) and the decisions that transport authorities/managers took at that moment can be compared to the ones that would be obtained using the recovery model. It can show

if those past recovery decisions were the optimal or instead, alternative decisions could have been proposed.

(c) *Alternative output information.* The current model obtains the (near-) optimal repair strategy, maximising the performance of the network. However, transport authorities/operators may also be interested in knowing the number of repair teams that should be assigned to each damaged location whilst ensuring certain levels of network connectivity and without having a significant increase in total travel cost. This can also be obtained from this model if certain modifications are done, such as adding a new restriction to the optimisation formulation that ensure minimum levels of connectivity and limits maximum values of travel costs. Repair teams can also be transformed into monetary values, so that they can know the amount of money they have to invest in order to maintain certain levels of connectivity and travel times.

8.12. Conclusions

This chapter has presented the application of the proposed recovery model to a real case study: the Scottish road network. A landslide-based damage scenario was generated producing a reduction of road capacity on certain road segments. The aim of the proposed model was to find the optimal repair strategies that maximised network connectivity and minimised total travel costs. The algorithm used to solve the bi-objective optimisation model was the Non-dominated Sorting Genetic Algorithm (NSGA-II). Drivers' decisions were simulated using the improved reinforcement learning traffic model presented in this thesis. External information was also provided to some drivers so they could make more informed decisions. Results showed a Pareto front of 13 optimal repair strategies that could be used by transport authorities and managers to make more optimal decisions. These solutions have been found after running the optimisation model for 60 generations. These solutions contained strategies with lower total travel cost values and higher connectivity values (e.g. the extreme repair strategy *a* of the Pareto front) and strategies with higher total travel cost values but lower connectivity values (e.g. the extreme repair strategy *m* of the Pareto front). Regarding the opening-closing dates of damaged road segments, only

two strategies (*a* and *j*) repaired the whole network within the simulation period (<47 days) while the remaining strategies needed more days to fully open damaged road segment DL8.

To the best of the author's knowledge, this is the first time that a recovery model that incorporates a reinforcement learning traffic model is applied to a real network. Results show the potential of this model to find strategies that enhance the resilience of road networks. Transport authorities and operators can benefit from this model as it suggests a list of optimal strategies to repair the network when multiple road segments are damaged and limited resources are available. The model constitutes the first step towards the development of future models that improve road network recovery using AI techniques (i.e. machine learning – reinforcement learning) to simulate drivers' reactions after the implementation of repair strategies.

CHAPTER 9

Conclusions and further research

9.1. Completion of the aim and objectives

This research has successfully developed a model to optimise the recovery of road networks after concurrent road capacity-reducing incidents. The methodology to obtain the optimal network recovery combined four main modules: (1) damage scenario generator that identified which road segments were damaged; (2) an infrastructure repair model that simulated how resources repaired damaged road segments; (3) a reinforcement-learning traffic module that simulated how drivers reacted and made decisions after changing network conditions; and (4) an optimisation module that found the optimal repair strategies that minimised total travel cost and maximised network connectivity. The following objectives were achieved in this thesis:

- ✓ A systematic literature review of current road recovery models after disruptive events was developed. This helped to identify recovery models, learn how other authors have modelled damage to infrastructure, drivers' behaviour and the repair process. It also identified the potential research gaps of the current state-of-the-art. A review of previous metrics that measured the performance of the system and techniques to solve optimization problems were also examined.
- ✓ A resource allocation model has been successfully developed, allowing the assignment of repair resources to damaged places, the provision of a repair scheduling plan and the calculation of damage evolution and repair over time.
- ✓ The development of an event-based mesoscopic traffic model to simulate the movement of individual or groups of vehicles through links at an aggregate level (based on the macroscopic fundamental diagrams). A detailed

explanation of how this new algorithm was implemented was included. This could potentially be used as a starting point for other researchers to develop new mesoscopic traffic simulators.

- ✓ The reformulation of the previous reinforcement-learning traffic model by incorporating departure time differences between travel options and differentiating between favourable and unfavourable options. The new model also incorporated the additional travel option that allowed drivers to decide not to travel using their own car and use alternative transport modes or cancel the trip.
- ✓ The understanding of the impact of the 'learning rate' parameter of the RL traffic model on the global network performance by undertaking a sensitivity analysis.
- ✓ The modelling of the on-board drivers' decision-making process by introducing a triggering option when drivers faced disruptions and a route choice algorithm that helped drivers find alternative routes after disruptive events. The consequences of on-board decisions were also incorporated into the drivers' probability of selecting travel options.
- ✓ The incorporation of external travel information in the model that allowed drivers to make more informed decisions.
- ✓ The application of the recovery model to a real case scenario (Scottish road network), demonstrating that the model could potentially obtain the (near-) optimal repair strategies after disruptive events.

9.2. Synthesis of key conclusions

After developing the literature review in Chapter 2, it was concluded that current methodologies used in road recovery models were overly simplistic, especially when simulating the dynamics of traffic demand and drivers' decision-making in multi-day damage scenarios. The majority of models loaded traffic onto the road network under the user equilibrium assumption which assumed that all drivers had complete knowledge at any time of all travel costs of any route. However, shortly after a disruptive event, drivers did not have perfect knowledge of traffic conditions and therefore they could not select the route with the minimal travel cost on a congested

network. They could not anticipate how other drivers would behave and therefore equilibrium conditions might not be reached immediately after the impact.

In order to overcome these limitations, Chapter 3 proposed the modelling framework of a new recovery model. Two functionality metrics were also proposed to measure the effectiveness of each repair strategy: a traffic-related metric, which measured the total travel cost, and a connectivity metric, which measured the demand that was not satisfied. The optimisation algorithm (NSGA-II) were also proposed.

The generation of damage scenarios was presented in Chapter 4. The methodology used hazard susceptibility data which allowed the modeller to identify those road segments that were more vulnerable to be damaged by a hazard event. A damage state (minor, moderate, extensive and collapse) was also assigned to each damaged infrastructure and the state was quantified in units of repair resources-time. This method provided a systematic framework that allowed modellers the generation of new damage scenarios.

A new three-stage repair model was also included in Chapter 4 and it simulated the road network repair process. It provided a framework that calculated the evolution of road capacities over time as a result of the allocation of repair teams to damaged road segments and the evolution of damage over time.

An event-based mesoscopic traffic model was required to simulate the movement of vehicles through links at an aggregate level based on the macroscopic fundamental diagrams. A new algorithm was implemented to send vehicles to next links. The algorithm consisted of two loops: the main ' node' loop, which was used to visit each node of the network and observe if there were vehicles to be sent to new links, and the 'packet' loop, which was inside the node loop, whose aim was to send those packets that were waiting at this node to neighbouring links.

A departure time and route choice model, which applied the idea of the reinforcement-learning algorithm, was presented in Chapter 6. Based on the difference between the expected and perceived travel cost, the driver was able to update the probability that was associated to the selection of each travel option. If the consequences of the decision that that driver took at the beginning of the day were good, then this driver would have more chances of repeating the some travel option the next day. If the consequences were negative, then the driver would have

less probabilities of repeating the same travel option the next day. This model improved the previous one by formulating a new updating probability scheme that took into account departure time differences between travel options. The new travel option of 'not travelling by car' was also added for the first time in this RL traffic model. That was an advantage compared to previous models due to the fact that, after the impact of weather-related hazards, some areas might be completely isolated or the detour route set in place might be too long and drivers might decide not to travel by car on that day. Therefore, a more realistic simulation of drivers' decision-making, such as the one presented in this thesis, contributes to a better prediction of the impact of repair strategies on the network.

Further improvements were introduced in Chapter 7. An on-board algorithm was presented that allowed drivers to decide at each intersection if they wanted to remain on the main route or they preferred to re-route. If they chose to re-route, a new algorithm was implemented to select the alternative route based on the travel time spent on known routes in previous days. The model also allowed drivers to abandon their trip and go back to the origin node if certain conditions were met. The option probability functions of the RL traffic model were also reformulated in order to incorporate the impact of on-board travel decisions.

For the first time, a RL traffic model added the possibility of providing external travel information to drivers: at the origin of the trip (pre-trip information) or on-route (GPS navigation or VMS). The results of applying the model to the Sioux Falls Network demonstrated the importance of including the provision of external information to road users. This information supported drivers to make better travel decisions, especially when multiple road closures existed and a global improvement in the network performance was observed when information was provided.

The recovery model was also applied to a real network, which was the Scottish road network. The aim was to demonstrate that the recovery model could potentially be applied to real networks and consequently, to find (near-) optimal repair strategies that maximised network connectivity and minimised total travel cost. Results from the analysis showed a Pareto front of 13 repair strategies after running the optimisation model for 60 generations. Transport authorities and operators could benefit from this model as it suggested a list of optimal strategies to repair the network when multiple road segments were damaged and limited repair resources were available. The model

constituted the first step towards the development of future models to improve road network recoveries using Artificial Intelligence techniques to simulate drivers' reactions after the implementation of repair strategies.

9.3. Limitations and recommendations for further research

The understanding of the model's limitations and constraints is required to apply the recovery model effectively to real networks. Although some limitations and recommendations for future research have already been described at the end of each chapter, in this section, a summary of the most important ones is presented.

Regarding the damage scenario simulation, the difficulty in obtaining fragility curves for certain infrastructure under the impact of a specific type of hazard makes the application of this approach to this project difficult. In addition, data from previous hazard impacts were often scarce and modellers cannot easily use these data to predict future events. Hazard susceptibility data were used in this model to overcome this lack of fragility data. However, these data could only indicate which road segments were more likely to be damaged. The modeller still needed to define thresholds that differentiated between damaged and undamaged road segments. In addition, the damage state (minor, moderate, severe, complete) of each damaged road segment was also a limitation of the model and a hypothetical uniform probability distribution was proposed in this model. The benefit of the proposed model compared to others that just generate a hypothetical impact was the use of susceptibility data to generate more realistic scenarios. Further research needs to be done in the area of hazard scenario simulation of this model and to apply existing fragility data to generate more realistic scenarios.

This model only simulates damage on road networks from a single-hazard impact. A single-hazard approach was a good starting point to understand how individual or independent hazards affect road networks, but it is not sufficient to capture all interactions that multiple hazards might have. It could potentially underestimate the impact that multiple hazards could generate. Therefore, further work should develop a multi-hazard approach to generate future damage scenarios on road networks.

Regarding the infrastructure repair model, it only assumes a single task and one type of resource is required to completely repair a damaged road segment. Resources, which were grouped into teams, were assumed to have the same productivity and saturation levels, which is not realistic. Depending on the type of repairs that are required, some tasks might require more specialised equipment or personnel. The impact that this might have on the model results are variations in the actual schedule of repairs due to the requirement of more (or less) time to complete tasks. This limitation could be overcome if future models included more types of repair teams (with different levels of productivity and saturation) and more variety of tasks.

Potential weaknesses of the RL traffic model focus on the following aspects:

(a) *Everyday activities*. The traffic model is focussed on simulating the decision-making process of those drivers that travel every day (e.g. commuting). The model could also consider leisure-based activities but it might be unrealistic to think that a driver undertake this leisure-based trip repeatedly every day. Future research should study the possibility of including these activities considering that drivers might travel every "X" days and therefore the learning process should be established between these "X" days.

(b) *Multi-modal approach*. After the closure of multiple road segments, alternative modes of travel could also help to improve the recovery of disrupted networks. These were considered as an additional measure of redundancy. That was the reason why those models that predict travel behaviour also need to consider alternative transport modes. The goal of the current model was not to develop a multimodal approach, but it has been forced to introduce aspects that would require a more sophisticated multi-modal model to determine which drivers would choose alternative modes of transport under disrupted conditions. This was one of the limitations of the current model and further work should incorporate a more sophisticated multi-modal modelling approach.

(c) *Initial path set generation*. The current path set generation found the K-shortest free-flow paths for each OD pair. The problem was that there could be too much overlap between these K-shortest paths. This meant that the heterogeneity of paths could be very limited under disrupted conditions. Future research should

improve the path set generation so that it finds the K-shortest paths but penalises those paths that share some links.

(d) *System optimum*. The proposed method to simulate drivers' decision making was based on the principle that drivers tend to minimise their individual travel costs when choosing a travel option on each day. However, the provision of more advanced personalised information to drivers might allow road managers to guide drivers' decisions towards the minimisation of total travel times. This follows the principle of system optimum, which benefits the whole system instead of individual agents. From a global perspective, this approach is more in accordance to the priorities of transport managers. Therefore, an alternative method should be implemented in the current model that allows the application of the system optimum principles.

(e) *Calibration and validation of results*. The model needs to calibrate its parameters to the traffic conditions that are applied and validate the simulation results using real traffic data. The lack of time has made this process impossible to complete.

Computational cost. The global optimisation model incurs high computational costs due to the time required to evaluate of the impact of each repair strategy on drivers' travel decisions. Some reasons for the high computational time were: the size of the transport network, the large amount of data that characterises the pre-disruption phase, the modelling of the warm-up and cool-down periods following the same principles as the peak period, among others. To increase the usability of the current model, the computational efficiency has to be improved allowing faster evaluation of repair strategies. Future research should investigate alternatives to reduce the high computational time and make it more affordable, such as the improvement of the efficiency of the algorithm, the usage of more powerful computers or the implementation of parallel computing in other parts of the model. A user interface can also be developed, facilitating the usage of the model and making it more attractive for infrastructure managers.

9.4. Contribution of this research: implications for theory and practice

This research contributed to the current body of knowledge in the area of road transport restoration and traffic modelling in the following ways:

- The development of a systematic review of recovery models that have been applied to road transport networks. This allowed readers to understand what a road recovery model looked like and what the current state-of-the-art was in the field of road transport network restoration modelling. It provided a methodology to identify road recovery models that could be used by other researchers. Current gaps and areas of further research were also highlighted so that it could contribute to the development of future research projects.

- The formulation of a multi-objective optimisation model that was capable of determining optimal repair strategies involving the allocation of limited repair resources to damaged locations, maximising the network performance. The novelty of the proposed recovery model led to the integration of: (1) an improved reinforcement-learning traffic model that simulated how drivers learn from day-to-day and adapt their behaviour to network changes and (2) an infrastructure repair model that simulated how repairs were carried out based on pre-defined repair strategies.

- The implementation of an improved reinforcement-learning stochastic traffic model that simulated the decision-making process of drivers after network disruptions. It allowed a more realistic representation of how drivers progressively adapt their travel behaviour and choose their travel options day after day. The improvements that this model provided compared to previous ones include:
    (1) The provision of new information to drivers, avoiding the assumption of 'perfect knowledge' (user equilibrium) that previous traffic assignment models used.
    (2) The addition of on-board decisions that allowed drivers to re-route or abandon their trip if they face disrupted road segments. This acquired

great importance in recovery models especially when dealing with road incidents.

(3) A reformulation of the RL updating probability scheme for selecting travel options, which included departure time differences between travel options, the consequences of on-board travel decisions and the addition of external travel information.

(4) The idea that bad memories were stronger and had longer lasting effects than good ones and the degradation of memories over time.

(5) The addition of travel demand variations after disruptive events that previous learning-based traffic assignment models did not include.

- Application of the model to a real road network. In this case, the north of Scotland was chosen as a case study. The example demonstrated the success in the applicability of the model to real networks and the potential to influence decision making.

The model has an important academic contribution in the area of RL modelling applied to the road transport field. Particularly, the improvements of the proposed RL traffic model benefit the research community as it goes a step beyond the previous RL models that have been developed during the past years. It is a more realistic model of how drivers react and make travel decisions with(out) the occurrence of disruptions. The assumption of user equilibrium cannot be accepted as not all drivers have 'perfect knowledge' of traffic conditions immediately after a hazardous event and, therefore, future studies that model travel behaviour need to use modelling techniques, such as the one presented in this thesis, that avoid reaching equilibrium conditions after the impact. The provision of external travel information to drivers also constitutes an important area that cannot be omitted in future transport models. Depending on the distribution of information, drivers are able to make more informed travel decisions and therefore, this has an impact on the global performance of the network. From a global point of view, the methodology proposed in this thesis to develop the recovery model may serve as a blueprint for similar analyses and it can be considered as the starting point for developing more advanced models that allow

a closer representation of how repairs are undertaken and their impact on the real world, and contribution to improving the recovery of transport systems.

The proposed new road recovery model not only contributes to academic research, but it is an important contribution to practice. Its value lies in its potential to improve the efficiency of road transport recovery management in such scenarios where multiple road segments are damaged and repair resources are limited. In these situations, transport managers need to prioritise repairs and assign resources to damaged locations in an efficient way. The model is able to recommend road recovery plans and it can help network managers find repair strategies that repair damaged road segments in an optimal way and improve the restoration of the system functionality. In other words, the outputs of the model are beneficial for government agencies and network managers to evaluate the impact of recovery strategies on transport systems, to improve the system's resilience under economic constraints (limited repair resources), and to evaluate contingency plans for transport management.

The recovery model can also contribute, from a planning point of view, to identifying critical road segments that, if disrupted, would cause the greatest disruption to the network. These are the areas that either transport authorities and/or transport operators may need to make more robust by allocating more resources during the recovery process or providing more information to drivers so that they can make more informed decisions, avoiding potential congestion in these areas if disrupted.

The provision of travel information can also play an important role in the recovery of road networks. It is noted that drivers make more informed decisions when information is disseminated. The type of information that should be provided to drivers is a topic that needs to be studied more in detail because, depending on the information that is provided, congestion can be solved in one place but created in another location. ITS provides road managers with the possibility of influencing drivers' behaviour by managing the information that is provided to them. This is an area that network managers need to take advantage of as ultimately it will help to improve the recovery of road networks.

REFERENCES

Abdellaoui, M., Bleichrodt, H. and Paraschiv, C. (2007) 'Loss Aversion Under Prospect Theory: A Parameter-Free Measurement', *Management Science*, 53(10), pp. 1659–1674. doi: 10.1287/mnsc.1070.0711.

Abdulhai, B. and Kattan, L. (2003) 'Reinforcement learning: Introduction to theory and potential for transport applications', *Canadian Journal of Civil Engineering*, 30(6), pp. 981–991. doi: 10.1139/l03-014.

Abdullah, B., Pringle, R. and Karakuls, G. J. (2003) 'Reinforcement Learning for True Adaptive Traffic Signal Control', *ASCE Journal of Transportation Engineering*, 129(3), pp. 278–285.

Abraham, A. and Jain, L. (2005) 'Evolutionary Multiobjective Optimization', in *Evolutionary Multiobjective Optimization*. London: Springer-Verlag, pp. 1–6. doi: 10.1007/1-84628-137-7_1.

de Abreu e Silva, J., de Oña, J. and Gasparovic, S. (2017) 'The relation between travel behaviour, ICT usage and social networks. The design of a web based survey', *Transportation Research Procedia*, 24, pp. 515–522. doi: 10.1016/j.trpro.2017.05.482.

Al-Rubaee, R. H. (2012) *A conceptual model to effectively prioritise recovery of roads damaged by natural/man-made disasters*. University of Birmingham. Available at: http://ethos.bl.uk/OrderDetails.do?uin=uk.bl.ethos.558932.

Alba, E. (2005) *Parallel Metaheuristics: A new class of algorithms*. New Jersey: Wiley Interscience.

Anderson, M., Bjork, R. and Bjork, E. (1994) 'Remembering can cause forgetting: retrieval dynamics in long-term memory', *Journal of Experimental psychology: learning memory and cognition*, 20(5), pp. 1063–1087.

Applied Technology Council (1985) *Earthquake damage evaluation data for California*. Redwood City CA. Available at: https://www.atcouncil.org/pdfs/atc13.pdf.

Arrighi, C. *et al.* (2019) 'Preparedness against mobility disruption by floods', *Science of the Total Environment*. The Authors, 654, pp. 1010–1022. doi: 10.1016/j.scitotenv.2018.11.191.

Aydin, N. Y. *et al.* (2018) 'Framework for improving the resilience and recovery of transportation networks under geohazard risks', *International Journal of Disaster Risk Reduction*. Elsevier Ltd, 31(July), pp. 832–843. doi: 10.1016/j.ijdrr.2018.07.022.

Barker, K., Ramirez-Marquez, J. E. and Rocco, C. M. (2013) 'Resilience-based network component importance measures', *Reliability Engineering & System Safety*. Elsevier, 117, pp. 89–97. doi: 10.1016/j.ress.2013.03.012.

Baroud, H. *et al.* (2014) 'Stochastic measures of network resilience: applications to waterway commodity flows', *Risk Analysis*, 34(7), pp. 1317–1335. doi: 10.1111/risa.12175.

Bartin, B. (2019) 'Use of learning classifier systems in microscopic toll plaza simulation models', *IET Intelligent Transport Systems*, 13(5), pp. 860–869. doi: 10.1049/iet-its.2018.5121.

Barzegar, S. *et al.* (2011) 'Formalized learning automata with adaptive fuzzy coloured Petri net; an application specific to managing traffic signals', *Scientia Iranica*, 18(3), pp. 554–565. doi: 10.1016/j.scient.2011.04.007.

Basavaraj, V. V. *et al.* (2017) 'Algorithm to prioritize the restoration of a multiple facility, multiple-hazard road network', *Proceedings of the Institution of Mechanical Engineers, Part O: Journal of Risk and Reliability*, 231(3), pp. 221–231. doi: 10.1177/1748006X17693484.

Baumeister, R. F. *et al.* (2001) 'Bad is stronger than good.', *Review of General Psychology*, 5(4), pp. 323–370. doi: 10.1037//1089-2680.5.4.323.

Bazzan, A. L. C. and Grunitzki, R. (2016) 'A multiagent reinforcement learning approach to en-route trip building', in *2016 International Joint Conference on Neural Networks (IJCNN)*. IEEE, pp. 5288–5295. doi: 10.1109/IJCNN.2016.7727899.

Bekhor, S., Ben-Akive, M. and Ramming, S. (2002) 'Adaptation of Logit Kernel to route choice situation', *Transportation Research Record No 1805*, 1805, pp. 78–85.

Ben-Akiva, M. *et al.* (1998) 'DynaMIT: a simulation-based system for traffic prediction', in *Proceedings of the DACCORD Short-term Forecasting Workshop*, pp. 1–12.

Ben-Akiva, M., Choudhury, C. and Toledo, Tomer (2009) 'Integrated lane-changing models', *Transport Simulation*.

Ben-Akiva, M., Choudhury, C. and Toledo, T. (2009) 'Lane Changing Models', in *Transport Simulation: Beyond Traditional Approaches*. Available at: www.geoconnexion.com.

Berdica, K. (2002) 'An introduction to road vulnerability: What has been done, is done and should be done', *Transport Policy*, 9(2), pp. 117–127.

Bevrani, K. and Chung, E. (2012) 'An Examination of the Microscopic Simulation Models to Identify Traffic Safety Indicators', *International Journal of Intelligent Transportation Systems Research*, 10(2), pp. 66–81. doi: 10.1007/s13177-011-0042-0.

Billah Kushal, T. R. and Illindala, M. S. (2020) 'Correlation-based feature selection for resilience analysis of MVDC shipboard power system', *International Journal of Electrical Power & Energy Systems*, 117, p. 105742. doi: 10.1016/j.ijepes.2019.105742.

Bliemer, M. *et al.* (2013) 'Requirements for Traffic Assignment Models for Strategic Transport Planning : A Critical Assessment', in *Australasian Transport Research Forum 2013 Proceedings*, pp. 1–25.

Blier, L., Wolinski, P. and Ollivier, Y. (2019) 'Learning with random learning rates', *Joint European Conference on Machine Learning and Knowledge Discovery in Databases*, pp. 449–464.

Bocchini, P. (2013) 'Computational procedure for the assisted multi-phase resilience-oriented disaster management of transportation systems', in *Safety, Reliability, Risk and Life-Cycle Performance of Structures and Infrastructures - Proceedings of the 11th International Conference on Structural Safety and Reliability, ICOSSAR 2013*. Department of Civil and Environmental Engineering, ATLSS Engineering Research Center, Lehigh University, Bethlehem, PA, United States: CRC Press, pp. 581–588. doi: 10.1201/b16387-86.

Bocchini, P. and Frangopol, D. M. (2011) 'A stochastic computational framework for the joint transportation network fragility analysis and traffic flow distribution under extreme events', *Probabilistic Engineering Mechanics*. Elsevier Ltd, 26(2), pp. 182–193. doi: 10.1016/j.probengmech.2010.11.007.

Bocchini, P. and Frangopol, D. M. (2012a) 'Optimal Resilience- and Cost-Based Postdisaster Intervention Prioritization for Bridges along a Highway Segment', *Journal of Bridge Engineering*, 17(1), pp. 117–129. doi: doi:10.1061/(ASCE)BE.1943-5592.0000201.

Bocchini, P. and Frangopol, D. M. (2012b) 'Restoration of Bridge Networks after an Earthquake: Multicriteria Intervention Optimization', *Earthquake Spectra*. Earthquake Engineering Research Institute, 28(2), pp. 426–455. doi: 10.1193/1.4000019.

Bocchini, P. and Frangopol, D. M. (2013) 'Connectivity-Based Optimal Scheduling for Maintenance of Bridge Networks', *Journal of Engineering Mechanics*, 139(6), pp. 760–769. doi: 10.1061/(asce)em.1943-7889.0000271.

Bombol, K., Koltovska, D. and Veljanovska, K. (2012) 'Application of Reinforcement Learning as a Tool of Adaptive Traffic Signal Control on Isolated Intersections', *IACSIT International Journal of Engineering and Technology*, 4(2), pp. 126–129.

Brabb, E. (1984) 'Innovative Approaches for Landslide Hazard Evaluation', in *IV International Symposium on Landslides*. Toronto, Canada, pp. 307–323.

Brander, A. W. and Sinclair, M. C. (1996) 'A Comparative Study of k-Shortest Path Algorithms', in *Performance Engineering of Computer and Telecommunications Systems*. London: Springer London, pp. 370–379. doi: 10.1007/978-1-4471-1007-1_25.

Brenner, T. (2004) 'Agent Learning Representation - Advice in Modelling Economic Learning', *Papers on Economics & Evolution, Max Planck Institute for Research into Economic Systems*.

Bruneau, M. *et al.* (2003) 'A Framework to Quantitatively Assess and Enhance the Seismic Resilience of Communities', *Earthquake Spectra*, 19(4), pp. 733–752. doi: 10.1193/1.1623497.

Bureau of Public Roads (1964) 'Traffic assignment manual'. Washington, DC.

Burghout, W. (2004) *Hybrid microscopic-mesoscopic traffic simulation*. Royal Institute of Technology.

Burghout, W., Koutsopoulos, H. N. and Andreasson, I. (2006) 'A discrete-event mesoscopic traffic simulation model for hybrid traffic simulation', in *IEEE Intelligent Transportation Systems Conference*. Toronto, Canada, pp. 1102–1107.

Bush, R. R. and Mosteller, F. (1951) 'A Mathematical Model for Simple Learning', in *Selected Papers of Frederick Mosteller*. New York, NY: Springer New York, pp. 221–234. doi: 10.1007/978-0-387-44956-2_12.

Buşoniu, L. *et al.* (2010) 'Online least-squares policy iteration for reinforcement learning control', in *Proceedings of the 2010 American Control Conference*.

Caliper Corporation (2008) 'TransCAD manual: Travel demand modeling with TransCAD'. Boston.

Carlos Lam, J. *et al.* (2020) 'Impact Assessment of Extreme Hydrometeorological Hazard Events on Road Networks', *Journal of Infrastructure Systems*, 26(2), p. 04020005. doi: 10.1061/(ASCE)IS.1943-555X.0000530.

Çelik, M. (2016) 'Network restoration and recovery in humanitarian operations: Framework, literature review, and research directions', *Surveys in Operations Research and Management Science*. Elsevier B.V., 21(2), pp. 47–61. doi: 10.1016/j.sorms.2016.12.001.

Cetin, N. (2005) *Large-Scale Parallel Graph-Based Simulations*. ETH Zurich.

Chakirov, A. and Fourie, P. J. (2014) *Enriched Sioux Falls Scenario with Dynamic And Disaggregate Demand*.

Chang, G., Mahmassani, H. S. and Herman, R. (1985) 'Macroparticle Traffic Simulation Model To Investigate Peak-Period Commuter Decision Dynamics', *Transportation Research Record*, pp. 107–121.

Chang, L. *et al.* (2010) *Transportations systems modeling and applications in earthquake engineering*.

Chang, L. *et al.* (2012) 'Bridge Seismic Retrofit Program Planning to Maximize Postearthquake Transportation Network Capacity', *Journal of Infrastructure Systems*, 18(2), pp. 75–88. doi: 10.1061/(asce)is.1943-555x.0000082.

Chang, S. E. (2003) 'Transportation planning for disasters: An accessibility approach', *Environment and Planning A*, 35(6), pp. 1051–1072. doi: 10.1068/a35195.

Chang, S. E. (2016) 'Socioeconomic Impacts of Infrastructure Disruptions', *Natural Hazard Science*, 1(May), pp. 1–31. doi: 10.1093/acrefore/9780199389407.013.66.

Chen, B. Y. *et al.* (2020) 'Efficient algorithm for finding k shortest paths based on re-optimization technique', *Transportation Research Part E: Logistics and Transportation Review*, 133, p. 101819. doi: 10.1016/j.tre.2019.11.013.

Chen, L. and Miller-Hooks, E. (2012) 'Resilience: An Indicator of Recovery Capability in Intermodal Freight Transport', *Transportation Science*, 46(1), pp. 109–123. doi: 10.1287/trsc.1110.0376.

Chen, Y. and Tzeng, G. (1999) 'A fuzzy multi-objective model for reconstructing post-earthquake road-network by genetic algorithm', *International Journal of Fuzzy Systems*, 1(2), pp. 85–95.

Chiu, Y. *et al.* (2011) *DynusT 3.0 User's Manual*.

Cimellaro, G. P., Reinhorn, A. M. and Bruneau, M. (2010) 'Framework for analytical quantification of disaster resilience', *Engineering Structures*. Elsevier Ltd, 32(11), pp. 3639–3649. doi: 10.1016/j.engstruct.2010.08.008.

Connor, A. M. and Shah, A. (2014) 'Resource allocation using metaheuristic search', in *Proceedings of the Fourth international Conference on Computer Science and Information Technology*. doi: 10.5121/csit.2014.4230.

Cosslett, S. (1977) 'The trip timing decision for travel to work by automobile', in McFadden (ed.) *Demand Model Estimation and validation*. Berkeley: Special Report UCB-ITS-SR-77-9, pp. 201–221.

Cotta, C., Talbi, E. G. and Alba, E. (2005) 'Parallel Hybrid Metaheuristics', *Parallel Metaheuristics: A New Class of Algorithms*, (November 2016), pp. 347–370. doi: 10.1002/0471739383.ch15.

Cui, Y. *et al.* (2017) 'Review: Multi-objective optimization methods and application in energy saving', *Energy*. Elsevier Ltd, 125, pp. 681–704. doi: 10.1016/j.energy.2017.02.174.

Dalezios, N. R. (2017) *Environmental hazards methodologies for risk assessment and management*. IWA Publishing.

Dalziell, E. (1998) *Risk assessment methods in road network evaluation: a study of the impact of natural hazards on the Desert Road, New Zealand*. University of Canterbury. Available at: http://ir.canterbury.ac.nz/handle/10092/5633.

Darwin, C. (1859) *On the origin of species by means of natural selection, or the preservation of favoured races in the struggle for life*. London.

Deb, K. *et al.* (2000) 'A Fast Elitist Non-dominated Sorting Genetic Algorithm for Multi-objective Optimization: NSGA-II', in, pp. 849–858. doi: 10.1007/3-540-45356-3_83.

Decò, A., Frangopol, D. M. and Bocchini, P. (2013) 'Pre-event probabilistic assessment of seismic resilience of bridge highway segments', in *Safety, Reliability, Risk and Life-Cycle Performance of Structures and Infrastructures - Proceedings of the 11th International Conference on Structural Safety and Reliability*, pp. 621–628.

Department for Transport (2017) 'TEMPRO—Trip End Model Presentation Program'. Department for Transport. Available at: https://www.gov.uk/government/publications/tempro-downloads.

Department for Transport (no date) *Guidance on Accessibility Planning in LTPs. Technical Annex 6*.

Dia, H., Harney, D. and Boyle, A. (2001) 'Dynamics of drivers'route choice decisions under advanced traveller information systems', *Road and Transport Research*, 10(4).

Dijkstra, E. W. (1959) 'A Note on Two Probles in Connexion with Graphs', *Numerische Mathematik*, 1(1), pp. 269–271. doi: 10.1007/BF01386390.

Duffy, J. (2006) 'Agent-based models and human subject experiments', in *Handbook of computational economics 2*, pp. 949–1011.

Duque, P. M. and Sörensen, K. (2011) 'A GRASP metaheuristic to improve accessibility after a disaster', *OR Spectrum*, 33(3), pp. 525–542. doi: 10.1007/s00291-011-0247-2.

Ebbinghaus, H. (1880) 'Ueber das Gedächtniß', *Passau: Passavia Universitätsverlag*.

Ekosgen (2016) *Argyll and Bute Transport Connectivity and Economy. Research Report*. Available at: http://www.hie.co.uk/regional-information/economic-reports-and-research/archive/argyll-and-bute-transport-connectivity-and-economy-research.html.

Emmerink, R. H. M. *et al.* (1996) 'Variable message signs and radio traffic information: an integrated empirical analysis of drivers' route choice behaviour', *Transportation Research Part A*, pp. 135–153.

Estes, W. (1950) 'Toward a statistical theory of learning', *Psychological review*, pp. 94–107.

Faturechi, R. and Miller-Hooks, E. (2014a) 'Measuring the performance of transportation infrastructure systems in disasters: A comprehensive review', *ASCE Journal of Infrastructure Systems*, 21(1), pp. 1–15. doi: 10.1061/(ASCE)IS.1943-555X.0000212.

Faturechi, R. and Miller-Hooks, E. (2014b) 'Travel time resilience of roadway networks under disaster', *Transportation Research Part B: Methodological*. Elsevier Ltd, 70, pp. 47–64. doi: 10.1016/j.trb.2014.08.007.

Federal Highway Administration (2004) *Traffic Analysis Toolbox Volume III: Guidelines for Applying Traffic Microsimulation Modeling Software*.

FEMA, F. E. M. A. (2013) *HAZUS-MH. Technical manual*, *Department of Homeland Security*. Washington, DC.

Feng, C.-M. and Wang, T. (2003) 'Highway Emergency Rehabilitation Scheduling in Post-Earthquake 72 Hours', *Journal of the Eastern Asia Society for Transportation Studies*, 5, pp. 3276–3285.

Ferreira, F. (2010) 'Dynamic Response Recovery Tool for Emergency Response within State Highway Organisations in New Zealand'.

Fishburn, P. C. and Kochenberger, G. A. (1979) 'Two-piece Von Neumann-Morgenstern utility functions', *Decision Sciences*, 10(4), pp. 503–518. doi: 10.1111/j.1540-5915.1979.tb00043.x.

Francis, R. and Bekera, B. (2014) 'A metric and frameworks for resilience analysis of engineered and infrastructure systems', *Reliability Engineering and System Safety*. Elsevier, 121, pp. 90–103. doi: 10.1016/j.ress.2013.07.004.

Furuta, H. *et al.* (2008) 'Optimal Restoration Scheduling of Damaged Networks Under Uncertain Environment by Using Improved Genetic Algorithm', *Tsinghua Science and Technology*, 13(SUPPL. 1), pp. 400–405. doi: 10.1016/S1007-0214(08)70181-0.

Gaver, D. P. (1968) 'Headstart Strategies for Combating Congestion', *Transportation Science*, 2(2), pp. 172–181. doi: 10.1287/trsc.2.2.172.

Gerami Matin, A., Vatani Nezafat, R. and Golroo, A. (2017) 'A comparative study on using meta-heuristic algorithms for road maintenance planning: Insights from field study in a developing country', *Journal of Traffic and Transportation Engineering (English Edition)*, 4(5), pp. 477–486. doi: 10.1016/j.jtte.2017.06.004.

Gibbons, A. (1985) *Algorithmic graph theory*. Cambridge: Cambridge University Press.

Gill, J. C. and Malamud, B. D. (2016) 'Hazard interactions and interaction networks (cascades) within multi-hazard methodologies', *Earth System Dynamics*, 7(3), pp. 659–679. doi: 10.5194/esd-7-659-2016.

Gläscher, J. *et al.* (2010) 'States versus Rewards: Dissociable Neural Prediction Error Signals Underlying Model-Based and Model-Free Reinforcement Learning', *Neuron*, 66(4), pp. 585–595. doi: 10.1016/j.neuron.2010.04.016.

Godart, B. and Vassie, P. R. (2001) *Bridge Management Systems: Extended Review of Existing Systems and Outline framework for a European System*.

Goldberg, D. E. (1989) *Genetic algorithms in search, optimization, and machine learning*. Addison-Wesley Publishing Company. doi: 10.5860/CHOICE.27-0936.

Gottman, J. (1995) *Why marriages succeed or fail*. New York: Simon & Schuster.

Greenshields, B. D. (1933) 'The Photographic Method of studying Traffic Behaviour', in *Proceedings of the 13th Annual Meeting of the Highway Research Board*.

Gulde, R. *et al.* (2020) 'Deep Reinforcement Learning using Cyclical Learning Rates', *ArXiv preprint arXiv:2008.01171*.

Habib, S. B. A. (2012) *Distributed algorithms in autonomous and heterogeneous networks*. Université d'Avignon.

Hackl, J., Adey, B. T. and Lethanh, N. (2018) 'Determination of Near-Optimal Restoration Programs for Transportation Networks Following Natural Hazard Events Using Simulated Annealing', *Computer-Aided Civil and Infrastructure Engineering*, 33(8), pp. 618–637. doi: 10.1111/mice.12346.

Haith, A. M. and Krakauer, J. W. (2013) 'Model-Based and Model-Free Mechanisms of Human Motor Learning', in *Progress in Motor Control. Advances in Experimental Medicine and Biology*. New York, NY: Springer New York, pp. 1–21. doi: 10.1007/978-1-4614-5465-6_1.

Henry, D. and Ramirez-Marquez, J. E. (2012) 'Generic metrics and quantitative approaches for system resilience as a function of time', *Reliability Engineering and System Safety*. Elsevier, 99, pp. 114–122. doi: 10.1016/j.ress.2011.09.002.

Highways Agency (1997) *Design Manual for Roads and Bridges (DMRB). DMRB 46/97. Assessment and preparation of road schemes. Assessment of road schemes. Traffic flow ranges for use in the assessment of new rural roads*.

Highways Agency (1999) *Design Manual for Roads and Bridges (DMRB). DMRB TA 79/99*.

HM Government (2002) *The Traffic Signs Regulations and General Directions order*. UK.

Holland, J. H. (1975) *Adaptation in Natural and Artificial Systems*. University of Michigan Press.

Hoogendoorn, S. and Knoop, V. (2013) 'Traffic flow theory and modelling', in *The transport system and transport policy: an introduction*. Cheltenham, UK: Edward Elgar Publishing Limited, pp. 125–159.

Hosny, M. I. (2010) *Investigating heuristic and meta-heuristic algorithms for solving pickup and delivery problems*. Cardiff University.

Hosseini, S., Barker, K. and Ramirez-Marquez, J. E. (2016) 'A review of definitions and measures of system resilience', *Reliability Engineering and System Safety*, 145, pp. 47–61. doi: 10.1016/j.ress.2015.08.006.

Huck, A., Monstadt, J. and Driessen, P. (2020) 'Building urban and infrastructure resilience through connectivity: An institutional perspective on disaster risk management in Christchurch, New Zealand', *Cities*, 98, p. 102573. doi: 10.1016/j.cities.2019.102573.

Hussain, K. *et al.* (2018) 'Metaheuristic research: a comprehensive survey', *Artificial Intelligence Reivew*.

ImageCat, I. (2005) 'REDARS'. Available at: http://www.imagecatinc.com/.

IPCC (2014) *Intergovernmental Panel on Climate Change, Fifth Assessment Report (AR5)*. Geneva.

Jamal, S. and Habib, M. A. (2020) 'Smartphone and daily travel: How the use of smartphone applications affect travel decisions', *Sustainable Cities and Society*, 53, p. 101939. doi: 10.1016/j.scs.2019.101939.

Janner, M. *et al.* (2019) 'When to Trust Your Model: Model-Based Policy Optimization', in *33rd Conference on Neural Information Processing Systems (NeurIPS 2019)*.

Jayakrishnan, R., Mahmassani, H. S. and Hu, T. Y. (1994) 'An evaluation tool for advanced traffic information and management systems in urban networks', *Transportation Research Part C*. doi: 10.1016/0968-090X(94)90005-1.

Jenelius, E., Mattsson, L.-G. and Levinson, D. (2011) 'Traveler delay costs and value of time with trip chains, flexible activity scheduling and information', *Transportation Research Part B: Methodological*, 45(5), pp. 789–807. doi: 10.1016/j.trb.2011.02.003.

Kahneman, D. and Tversky, A. (1979) 'Prospect Theory: An Analysis of Decision under Risk', *Econometrica*, 47(2), p.

263. doi: 10.2307/1914185.

Kandil, A. and El-Rayes, K. (2006) 'Parallel Genetic Algorithms for Optimizing Resource Utilization in Large-Scale Construction Projects', *Journal of Construction Engineering and Management*, 132(5), pp. 491–498. doi: 10.1061/(ASCE)0733-9364(2006)132:5(491).

Kansky, K. J. (1963) *Structure of transportation networks: relationships between network geometry and regional characteristics*. University of Chicago.

Karamlou, A. and Bocchini, P. (2014) 'Optimal bridge restoration sequence for resilient transportation networks', in *Structures Congress 2014 - Proceedings of the 2014 Structures Congress*. Department of Civil and Environmental Engineering, Advanced Technology for Large Structural Systems (ATLSS) Engineering Research Center, Lehigh University, 117 ATLSS Drive, Bethlehem, PA, United States, pp. 1437–1447. doi: 10.1061/9780784413357.127.

Karamlou, A. and Bocchini, P. (2016) 'Sequencing algorithm with multiple-input genetic operators: Application to disaster resilience', *Engineering Structures*. Elsevier Ltd, 117, pp. 591–602. doi: 10.1016/j.engstruct.2016.03.038.

Karamlou, A., Bocchini, P. and Christou, V. (2016) 'Metrics and algorithm for optimal retrofit strategy of resilient transportation networks', in *Maintenance, monitoring, safety, risk and resilience of bridges and bridge networks*, pp. 1121–1128.

Karlaftis, M. G., Kepaptsoglou, K. and Lambropoulos, S. (2007) 'Fund allocation for transportation network recovery following natural disasters', *Journal of Urban Planning and Development*, 133(1), pp. 82–89. Available at: http://ascelibrary.org/doi/abs/10.1061/(ASCE)0733-9488(2007)133:1(82).

Kasmalkar, I. G. *et al.* (2020) 'When floods hit the road: Resilience to flood-related traffic disruption in the San Francisco Bay Area and beyond', *Science Advances*, 6(32), pp. 1–9. doi: 10.1126/sciadv.aba2423.

Kaviani, A. *et al.* (2018) *A model for multi-class road network recovery scheduling of regional road networks*, *Transportation*. Springer US. doi: 10.1007/s11116-017-9852-5.

Kilanitis, I. and Sextos, A. (2019) 'Integrated seismic risk and resilience assessment of roadway networks in earthquake prone areas', *Bulletin of Earthquake Engineering*. Springer Netherlands, 17(1), pp. 181–210. doi: 10.1007/s10518-018-0457-y.

Konstantinidou, M. A., Kepaptsoglou, K. L. and Karlaftis, M. G. (2014) 'Transportation Network Post-Disaster Planning and Management : A Review Part I : Post-Disaster Transportation Network Performance', *International Journal of Transportation*, 2(3), pp. 1–16. doi: 10.14257/ijt.2014.2.3.01.

Kora, P. and Yadlapalli, P. (2017) 'Crossover operators in Genetic Algorithms: a review', *International Journal of Computer Applications*, 162.

Koski, H. A. (2002) 'Information and communication technologies in transport', *SOcial change and sustainable transport*, pp. 43–47.

Kristoffersson, I. and Engleson, L. (2009) 'A dynamic transportation model for the Stockholm area: Implementation issues regarding departure time choice and OD-pair reduction', *Networks and Spatial Economics*, 9(4), pp. 551–573.

Kurauchi, F. *et al.* (2009) 'Network Evaluation Based on Connectivity Vulnerability', *Transportation and Traffic Theory 2009: Golden Jubilee*, pp. 637–649. doi: 10.1007/978-1-4419-0820-9_31.

Kurdi, B., Gershman, S. J. and Banaji, M. R. (2019) 'Model-free and model-based learning processes in the updating of explicit and implicit evaluations', *Proceedings of the National Academy of Sciences*, 116(13), pp. 6035–6044. doi: 10.1073/pnas.1820238116.

Latuconsina, R. and Purboyo, T. W. (2017) 'Shortest Path Algortihms: State of the Art', *International Journal of Applied Engineering Research*, 12(23).

Leblanc, L. J. (1975) 'Algorithm for the Discrete Network Design Problem.', *Transportation Science*, 9(3), pp. 183–199. doi: 10.1287/trsc.9.3.183.

Lei, X. and Shi, Z. (2004) 'Overview of multi-objective optimization methods', *Journal of Systems Engineering and Electronics*, 15(2), pp. 142–146.

Leonard, D. R., Power, P. and Taylor, N. B. (1989) 'CONTRAM: structure of the model', *Transportation Research Laboratory*. Crowthorn.

Lertworawanich, P. (2012) 'Highway network restoration after the great flood in Thailand', *Natural Hazards*, 64(1), pp. 873–886. doi: 10.1007/s11069-012-0278-2.

Lewis, R. (2020) 'Algorithms for Finding Shortest Paths in Networks with Vertex Transfer Penalties', *Algorithms*, 13(11), p. 269. doi: 10.3390/a13110269.

Li, Z. *et al.* (2019) 'Resilience-based transportation network recovery strategy during emergency recovery phase under uncertainty', *Reliability Engineering and System Safety*. Elsevier Ltd, 188(April), pp. 503–514. doi: 10.1016/j.ress.2019.03.052.

Liao, T. Y., Hu, T. Y. and Ko, Y. N. (2018) 'A resilience optimization model for transportation networks under disasters', *Natural Hazards*, 93(1), pp. 469–489. doi: 10.1007/s11069-018-3310-3.

Lu, G. *et al.* (2016) 'An optimal schedule for urban road network repair based on the greedy algorithm', *PLoS ONE*, 11(10), pp. 1–15. doi: 10.1371/journal.pone.0164780.

Maerivoet, S. and De Moor, B. (2005) 'Transportation Planning and Traffic Flow Models', *ArXivPrepr. Physics 0507127*.

Magzhan, K. and Jani, H. M. (2013) 'A review and evaluation of Shortest Path Algorithms', *International Journal of Scientific & Technology research*, 2(6).

Mahut, M. (2001a) *A discrete flow model for dynamic network loading*. University of Montreal, Canada.

Mahut, M. (2001b) *A multi-lane extension of the Space-Time Queue Model of Traffic Dynamics*. Axores Islands: TRISTAN IV.

Mahut, M. and Florian, M. (2011) 'Traffic Simulation with Dynameq', in *Fundamentals of Traffic Simulation*.

Mai, C., Konakli, K. and Sudret, B. (2017) 'Seismic fragility curves for structures using non-parametric representations', *Frontiers of Structural and Civil Engineering*, 11(2), pp. 169–186. doi: 10.1007/s11709-017-0385-y.

Maravall, D., de Lope, J. and Fuentes, J. P. (2013) 'Fusion of probabilistic knowledge-based classification rules and learning automata for automatic recognition of digital images', *Pattern Recognition Letters*, 34(14), pp. 1719–1724. doi: 10.1016/j.patrec.2013.03.019.

Martinez-Pastor, B. *et al.* (2015) 'Evaluation of resilience in traffic networks: models and characteristics', in *Proceedings of the Irish Transportation Research Network ITRN*. Available at: http://www.itrn.ie/uploads/MartinezPastor.pdf.

Martinez-Pastor, B. (2017) *Resilience of Traffic Networks to Extreme Weather Events: Analysis and Assessment*. University of Dublin, Trinity College.

Mattsson, L.-G. and Jenelius, E. (2015) 'Vulnerability and resilience of transport systems - A discussion of recent research', *Transportation Research Part A: Policy and Practice*, 81. doi: 10.1016/j.tra.2015.06.002.

May, A. D. (1990) *Traffic Flow fundamentals*. New Jersey: Englewood Cliffs.

Mehlhorn, S. A. A. (2009) *Method for prioritizing highway routes for reconstruction after a natural disaster*. The University of memphis. Available at: http://www.memphis.edu/cifts/pdfs/Sandy_dissertation.pdf.

Merz, P. and Freisleben, B. (2002) 'Greedy and Local Search Heuristics for Unconstrained Binary Quadratic Programming', *Journal of Heuristics*, 8(2), pp. 197–213. doi: https://doi.org/10.1023/A:1017912624016.

Míča, O. (2015) 'Comparison of metaheuristic methods by solving travelling salesman problem', in *The International Scientific Conference INPROFORUM*.

Miles, S. B., Burton, H. V. and Kang, H. (2018) 'Community of Practice for Modeling Disaster Recovery', *Natural Hazards Review*, 20(1), p. 04018023. doi: 10.1061/(asce)nh.1527-6996.0000313.

Mohammadi Ziabari, S. S. and Treur, J. (2019) 'A Modeling Environment for Dynamic and Adaptive Network Models Implemented in MATLAB', in *Fourth International Congress on Information and Communication Technology*, pp. 91–111. doi: 10.1007/978-981-15-0637-6_8.

Mohan, R. and Ramadurai, G. (2013) 'State-of-the art of macroscopic traffic flow modelling', *International Journal of Advances in Engineering Sciences and Applied Mathematics*, 5(2–3), pp. 158–176. doi: 10.1007/s12572-013-0087-1.

Moher, D. *et al.* (2009) 'Preferred Reporting Items for Systematic Reviews and Meta-Analyses: The PRISMA Statement', *PLoS Medicine*, 6(7). doi: 10.1371/journal.pmed.1000097.

Najim, K. and Poznyak, A. S. (1994) *Learning Automata: Theory and Applications*. 1st Editio. Oxford, England: Pergamon.

Nakanishi, H., Matsuo, K. and Black, J. (2013) 'Transportation planning methodologies for post-disaster recovery in regional communities: the East Japan Earthquake and tsunami 2011', *Journal of Transport Geography*, 31, pp.

181–191. doi: 10.1016/j.jtrangeo.2013.07.005.

Narendra, K. S. and Thathachar, M. a. L. (1974) 'Learning Automata - A Survey', *IEEE Transactions on Systems, Man, and Cybernetics*, SMC-4(4), pp. 323–334. doi: 10.1109/TSMC.1974.5408453.

National Records of Scotland (2011) *SNS Data Zone 2011*. Available at: https://www.scotlandscensus.gov.uk/variables-classification/sns-data-zone-2011 (Accessed: 11 November 2020).

Nifuku, T. (2015) *Probabilistic post-earthquake restoration process with repair prioritization of highway network system for disaster resilience enhancement*. University of California. Available at: http://escholarship.org/content/qt5fr2p0vw/qt5fr2p0vw.pdf.

Nogal, M. *et al.* (2015) 'Dynamic restricted equilibrium model to determine statistically the resilience of a traffic network to Extreme weather events', *12th International Conference on Applications of Statistics and Probability in Civil Engineering, ICASP 2015*.

Nogal, M. *et al.* (2016) 'Resilience of traffic networks: From perturbation to recovery via a dynamic restricted equilibrium model', *Reliability Engineering and System Safety*, 156, pp. 84–96. doi: 10.1016/j.ress.2016.07.020.

Noland, R. B. and Small, K. A. (1995) 'Travel-time uncertainty, departure time choice, and the cost of the morning commute', *Transportation Research Record*.

NSW Roads & Maritime Services (2013) *Traffic Modelling guidelines*. New South Wales.

Obaidat, M. S., Papadimitriou, G. I. and Pomportsis, A. S. (2002) 'Learning Automata: theory, paradigms and applications', *IEEE Transactions on Systems, Man, and Cybernetics*, 32(6), pp. 706–709.

de Oliveira Ramos, G. and Grunitzki, R. (2015) 'An Improved Learning Automata Approach for the Route Choice Problem', in *Agent Technology for Intelligent Mobile Services and Smart Societies*. Springer Berlin, pp. 56–67.

Oommen, B. J. and Hashem, M. K. (2010) 'Modeling a Student's Behavior in a Tutorial- Like System Using Learning Automata', *IEEE Transactions on Systems, Man, and Cybernetics, Part B (Cybernetics)*, 40(2), pp. 481–492. doi: 10.1109/TSMCB.2009.2027220.

Orabi, W. *et al.* (2009) 'Optimizing postdisaster reconstruction planning for damaged transportation networks', *Journal of Construction Engineering and Management*, 135(10), pp. 1039–1048.

Orabi, W. *et al.* (2010) 'Optimizing resource utilization during the recovery of civil infrastructure systems', *Journal of Management in Engineering*, 26(4), pp. 237–246. doi: 10.1061/(ASCE)ME.1943-5479.0000024.

Ordnance Survey (2019) *OS Open Roads*. Available at: https://www.ordnancesurvey.co.uk/business-government/products/open-map-roads.

Ortuzar, J. de D. and Willumsen, L. G. (2011) *Modelling Transport*. 4th Editio, *WILEY*. 4th Editio. John Wiley & Sons. doi: 10.1002/9781119993308.

Ozbay, K. *et al.* (2013) 'Probabilistic programming models for traffic incident management operations planning', *Annals of Operations Research*, 203(1), pp. 389–406. doi: 10.1007/s10479-012-1174-6.

Ozbay, K., Datta, A. and Kachroo, P. (2001) 'Modeling Route Choice Behavior with Stochastic Learning Automata', *Transportation Research Record: Journal of the Transportation Research Board*, 1752(01), pp. 38–46. doi: 10.3141/1752-06.

Ozbay, K., Datta, A. and Kachroo, P. (2002) 'Application of Stochastic Learning Automata for Modeling Departure Time and Route Choice Behavior', *Transportation Research Record: Journal of the Transportation Research Board*, 1807(1), pp. 154–162. doi: 10.3141/1807-19.

Padgett, J. E. and DesRoches, R. (2007) 'Bridge Functionality Relationships for Improved Seismic Risk Assessment of Transportation Networks', *Earthquake Spectra*, 23(1), pp. 115–130. doi: 10.1193/1.2431209.

De Palma, Andre and Marchal, F. (1998) 'METROPOLIS. A dynamic simulation model designed for ATIS applications', in *1st International Conference on Traffic and Transportation Studies (ICTTS 98)*, pp. 770–781.

de Palma, A. *et al.* (1983) 'Stochastic Equilibrium Model of Peak Period Traffic Congestion', *Transportation Science*, 17(4), pp. 430–453. doi: 10.1287/trsc.17.4.430.

Parvaneh, Z., Arentze, T. A. and Timmermans, H. J. P. (2010) 'Effects of advanced information and communication technology on activity-travel pattern: Conceptualization and modelling approach', in *10th International Conference on Design and Decision Support Systems*. Eindhoven: Eindhoven University of Technology.

Pavlov, I. P. (1927) *Conditioned Reflexes*. Oxford, England: Oxford University Press.

Peeling, J. *et al.* (2016) *The Value of the Trunk Road Network to Society and the Economy in Scotland*. Available at: https://www.transport.gov.scot/publication/the-value-of-the-trunk-road-network-to-society-and-the-economy-in-scotland/.

Pillay, N. and Qu, R. (2019) *Hyper-heuristics: Theory and Applications*. Cham, Switzerland: Springer International Publishing AG.

Postance, B. *et al.* (2017) 'Extending natural hazard impacts: an assessment of landslide disruptions on a national road transportation network', *Environmental Research Letters*, 12(1). doi: 10.1088/1748-9326/aa5555.

Postance, B. F. (2017) *Indirect impact of landslide hazards on transportation infrastructure*, *Loughborough University Institutional Repository*. Loughborough University. Available at: https://dspace.lboro.ac.uk/2134/32771.

Pourghasemi, H. R. *et al.* (2020) 'Assessing and mapping multi-hazard risk susceptibility using a machine learning technique', *Scientific Reports*, 10(1), p. 3203. doi: 10.1038/s41598-020-60191-3.

Qu, Z. *et al.* (2013) 'The Departure Characteristics of Traffic Flow at the Signalized Intersection', *Mathematical Problems in Engineering*, 2013, pp. 1–11. doi: 10.1155/2013/671428.

Rachunok, B. and Nateghi, R. (2020) 'The sensitivity of electric power infrastructure resilience to the spatial distribution of disaster impacts', *Reliability Engineering & System Safety*, 193, p. 106658. doi: 10.1016/j.ress.2019.106658.

Rakhecha, A. (2019) *Learn Computer Science - Understand Learning Rate by a Child's interaction with Dogs*, *OpenGenus IQ*. Available at: https://iq.opengenus.org/learning-rate/ (Accessed: 27 October 2020).

Reed, D. A., Kapur, K. C. and Christie, R. D. (2009) 'Methodology for assessing the resilience of networked infrastructure', *IEEE Systems Journal*, 3(2), pp. 174–180.

Reeves, C. R. (1996) 'Heuristic Search Methods: a review', in *Operational Research Society*. Birmingham, pp. 122–149.

Reggiani, A., Nijkamp, P. and Lanzi, D. (2015) 'Transport resilience and vulnerability: The role of connectivity', *Transportation Research Part A: Policy and Practice*. Elsevier Ltd, 81, pp. 4–15. doi: 10.1016/j.tra.2014.12.012.

Roozemond, D. A. and Veer, P. van der (1998) 'Usability of Intelligent Agent Systems in Urban Traffic Control', in *International Conference on Applications of Artificial Intelligence in Engineering*.

Rozin, P. and Royzman, E. B. (2001) 'Negativity Bias, Negativity Dominance, and Contagion', *Personality and Social Psychology Review*, 5(4), pp. 296–320. doi: 10.1207/S15327957PSPR0504_2.

Rus, K., Kilar, V. and Koren, D. (2018) 'Resilience assessment of complex urban systems to natural disasters: A new literature review', *International Journal of Disaster Risk Reduction*. Elsevier Ltd, 31(May), pp. 311–330. doi: 10.1016/j.ijdrr.2018.05.015.

Saaty, T. L. (1980) *The Analytic Hierarchy Process: planning, priority setting, resource allocation*. New York: McGraw-Hill International Book Company.

Said, G. A. E. A., Mahmoud, A. M. and El-Horbaty, E.-S. M. (2014) 'A Comparative Study of Meta-heuristic Algorithms for Solving Quadratic Assignment Problem', *International Journal of Advanced Computer Science and Applications*, 5(1), pp. 1–6.

Sangaiah, A. K. *et al.* (2020) 'IoT Resource Allocation and Optimization Based on Heuristic Algorithm', *Sensors*, 20(2), p. 539. doi: 10.3390/s20020539.

Sato, T. and Ichii, K. (1995) 'Optimization of post-earthquake restoration of lifeline networks using genetic algorithms', in *Proceedings of the 6th U.S.–Japan Workshop on Earthquake Disaster Prevention for Lifeline Systems*. Osaka City, Japan, pp. 235–250.

Schoon, I. (2006) *Risk and Resilience: Adaptations in Changing Times*. Cambridge: Cambridge University Press. doi: 10.1017/CBO9780511490132.

Schwarz, S. (2018) 'Resilience in psychology: A critical analysis of the concept', *Theory & Psychology*, 28(4), pp. 528–541. doi: 10.1177/0959354318783584.

Scottish Government (2011) *Scotland's Census 2011*.

Shalev, J. (2000) 'Loss aversion equilibrium', *International Journal of Game Theory*, 29(2), pp. 269–287.

Shinozuka, M. *et al.* (2003) 'Effect of seismic retrofit of bridges on transportation networks', *Earthquake Engineering*

and Engineering Vibration, 2(2), pp. 169–179. doi: 10.1007/s11803-003-0001-0.

Shinozuka, M. *et al.* (2005) *Socio-Economic Effect of Seismic Retrofit Implemented on Bridges in the Los Angeles Highway Network*, *Report No. CA F/CA/SD-2005/03*. Sacramento, CA. Available at: http://www.dot.ca.gov/newtech/researchreports/reports/2008/06-0145.pdf.

Shoufeng, L., Ximin, L. and Shiqiang (2008) 'Q-Learning for Adaptive Traffic Signal Control Based on Delay Minimizations Strategy', in *IEEE International Conference on Networking Sensing and Control*.

Shumeet, B. and Caruana, R. (1995) 'Removing the genetics from the standard genetic algorithm', in *Machine Learning Proceedings*, pp. 38–46.

Singh, P. *et al.* (2018) 'Vulnerability assessment of urban road network from urban flood', *International Journal of Disaster Risk Reduction*. Elsevier Ltd, 28(March), pp. 237–250. doi: 10.1016/j.ijdrr.2018.03.017.

Small, K. A. (1982) 'The scheduling of consumer activities: work trips', *The American Economic Review*, 72(3), pp. 467–480.

Smith, L. (2017) 'Cyclical Learning Rates for Training Neural Network', *IEEE Winter Conference on Applications of Comupter Vision (WACV)*, 24, pp. 464–472.

Soldi, D., Candelieri, A. and Archetti, F. (2015) 'Resilience and Vulnerability in Urban Water Distribution Networks through Network Theory and Hydraulic Simulation', *Procedia Engineering*, 119, pp. 1259–1268. doi: 10.1016/j.proeng.2015.08.990.

Spiliopoulou, A. *et al.* (2015) 'Macroscopic Traffic Flow Model Calibration Using Different Optimization Algorithms', *Transportation Research Procedia*. Elsevier B.V., 6(June 2014), pp. 144–157. doi: 10.1016/j.trpro.2015.03.012.

Standish, R. J. *et al.* (2014) 'Resilience in ecology: Abstraction, distraction, or where the action is?', *Biological Conservation*, 177, pp. 43–51. doi: 10.1016/j.biocon.2014.06.008.

Stevanovic, A. and Nadimpalli, B. (2010) *Seismic Vulnerability & Emergency Response Analyses of UDOT Lifelines*. Utah. Available at: http://www.mountain-plains.org/pubs/pdf/MPC10-217.pdf.

Sullivan, J. L. *et al.* (2010) 'Identifying critical road segments and measuring system-wide robustness in transportation networks with isolating links: A link-based capacity-reduction approach', *Transportation Research Part A: Policy and Practice*. Elsevier Ltd, 44(5), pp. 323–336. doi: 10.1016/j.tra.2010.02.003.

Sumalee, A. and Watling, D. P. (2008) 'Partition-based algorithm for estimating transportation network reliability with dependent link failures', *Journal of Advanced Transportation*, 42(3), pp. 213–238. doi: 10.1002/atr.5670420303.

Sun, W., Bocchini, P. and Davison, B. D. (2018) 'Resilience metrics and measurement methods for transportation infrastructure : the state of the art', *Sustainable and Resilient Infrastructure*. Taylor & Francis, 9689, pp. 1–33. doi: 10.1080/23789689.2018.1448663.

Sutton, R. S. and Barto, A. G. (1981) 'Toward a modern theory of adaptive networks', *American Psychological Association*, 88(2), pp. 135–170.

Sutton, R. S. and Barto, A. G. (1998) *Reinforcement Learning: An Introduction*. Cambridge: MIT Press.

Tarbotton, C. *et al.* (2012) 'GIS-based techniques for assessing the vulnerability of buildings to tsunami: current approaches and future steps', *Geological Society, London, Special Publications*, 361(1), pp. 115–125. doi: 10.1144/SP361.10.

Tavares, A. R. and Bazzan, A. L. C. (2012) 'Independent learners in abstract traffic scenarios', *Revista de Informática Teórica e Aplicada*.

The MathWorks Inc. (2018) 'MATLAB-R2018b'. Natick, MA.

Thonhofer, E. *et al.* (2018) 'Macroscopic traffic model for large scale urban traffic network design', *Simulation Modelling Practice and Theory*, 80, pp. 32–49. doi: 10.1016/j.simpat.2017.09.007.

Thorhauge, M., Cherchi, E. and Rich, J. (2014) 'Building efficient stated choice design for departure time choices using the scheduling model: Theoretical considerations and practical implementations', in *Selected Proceedings from the Annual Transport Conference at Aalborg University*, pp. 1–15.

Thorndike, E. (1898) 'Animal intelligence: An experimental study of the associative processes in animals', *Psychological Monographs: General and Applied*, 2(4).

Thorndike, E. (1911) *Animal Intelligence: Experimental Studies*. New York: Macmillan.

Toledo, T. *et al.* (2005) 'Microscopic Traffic Simulation: Models and Application', in *Simulation Approaches in*

Transportation Analysis. New York: Springer-Verlag, pp. 99–130. doi: 10.1007/0-387-24109-4_4.

Traffic Engineering, Operations & Safety Manual (2005). Wisconsin.

Tugend, A. (2012) 'Praise Is Fleeting, but Brickbats We Recall', *The New York Times*, 24 March.

Tuzun Aksu, D. and Ozdamar, L. (2014) 'A mathematical model for post-disaster road restoration: Enabling accessibility and evacuation', *Transportation Research Part E: Logistics and Transportation Review*. Elsevier Ltd, 61, pp. 56–67. doi: 10.1016/j.tre.2013.10.009.

Tversky, A. and Kahneman, D. (1992) 'Advances in prospect theory: Cumulative representation of uncertainty', *Journal of Risk and Uncertainty*, 5(4), pp. 297–323. doi: 10.1007/BF00122574.

Twumasi-Boakye, R. and Sobanjo, J. (2018) 'Civil infrastructure resilience: state-of-the-art on transportation network systems', *Transportmetrica A: Transport Science*, 9935. doi: 10.1080/23249935.2018.1504832.

Twumasi-Boakye, R. and Sobanjo, J. O. (2018) 'Resilience of Regional Transportation Networks Subjected to Hazard-Induced Bridge Damages', *Journal of Transportation Engineering, Part A: Systems*, 144(10), p. 04018062. doi: 10.1061/jtepbs.0000186.

Twumasi-Boakye, R. and Sobanjo, J. O. (2019) 'A computational approach for evaluating post-disaster transportation network resilience', *Sustainable and Resilient Infrastructure*. Taylor, 9689(May), pp. 1–17. doi: 10.1080/23789689.2019.1605754.

UK Met Office (2018) *UKCP18 Headline Findings*. Available at: https://www.metoffice.gov.uk/binaries/content/assets/mohippo/pdf/ukcp18/ukcp18-headline-%0Afindings.pdf.

Unal, M. (2015) *Restoration decision-making of disrupted infrastructure networks: a design by shopping and data visualization approach*. The Pennsylvania State University.

UNISDR (2009) *UNISDR terminology on disaster risk reduction*. Switzerland. Available at: http://www.unisdr.org/we/inform/terminology.

Unsal, C., Kachroo, P. and Bay, J. S. (1999) 'Multiple stochastic learning automata for vehicle path control in an automated highway system', *IEEE Transactions on Systems, Man, and Cybernetics - Part A: Systems and Humans*, 29(1), pp. 120–128. doi: 10.1109/3468.736368.

Vickrey, W. S. (1969) 'Congestion Theory and Transport Investment', *The American Economic Review*, 59(2).

Violante, A. (2019) *Simple Reinforcement Learning: Q-learning*, *Towards data science*. Available at: https://towardsdatascience.com/simple-reinforcement-learning-q-learning-fcddc4b6fe56 (Accessed: 14 October 2020).

Vishnu, N., Kameshwar, S. and Padgett, J. E. (2019) 'A framework for resilience assessment of highway transportation networks', in *Routledge Handbook of Sustainable and Resilient Infrastructure*, pp. 216–237.

Vodák, R., Bíl, M. and Křivánková, Z. (2018) 'A modified ant colony optimization algorithm to increase the speed of the road network recovery process after disasters', *International Journal of Disaster Risk Reduction*, 31(December 2017), pp. 1092–1106. doi: 10.1016/j.ijdrr.2018.04.004.

Vugrin, E. D., Turnquist, M. A. and Brown, N. J. K. (2014) 'Optimal recovery sequencing for enhanced resilience and service restoration in transportation networks', *International Journal of Critical Infrastructures*. Inderscience Publishers, 10(3–4), pp. 218–246. doi: 10.1504/IJCIS.2014.066356.

Wahba, M. and Shalaby, A. (2005) 'Multiagent Learning-Based Approach to Transit Assignment Problem: A Prototype', *Transportation Research Record Journal of the Transportation Research Board*, (1926), pp. 96–105. doi: 10.1177/0361198105192600112.

Wahba, M. and Shalaby, A. (2006) 'A General Multi-agent Modelling Framework for the Transit Assignment Problem – A Learning-Based Approach', in Böhme T., Larios Rosillo V.M., Unger H., U. H. (ed.) *International Workshop on Innovative Internet Community Systems*. Springer, pp. 276–295. doi: https://doi.org/10.1007/11553762_26.

Wan, C. *et al.* (2018) 'Resilience in transportation systems: a systematic review and future directions', *Transport Reviews*, 38(4), pp. 479–498. doi: 10.1080/01441647.2017.1383532.

Wang, P. and Yodo, N. (2016) 'Engineering Resilience Quantification and System Design Implications: A Literature Survey', *Journal of Mechanical Design*, 138(c). doi: 10.1115/1.4034223.

Wang, W. *et al.* (2020) 'An Integrated Approach for Assessing the Impact of Large-Scale Future Floods on a Highway Transport System', *Risk Analysis*, 40(9), pp. 1780–1794. doi: 10.1111/risa.13507.

Wang, Y. *et al.* (2018) 'Dynamic traffic assignment: A review of the methodological advances for environmentally sustainable road transportation applications', *Transportation Research Part B: Methodological*. Elsevier Ltd, 111, pp. 370–394. doi: 10.1016/j.trb.2018.03.011.

Wang, Z., He, S. Y. and Leung, Y. (2018) 'Applying mobile phone data to travel behaviour research: A literature review', *Travel Behaviour and Society*, 11, pp. 141–155. doi: 10.1016/j.tbs.2017.02.005.

Wardrop, J. G. (1952) 'Some theoretical aspects of road traffic research', in *Proceedings of the institution of civil engineers*, pp. 325–362.

Watkins, C. (1989) *Learning from Delayed Rewards*. Cambridge University.

Watkins, C. and Dayan, P. (1992) 'Q-learning', *machine Learning*, 8, pp. 279–292.

Wauters, T. *et al.* (2013) 'Boosting Metaheuristic Search Using Reinforcement Learning', *Studies in Computational Intelligence*, pp. 433–452. doi: 10.1007/978-3-642-30671-6_17.

Wei, F., Ma, S. and Jia, N. (2014) 'A Day-to-Day Route Choice Model Based on Reinforcement Learning', *Mathematical Problems in Engineering*, 2014, pp. 1–19. doi: 10.1155/2014/646548.

Wilson, R. J. (1996) *Introduction to graph theory*. 4th editio. Longman.

Winter, M. G. *et al.* (2013) 'Landslide hazard and risk assessment on the Scottish road network', *Geotechnical Engineering*, 166(GE6), pp. 522–539. doi: http://dx.doi.org/10.1680/geng.12.00063.

Wu, Y. and Chen, S. (2019) 'Resilience modeling of traffic network in post-earthquake emergency medical response considering interactions between infrastructures, people, and hazard', *Sustainable and Resilient Infrastructure*. Taylor, 4(2), pp. 82–97. doi: 10.1080/23789689.2018.1518026.

Xiao, L., Liu, R. and Huang, H. (2014) 'Congestion Behavior under Uncertainty on Morning Commute with Preferred Arrival Time Interval', *Discrete Dynamics in Nature and Society*, 2014, pp. 1–9. doi: 10.1155/2014/767851.

Yamasaki, T. and Miwa, H. (2017) 'Method for determining recovery order against intermittent link failures', in Barolli, L., Woungang, I., and Hussain, O. K. (eds) *Advances in Intelligent Networking and Collaborative Systems*. Cham: Springer International Publishing (Lecture Notes on Data Engineering and Communications Technologies), pp. 403–412. doi: 10.1007/978-3-319-65636-6.

Yanmaz-Tuzel, O. and Ozbay, K. (2009) 'Modeling Learning Impacts on Day-to-day Travel', in *Transportation and Traffic Theory 2009: Golden Jubilee*. Boston: Springer.

Ye, Q. and Ukkusuri, S. V. (2015) 'Resilience as an Objective in the Optimal Reconstruction Sequence for Transportation Networks', *Journal of Transportation Safety & Security*, 7(1), pp. 91–105. doi: 10.1080/19439962.2014.907384.

Yen, J. Y. (1971) 'Finding the K Shortest Loopless Paths in a Network', *Management Science*, 17(11), pp. 712–716. doi: 10.1287/mnsc.17.11.712.

Zamanifar, M. and Seyedhoseyni, S. M. (2017) 'Recovery planning model for roadways network after natural hazards', *Natural Hazards*. Springer Netherlands, 87(2), pp. 699–716. doi: 10.1007/s11069-017-2788-4.

Zang, X. *et al.* (2020) 'MetaLight: Value-Based Meta-Reinforcement Learning for Traffic Signal Control', in *Proceedings of the AAAI Conference on Artificial Intelligence*, pp. 1153–1160.

Zhang, M.-X., Zhang, B. and Zheng, Y.-J. (2014) 'Bio-Inspired Meta-Heuristics for Emergency Transportation Problems', *Algorithms*, 7(1), pp. 15–31. doi: 10.3390/a7010015.

Zhang, N., Alipour, A. and Coronel, L. (2018) 'Application of novel recovery techniques to enhance the resilience of transportation networks', *Transportation Research Record*, 2672(1), pp. 138–147. doi: 10.1177/0361198118797510.

Zhang, Q. *et al.* (2020) 'Assessing potential likelihood and impacts of landslides on transportation network vulnerability', *Transportation Research Part D: Transport and Environment*, 82, p. 102304. doi: 10.1016/j.trd.2020.102304.

Zhang, W. *et al.* (2018) 'A Stage-wise Decision Framework for Transportation Network Resilience Planning', *arXiv preprint*, pp. 1–27. Available at: http://arxiv.org/abs/1808.03850.

Zhang, W. and Wang, N. (2016) 'Resilience-based risk mitigation for road networks', *Structural Safety*. Department of Industrial and Systems Engineering, University of Oklahoma, United States School of Civil Engineering and Environmental Science, University of Oklahoma, United States: Elsevier Ltd, 62, pp. 57–65. doi: 10.1016/j.strusafe.2016.06.003.

Zhang, W., Wang, N. and Nicholson, C. (2017) 'Resilience-based post-disaster recovery strategies for road-bridge networks', *Structure and Infrastructure Engineering*. Taylor, 13(11), pp. 1404–1413. doi: 10.1080/15732479.2016.1271813.

Zhang, X. *et al.* (2018) 'Resilience-based network design under uncertainty', *Reliability Engineering & System Safety*. Department of Civil and Environmental Engineering, Vanderbilt University, Nashville, TN, 37235, United States NASA Ames Research Center, Intelligent Systems Division, Moffett Field, CA 94035, United States, 169, pp. 364–379. doi: 10.1016/j.ress.2017.09.009.

Zhang, X. and Miller-Hooks, E. (2014) 'Scheduling short-term recovery activities to maximize transportation network resilience', *Journal of Computing in Civil Engineering*, 29(6), pp. 1–10. doi: 10.1061/(ASCE)CP.1943-5487.0000417.

Zhou, B. *et al.* (2020) 'A reinforcement learning scheme for the equilibrium of the in-vehicle route choice problem based on congestion game', *Applied Mathematics and Computation*, 371, p. 124895. doi: 10.1016/j.amc.2019.124895.

Zhou, X. and Taylor, J. (2014) 'DTALite: a queue-based mesoscopic traffic simulator for fast model evaluation and calibration', *Cogent Eng.*, 1(1).

Zhou, Y., Banerjee, S. and Shinozuka, M. (2010) 'Socio-economic effect of seismic retrofit of bridges for highway transportation networks: a pilot study', *Structure and Infrastructure Engineering*, 6(1–2), pp. 145–157. doi: 10.1080/15732470802663862.

Zhou, Y., Wang, J. and Yang, H. (2019) 'Resilience of Transportation Systems : Concepts and Comprehensive Review', *IEEE Transactions on Intelligent Transportation Systems*. IEEE, PP(c), pp. 1–15. doi: 10.1109/TITS.2018.2883766.

APPENDICES

Appendix 1. Sioux falls network characteristics

Table A.1. XY coordinates of nodes

Node	X-coord (m)	Y-coord (m)
1	10.25	612.62
2	68.96	605.56
3	5.44	572.56
4	19.10	564.37
5	48.94	564.17
6	69.53	576.57
7	86.67	563.66
8	68.82	562.10
9	48.96	551.22
10	49.00	544.69
11	19.16	543.92
12	0.03	543.91
13	0.00	514.83
14	19.12	529.40
15	49.00	529.41
16	68.90	546.66
17	68.95	537.56
18	86.27	546.70
19	69.00	529.37
20	68.71	515.31
21	49.04	514.87
22	49.01	522.14
23	19.13	522.12
24	19.21	514.82

Table A.2. Link description, length, capacity and susceptibility to hazards

Link Number	Node_1	Node_2	Length (km)	Capacity (veh/h)	Susceptibility to hazard impacts (2->high susceptible; 0->No susceptible)
1	1	2	6.5	1554.01	0
2	2	1	6.5	1404.21	0
3	1	3	6	1554.01	0
4	3	1	6	297.49	0
5	2	6	4.5	1404.21	2
6	6	2	4.5	1026.63	2
7	3	4	2	1404.21	2

Link Number	Node_1	Node_2	Length (km)	Capacity (veh/h)	Susceptibility to hazard impacts (2->high susceptible; 0->No susceptible)
8	4	3	2	1026.63	2
9	3	12	4.5	1066.97	0
10	12	3	4.5	294.53	0
11	4	5	3.5	1066.97	0
12	5	4	3.5	296.88	0
13	4	11	3.1	600	0
14	11	4	3.1	297.49	0
15	5	6	3.6	296.88	0
16	6	5	3.6	293.92	0
17	5	9	2	470.51	2
18	9	5	2	1404.21	2
19	6	8	2.2	293.92	0
20	8	6	2.2	470.51	0
21	7	8	2	303.01	2
22	8	7	2	302.75	2
23	7	18	2.6	600	0
24	18	7	2.6	303.01	0
25	8	9	3.6	834.95	0
26	9	8	3.6	834.95	0
27	8	16	2.4	600	0
28	16	8	2.4	810.72	0
29	9	10	1	291.3	0
30	10	9	1	299.61	0
31	10	11	3.5	294.53	0
32	11	10	3.5	600	0
33	10	15	2.3	294.53	2
34	15	10	2.3	292.59	2
35	10	16	2.3	1404.21	2
36	16	10	2.3	294.53	2
37	10	17	3.5	1554.01	0
38	17	10	3.5	1554.01	0
39	11	12	2	305.48	2
40	12	11	2	292.59	2
41	11	14	2.2	307.65	2
42	14	11	2.2	295.49	2
43	12	13	4.5	810.72	0
44	13	12	4.5	307.65	0
45	13	24	2.1	873.89	2
46	24	13	2.1	575.95	2
47	14	15	3.3	302.75	0
48	15	14	3.3	291.3	0

Link Number	Node_1	Node_2	Length (km)	Capacity (veh/h)	Susceptibility to hazard impacts (2->high susceptible; 0->No susceptible)
49	14	23	1.1	313.79	0
50	23	14	1.1	1180.79	0
51	15	19	2.2	299.61	0
52	19	15	2.2	313.79	0
53	15	22	1.1	289.44	0
54	22	15	1.1	1404.21	0
55	16	17	1.4	1180.79	2
56	17	16	1.4	1404.21	2
57	16	18	2	873.89	0
58	18	16	2	289.44	0
59	17	19	1.3	300.16	0
60	19	17	1.3	1404.21	0
61	18	20	5.5	300.16	0
62	20	18	5.5	303.59	0
63	19	20	2.1	304.54	0
64	20	19	2.1	303.59	0
65	20	21	2.3	313.79	0
66	21	20	2.3	293.12	0
67	20	22	2.5	575.95	0
68	22	20	2.5	304.54	0
69	21	22	1.1	313.79	0
70	22	21	1.1	300	0
71	21	24	3.3	295.49	0
72	24	21	3.3	300	0
73	22	23	3.3	304.71	0
74	23	22	3.3	305.48	0
75	23	24	1.1	293.12	0
76	24	23	1.1	304.71	0

Traffic demand

Table A.3. Disruption scenario: damage state, quantification and road capacity

OD pair	Initial node	Final node	Traffic demand (users/h)
1	1	13	10
2	1	18	140
3	1	20	880
4	2	13	50
5	2	18	20
6	2	20	50

7	7	12	650
8	7	13	610
9	7	20	10
10	12	7	650
11	13	1	10
12	13	2	50
13	13	7	610
14	18	1	140
15	18	2	20
16	20	1	880
17	20	2	50
18	20	7	10
	TOTAL		4840

Appendix 2. Sensitivity analysis of parameters (CHAPTER 4)

CHAPTER 4: Damage scenario simulation and three-stage road infrastructure repair model

A sensitivity analysis is carried out in order to understand the effect of certain inputs and parameters on the model outputs. For more information about the network and other data, please refer to Chapter 4.

Base damage value (D) and available repair teams

The number of the available repair teams is modified in order to see how the model changes to variations of resources, while keeping the rest of the parameters fixed. The results are shown in Figure A.*1*. As observed, the more teams available to repair the network, the less number of days are required to physically repair the network. It is also observed that, due to the saturation of repair teams working at the same damaged road segment, the addition of more repair teams cannot reduce the total repair time. This information can be useful for transport operators as they can know if it is worth adding/reducing repair teams to get a faster repair time.

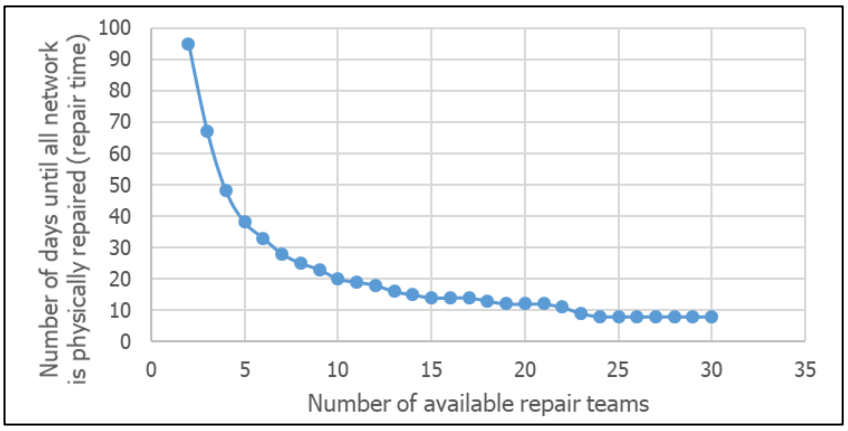

Figure A.1. Relationship between the number of available repair resources and the amount of time required to totally repair the road network. Damage base D=10res-day.

In addition, the analysis of the effect of the base damage value (D) on the model output is also analysed. As expected, the more damage on the network, the more repair time is required to repair the network for a fixed number of repair resources.

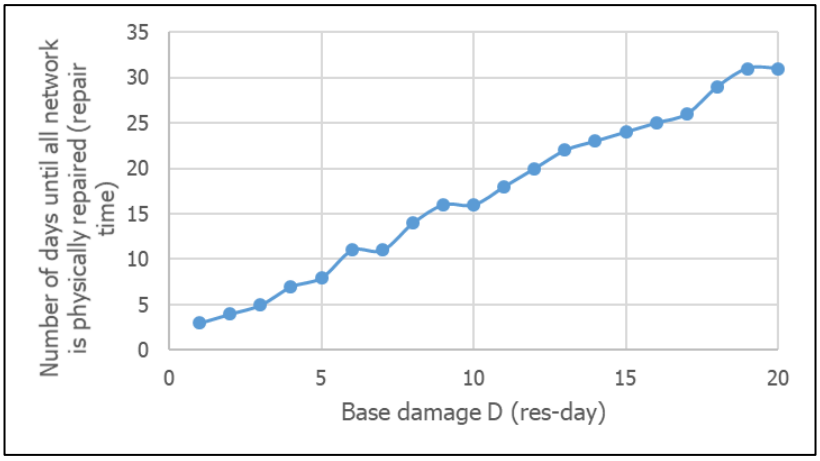

Figure A.2. Relationship between the base damage value (D) and the amount of time required to totally repair the road network. Available repair teams = 13.

Results from both variables (Base damage value and available repair teams) can be combined together as shown in Figure A.*3*. The vertical axis represents the base damage variable and the horizontal axis the available number of repair teams. Each number on the table shows the number of days that are expected to repair the whole network. The column of repair times that is highlighted (13 available teams) provides the same results as the one shown in Figure A.*2*. On the other hand, the row of repair times when base damage is 10 res-day represents the results shown in Figure A.*1*. As observed, both variables have a significant importance in the calculation of repair time. A deficit of repair teams may lead to really high repair times, especially if base damage is high too. If extreme values are not considered, the rest of the values of repair teams acquire similar results. These results can also be useful for transport operators as they can see how adding or reducing available resources can enhance the repair time.

Base Damage (D)	1	2	3	4	5	6	7	8	9	10	11	12	13	14	15	16	17	18	19	20	21	22	23	24	25	26	27	28	29	30
20	380	191	128	95	77	67	56	50	44	40	37	34	31	30	29	29	28	25	24	24	23	21	18	17	17	16	16	16	16	16
19	365	182	125	91	75	64	54	48	42	40	36	32	31	29	29	29	27	26	24	24	22	20	19	17	16	16	16	16	16	16
18	347	174	115	87	73	59	51	46	41	39	35	32	29	28	27	27	25	24	23	23	22	19	16	16	16	16	16	16	16	16
17	330	167	111	86	66	56	48	42	38	35	32	29	26	26	25	25	24	22	21	20	19	17	15	14	14	14	14	14	14	14
16	305	152	105	77	63	54	46	40	36	32	30	27	25	24	23	23	22	21	20	19	18	16	15	14	14	13	13	13	13	13
15	286	147	95	73	60	50	43	39	34	32	29	26	24	23	22	22	22	19	19	19	18	16	14	13	13	13	13	13	13	13
14	270	138	92	68	56	45	39	35	31	30	26	24	23	21	21	21	20	18	18	18	17	15	14	12	12	12	12	12	12	12
13	251	128	87	64	54	45	38	34	30	29	26	24	22	21	21	21	19	18	17	17	16	13	12	12	12	12	12	12	12	12
12	234	115	77	60	49	41	35	30	28	25	22	21	20	19	18	18	17	16	15	14	14	12	12	11	10	10	10	10	10	10
11	212	106	72	53	47	39	33	29	27	24	22	20	18	18	17	17	17	15	14	14	13	12	10	10	10	10	10	10	10	10
10	191	95	67	48	38	33	28	25	23	20	19	18	16	15	14	14	14	13	12	12	12	11	9	8	8	8	8	8	8	8
9	174	87	60	45	38	32	27	23	21	20	18	16	16	15	14	14	13	12	12	12	11	10	8	8	8	8	8	8	8	8
8	152	77	52	38	32	28	24	21	18	16	15	15	14	12	13	12	11	11	10	10	9	8	7	8	7	7	7	7	7	7
7	138	71	48	34	28	24	21	17	16	15	13	12	11	11	11	10	10	9	9	8	8	7	6	6	6	6	6	6	6	6
6	115	60	38	29	27	23	20	17	15	13	12	11	11	10	9	9	9	8	8	8	7	6	6	6	6	6	5	5	5	5
5	95	49	33	26	19	16	15	13	12	10	9	9	8	8	7	7	7	7	7	6	6	6	5	5	4	4	4	4	4	4
4	77	38	29	19	18	13	11	10	10	10	8	7	7	7	7	7	6	6	6	6	5	5	4	4	4	4	4	4	4	4
3	60	30	19	15	13	10	10	8	7	6	6	6	5	5	5	4	5	4	4	4	3	3	3	3	3	3	3	3	3	3
2	38	19	14	10	9	9	6	6	5	5	4	4	4	3	3	3	3	3	3	2	2	2	2	2	2	2	2	2	2	2
1	19	11	10	7	5	5	4	5	3	3	3	3	3	2	2	2	2	2	2	2	2	2	2	2	2	2	1	1	1	1

Available repair teams

Figure A.3. Time (days) required to physically repair the road network depending on the number of available repair teams and damage base value. Note that these values are obtained using the repair strategy defined on the illustrative example of Chapter 4.

Productivity values and saturation level

The variables 'saturation level of repair teams' and 'productivity gradient' are also analysed in this section. The saturation level is set to 5 teams because, for this particular example, the repair strategy requires a maximum of 5 teams per damaged road which means that the saturation level cannot be exceeded. As observed, the difference in gradient for the same saturation level is not that high compared to changes on the saturation level for a fixed gradient value.

Max number of repair teams working at the same place (saturation value)	1	2	3	4	5	6	7	8	9	10	11	12	13	14	15	16	17	18	19	20	Gradient, k
5	16	8	6	4	4	3	3	2	2	3	3	3	3	3	3	3	3	3	3	2	
4	19	18	15	11	13	13	10	10	10	10	10	12	12	11	11	11	11	11	11	11	
3	25	22	15	18	14	14	14	14	14	14	14	14	14	14	14	14	14	14	14	14	
2	35	35	35	35	35	35	35	35	35	35	35	35	35	35	35	35	35	35	35	35	
1	71	71	71	71	71	71	71	71	71	71	71	71	71	71	71	71	71	71	71	71	

Figure A.4. Time (days) required to repair the network depending on different values of productivity

It is also observed how the model outputs change depending on the saturation level of teams and the available number of repair teams to repair all damage locations (see Figure A.*5*). As observed, if the number of saturation teams is quite low, there is a significant effect on the repair time. However, the difference in repair time is lower when the saturation level is closer to the number of teams required by the repair strategy. This evidences that ideally the number of required teams (by the repair strategy) should be closer to the number of saturation teams to get a better value of global repair time.

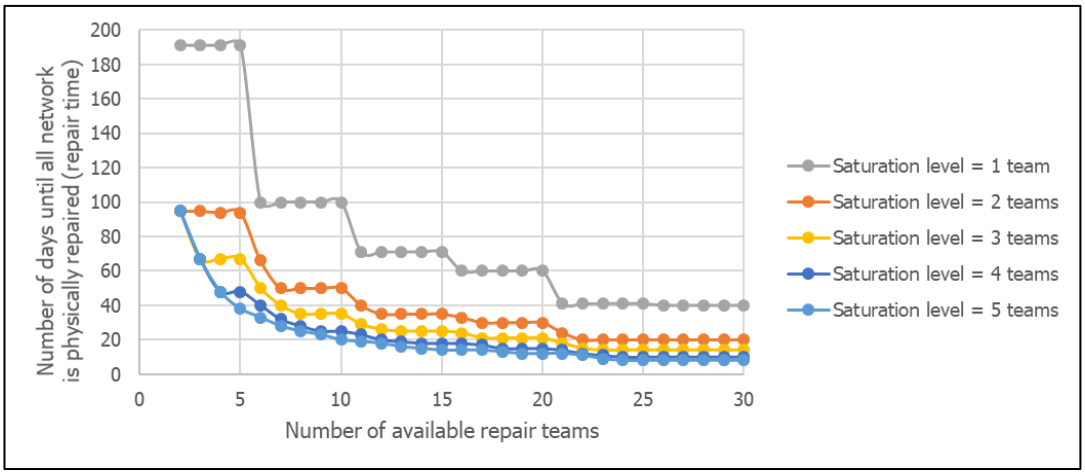

Figure A.5. Available repair teams profile with different saturation levels.

Appendix 3. Maps

This figure has been removed for copyright reasons.

The reader can use the following link to access the image:

https://www.nhshighland.scot.nhs.uk/OurAreas/HHSCS/Pages/welcome.aspx

Figure A.6. Location of NHS Hospitals in the North-West of Scotland. Source: https://www.nhshighland.scot.nhs.uk/OurAreas/HHSCS/Pages/welcome.aspx

Figure A.7. Map of ferry services in Scotland. Source: https://www.audit-scotland.gov.uk/transport-scotlands-ferry-services

Figure A.8. Locations of the main airports in Scotland. Source: https://www.mapsofworld.com/international-airports/europe/scotland.html

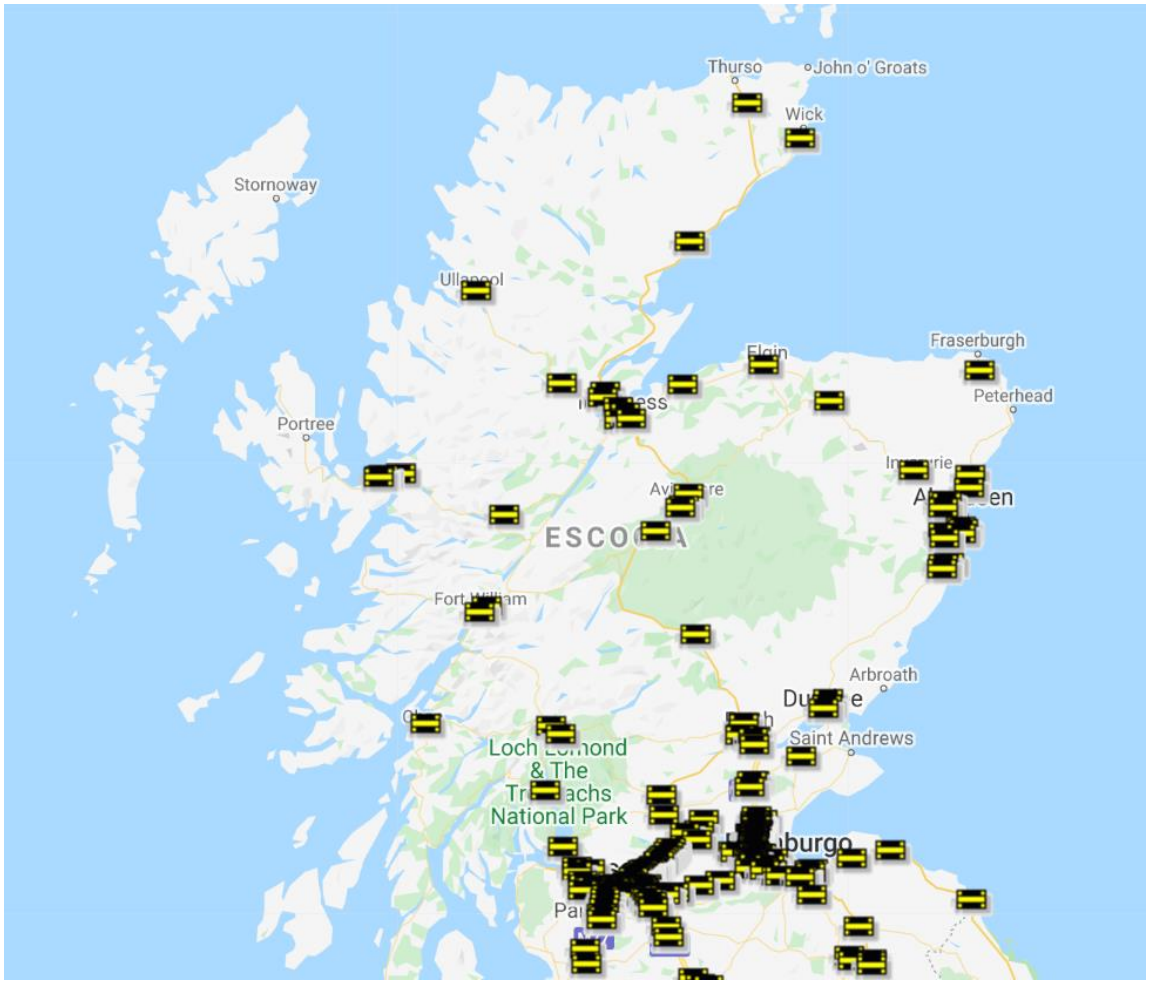

Figure A.9. Map of Scotland showing the location of the VMS. Source: Traffic Scotland Website. Date of access: November 2019. Map data ©2019 GeoBasis-DE/BKG (©2009) https://trafficscotland.org/map/index.aspx?type=8

Appendix 4. Fictitious/Real case applications of recovery models

Table A.4. Summary of fictitious/real case scenarios modelled in reviewed publications

Application to road networks	Nodes	Links	Bridges	% Damaged asset*	References
Road network in Lehigh Valley, Pennsylvania (US)	6	8	13	100%	(Unal, 2015)
Hypothetical road network	6	16	-	-	(Faturechi and Miller-Hooks, 2014b)
Hypothetical road network. Seervada Park	7	12	-	42%	(Henry and Ramirez-Marquez, 2012; Baroud *et al.*, 2014)
	7	12	-	-	(X. Zhang *et al.*, 2018)
Hypothetical road network	8	12	24	100%	(Bocchini, 2013)
Hypothetical road network	8	13	8	62%	(Twumasi-Boakye and Sobanjo, 2019)
Freight transport network in the Western US	8	12	-	-	(Chen and Miller-Hooks, 2012; Zhang and Miller-Hooks, 2014)
Hypothetical road network	9	30	-	13%	(Vugrin, Turnquist and Brown, 2014)
Road network in Greece	9	12	9	50%	(Kilanitis and Sextos, 2019)
Hypothetical road network	9	12	-	25%	(Ye and Ukkusuri, 2015)
Hypothetical road network	10	13	8	100%	(Karamlou and Bocchini, 2014)
	10	26	8	100%	(Karamlou, Bocchini and Christou, 2016)
Road network in the area of Santa Barbara, California (US)	11	28	38	100%	(Bocchini and Frangopol, 2012b)
Hypothetical road network	12	17	-	24%	(Ferreira, 2010)
Hypothetical road network	13	32	-	31%	(Lertworawanich, 2012)
Road network in Izu peninsula (Japan)	14	20	-	55%	(Sato and Ichii, 1995)
Road network in San Diego, California (US)	16	52	238	34%	(Karamlou and Bocchini, 2016)
Hypothetical road network	20	30	-	-	(Barker, Ramirez-Marquez and Rocco, 2013; X. Zhang *et al.*, 2018)
Road network of a virtual community called Centerville	20	33	8	-	(Wu and Chen, 2019)
Hypothetical road network	30	37	-	-	(Zhang and Wang, 2016; Zhang, Wang and Nicholson, 2017)
Road network in Sioux Falls, South Dakota (US)	-	-	-	-	(Orabi *et al.*, 2010)
	24	76	-	10%	(Lu *et al.*, 2016)
	24	76	-	-	(Basavaraj *et al.*, 2017)
	24	76	-	4%	(Kaviani *et al.*, 2018)
	24	76	-	13%	(Chen and Tzeng, 1999)
	24	76	-	16%	(Vodák, Bíl and Křivánková, 2018)
	24	76	-	8%	(Ye and Ukkusuri, 2015)
Highway network in Shelby County, Tennessee (US)	-	-	100	83%	(Mehlhorn, 2009)
	-	-	7	-	(Orabi *et al.*, 2009)
	34	46	24	85%	(Vishnu, Kameshwar and Padgett, 2019)
	34	46	24	80%	(W. Zhang *et al.*, 2018)
Highway network in Nantou (Taiwan)	52	62	-	16%	(Feng and Wang, 2003)
Hypothetical road network	62	122	-	25%	(Li *et al.*, 2019)
Hypothetical road network	82	92	-	-	(Yamasaki and Miwa, 2017)
Road network in Los Angeles metropolitan area, Califonia (US)	-	-	524	-	(Nifuku, 2015)
	118	185	2727	-	(Shinozuka *et al.*, 2003)
	-	-	3133	-	(Zhou, Banerjee and Shinozuka, 2010)
Road network in Kaohsiung City (Taiwan)	132	196	-	12%	(Liao, Hu and Ko, 2018)
Road network in Kobe (Japan)	164	228	-	39%	(Furuta *et al.*, 2008)
Road network in Haiti	216	281	-	10%	(Duque and Sörensen, 2011)
Road network in Cuenca (Spain)	323	672	-	3%	(Nogal *et al.*, 2016)
Rural road network in Sindhupalchok District (Nepal)	457	557	-	12%	(Aydin *et al.*, 2018)
Road network of the Zlín region (Czech Republic)	723	974	-	5%	(Vodák, Bíl and Křivánková, 2018)
Road network in the Canton of Grisons (Switzerland)	37**	2011	116	-	(Hackl, Adey and Lethanh, 2018)
Road network in Chicago (US)	935	2950	-	100%	(Basavaraj *et al.*, 2017)
Highway network in Seattle, Washington (US)	6187	16769	106	-	(Chang, 2003)
Road network in the Memphis metropolitan area, Tennessee (US)	12821	15758	616	-	(Chang *et al.*, 2012)
Road network in Leon County, Florida (US)	2240**	27930	-	10 bridges	(Twumasi-Boakye and Sobanjo, 2019)

Application to road networks	Nodes	Links	Bridges	% Damaged asset*	References
Road network in the Tampa Bay area – Florida (US)	3029**	31797	-	5 bridges	(Twumasi-Boakye and J. O. Sobanjo, 2018)
Two road networks in two districts in Istanbul (Turkey)	-	212 and 386	-	20%	(Tuzun Aksu and Ozdamar, 2014)
Road network in San Francisco Bay Area (US)	-	-	-	664 bridges	(Zhang, Alipour and Coronel, 2018)
Road sections in Baghdad city (Iraq)	-	-	-	-	(Al-Rubaee, 2012)
Two scenario (SC) earthquakes affecting bridges in Athens (Greece)	-	-	400	SC1: 15% SC2: 35%	(Karlaftis, Kepaptsoglou and Lambropoulos, 2007)
Road network in Tehran (Iran)	-	-	-	-	(Zamanifar and Seyedhoseyni, 2017)
Road network in Salt Lake County, Utah (US)	-	-	-	-	(Stevanovic and Nadimpalli, 2010)
Hypothetical highway segment	-	-	3		(Bocchini and Frangopol, 2012a; Decò, Frangopol and Bocchini, 2013)
Road network in South Jersey, New Jersey (US)	-	-	-	-	(Ozbay *et al.*, 2013)

* Ratio between damaged assets and total number of assets
**Zones, not nodes.

Appendix 5. Free flow travel time and capacity estimation for Scottish roads

A5.1. Free flow travel time

The free flow travel time considered in the Scottish case study is obtained dividing the desired travel speed by the length of the road.

The desired speed is the one considered in the following table:

Table A.5. Desired speed considered in the Scottish case study

Route Hierarchy	Form of Way	Desired Speed (km/h)
Motorway		108
A Road or A Road Primary	Dual	92
B Road or B Road Primary	Dual	72
A Road or A Road Primary	any other	40
B Road or B Road Primary	any other	40
Minor Road		39
Local Road		32
all other		16

A5.2 Capacity estimation

RURAL ROADS (based on DMRB 46/97)

The DMRB 46/97 provides a method to estimate the capacity of rural roads that depends on the number of lanes and the width of the road. The formula used to calculate the capacity is the following:

$$q'_{max} = q_{max} \cdot lanes \cdot W_f \quad \text{(A.8)}$$

Where:

q'_{max}, is the updated capacity affected by the width of the road.

q_{max}, is the maximum hourly lane throughput. Based on the road standard, this parameter takes a value of 1380 veh/h/lane for single carriageway; 2100 veh/h/lane for dual carriageway; 2300 veh/h/lane for motorways.

$lanes$, number of lanes.

W_f, is the width factor. For motorways, $W_f = 1$; For dual carriageways, the factor is given by Equation (A.9) and for single carriageways, Equation (A.10).

$$W_f = \frac{Carriageway\ width}{lanes \cdot 3{,}65} \quad \text{(A.9)}$$

$$W_f = 0{,}171 \cdot Carriageway\ width - 0{,}25 \quad \text{(A.10)}$$

Where,

$Carriageway\ width$, is defined as the total paved width of the carriageway less the width of ghost islands and hard strips.

URBAN ROADS (based on DMRB TA 79/99)

The DMRB TA 79/99 differentiates between different road types: (1) UM: Motorways; (2) UAP1: single/dual carriageway road with limited access; (2) UAP2: single/dual carriageway road with frontage access and more than two side roads per km; (3) UAP3: variable standard road carrying mixed traffic, frontage access, bus stops and pedestrian crossings; (4) UAP4: Busy street carrying local traffic. The model presented in this thesis assumes in the Scottish case study that an A road Primary corresponds to a UAP1, an A road or B road to UAP2, a minor road to UAP3 and for the rest of roads UAP4.

According to the DMRB TA 79/99, the estimated capacities for urban roads are the following:

Motorway
UM (2 lanes). Capacity = 4000 veh/h each way
UM (3 lanes). Capacity = 5600 veh/h each way
UM (4 lanes). Capacity = 7200 veh/h each way
UM (5 lanes). Capacity = 8800 veh/h each way

UAP1
UAP1 2-way, 2 lane. Capacity = 1590 veh/h each way
UAP1 2-way, 4 lane. Capacity = 2800 veh/h each way
UAP1 1-way, 1 lane. Capacity = 1590 veh/h
UAP1 1-way, >1 lane. Capacity = 2800 veh/h

UAP2
UAP2 2-way, 2 lane. Capacity = 1470 veh/h each way, if > 2 lanes then 1650 veh/h each way
UAP2 1-way. Capacity = 1470 veh/h, if > 1 lane then 1650 veh/h.

UAP3
UAP3 2-way for 2 lanes = 1300 veh/h each way, else if >2 lanes then 1620 veh/h
UAP3 1-way for 1 lane = 1300 veh/h, else if > 1 lane then 1620 veh/h

UAP4
UAP4 2-way for 2 lanes = 1140 veh/h each way, else if >2 lanes then 1410 veh/h
UAP4 1-way for 1 lane = 1140 veh/h, else if > 1 lane then 1410 veh/h

Appendix 6. Disruption scenario for the Scottish case study

A6.1. Damaged links

A total number of 8 bidirectional road segments (16 in total) are considered as damaged: DL1 (Links 293 and 294), DL2 (Links 441 and 442), DL3 (Links 403 and 404), DL4 (Links 159 and 160), DL5 (Links 143 and 144), DL6 (Links 347 and 348), DL7 (Links 305 and 306) and DL8 (Link 123 and 124).

Appendix 7. Image of Research

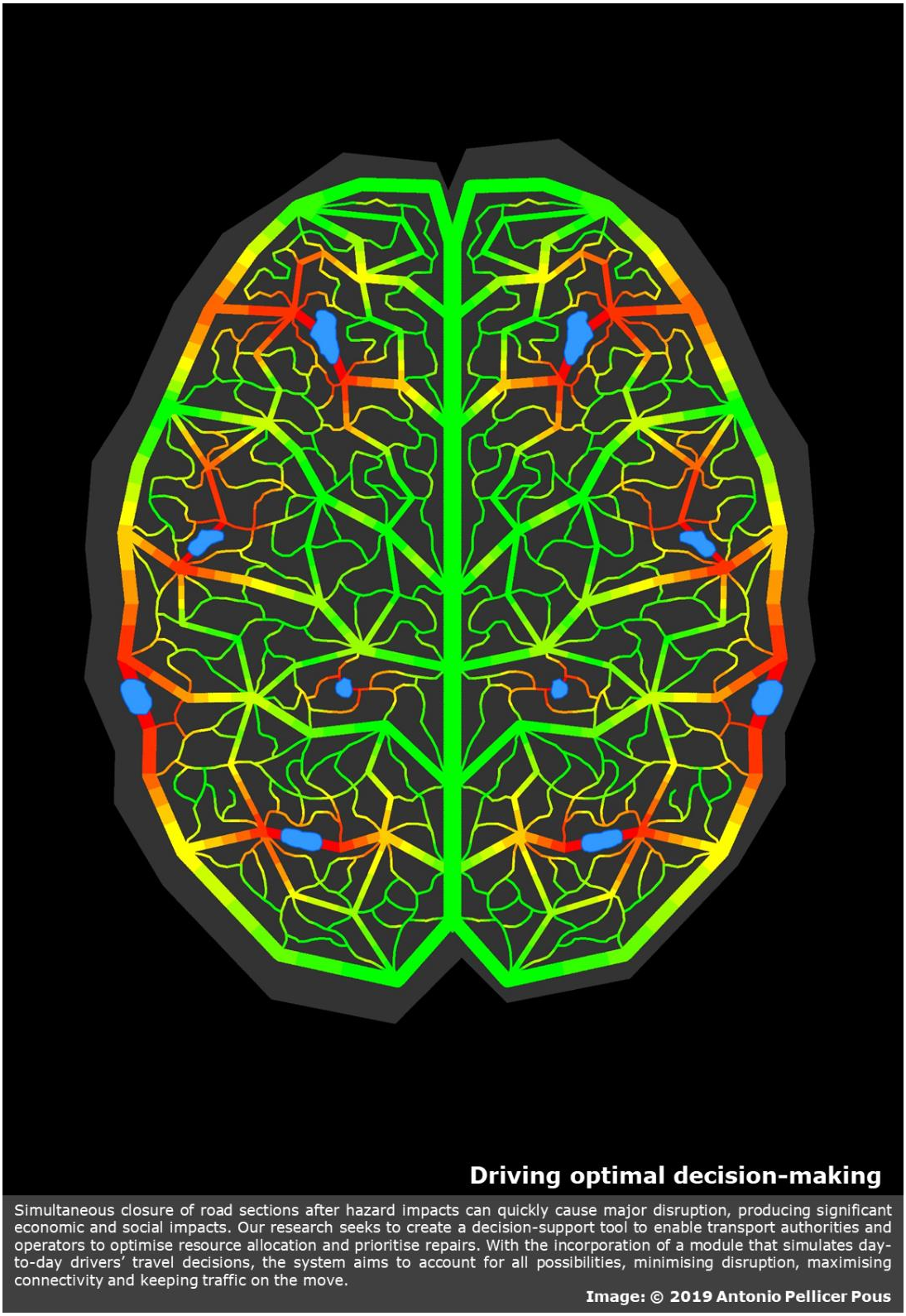

Figure A.10. Image can be found at:

https://www.imagesofresearch.strath.ac.uk/2019/gallery.php